PROCESSING OF TOUGHENED CYANATE ESTER MATRIX COMPOSITES

by

Anand V. Rau

Dissertation submittted to the Faculty of the
Virginia Polytechnic Institute and State University
in partial fulfillment of the requirements for the degree of

Doctor Of Philosophy
in
Engineering Mechanics

APPROVED:

Dr. Alfred C. Loos, Chairman

Dr. Zafer Gürdal

Dr. Ronald G. Kander

Dr. Tangavelu Kuppusamy

Dr. Saad A. Ragab

November, 1996
Blacksburg, Virginia 24061

KEY WORDS: Toughened Resins, Cyanate Esters, Fabric Composites, Resin Transfer Molding, Process Optimization, Damage Tolerance.

PROCESSING OF TOUGHENED CYANATE ESTER MATRIX COMPOSITES

by

Anand V. Rau

A. C. Loos, Chairman

Engineering Mechanics

ABSTRACT

This investigation explored the feasibility of recently developed toughened cyanate ester networks as candidate materials for high performance composite matrix applications. The resin investigated was a Bisphenol-A cyanate ester toughened with hydroxy functionalized phenolphthalein based amorphous poly(arylene ether sulfone). The thermoplastic modified toughened networks exhibited improvement in the fracture toughness over the base cyanate ester networks without significant reductions in mechanical properties or glass transition temperature.

Void free, unidirectional carbon fiber prepreg was successfully manufactured with the toughened cyanate resin using a solventless hot-melt technique. The resin mass fraction of the prepregs was between 31 and 35%. The carbon fiber, toughened cyanate ester prepreg was fabricated into composite panels for mechanical and physical testing. The cure cycle used to manufacture the composite laminates was developed with the aid

of a process simulation model developed by Loos and Springer. In order to accurately simulate the resin curing and flow processes, the cure reaction kinetics and melt viscosity was characterized as a function of temperature and degree of cure and input into the simulation model. The model generated cure cycle was used in the manufacture 8-ply unidirectional and 16-ply quasi-isotropic composite laminates. The manufactured laminates were well consolidated to the specified fiber volume fraction between 59 and 60%. Photomicrographs showed that the laminates are void free, the fiber and resin distribution is uniform and fiber wet-out is very good. Mechanical tests were performed to measure the impact damage resistance and shear properties of the toughened cyanate ester resin composites. The results show improvements in impact damage resistance compared with the commonly used hot-melt epoxy resin composites. The influence of processing on performance was observed from the results of shear tests.

Carbon fabric composite panels were manufactured by liquid molding processes (resin transfer molding and resin film infusion), with a series of four toughened cyanate ester resins generated by varying the concentration and the molecular weight of the toughener. The panels were subjected to physical, damage tolerance, and fracture toughness tests. The results of physical testing indicate consistently uniform quality, and the void content was found to be less than 2%. The toughened cyanate ester composites exhibited significantly improved impact damage *resistance* and *tolerance* compared with hot-melt epoxy systems. Marked increase in the mode II fracture toughness were observed with an increase in the concentration and the molecular weight of the toughener.

To my parents, Vijaya and Ganapathi Rau

ACKNOWLEDGEMENTS

I would like to express my gratitude to Dr. A. C. Loos, my advisor, for his support, encouragement, and guidance. I am greatly appreciative of all the research and learning opportunities that he has provided me over the years.

I wish to extend my sincere thanks to the members of my advisory committee, Dr. Gürdal, Dr. Kander, Dr. Kuppusamy, and Dr. Ragab, for kindly serving on my committee and for reviewing this manuscript. I am very appreciative of their valuable suggestions, remarks, and support.

I would like to acknowledge the NSF Center for High Performance Polymeric Adhesives and Composites, Virginia Tech, for the financial support. My association with the faculty, staff, and students affiliated with the Center has been educative and pleasant.

The assistance of Bob Davis, Bill Shaver, Bob Simonds, and Duane Taylor, of the ESM Department, during the course of my research work was extremely valuable. I am very grateful to Joe Price-O'Brien (a.k.a. Obie) who has always been willing (and able) to iron out many of my research related problems. I wish to thank Obie (WA4DOX) for the endless supply of coffee and for providing the activation energy to obtain my amateur radio license (KF4JFD).

My fellow students who have called 205 Hancock Hall "lab", have enriched my experience at Virginia Tech. I sincerely thank all of them, those who have taught me and those who have been at the "receiving" end.

My parents have been a constant source of support, encouragement, and strength. I wish to thank them by emulation, as words fail me, for putting their son's education above all else.

To my wife and son: thank you for your care, support, and patience.

TABLE OF CONTENTS

LIST OF ILLUSTRATIONS

LIST OF TABLES

1.0 INTRODUCTION

Fiber-reinforced composite materials are gaining wider acceptance as high performance materials in a variety of industries, from aerospace to sporting goods. However, concerns about damage tolerance of high performance composite materials have inhibited widespread immediate use of these lightweight materials. Impact damage tolerance is an issue of significant concern, especially in the aerospace industry.

Impact damage can result from low energy (dropped tools), medium energy (runway debris), and high energy (bird strikes/bullets). High and medium energy impacts typically cause damage which are visible on the surface. However, low energy impacts can cause internal delamination type damage with little or no evidence on the surface. Such damage is termed "barely visible impact damage" (BVID). While visible damage can be easily identified and repaired, detecting BVID requires the use of expensive non-destructive inspection equipment. Delaminations, a type of internal damage, greatly

reduce the fatigue and compressive strengths of the component, and if not detected may lead to catastrophic failures.

Recent studies have shown that damage resistance of composite materials is highly dependent on the matrix material. While thermoplastic resins can provide enhanced resistance to impact damage, they are expensive and not easily processed. Traditional thermosetting resins such as epoxies, cyanate esters and bismaleimides are cheap and easy to process, however, they are also brittle and have poor impact damage resistance.

The need to improve the impact damage tolerance of composite materials is widely recognized. Matrix toughening to improve damage tolerance is one approach to this end. Tough, ductile polymers are often incorporated in thermosetting resins systems to overcome their inherent brittleness. Such modified systems tend to bridge the gap between the easily melt-processable, but brittle thermosets on one hand and the tough, but difficult to melt-process thermoplastics on the other. The improvement in toughness is almost always accompanied by increased melt viscosity, which adversely affects the ease of processability.

The cost of manufacturing composite components is yet another impediment to their widespread use. It was reported that manufacturing costs account for up to 70% of the cost of high performance composites. Therefore, reduction in manufacturing cost is of prime importance, especially in the automotive industry. Spurred by the need for cost-effectiveness, net-shape manufacturing techniques, such as liquid molding, electrostatic

dry powder prepregging, on-line consolidation, etc., have been developed. Further, process automation helps achieve cost reductions, in addition to reliability in processing.

Resin Transfer Molding (RTM) is a net-shape, liquid molding process for the manufacture of fiber reinforced polymeric composite components. In this process, a dry preform of reinforcing fiber is placed in a cavity of a matched mold, usually made of metal. The mold cavity is machined to the final shape and dimensions of the required part. Liquid resin at low viscosity is then injected under pressure into the mold cavity until the preform is fully saturated with the resin. Upon full infiltration of the preform the resin is cured by the application of heat to the mold assembly. The fully cured component is then de-molded and finished. Thus, the composite components manufactured by the RTM process would need little, if any, further processing.

RTM offers the ability to manufacture complex components to close dimensional tolerances, good surface finish, low void content and controlled fiber content/ architecture. In addition, this process is amenable to extensive automation. These advantages coupled with the low capital requirements has, in recent years, drawn the attention of a variety of industries to the potential of this process.

There are two major steps involved in the RTM process, which are identified as follows:

- Resin injection until complete infiltration of preform
- Subsequent thermal processing until full cure of resin

In order to realize the full potential of the RTM process, it is necessary to efficiently design processing equipment and conditions. This requires an understanding of the physical factors of the above sub-processes and the identification of the significant process variables. Knowledge of the resin and preform characteristics help understand their interaction during infiltration. Again, resin characterization is vital for the curing process.

Currently a variety of thermosetting resin systems tailored for use in the RTM process are commercially available. At the infiltration step, resin systems specifically designed for the RTM process allow a greater latitude in operating conditions as compared to toughened thermosetting resin systems. The increased melt viscosity, resulting from the addition of the toughness modifier to thermosetting resin systems, forms a formidable challenge in the injection stage.

While initially dissolved in the thermoset resin, the toughener may, under the right conditions, "separate" out of the solution. This phenomenon known as phase-separation occurs commonly during the curing process. The rate of phase separation and the resulting morphology is strongly influenced by the thermal cure profile. The final phase separated morphology in the resin has a direct bearing on the toughness and damage tolerant properties of the composite material.

It is therefore necessary to develop science based methodologies to describe and simulate the sub-processes and further to design optimal processing conditions that yield a quality composite part/ component with the desired properties. Also, it is important to

develop appropriate process control equipment which would facilitate the incorporation of optimal processing profiles at all stages of operation.

Given a resin system and a reinforcing preform, is it possible to successfully implement the RTM process? If it is indeed possible, what are the optimal processing conditions for injection and subsequent cure? These questions can be answered either by an experimental procedure which would be time and material intensive or by turning to scientific tools to provide the answers. This work attempts to address some of these issues.

The focus of this work was to explore the feasibility of toughened cyanate ester networks as potential candidates for high performance composite matrix applications. The specific objectives were to manufacture carbon fiber composites with the toughened cyanate ester resin systems and to perform physical and mechanical tests to evaluate the quality and mechanical performance of the composites manufactured.

An initial study (Chapter 2) was conducted to evaluate the processability of a toughened cyanate ester resin system by the conventional prepregging/compression molding techniques. This was then followed by a liquid molding processability study (Chapter 3.0) on a variety of toughened cyanate ester formulations. Carbon fabric reinforced composite laminates were manufactured and subjected to physical and mechanical testing. Finally, in Chapter 4.0, a systematic procedure is developed, based on optimization techniques and flow modeling, to design the injection parameters for the RTM process.

2.0 PREPREGGING AND COMPOSITE MANUFACTURE WITH TOUGHENED CYANATE ESTER RESIN SYSTEMS

2.1 INTRODUCTION

The matrix resin plays a vital role in the performance of advanced structural composite materials used in the aerospace and electronic industries. Traditionally, low cost, and easy to process resin systems such as epoxies and bismaleimides have been used as matrix materials. The major drawback of these highly crosslinked resins is their inherent brittleness. Cano and Dow recognized the limitation of brittle epoxies for use in primary aircraft structures in their study of commercial toughened composite material systems [1]. Williams [2] draws the following conclusions based on impact studies comparing brittle and toughened matrix composites:

- Tough resin systems reduce the size of impact damage zone

- Tough resin systems can improve the compression strength of impact damaged laminates

In order to improve the toughness of such brittle thermosetting resin systems, often elastomers have been incorporated [3-7] into the base thermoset resin. The addition of an elastomeric second phase improves the toughness of thermosets. However, associated with this is a decrease in modulus and high temperature capability. This penalty precludes the use of elastomer toughened thermosets in many high performance structural composite applications.

In some cases, toughening is effected by controlling the crosslinked structure through chemical reactions alone and not through the inclusion of a secondary ductile phase. Lee and coworkers report the development of a new toughened epoxy, RX 104, based on this approach [14].

- McGrath and coworkers have demonstrated that the incorporation of tough ductile, functionally terminated high temperature thermoplastic modifiers in thermosetting systems results in improvements in toughness along with retention of high modulus and thermal stability [8-13]. Resin toughening with reactive thermoplastics, through chemical bonding between thermoplastic and thermoset phases, results in toughened resins with superior properties as compared to non-reactive thermoplastic modified systems.

The resin used in the present investigation is a Bisphenol-A cyanate ester toughened with hydroxy functionalized phenolphthalein based amorphous poly(arylene ether sulfone). The thermoplastic modified toughened networks exhibited improvement

in the fracture toughness over the base cyanate ester networks without significant reductions in mechanical properties or glass transition temperature. Details of toughener chemistry and synthesis is reported by Srinivasan [12].

A variety of factors contribute to influence the properties of toughened thermosets including toughener concentration, molecular weight, and formulation [3,6,7,11,15]. Further, cure conditions also have a significant effect on the development of morphology and on the mechanical behavior of the toughened system [4,6,10,16,17]. While improvements in toughness of the cured resin is achieved through the addition of the ductile second phase to the base thermoset resin, the viscosity of the uncured toughened resin is significantly increased. Thermosets are easily processed, however, increased resin viscosity resulting from the toughening process has an adverse effect on the ease of processability. Therefore, in the manufacture of advanced fiber reinforced composites with toughened resin systems a good understanding of resin behavior is necessary. Further, close control of process parameters is required to successfully manufacture high quality composites.

In order to efficiently manufacture composite components, a model based approach to processing is necessary. The steps involved in such an approach to process development and material evaluation is schematically shown in Fig. 2.1. This approach involves characterizing the resin system as the first step. An understanding of the cure kinetics and viscosity behavior of the resin system is essential nearly at all the stages of

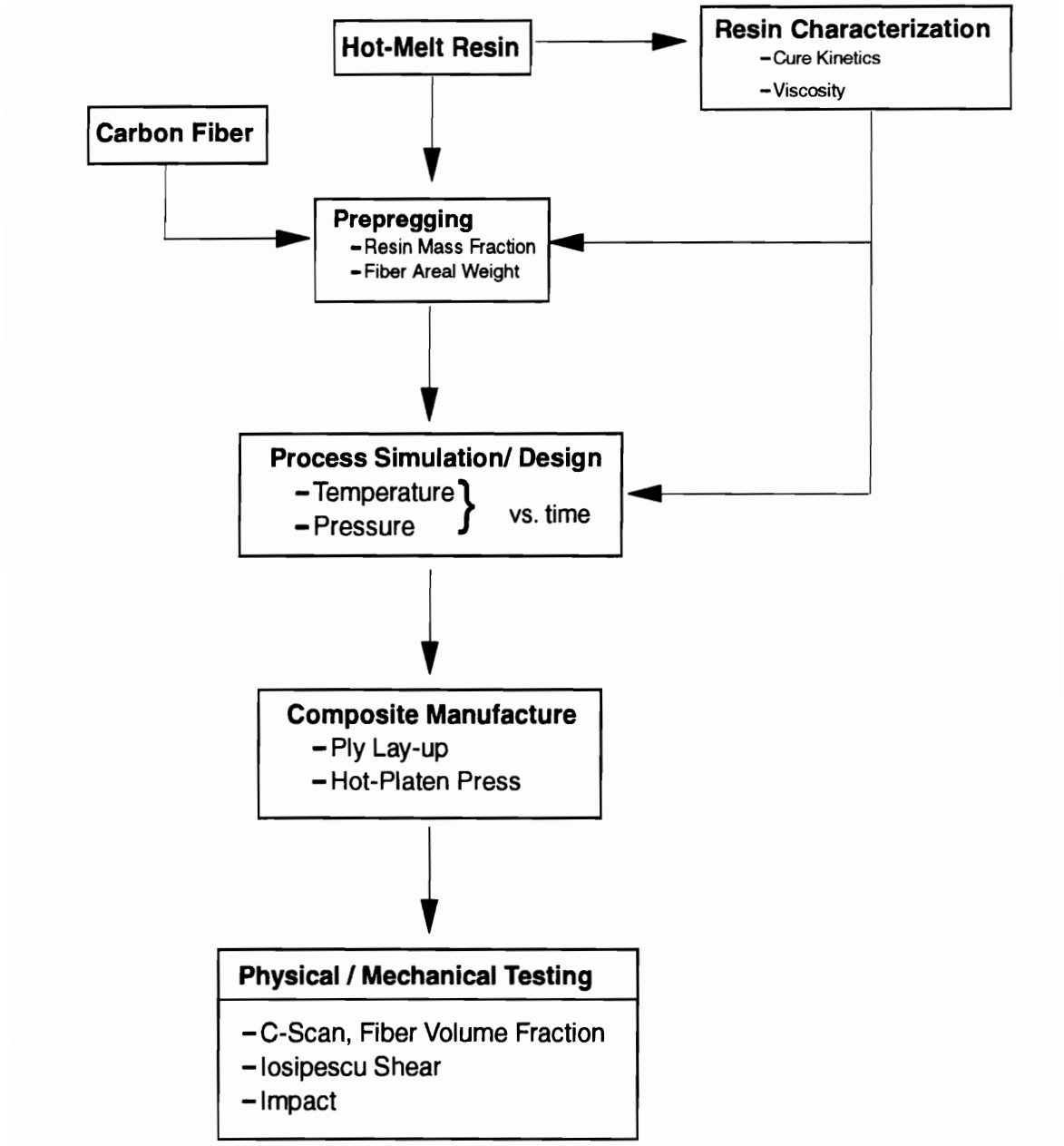

Figure 2.1 Schematic representation of a model based approach to composite processing.

processing. Science based process simulation models, in conjunction with the characterization data, provide a means to develop processing cycles which when applied during processing produce quality composites in the desired configuration. This necessitates the use of sophisticated control equipment for composite manufacture to accurately implement the model generated process cycles. Thus, composite components can be produced without extensive process trials. Also, based on the report published by Cano and Dow [1], commercially available toughened thermoset systems are 2-5 times more expensive than a common brittle thermoset. The need to closely control the processing of toughened resin systems coupled with their cost makes the modeling approach more relevant when compared to a trial-and-error based procedure.

This investigation examines the use of novel, toughened cyanate ester networks for high performance composite matrix applications. Specifically, the study involves the characterization of the resin system using thermal analysis, the manufacture of carbon fiber prepreg tapes, and through the use of simulation models, develop processing parameters for composite curing and consolidation. The fabrication of composite specimens from prepreg tape for physical and mechanical testing 'closes the loop' in assessing the processability and mechanical performance of the material system under evaluation.

2.2 MATERIALS AND CHARACTERIZATION

2.2.1 Materials

A commercially available bisphenol-A based cyanate ester network system under the trade name AroCy B10 (T_g ~265-270 °C) provided by Ciba-Geigy, Inc. was the base thermosetting resin system. The thermoplastic toughener chosen was a hydroxy functionalized phenolphthalein based amorphous poly(arylene ether sulfone) (T_g ~260 °C), molecular weight 15,000 g/mol, synthesized at Virginia Tech by McGrath and coworkers [9,12]. The toughened resin system formulated for this investigation had 25 wt.% of the reactive toughener dissolved in AroCy B-10 thermoset. For convenience of reference, this system was designated "VTUFF1525", indicating the toughener molecular weight and concentration. Aluminum acetylacetonate [Al(acac)], at a concentration of 250 ppm, and nonyl phenol, at a concentration of 2 phr, constituted the catalysts for this system. For processability studies, the resin system was supplied with the toughener predissolved in the cyanate thermoset resin.

AS4 carbon fiber in 12,000 filament count tow form from Hercules, Inc., was used as the reinforcement material.

2.2.2 Cure Kinetics Characterization

Characterizing the cure kinetics involves measuring the parameters associated with the exothermic cure reaction and then developing a mathematical model for the cure rate in terms of temperature and degree of cure. The instrument employed in this investigation to make these measurements was a DuPont Model 910 differential scanning calorimeter (DSC) controlled by TA Instruments Model 9900 computer.

The toughened resin system was melted at 105 °C and an appropriate amount of catalyst was added to the molten resin while continuously stirring. The catalyzed resin was degassed under full vacuum for 10-15 minutes. Typically, a 5-10 milligram sample of resin was encapsulated in a hermetic aluminum DSC pan.

Initially, temperature and enthalpy calibrations were performed on the DSC. A two-point temperature calibration was performed based on the observed and actual melting points of high purity standard indium (m.p. 156.7 °C) and lead (m.p. 327.4 °C). The calibration software automatically corrects the cell constant, a ratio of the measured to standard heat of fusion of indium.

Dynamic scans at various heating rates between 1.0 and 5.0 °C/min were performed on uncured resin.

Isothermal measurements were made at constant temperatures between 120 and 180 °C. The signal corresponding to the rate of heat generation was monitored until the signal value remained constant for an extended period of time, indicating the cessation of the cure reaction at that particular temperature. The sample was then cooled to room

temperature and dynamically rescanned at 2.5 °C/min to measure the residual heat of reaction.

The data analysis software available on the TA9900 computer was used to calculate the ultimate heat of reaction, H_u, for each of the dynamic scans. The area under the exothermic peak resulting from a dynamic scan, referenced to a baseline established between operator selected start and end points, yields the ultimate heat of reaction. In order to determine the start and end points of the exothermic peak with reasonable accuracy, the derivative of the rate of heat generation signal with respect to temperature was used. At the starting point of the exotherm, the derivative signal deviates from a zero value and returns to zero value again at the end of the exotherm. The derivative signal goes through an inflection at the temperature at which the rate of heat generation reaches a maximum. This is commonly referred to as the peak temperature.

For isothermal measurements, the DSC cell was preheated to the desired isothermal scan temperature. The cell was then rapidly opened and the sample pan containing the uncured resin was quickly placed in the cell. The data acquisition procedure was initiated when the displayed temperature stabilized to within 4-5 °C of the scan temperature. This procedure allowed the baseline to be established as outlined above. The isothermal heat of reaction, H_i, was calculated from the area under the exotherm peak resulting from an isothermal scan. The total heat of reaction, H_T is expressed as follows

$$H_T = H_t + H_{res} \quad 2.1$$

where, H_{res} is the residual heat of reaction obtained from the dynamic rescan performed on the isothermally scanned sample.

Further, from isothermal scans, the cure rate and degree of cure data as a function of time for each scan temperature were obtained. The data were then fit to a two part mathematical model proposed by Chen and Macosko [18]. A nonlinear multiple regression software using a modified Levenberg-Marquardt algorithm was used to fit the data to the model [20].

2.2.3 Viscosity Characterization

The viscosity-time characteristics of the toughened cyanate resin system were measured at elevated temperatures using a Bohlin rheometer. Viscosity measurements were made using 25 mm diameter parallel plates. The isothermal measurements were made at three different temperatures: 140, 150, and 160 °C, at a shear rate of 10 s^{-1}. An appropriate quantity of resin was used in order to maintain a plate gap of 1-2 mm.

The cure kinetics model was used to convert the isothermal viscosity-time curves to viscosity-conversion curves. The transformed data were then fit to a mathematical model proposed by Castro and Macosko [19]. Further, a model based on the viscosity-time data alone, analogous to the Castro and Macosko model, is proposed.

2.3 HOT-MELT PREPREGGING

Pre-impregnating the reinforcing fibers with the matrix resin to form pre-impregnated tapes or prepreg is a commonly used technique in industry. Prepreg, an intermediate product wherein the matrix resin is only marginally cured (B-staged), is then "laid-up" in desired orientations and processed into a composite laminate. The processing, carried out either in an autoclave or in a hot-platen press, involves the application of heat and pressure to consolidate and fully cure the composite. It is quite obvious that the quality of the prepreg has a direct bearing on the quality of the resulting composite.

While prepregging equipment may vary in operational details, the technique involves passing dry reinforcing fibers (or woven fabric) through a bath of resin, heated to maintain it in a low viscosity liquid state. The parameters of the process are set so as to yield prepreg tape with just the right amount of resin. Less than an optimum amount leads to a "dry" composite with higher than desired fiber volume fraction. On the other hand, a high resin content in the prepreg requires more resin to be bled off during consolidation which is essentially a waste of expensive material.

The equipment used in this investigation was a lab scale Model 30 prepregger manufactured by Research Tools Corporation, Ovid, Michigan. In this apparatus, a single tow of reinforcing fiber is passed through a wedge-slit die, at the bottom of a heated resin pot containing the matrix resin. The wetted tow is then passed between a pair of flattening pins and around a guide roller before being wound on a drum. The flattening ping and the guide rollers can also be independently heated.

Figure 2.2 shows a schematic representation of this prepregger and the resin pot with the wedge slit die and impregnation bars. The wedge-slit die, where most of the impregnation occurs, has to be of appropriate dimensions to permit the desired amount of resin to be deposited on the fiber tow as it is drawn through the die.

In a study of resin impregnation rates using wedge-slit dies, Chmielewski, Jayaraman, and Petty [21] developed a mathematical model to analyze the resin impregnation at the die. The model has been used to predict resin content in the impregnated tow for a given set of process parameters. The following are the typical parameters for prepreg manufacture on the Model 30 prepregger:

- resin type
- resin pot temperature
- resin viscosity-time characteristics at the prepregging temperature
- fiber tow velocity and tension
- wedge-slit die size

The bundle area of the fiber tow used in this investigation was 0.53 mm^2. A wedge-slit die with slit dimensions of 5.59 mm x 0.165 mm (0.22 in. x 0.0065 in.) was initially selected. In the manufacture of prepreg on the Model 30 prepregger, the impregnated tow is wound on a traversing drum which requires a small degree of overlap of tows as they are wound. This is necessary to prevent the tows from separating upon removal of the completed prepreg tape.

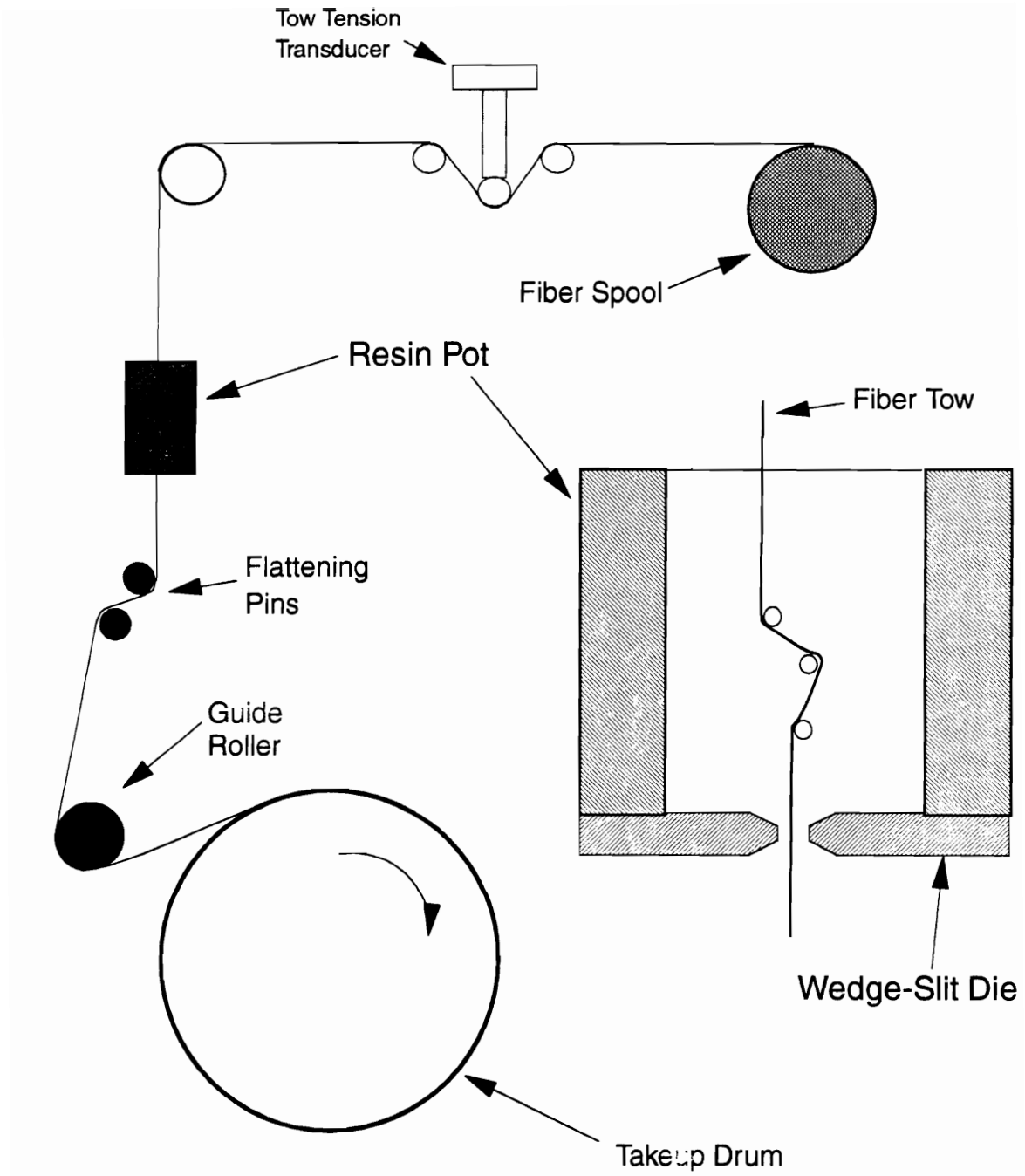

Figure 2.2 Schematic representation of Model 30 prepregger and resin pot.

With the above wedge-slit die, the need to overlap tows resulted in excessive prepreg tape thickness. Also, the minimum fiber volume fraction that could be attained with this die was about 57.5% which was perilously close to that desired in the composite of 60%. Hence new dies were manufactured to slit dimensions of 7.62 mm x 0.127 mm (0.3" x 0.005"). This change resulted in thinner prepreg and also provided wider processing margin by reducing minimum fiber volume fraction.

For prepregging with the toughened cyanate ester resin system, the resin pot was maintained at 104 °C. At this temperature the resin viscosity was sufficiently low to permit excellent wet-out of the fiber tow. In addition, the resin system exhibited a wide processing window at this temperature. The flattening pin and guide rollers were maintained at temperatures of 115 and 120 °C, respectively. The higher temperatures were necessary to maintain the resin in the tow in a liquid state as it was being place on the take-up drum.

The rotational speed of the drum controlled the residence time of a given section of the tow in the resin pot which also influences the degree of impregnation. High drum speeds tends to break the fragile fiber tow. The traverse speed of the drum adjusted relative to drum rotation determines the degree of overlap between successive tows. These parameters were selected such that prepreg tape with the desired resin content was successfully produced without tow breakage.

Finally, the resin mass fraction of each prepreg batch produced was determined by matrix digestion in accordance with ASTM D3171-76 Standard Test Method for Fiber Content of Resin-Matrix Composites by Matrix Digestion.

2.4 PROCESS DEVELOPMENT

In order to manufacture a composite panel from prepreg tape it is necessary to develop a process cycle to consolidate and fully cure the material. It is now widely known that experimental development of process cycles is both time consuming and expensive. Science based simulation models alleviate this problem.

A computer code based on mathematical models, CUREV1, developed by Loos and Springer [22] was used in this investigation to develop processing cycles for fabrication of composite laminates from the carbon fiber, toughened cyanate ester prepreg. A schematic diagram of the process simulation model CUREV1 is shown in Fig. 2.3. The important user inputs to the code include:

- geometry and the ply lay-up sequence of the laminate
- fiber/ matrix physical and thermal properties
- prepreg properties: resin mass fraction, fiber areal weight, ply thickness
- resin characterization data
- temperature/ pressure profile as a function of time

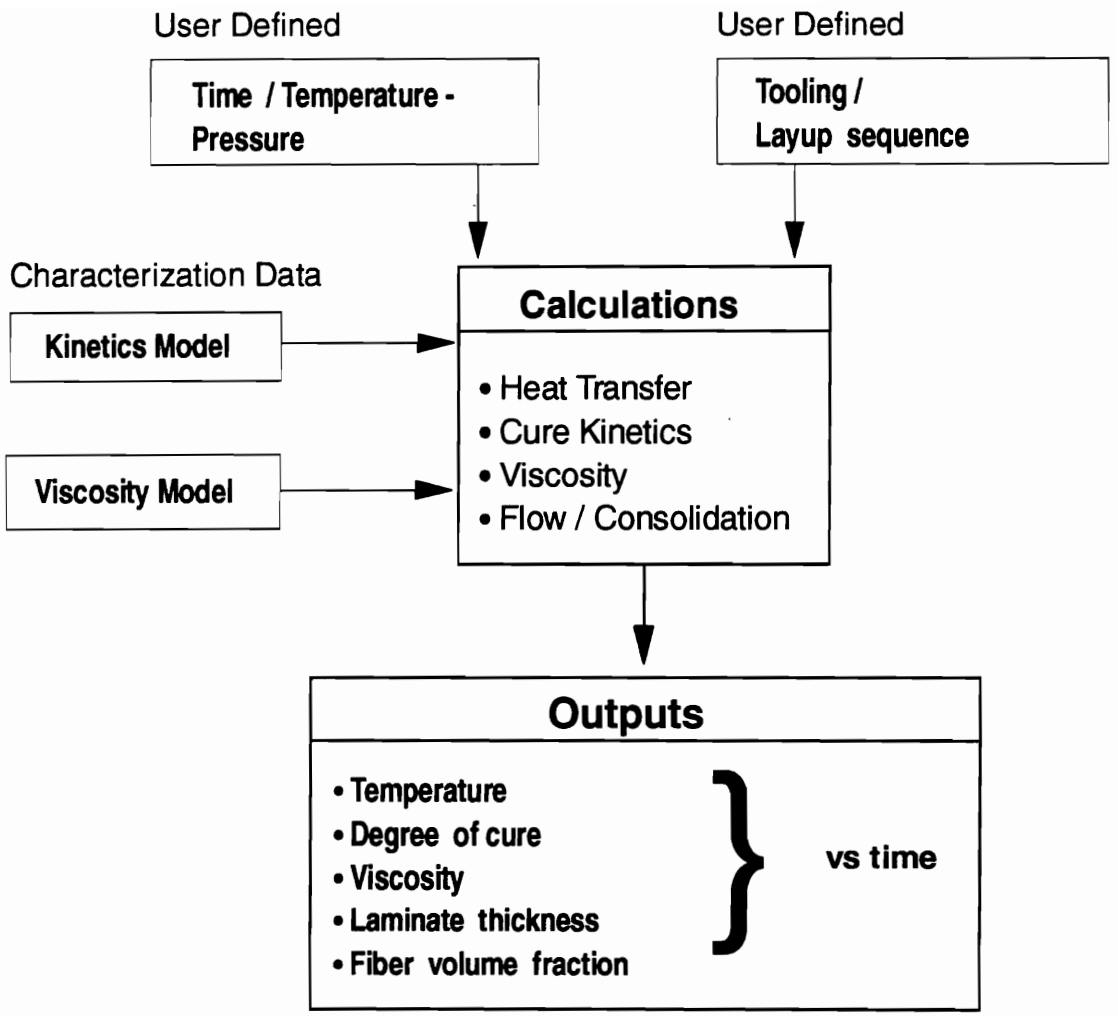

Figure 2.3 Schematic representation of CUREV1 process simulation model.

A typical time-temperature-pressure profile, also known as cure cycle, is shown in Fig. 2.4. This is an example of a two stage cure cycle, referring to the two temperature steps. Region 1, represents the initial heating-up or "ramp" at a constant rate up to a specified temperature, known as the hold temperature. At this temperature, represented by region 2 in the figure, the temperature is constant for a period of time. Usually, but not necessarily, at some instant during this hold the consolidation pressure is applied. In this example, the time of pressure application is indicated by t_p . At the end of the region 2 hold period, the temperature is increased at a constant heating rate (region 3) to a final cure temperature. Region 4 represents the high temperature hold wherein the composite is fully cured, followed by a cool down to ambient temperature. The rate of cooling in region 5 may be closely controlled, depending on the matrix material. The applied consolidation pressure is released during the cool down.

The consolidation pressure is applied in region 2 and is influenced by the initial hold temperature and the duration of hold. Also, proper choice of the time of application and the magnitude of pressure are critical to achieving the desired fiber volume fraction. Further, the choice of the region 4 temperature is based on the curing behavior of the resin. The temperature of the second hold must be sufficiently high in order to fully cure the resin. However, not so high as to cause devitrification and thermal degradation.

A user defined cure cycle, specifying the regions 1 to 4, forms an input to CUREV1. Using these inputs as boundary conditions, through-the-thickness heat transfer, resin flow, and consolidation analyses are performed by the simulation model.

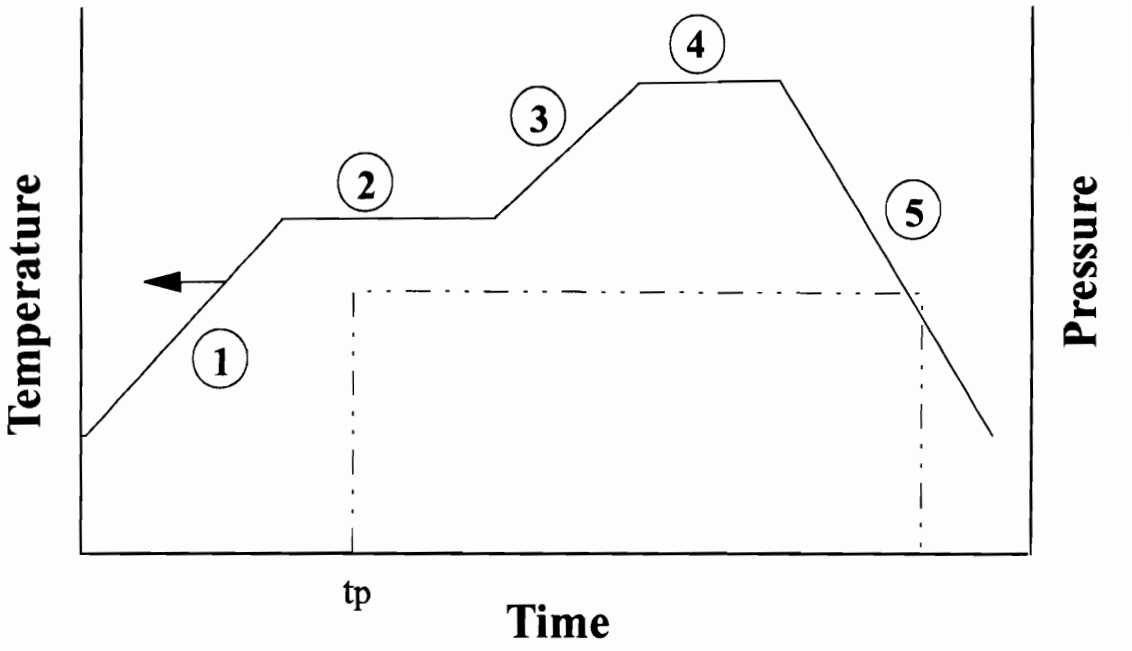

Figure 2.4 Example of a typical cure cycle showing different processing events.

The results of the simulation include the temperature and degree of cure distributions inside the composite over the entire cure cycle. Also, laminate thickness and the fiber volume fraction as a function of time are obtained.

This study, part of a larger multidisciplinary research effort on the toughened cyanate ester resin system, drew information from work of other researcher in the group. The cure cycle development for composite manufacture was based on investigations of Brown, et. al. [10,15]. The research work performed by Brown involved the development of controlled morphologies in the toughened resin system by in-situ cure monitoring using Fourier Transform Near Infrared (FTNIR) spectroscopy. In this work, different phase-separated morphologies were developed in neat resin samples by varying both the temperature and the duration of the initial hold (region 2 in fig. 3.4). The duration of the hold was specified in terms of the time required to achieve a specified degree of cure of the resin.

Based on the above mentioned study, a temperature of 150 °C was selected for the initial hold. The duration of the hold at 150 °C was determined by the simulation model, using the cure kinetics submodel. Two cases were investigated. One with a hold period such that the degree of cure at the beginning of region 3 (in Fig. 2.4) was 0.3 (or 30%) and the other with the same hold temperature but the period extended to achieve a degree of cure of 0.6 (60%) at the beginning of region 3. The heating rates in regions 1 and 3 were set at 2.0 °C/min. The final cure temperature and the duration of hold at this

temperature was governed by the cure kinetics. Thus, CUREV1 was used to obtain the cure cycle.

Process cycles for the manufacture of 8-ply unidirectional and 16-ply quasi-isotropic composite laminates on a hot-platen press were generated by the model. The cure cycle was required to yield a nominal fiber volume fraction of 0.6 (60 %) and a final degree of cure in excess of 0.98 (98%) in the composite.

2.5 COMPOSITE LAMINATE MANUFACTURE

2.5.1 Process Control System

The effort of process simulation and cure cycle development would be rendered futile if the model prescribed conditions are not implicitly adhered to during the actual manufacture of composite laminates. Therefore, accuracy of model predictions can be verified only if the process control equipment is capable of faithfully executing the specified cure cycle. A computer controlled process control system was built around a hot-platen press toward this end.

The model generated cure cycle was programmed into the control software of the hot-platen press. Also, the process variables associated with the laminate manufacture were acquired in real time and stored. The data include the programmed temperature cycle, the platen temperatures, applied consolidation pressure, and mold temperature. A

type-J thermocouple placed within the mold provided the signal for mold temperature measurement. After the completion of the cure cycle, the computer data file was read into a spreadsheet software for reference and analysis.

2.5.2 Composite Laminate Manufacture

Two different steel molds were used in the laminate manufacture depending on the desired size of the laminate. Figure 2.5 shows the details of the mold construction. The two molds were similar in construction and differed only in dimensions. Both molds had a provision to insert a thermocouple, for temperature measurement, into the mold cavity. The molds were prepared for laminate manufacture by first disassembling and cleaning all surfaces thoroughly. A coat of a release agent (Miller-Stephenson MS-136/CO2) was then sprayed on all the mold surfaces. The mold sides were then assembled and fastened to the mold bottom plate with screws coated with an anti-seize compound (DOW CORNING® 1000 Anti-seize paste). 8-ply unidirectional and 16-ply quasi-isotropic $[\pm 45°/0°/90°]_{2s}$ composite laminates were manufactured in this investigation. The unidirectional panels were manufactured in a 76.2 mm x 76.2 mm square mold and the quasi-isotropic panel was manufactured in a 152.4 mm x 152.4 mm mold.

In either case, with the mold top plate as a template, the AS4 carbon fiber/toughened resin prepreg was cut using a razor blade in the desired ply orientation.

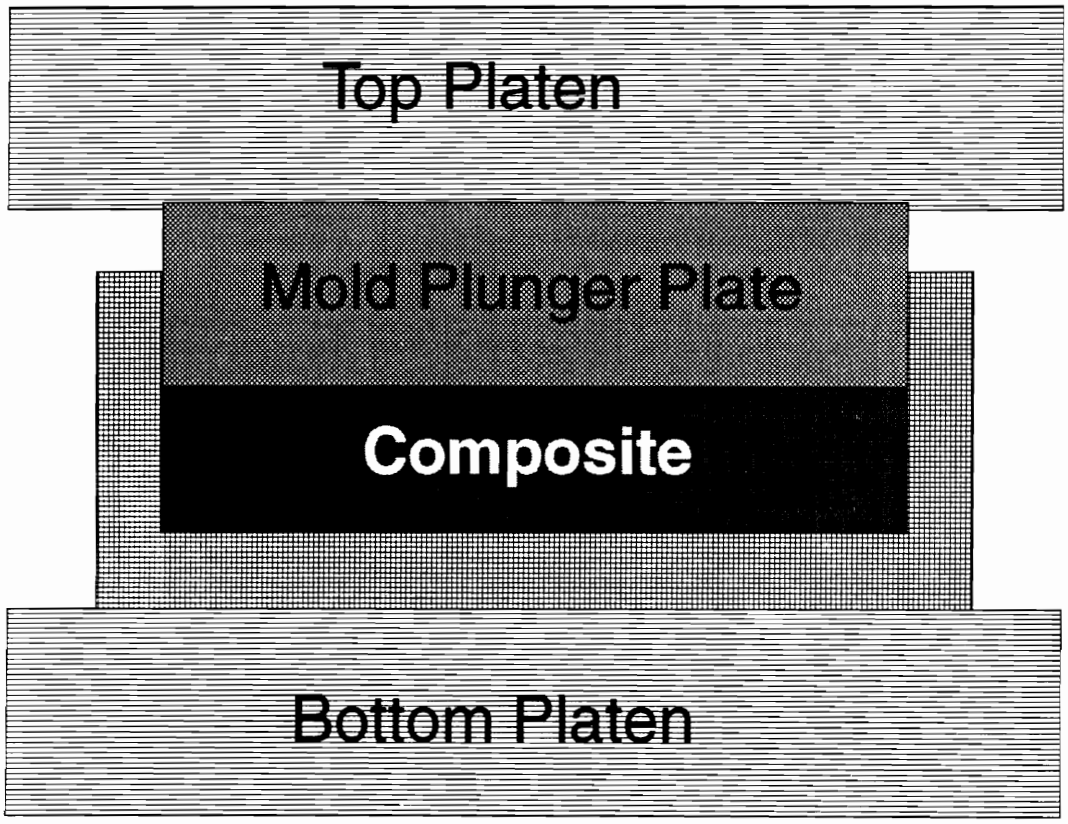

Figure 2.5 Schematic of metal mold for composite manufacture in a hot-platen press.

To prevent sticking of the composite laminate to the mold surfaces, two pieces of Teflon™ release cloth were cut to the same dimensions as the prepreg plies. One Teflon™ release cloth was placed between the bottom mold surface and the prepreg plies and the other was placed on top of the prepreg ply stack, before installing the mold top plate. A type-J thermocouple was inserted into the mold cavity through a slot provided in the mold.

The assembled mold was then placed between the platens of the computer controlled press. The mold thermocouple was then connected to an appropriate terminal of the data acquisition system. A glass fabric skirt was placed around the mold, between the platens to minimize heat loss. Then, a computer program file containing the cure cycle information was loaded into the control software and the manufacture was started. During processing, operator intervention was not required, except to apply the desired consolidation pressure at the time specified by the process simulation model.

At the end of the process cycle, the platens and the mold were cooled down to ambient temperature and the laminate was removed from the mold. Resin flash bled out of the panel, but retained within the mold cavity, was carefully collected and identified along with the respective panels for later use in testing.

2.6 PHYSICAL AND MECHANICAL TESTING

2.6.1 Physical Testing

In order to evaluate the quality of the toughened cyanate ester composite laminates manufactured, physical testing was performed. First, the laminates were nondestructively examined by the ultrasonic C-scan technique. The instrument available at Virginia Tech is a reflective ultrasonic scanner. A transducer designed to operate at a frequency of 10 MHz was used.

To estimate the composite fiber volume fraction, a method based on measurement of density as specified by BASF product development specification no. CS-200-T was employed. The procedure involved is similar to that in ASTM D 792-86. The ASTM test method is for measuring the density of plastics by displacement of a liquid. Following the BASF procedure, the composite density is measured, and then by using the rule of mixtures, the fiber volume fraction is estimated. This procedure also requires the density of the constituents. The density of the matrix resin was measured and density of the carbon fiber as reported by the manufacturer was used.

2.6.2 Microscopy

Specimens from both the unidirectional and the quasi-isotropic panels were machined from the laminates for optical microscopy. The machined specimens were

encapsulated in an epoxy potting resin (Buehler). The potted specimen were then polished, first on emery cloth and then on a polishing wheel with alumina powder. The polished specimens were observed for manufacturing related flaws under a Nikon optical microscope at different magnifications. Representative areas of the specimen were then photographed.

The flash resin obtained from the unidirectional laminate manufacture (Section 2.5.2) was analyzed by transmission electron microscopy (TEM). The objective of this analysis was to detect the phase-separated morphology in the flash resin, which had also been subjected to the same thermal cure cycle as the composite. The resin samples were microtomed and stained with ruthenium oxide to enhance the contrast between the thermoset and the thermoplastic phases. TEM photomicrographs were then produced of the morphologies considered most representative of the specimen.

2.6.3 Iosipescu Shear Testing

The unidirectional laminates were machined for 90° Iosipescu shear testing on a modified Wyoming fixture. The test specimen geometry used is as shown in Fig. 2.6. Three test specimens were obtained from each of the 76 mm x 76 mm unidirectional laminates. Precision strain gages, type CEA-13-250UW-350 from Measurements Group, Inc., Raleigh, North Carolina, were bonded to both surfaces of the test specimen, midway between the notch roots.

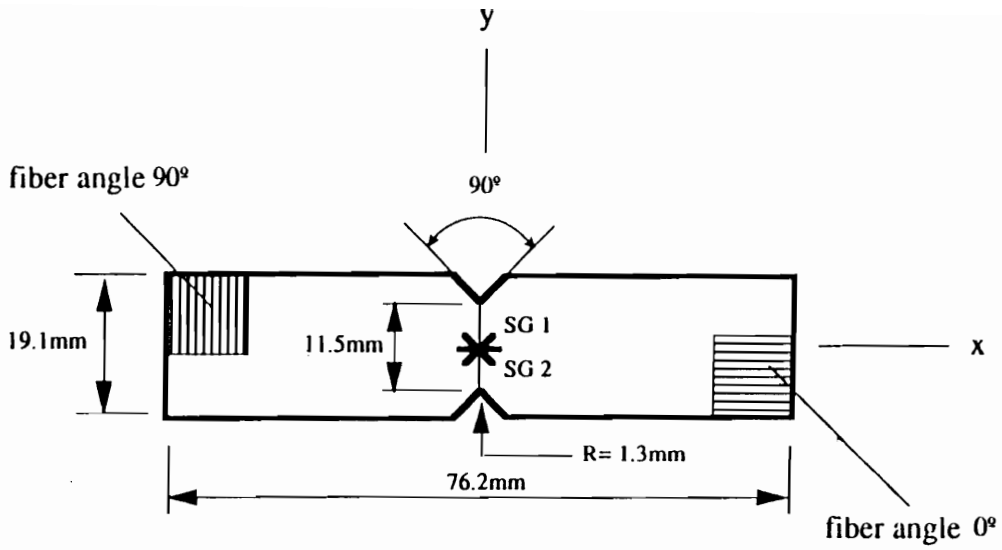

Figure 2.6 Geometry and dimensions of the Iosipescu shear test specimen.

The specimen were then tested on an Instron testing machine. Load and strain data during the test were acquired and collected in real time on a IBM PC based data acquisition system. The load-strain data were then converted to shear stress-strain data. The data were then fit to a fourth order polynomial with strain data as the dependent variable. The initial shear modulus, the shear strength, and the strain at failure were obtained as a result of the data reduction. For each specimen, the strain outputs from the two strain gages were averaged, provided there were no spurious signals from any of the gages during testing.

2.6.4 Gas Gun Impact Testing

Evaluation of impact damage properties of the carbon fiber/ toughened cyanate ester composite material was performed on an impact testing instrument developed at Virginia Tech by Morton and co-workers. The details of the development of this test procedure and equipment are described by Teh [23]. Figure 2.7 shows a schematic representation the gas-gun impact testing apparatus. In this test, a 35 g plastic impactor with a steel nose is loaded in the gun barrel. The impactor is then shot at the test specimen placed at a short distance away from the end of the gun barrel. The velocity of the impactor is measured by a light gate arrangement. Different impactor velocities can be attained by varying the nitrogen gas pressure and/or the initial position of the impactor in the gun barrel.

The 152 mm x 152 mm quasi-isotropic composite laminate was used in the impact damage evaluation. The panel was machined into four 76 mm x 76 mm test specimens. This test procedure calls for a minimum of four specimens. The four specimens are impacted at different velocities and the damage areas are then measured by ultrasonic C-scan. Then, the damage area is plotted as a function of the incident velocity of the impactor. Fig. 2.8 shows a typical plot of damage area versus incident impact velocity [23]. The two parameters defining the impact damage resistance of the composite are obtained by fitting a linear least squares curve through the data points. The x-axis intercept of the regression line yields the critical velocity to initiate damage, Vc (ms^{-1}), in the material. The slope of the line yields the parameter C (mm^2/ms^{-1}) which is a measure of the rate of damage growth with increasing impact velocity.

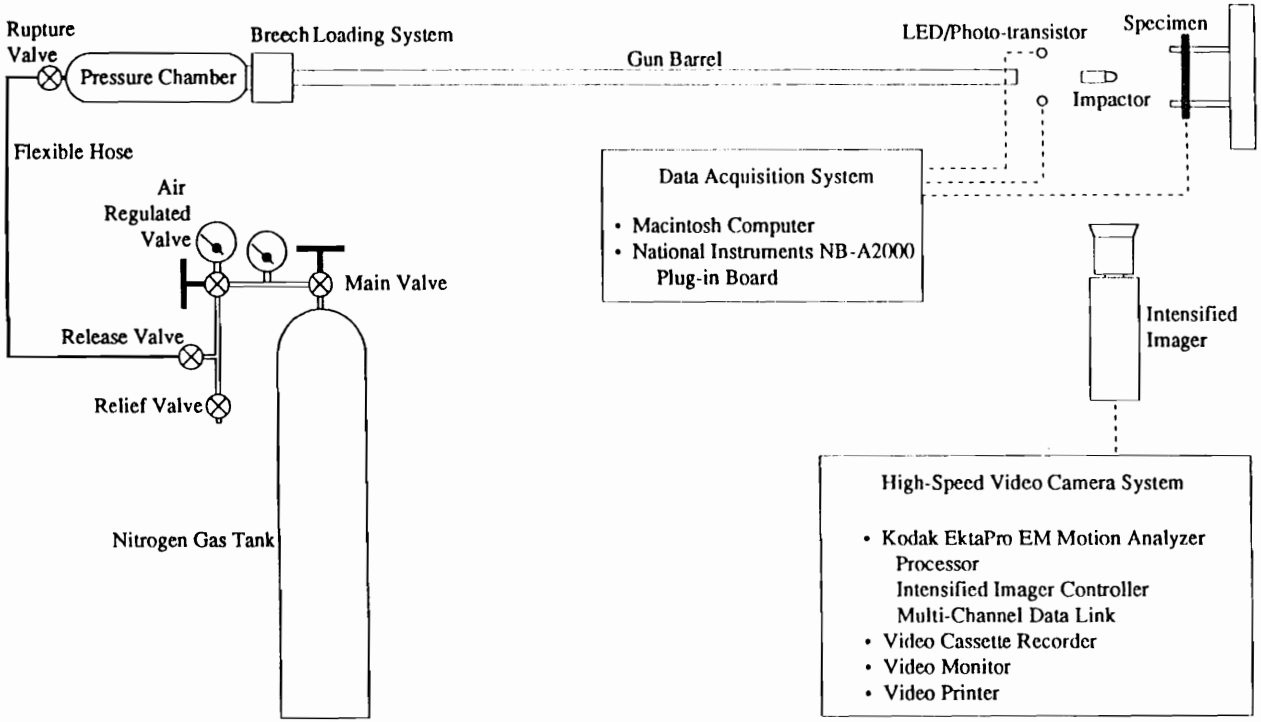

Figure 2.7 Schematic representation of the gas gun impact test facility at Virginia Tech (from Teh [23]).

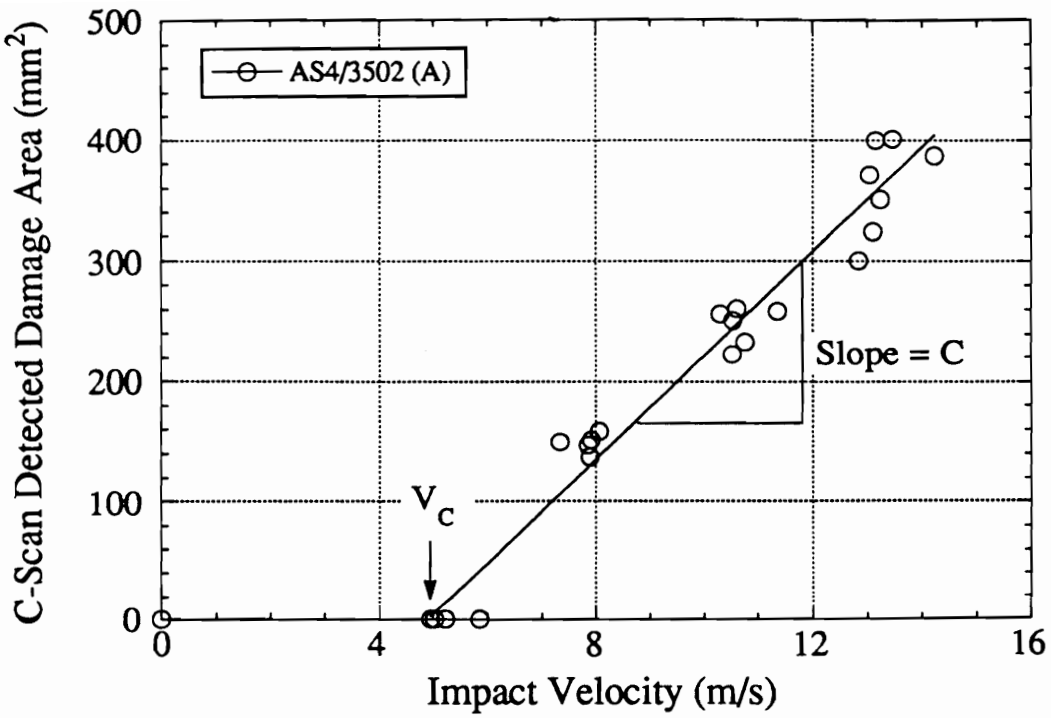

Figure 2.8 Typical plot of impact damage area as a function of impact velocity showing the parameters determined [23].

2.7 RESULTS AND DISCUSSIONS

2.7.1 Resin Characterization

The isothermal DSC measured curing behavior, represented by the cure reaction rate as a function of degree of cure at four different temperatures 140, 150, 160, and 180 °C are shown in Fig 2.9 (top) and (bottom) and Fig. 2.10 (top) and (bottom), respectively. A two part cure kinetics model of the following form was used to describe the curing behavior,

$$\frac{d\alpha}{dt} = (k_1 + k_2\,\alpha^m)\,(1-\alpha)^{n_1} \quad ;\ \alpha < \alpha_d \tag{2.2}$$

$$\frac{d\alpha}{dt} = k_3\,(\alpha_p-\alpha)^{n_2} \quad ;\ \alpha \geq \alpha_d \tag{2.3}$$

where, the reaction rate constants k_i were described by an Arrhenius type expression as follows

$$k_i = A_i\, e^{-\frac{E_i}{RT}}, \qquad i = 1\text{-}3 \tag{2.4}$$

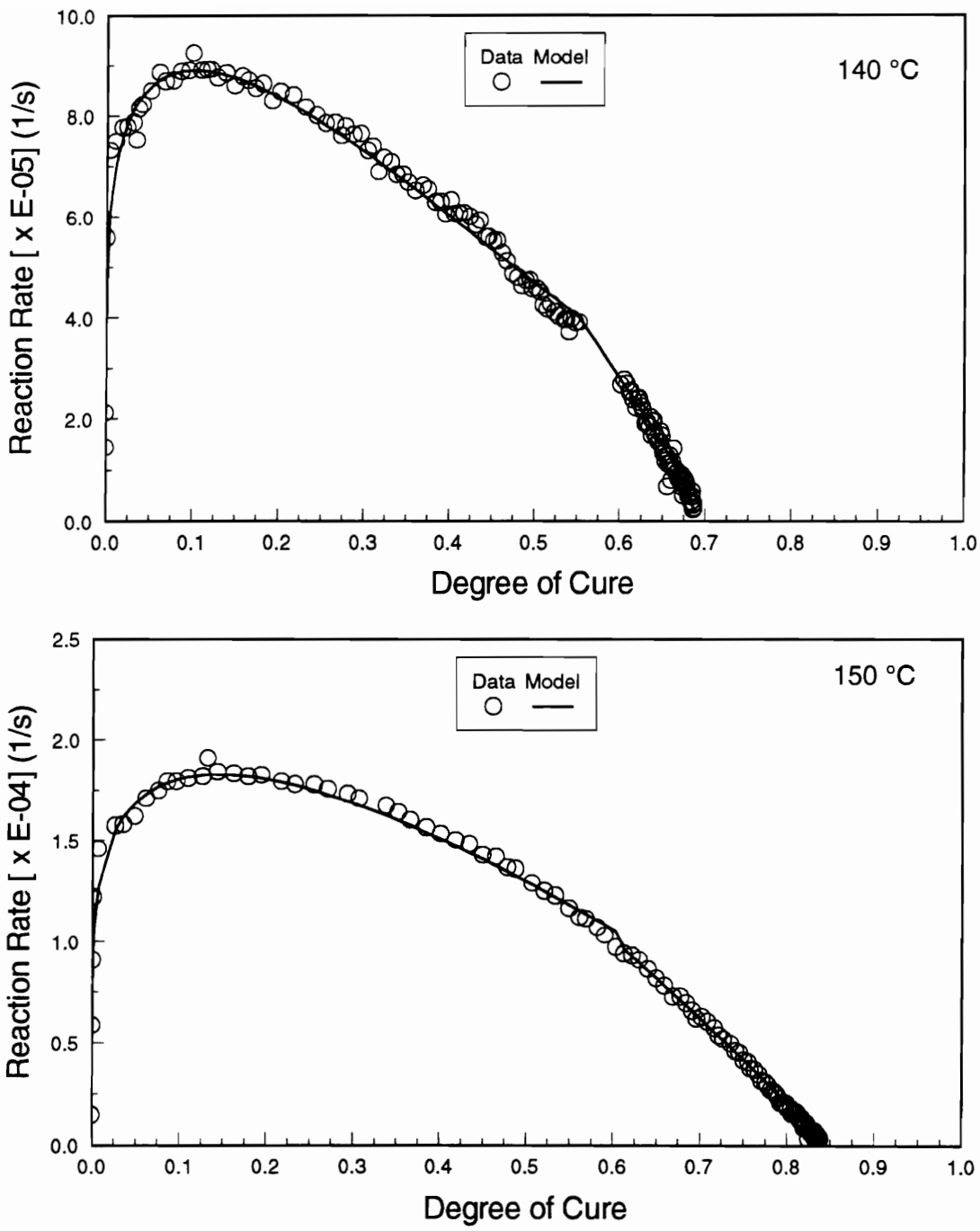

Figure 2.9 Measured and model generated reaction rate as a function of conversion. 140 °C (top) and 150 °C (bottom).

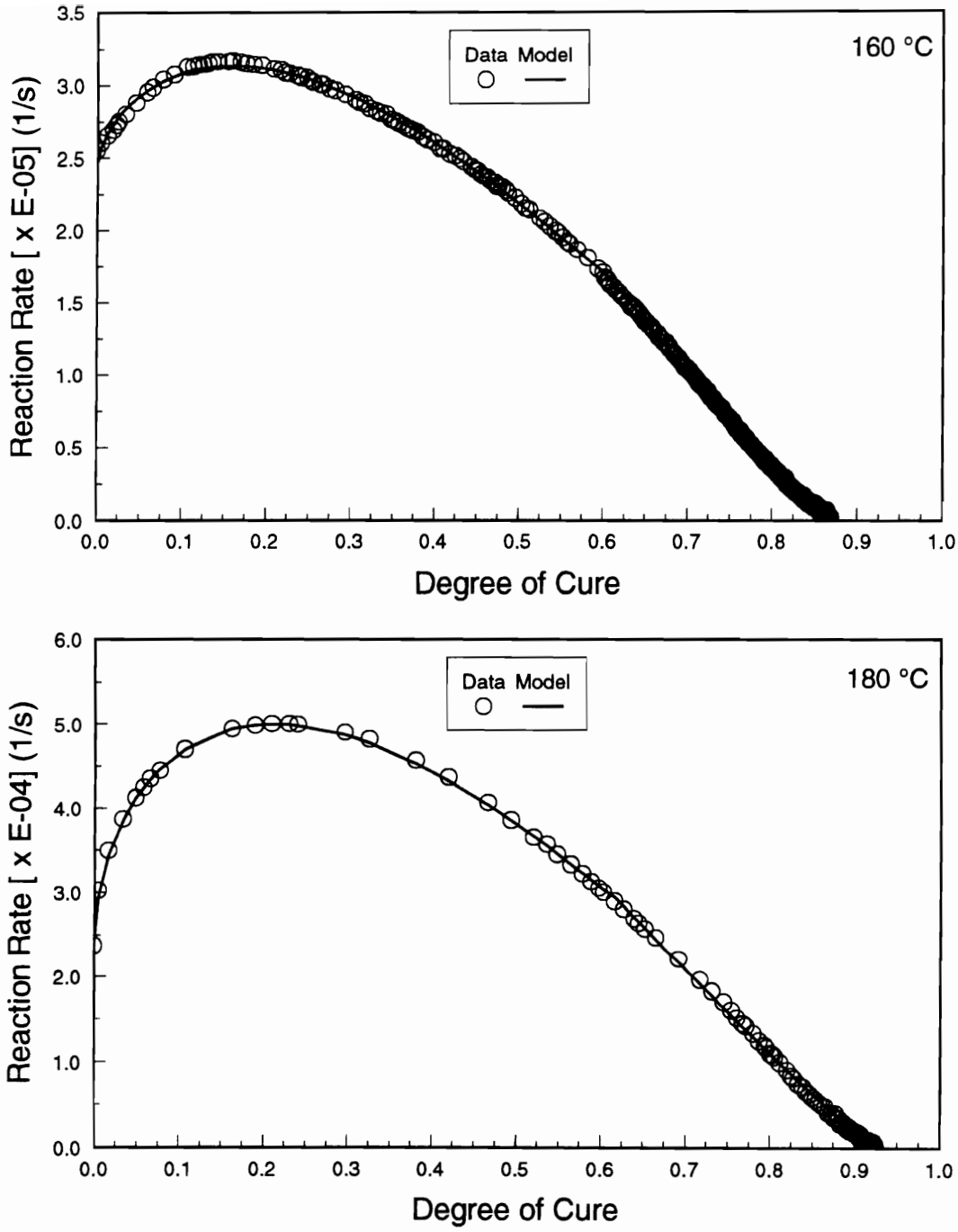

Figure 2.10 Measured and model generated reaction rate as a function of conversion. 160 °C (top) and 180 °C (bottom).

The parameters A_i and E_i were determined by constructing an Arrhenius plot and measuring the intercept and the slope of a linear regression curve fit to the data. The Arrhenius plot for rate constants k_1 and k_2 is shown in Fig. 2.11(top) and that for k_3 in Fig. 2.11(bottom). Further, in equations 2.2 and 2.3, α_d is onset of diffusion control, chosen as 0.6 in this case. The onset of diffusion control occurs as the T_g of the curing resin system approaches the isothermal cure temperature. Due to decreasing molecular mobility in the cross-linked network, the reaction rate decreases. Thus, at a given isothermal temperature, there is maximum degree of cure that cannot be exceeded, at which point the reaction stops altogether. In eq. (2.3), α_p represents this maximum degree of cure or plateau conversion. An increase in temperature above the isothermal cure temperature is necessary to increase the molecular mobility and hence resume the cure reaction [24-26,28]. An empirical model of this form was proposed by Chen and Macosko [27]. For instance, the toughened cyanate resin system exhibits a plateau conversion of 0.84 at 150 °C. The plateau conversion is represented in the form $\alpha_p = A + BT$, where the constants A and B determined by a linear least squares regression fit to the data. The values of the constants were A = -0.336, and B = 2.78E-03, for the temperature, T, specified in the Kelvin scale.

Fig. 2.12 shows the measured and model predicted conversion as a function of time at the four DSC isothermal scan temperatures.

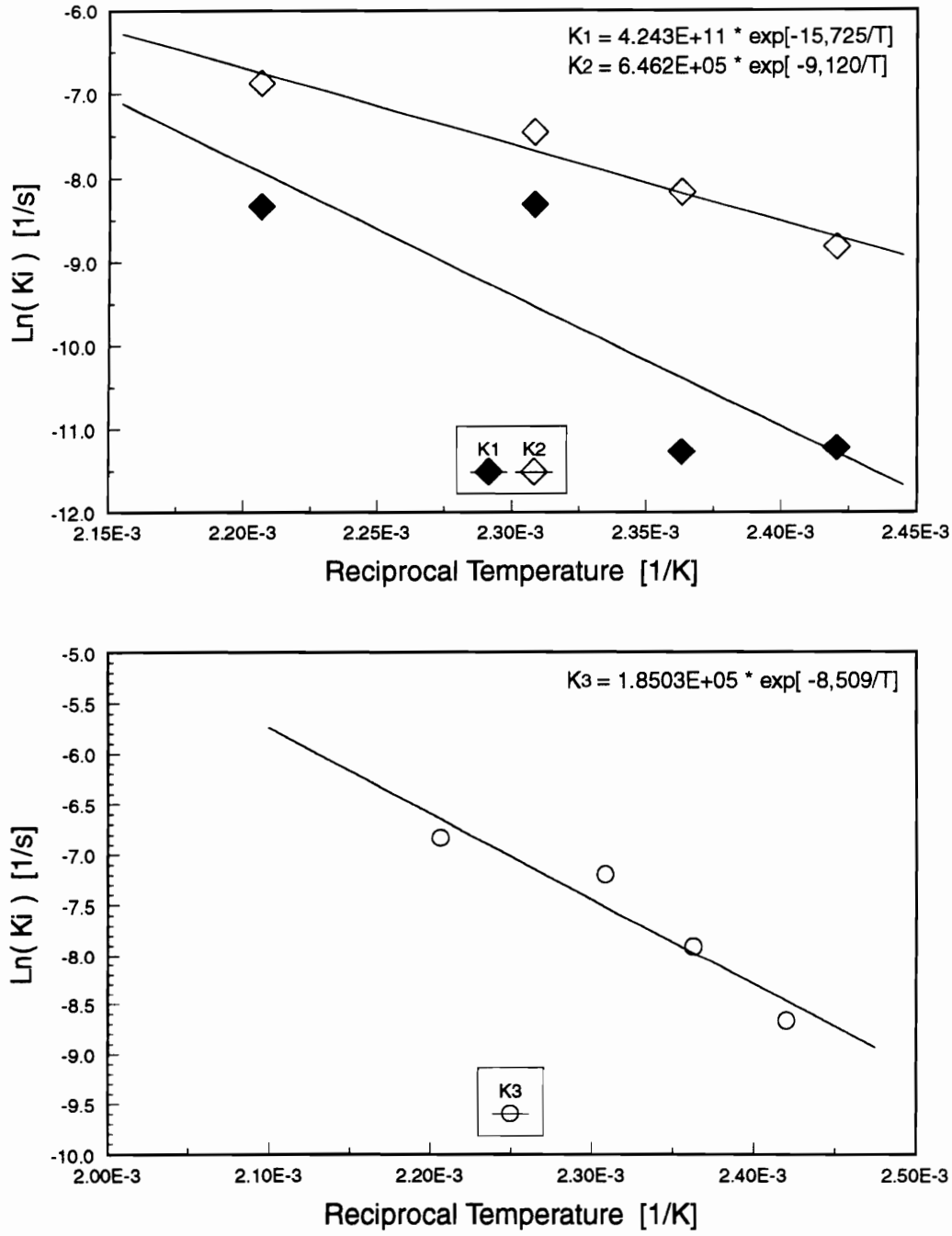

Figure 2.11 Arrhenius plots of the reaction rate constants for cure kinetics model. Rate constants k_1 and k_2 in the kinetic controlled region (top). Rate constant k_3 in the diffusion controlled region (bottom).

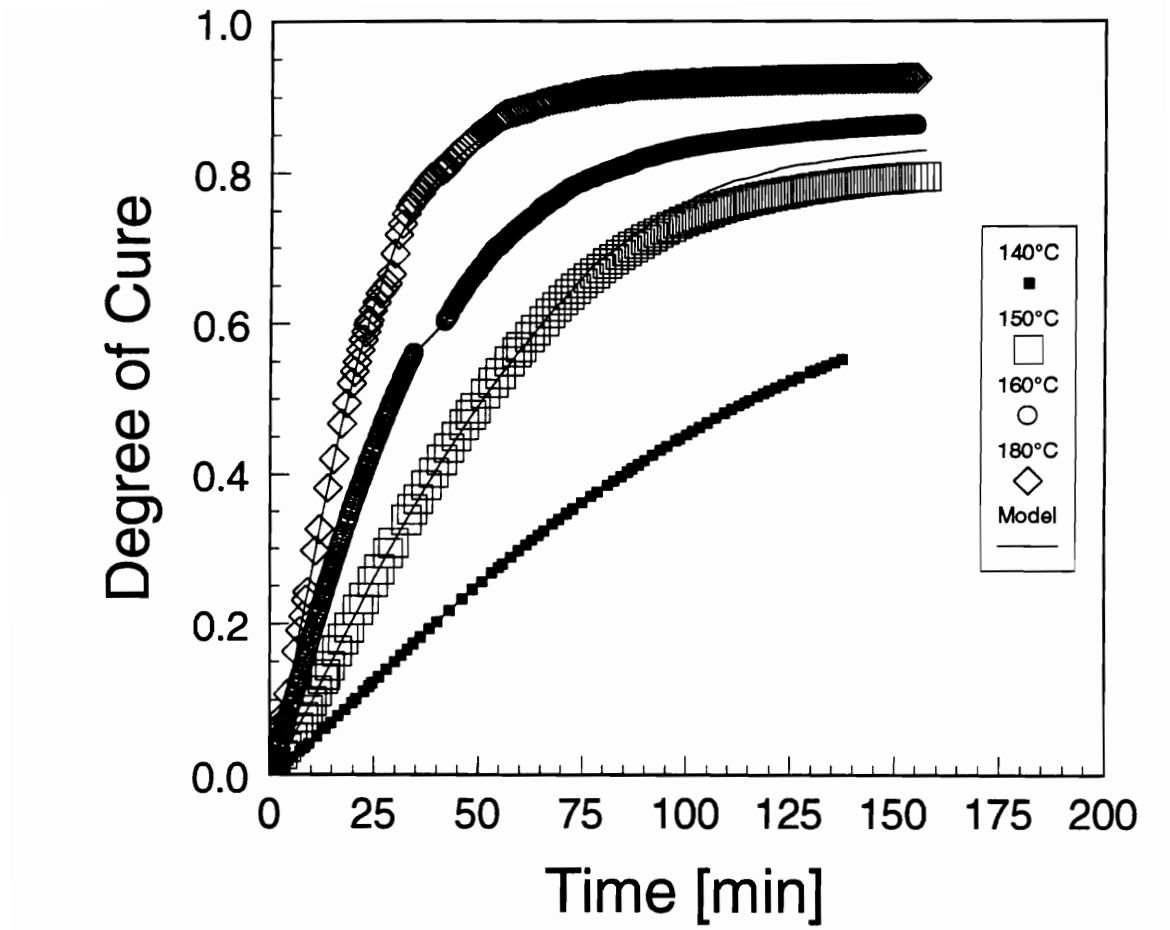

Figure 2.12 Measured and model generated conversion as a function of time at different isothermal cure temperatures for the toughened cyanate ester resin system.

In order to characterize the viscosity behavior of the toughened cyanate ester resin system, isothermal viscosity measurements were performed at three different temperatures, 140, 150, and 160 °C on a Bohlin rheometer. The measured resin viscosity as a function of time at these temperatures is shown in Fig. 2.13. The viscosity data indicate a typical thermoset behavior. The resin viscosity, initially low in the uncured state, builds up rapidly to gel. With increasing temperature, this rapid increase in viscosity occurs at earlier times. The viscosity time data was converted to viscosity-conversion data using the cure kinetics model.

The data were then fitted to an empirical chemorheological model proposed by Castro and Macosko [19]. Eq. (2.5) shows the form of the model which correlates the resin viscosity to both, temperature and conversion

$$\mu(\alpha,T) = \mu_o \left(\frac{\alpha_g}{\alpha_g - \alpha}\right)^{f(\alpha)} \tag{2.5}$$

where, α_g is the gel point conversion, and $f(\alpha) = A + B\alpha$.

The initial viscosity term, μ_0, is expressed in terms of temperature by an Arrhenius type expression,

$$\mu_o = A_\mu e^{\frac{E_\mu}{RT}} \tag{2.6}$$

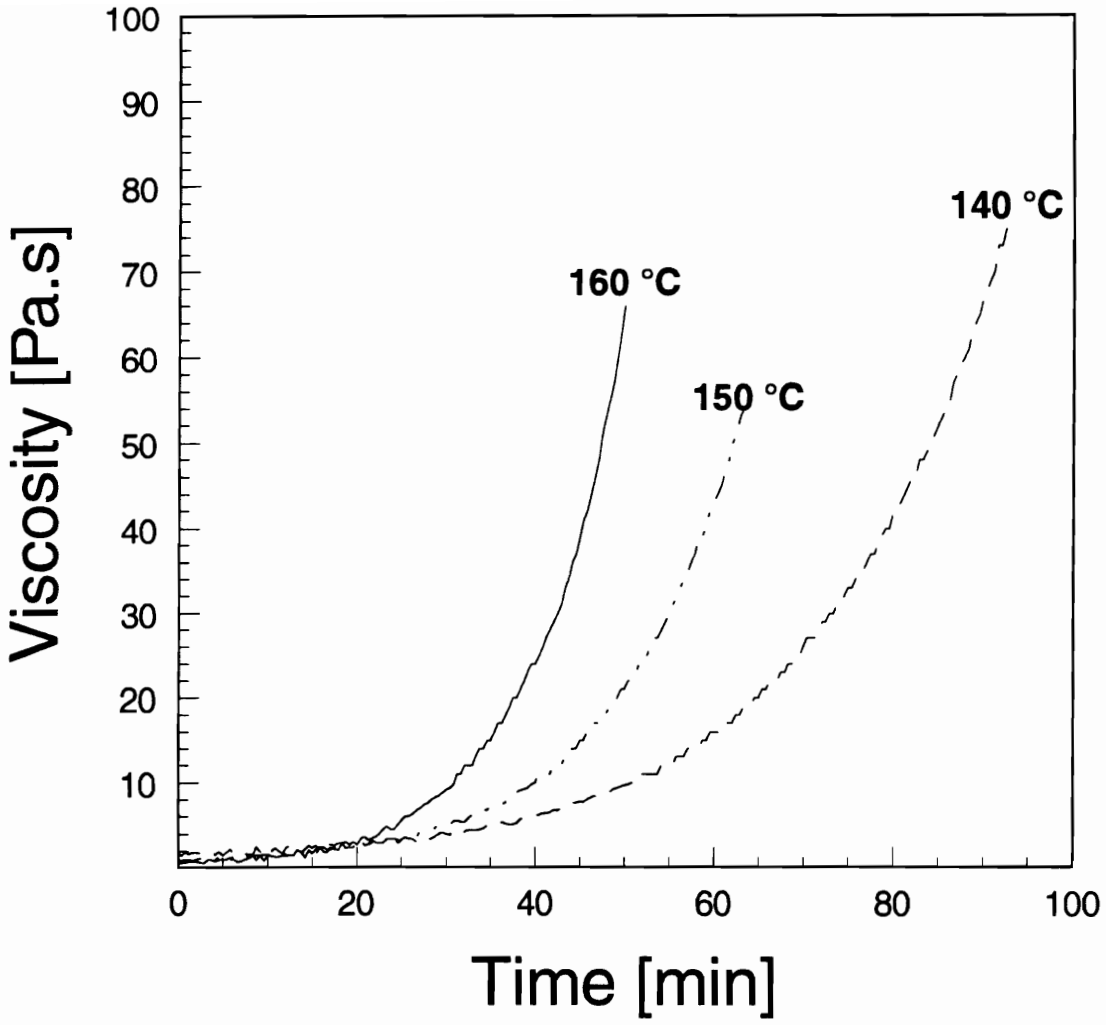

Figure 2.13 Measured viscosity as a function of time at different isothermal temperatures for the toughened cyanate ester resin system.

where, A_μ and E_μ are parameters determined by constructing an Arrhenius plot and measuring the intercept and the slope of a linear regression curve fit to the μ_o versus temperature data. First, the isothermal viscosity-conversion data were fit to eq. (2.5) and μ_0, α_g, A, and B were determined. Then, the initial viscosity from each data set was fit to eq. (2.6). The parameters A_μ, and E_μ, were obtained as a result. Fig. (2.14) shows the plot of the natural logarithm of μ_0 data versus reciprocal temperature [K^{-1}]. Plots comparing the measured data and model generated viscosity-conversion profiles for each of the isothermal temperatures, 140, 150, and 160 °C are shown in Figures 2.15 - 2.17, respectively.

In order to provide a rapid method of viscosity characterization, perhaps for use in preliminary evaluations, a simplified model is proposed. The proposed model is analogous to the Castro-Macosko model but does not require the correlation to the degree of cure. The form of the model is as follows:

$$\mu(t, T) = \mu_o \left(\frac{t_g}{t_g - t}\right)^{f(T)} \qquad (2.7)$$

Here, viscosity is expressed only in terms of time and temperature. Comparing eqs (3.5) and (3.7), it is seen that the term α_g, representing conversion at gel point, is replaced by the parameter t_g, which may be considered the "time-to-gel". Also, the exponent $f(\alpha)$, a function of conversion, has been replaced by f(T), a function of

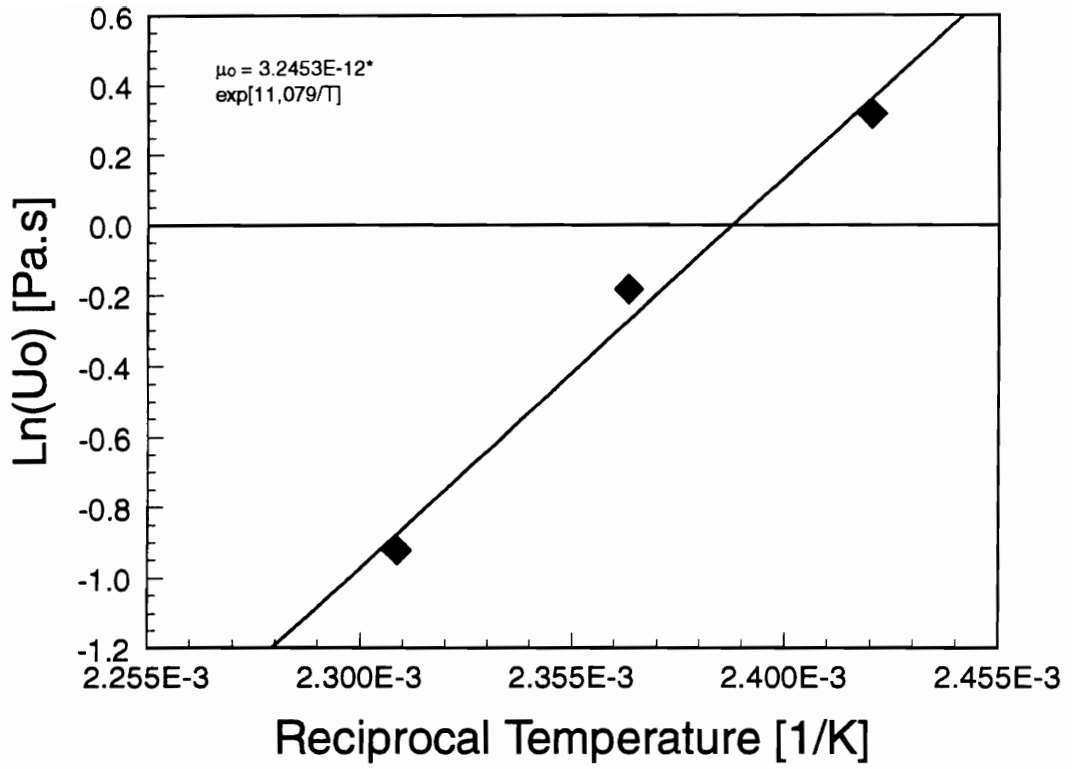

Figure 2.14 Arrhenius plot showing the temperature dependence of initial viscosity for the Castro-Macosko model.

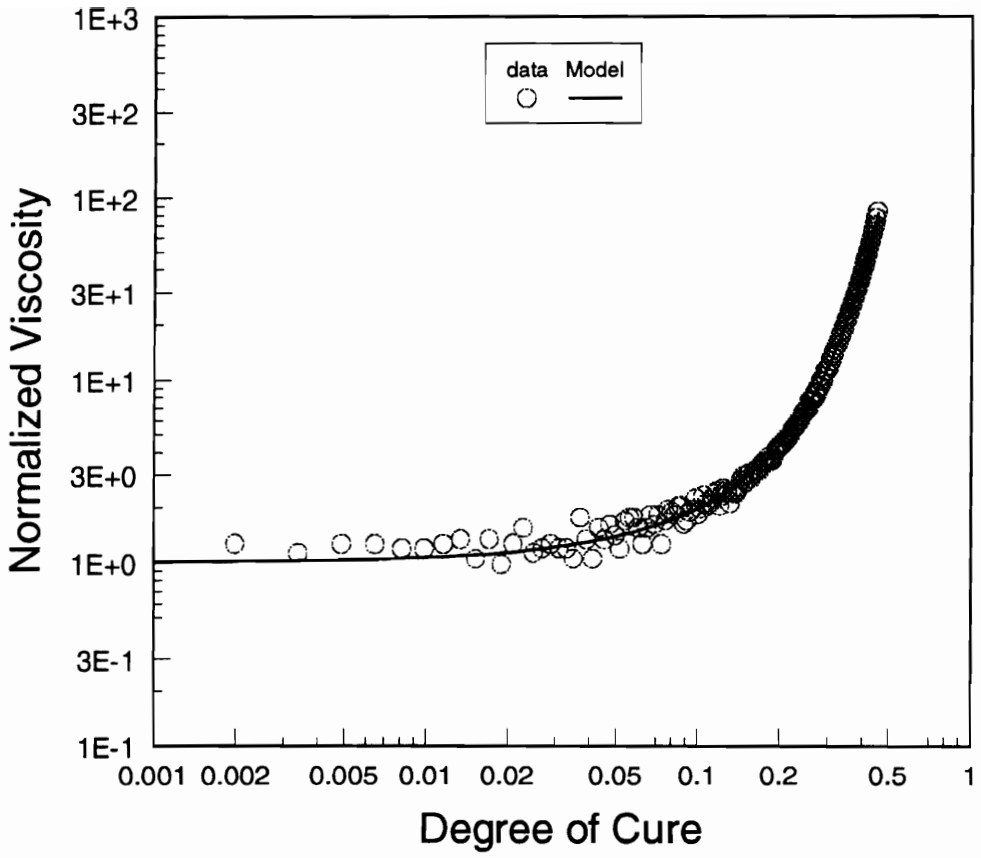

Figure 2.15 Measured and model predicted viscosity as a function of degree of cure (at 140 °C) for the toughened cyanate ester resin system.

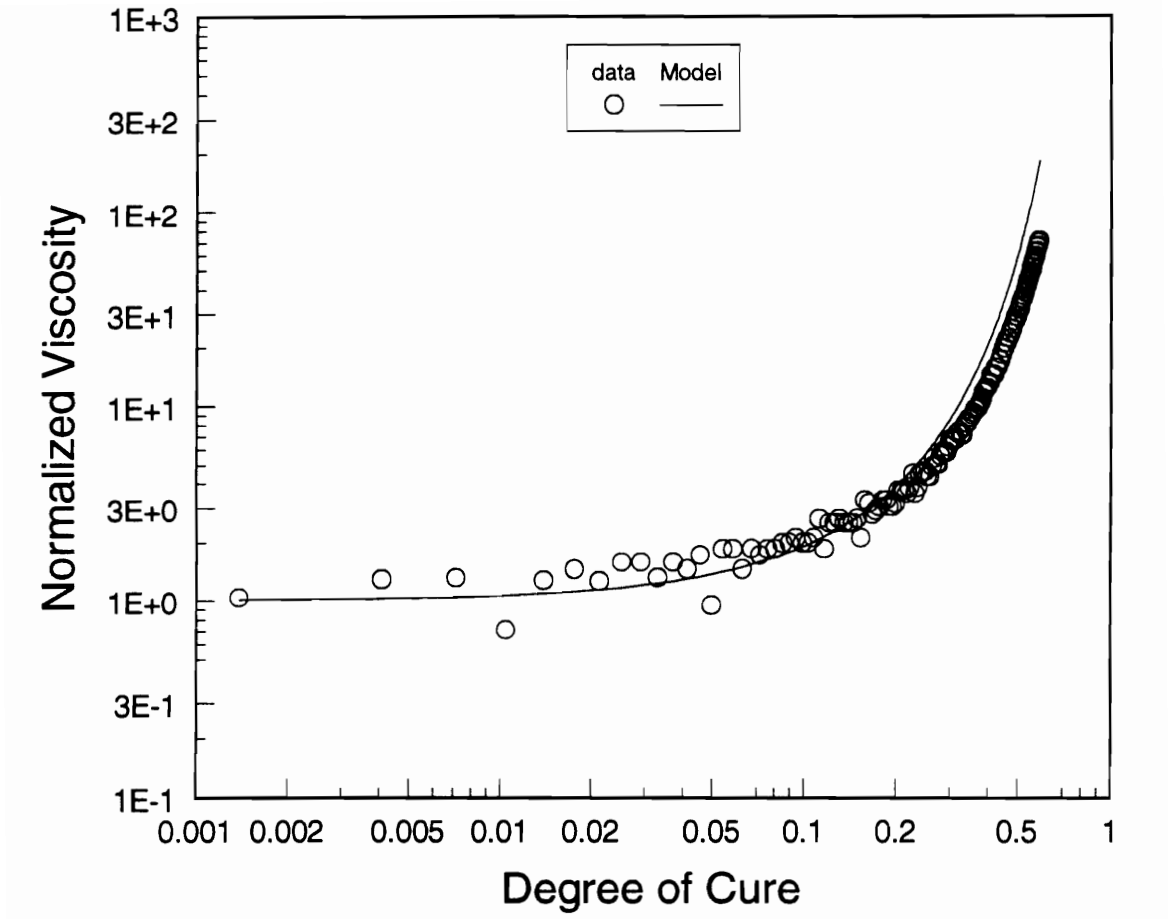

Figure 2.16 Measured and model predicted viscosity as a function of degree of cure (at 150 °C) for the toughened cyanate ester resin system.

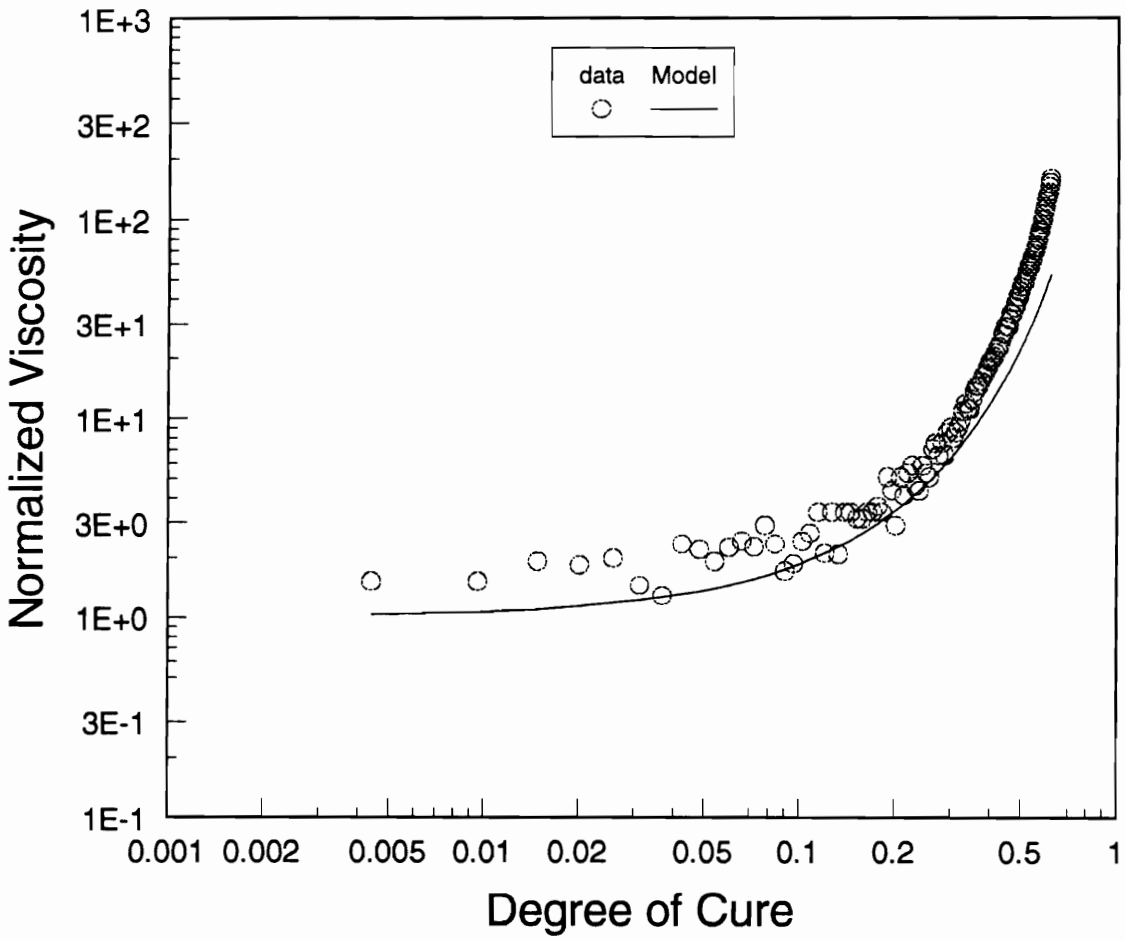

Figure 2.17 Measured and model predicted viscosity as a function of degree of cure (at 160 °C) for the toughened cyanate ester resin system.

temperature. The exponent is expressed as $f(T) = p + qT$, where p and q are parameters and the temperature is expressed in Kelvin. The initial viscosity term, however, is given by the same Arrhenius type expression as in eq. (2.6). The temperature dependence of μ_g and t_g are shown in Fig. 2.18 (top) and bottom, respectively. The plot show good correlation to the Arrhenius form expression for both, the initial viscosity and the "time-to-gel" data. Fig. (2.19) shows the comparison between the measured and model generated (eq. 3.7) viscosity-time profiles at the three isothermal temperatures 140, 150, and 160 °C. Although there is a good agreement between the data and the model predictions, the limitations of this model must be recognized. Caution should be exercised in using such a model for process simulation because this model does not take into consideration the initial state of cure of the resin. In carrying through from simulation to actual manufacture, the state of cure of the resin system must be identical to that used in viscosity measurements. Failure to ensure this can lead to significant discrepancy between predicted and actual behavior.

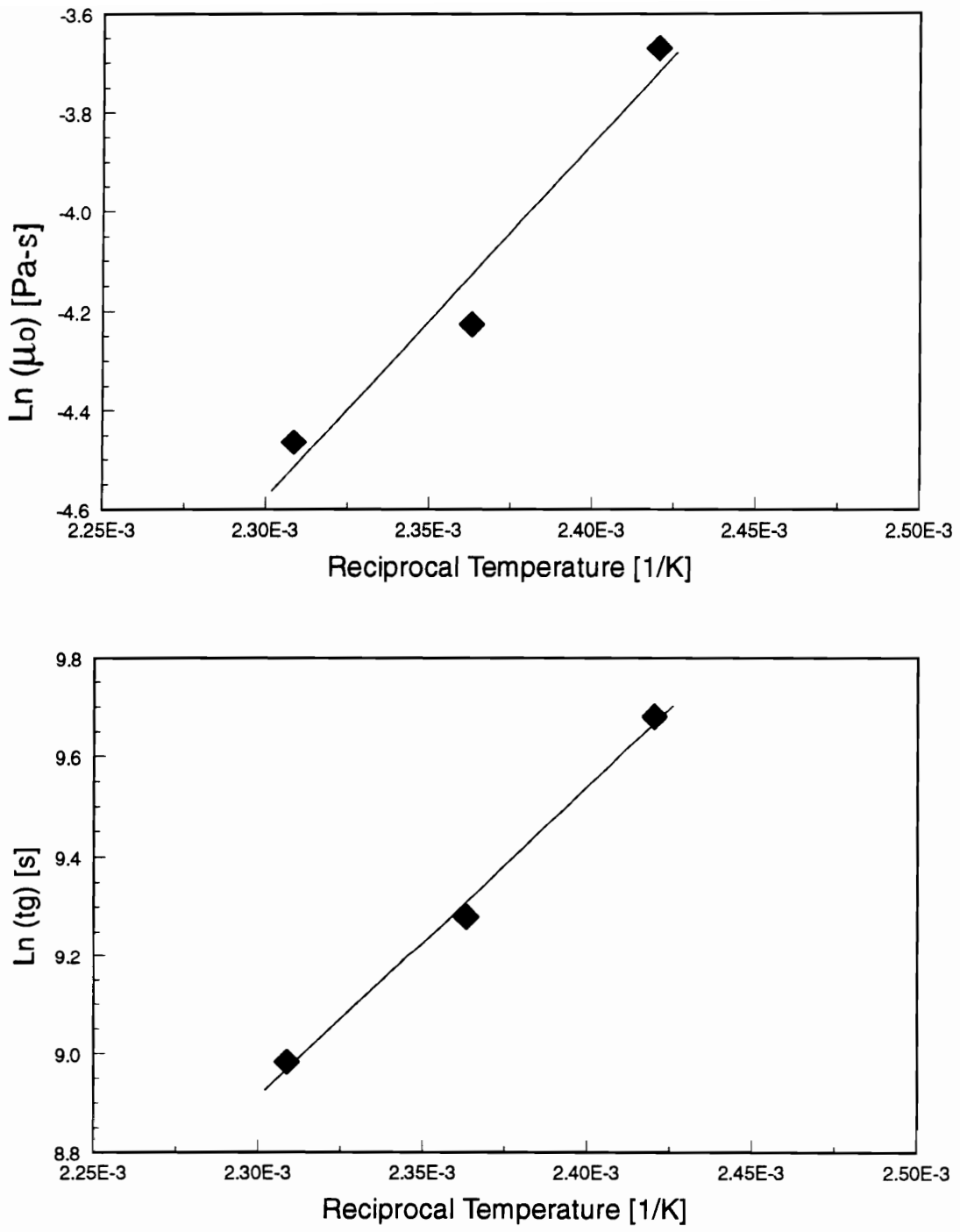

Figure 2.18 Temperature dependence of the initial viscosity, μ_o (top), and 'time-to-gel', t_g (bottom), for the proposed model.

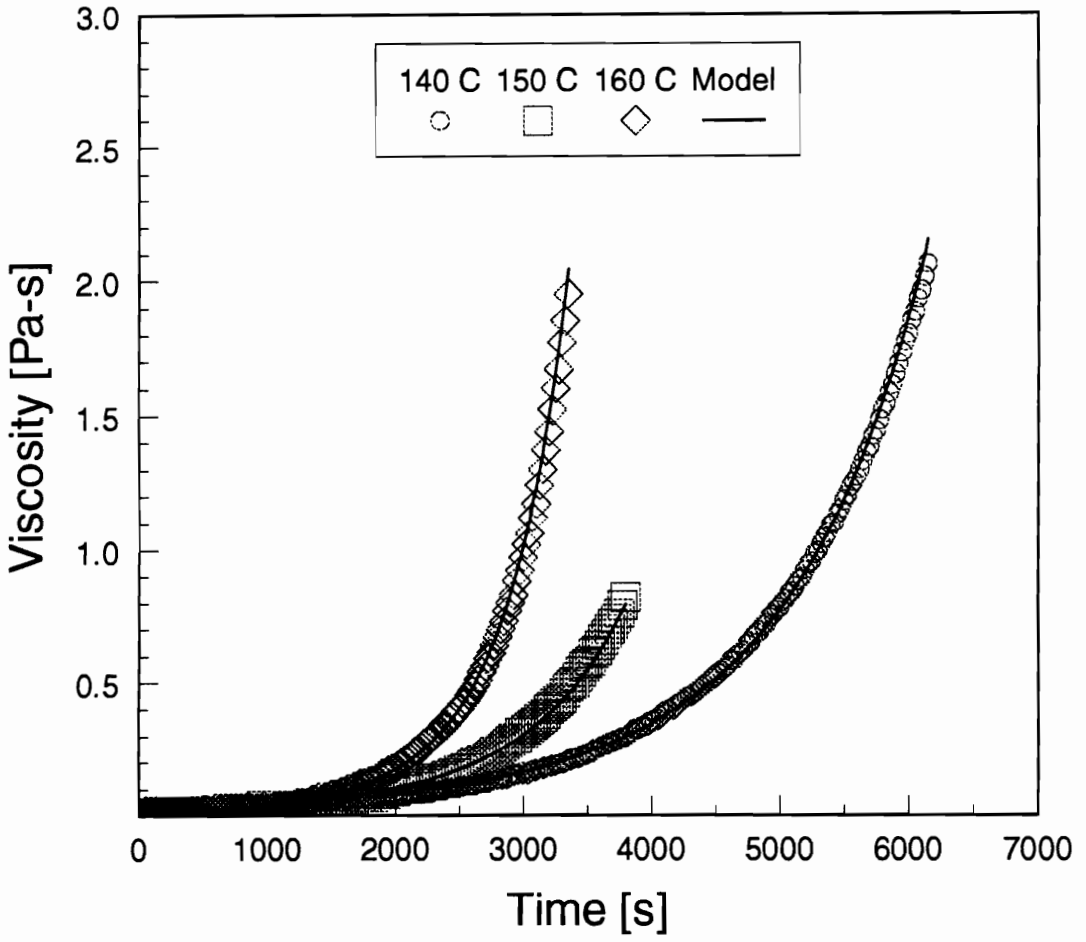

Figure 2.19 Comparison of measured and proposed model predicted viscosity as a function of time at 140, 150, and 160 °C for the toughened cyanate ester resin system.

2.7.2 Prepregging

Several batches of unidirectional AS4-12k-unsized carbon fiber reinforced toughened cyanate ester resin prepreg tape were successfully manufactured using the Model 30 prepregger. The relatively low viscosity of the resin, ~11-12 Pa.s at 110 °C, permitted excellent wet out of the fibers. Also, the low resin viscosity allowed the use of a low level of tow tension which helps avoid excessive filament breakage leading to tow breakage. Close monitoring and adjustment of the prepregger operation resulted in prepreg tape the desired resin mass fraction. Figure 2.20 shows the results of acid digestion studies performed to estimate the resin mass fraction in the prepregs from various production batches. Only those with adequate resin content were used in composite manufacture.

2.7.3 Process Simulation

The CUREV1 process simulation model was used to develop the cure cycle as outlined in Section 2.4. The characterization models, eqs.(3.2) and (3.3) for cure kinetics and eq.(3.5) for viscosity behavior, were incorporated into the code. The heating rates (regions 1 and 3 in Fig. 2.4) were constrained to 2.0 °C/min. Also, the initial hold temperature was set to 150 °C (region 2 in Fig. 2.4). The model was used to predict the duration of the initial hold required to obtain a degree of cure of 0.3 (30%) or 0.6 (60%) at the end of the hold period.

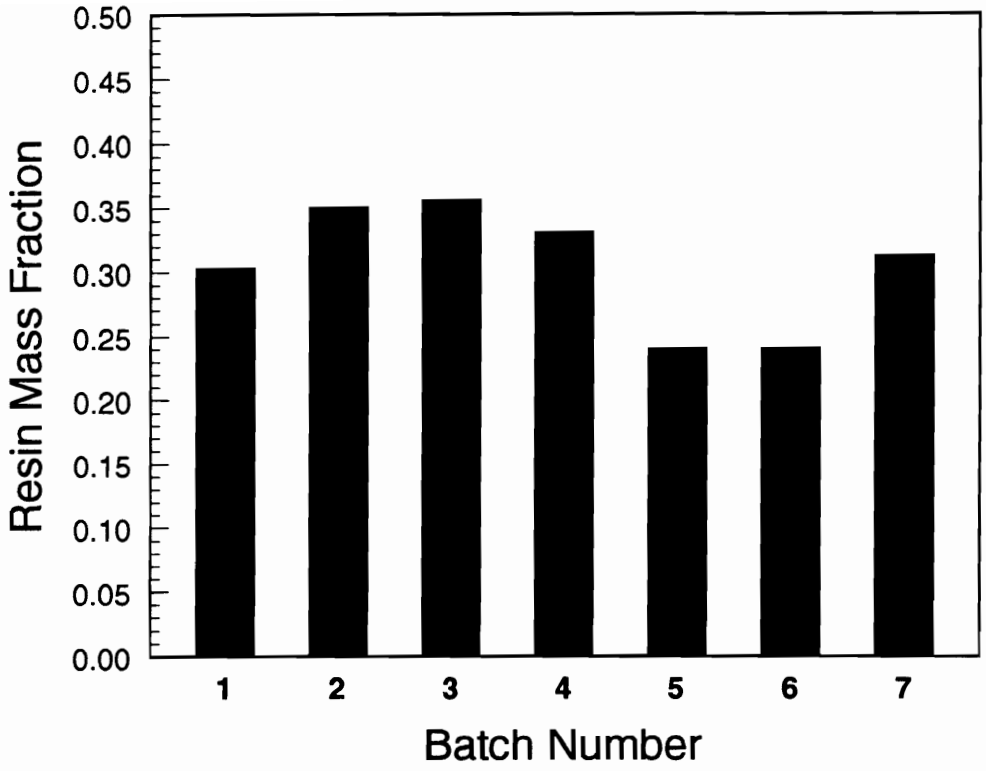

Figure 2.20 Resin mass fraction of the various AS4 carbon fiber/ toughened cyanate ester prepreg batches determined by acid digestion.

After the initial hold period, the cure temperature was increased at the prescribed rate to the final cure temperature and held at that temperature until the desired final degree of cure (α=0.98) was attained as predicted by the cure kinetics model. The time and level of pressure application were adjusted to yield the desired fiber volume fraction.

For the first case of $\alpha = 0.3$, the model generated cure cycle is shown in Fig. 2.21. The model predicted an initial hold period of 20 minutes followed by a ramp to 200 °C and a final hold of 52 minutes. A compaction pressure of 379 kPa, applied at a cycle time of 100 minutes, was predicted to fully consolidate the laminate without excessive resin bleed. Fig. 2.22 shows the model predicted degree of cure during the cure cycle. The degree of cure and cycle temperature profile are plotted against the cycle time (x-axis). Likewise, the model predicted viscosity during the cure cycle is shown in Fig 2.23. Model results show that at the point of pressure application, a resin viscosity greater than 10-15 Pa·s is necessary to prevent excessive resin bleed from the laminate.

Further, the viscosity model is valid up to a resin conversion of 0.6 (60%), the degree of cure at gel. Beyond this point, the resin flow sub-model was bypassed in the simulation. Figure 2.24 shows the matrix volume fraction, ν_m, and the cure temperature profile as functions of time. The model predicts a final fiber volume fraction ($\nu_f = 1-\nu_m$) of about 61.5%.

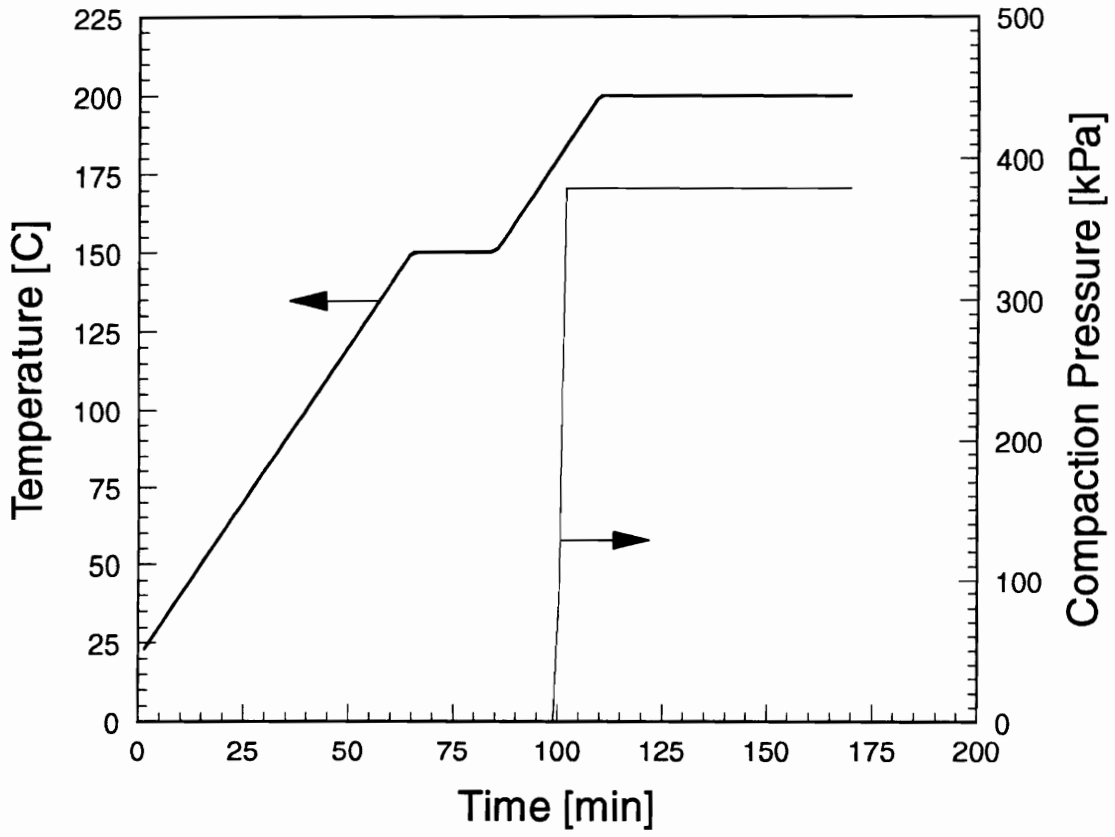

Figure 2.21 Cure cycle developed using the CUREV1 simulation model showing the time-temperature-pressure profile for $\alpha = 0.3$ at the end of initial hold case.

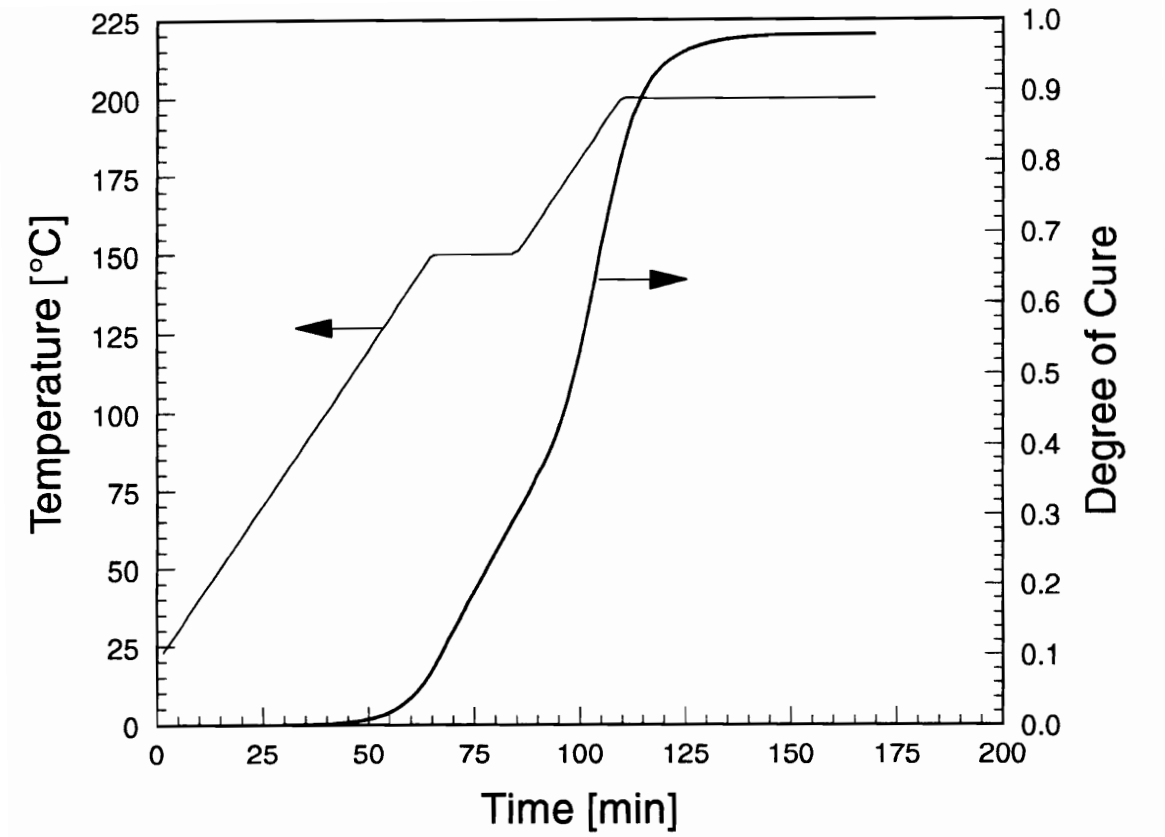

Figure 2.22 CUREV1 predicted degree of cure for the $\alpha = 0.3$ case.

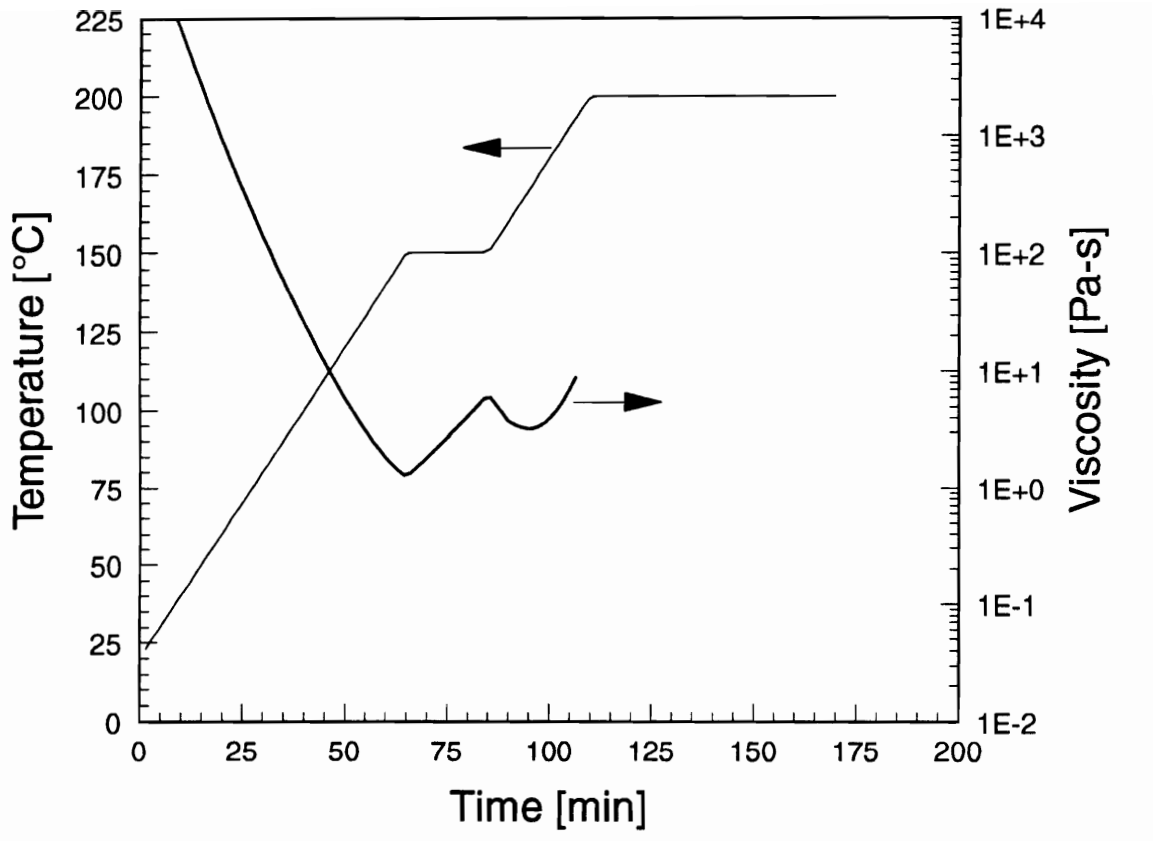

Figure 2.23 CUREV1 predicted viscosity profile for the $\alpha = 0.3$ case.

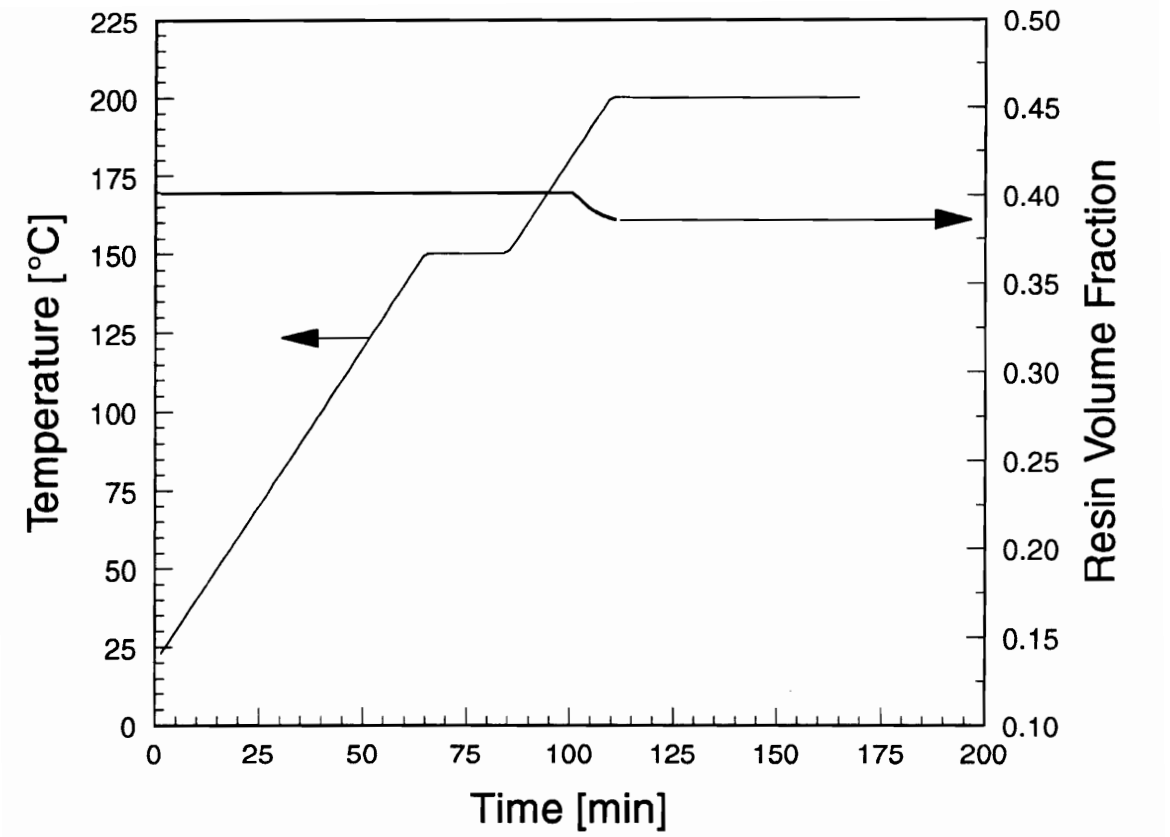

Figure 2.24 CUREV1 predicted resin volume fraction for the $\alpha = 0.3$ case.

A similar analysis was performed for the second case of a desired degree of cure of $\alpha = 0.6$ at the end of the initial hold. Fig. 2.25 shows the model predicted time-temperature-pressure cure cycle. The duration of the initial hold at 150 °C for this case is 55 minutes. A pressure of 414 kPa, applied at the same instant of time in the cure cycle as in the previous case, is predicted by the model for full consolidation of the laminate. Comparing Figs. 2.21 and 2.25, it is seen that for the first case, the consolidation pressure was applied during the second ramp to final cure. However, in the second case, the consolidation pressure is applied during the initial hold at 150 °C. Again, the development of the cure state of the resin in the composite is shown in Figure 2.26. At the end of the initial hold of 55 minutes at 150 °C, the degree of cure reaches the desired value of 0.6 (60%). Thereafter, the temperature is raised at 2.0 °C/min to the final cure temperature. Fig. 2.27 shows the resin viscosity during the cure cycle. Based on this cure cycle, CUREV1 predicts a final fiber volume fraction of about 0.6 (60%) in the composite. Fig. 2.28 shows the resin volume fraction during the cure cycle.

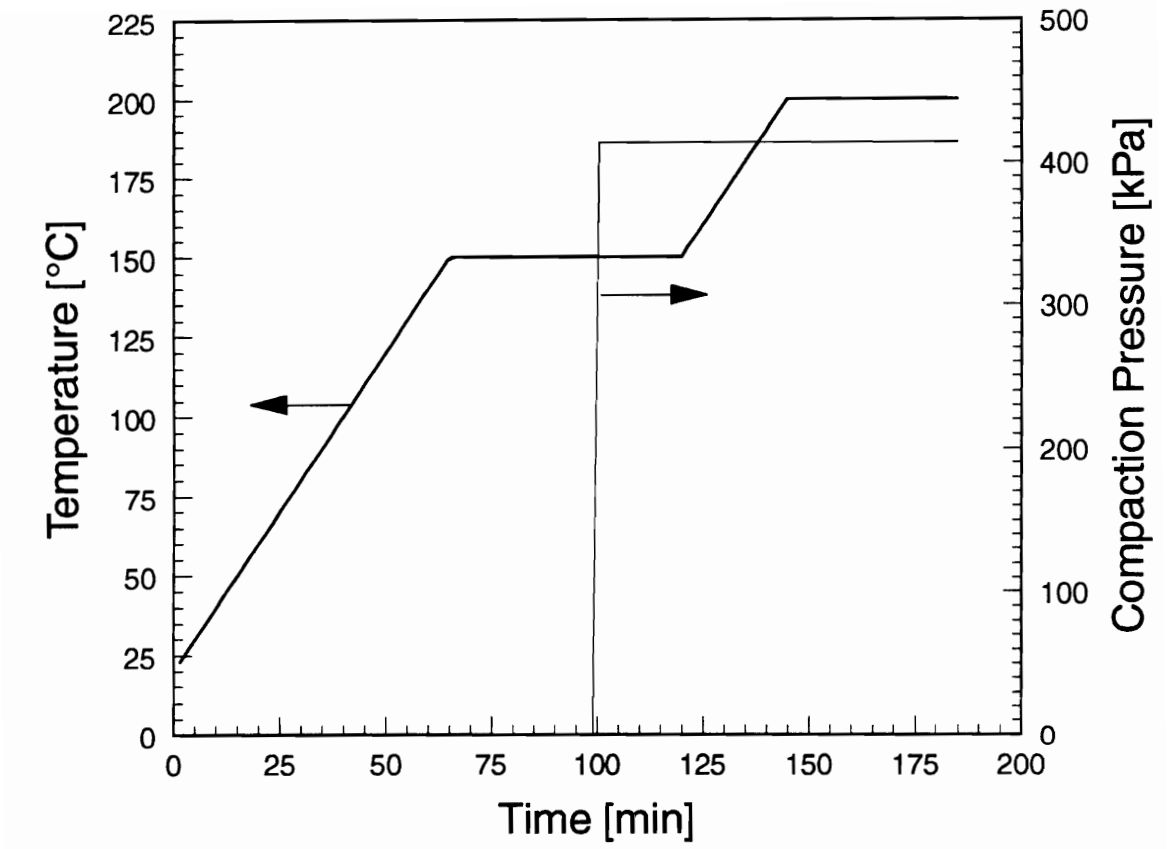

Figure 2.25 Cure cycle developed using the CUREV1 simulation model showing the time-temperature-pressure profile for $\alpha = 0.6$ at the end of the initial hold case.

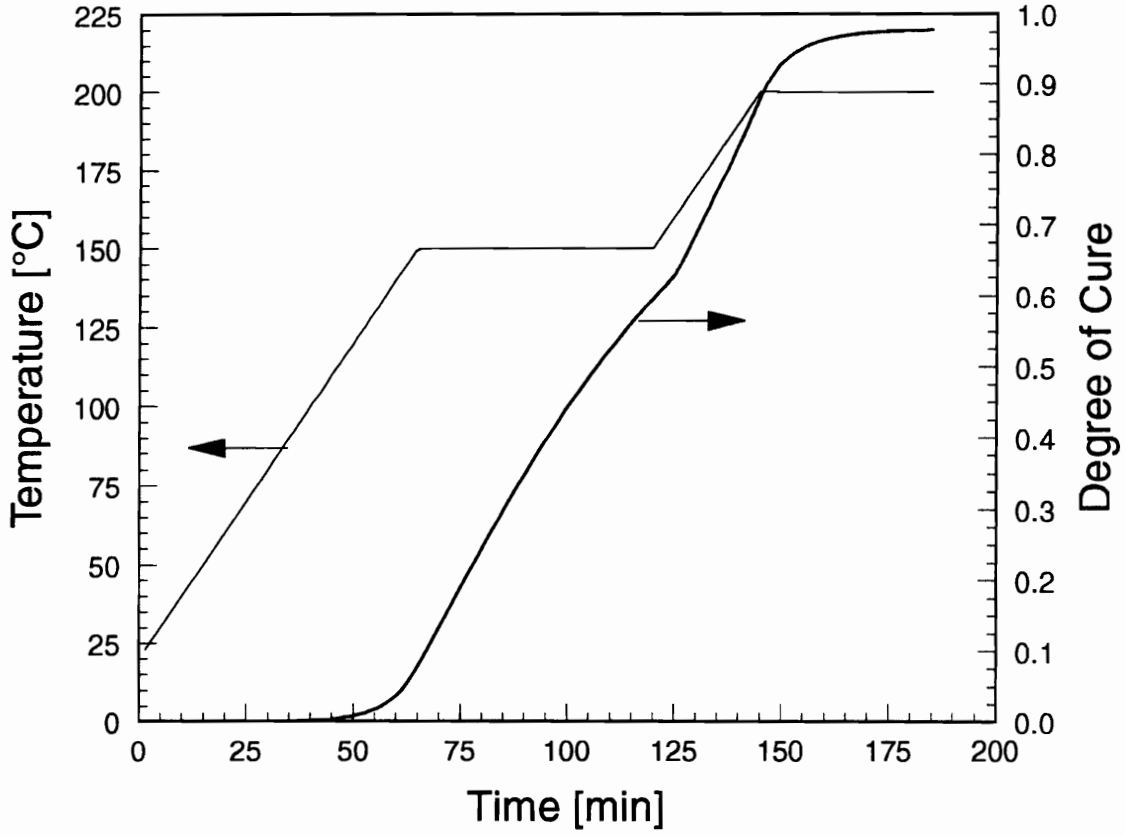

Figure 2.26 CUREV1 predicted degree of cure for the $\alpha = 0.6$ case.

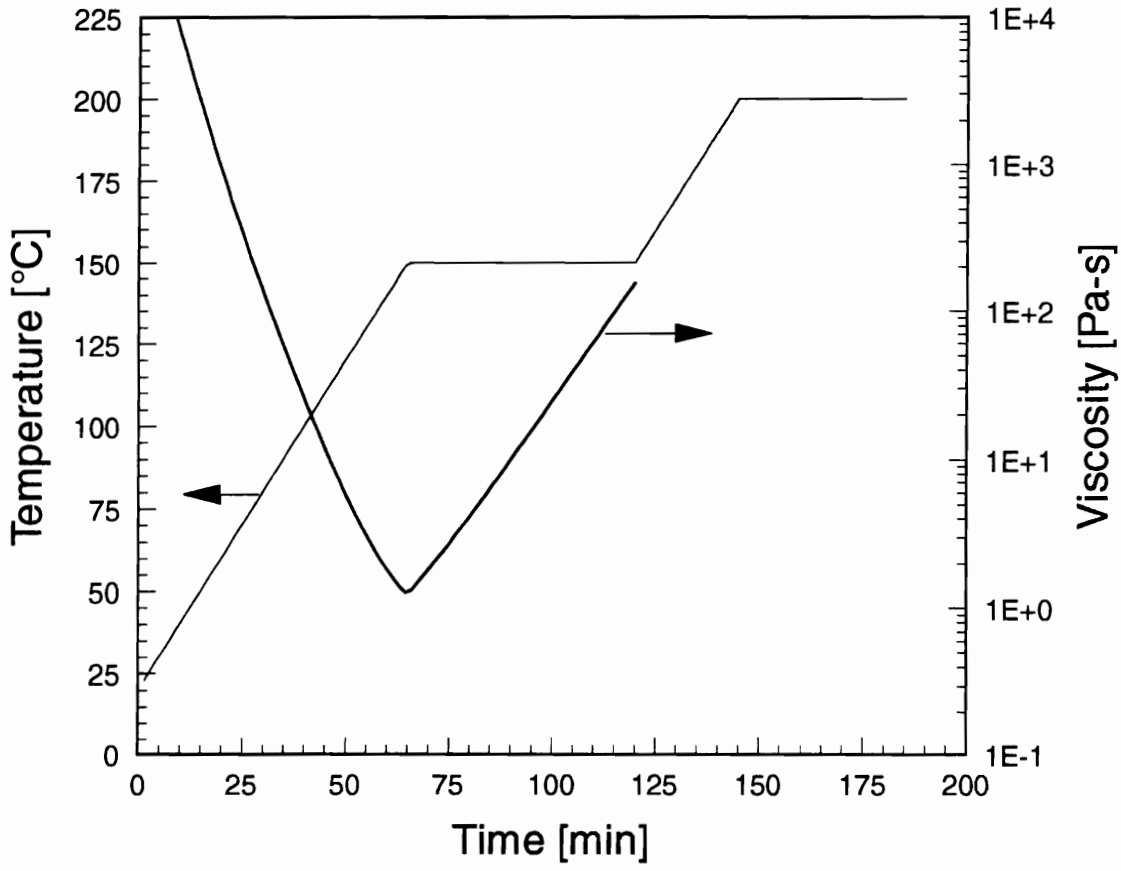

Figure 2.27 CUREV1 predicted viscosity profile for the $\alpha = 0.6$ case.

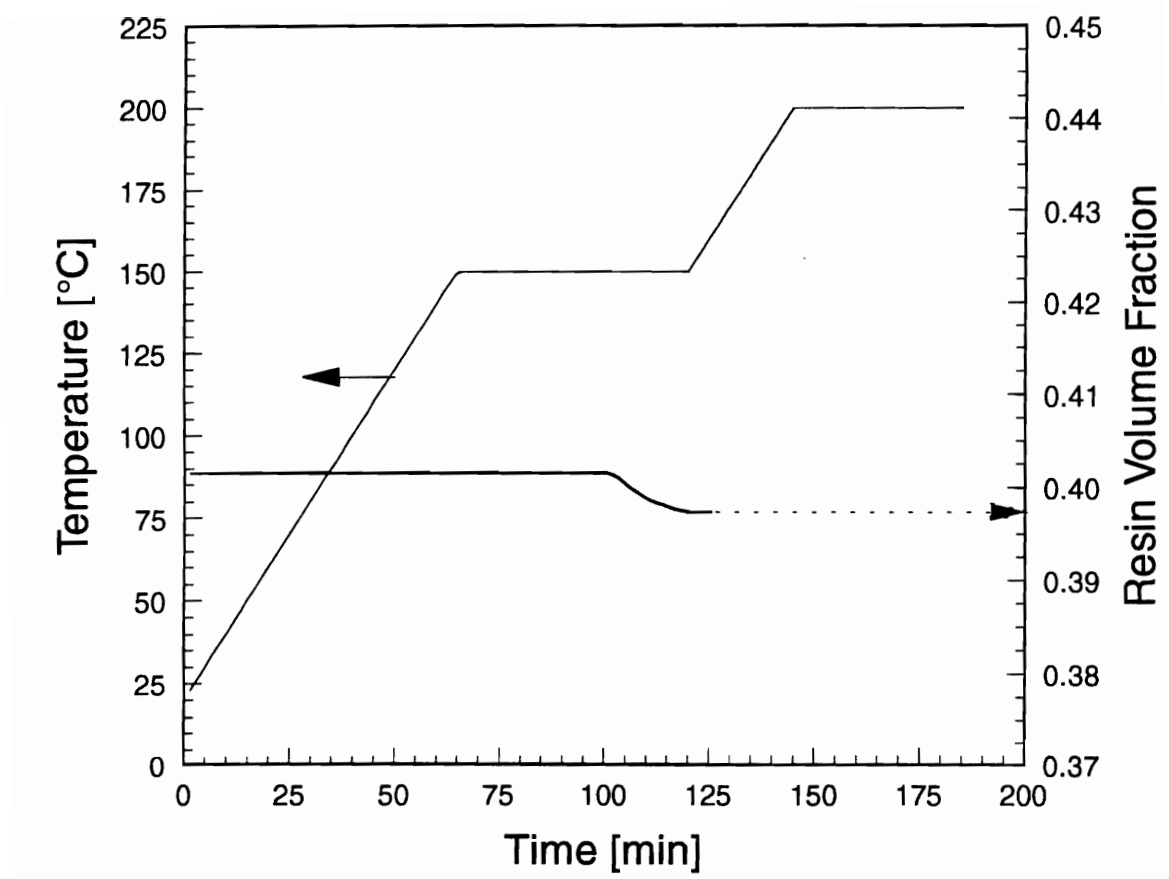

Figure 2.28 CUREV1 predicted resin volume fraction for the $\alpha = 0.6$ case.

2.7.4 Composite Manufacture

The model generated cure cycles were programmed into the CONTROL/EG (Rev. 3.54 from Quinn-Curtis Inc., Needham, MA), a process control and data acquisition software for the computer controlled hot-platen press. During processing, the process variables were continuously monitored and the acquired data stored. The mold temperature, measured by a thermocouple placed in the mold, was also acquired. The platen temperature was closely controlled to follow the desired cure cycle. Fig. 2.29 shows a plot of the programmed cure cycle along with the average of the measured top and bottom platen temperatures. Also, the mold temperature, as acquired, is also plotted. The plot shows the excellent control of platen temperature performed by the closed-loop computer control system. The mold temperature also follows the platen temperature closely. The control software allows the duration of the hold to be programmed so that the *mold* was exposed for the desired period of time at 150 °C. At the final cure temperature, the data shows a small overshoot in mold temperature of about 2-5 °C above the programmed cycle temperature. At the end of the final cure period, the platens were cooled at 4.0 °C/min to room temperature as shown in this figure.

Similarly, Fig. 2.30 shows a plot of the data acquired from the panel manufactured with the model predicted cycle to achieve a degree of cure of $\alpha = 0.6$ at the end of the initial hold. Again, the good performance of the computer controlled press is evident.

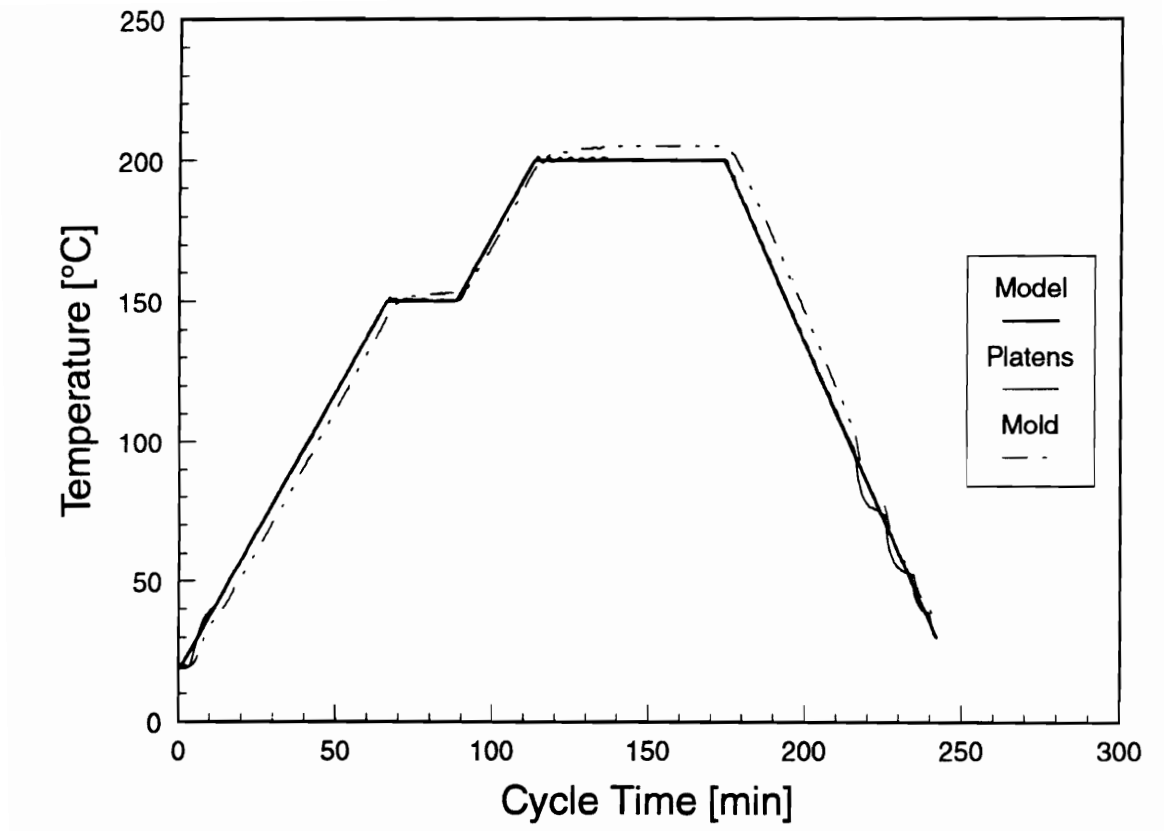

Figure 2.29 Temperature-time plot of data acquired from the computer controlled hot-platen press for panels manufactured with an initial hold of 20 min. at 150 °C

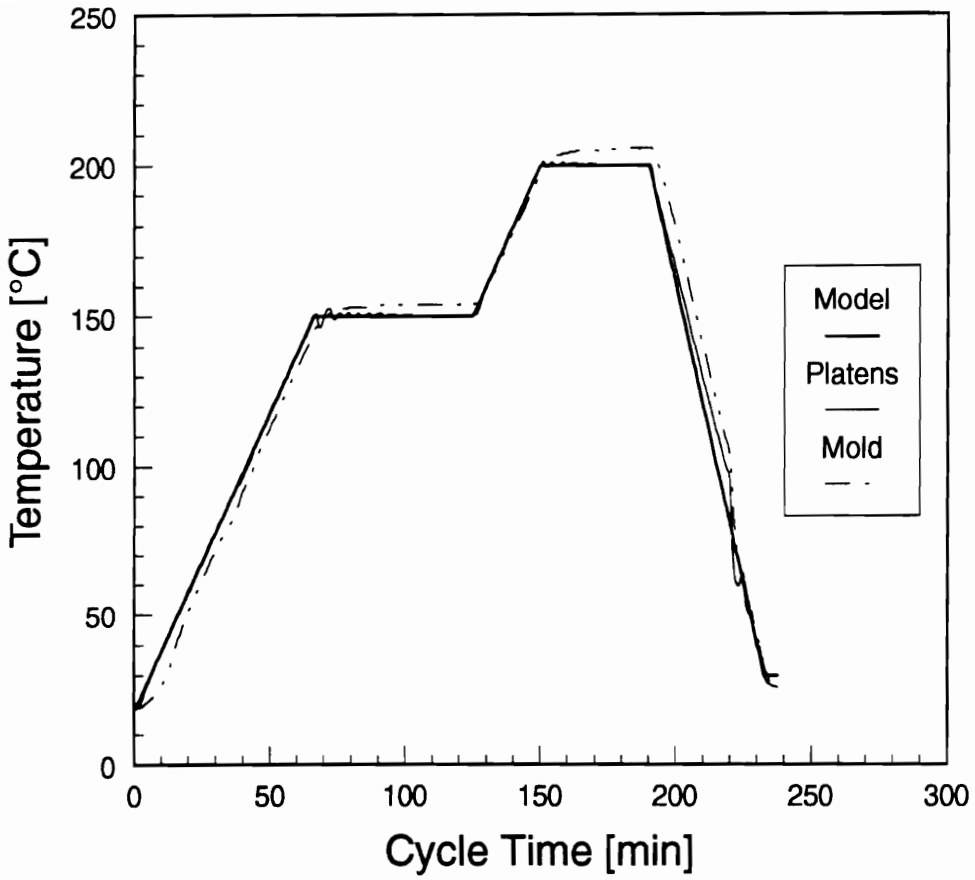

Figure 2.30 Temperature-time plot of data acquired from the computer controlled hot-platen press for panels manufactured with an initial hold of 55 min. at 150 °C

A close look at the platen temperature at the beginning of the 150 °C hold shows mild initial oscillations about the set-point temperature which, however, are damped are quickly damped out.

A total of four 76 mm x 76 mm, 8-ply unidirectional composite laminates were manufactured, two panels for each of the two initial hold period cases. Of the two panels manufactured in each case, two different levels of compaction pressures were applied. Also, a 152 mm x 152 mm, 16-ply quasi-isotropic laminate was manufactured on the hot-platen press for impact testing.

2.7.5 Physical Testing

Ultrasonic C-scans showed all the 8-ply unidirectional panels to be uniformly consolidated and free of large scale imperfections. A C-scan of the 16-ply quasi-isotropic laminate showed a reticular pattern. This was entirely due to surface undulations only.

Further, the 8-ply unidirectional panels were tested for the fiber content by the density measurement technique. Each panel was machined into 76 mm x 25 mm strips for this test. Fig 2.31 compares the measured and the model predicted fiber volume fractions for the two cure cycle cases. Error bars indicate very small variation in fiber volume fraction over the entire panel. The data indicate that the panels manufactured with an initial hold period of 55 minutes have fiber volume fractions barely above 60%, while those manufactured with an initial hold of 20 minutes have fiber contents just below

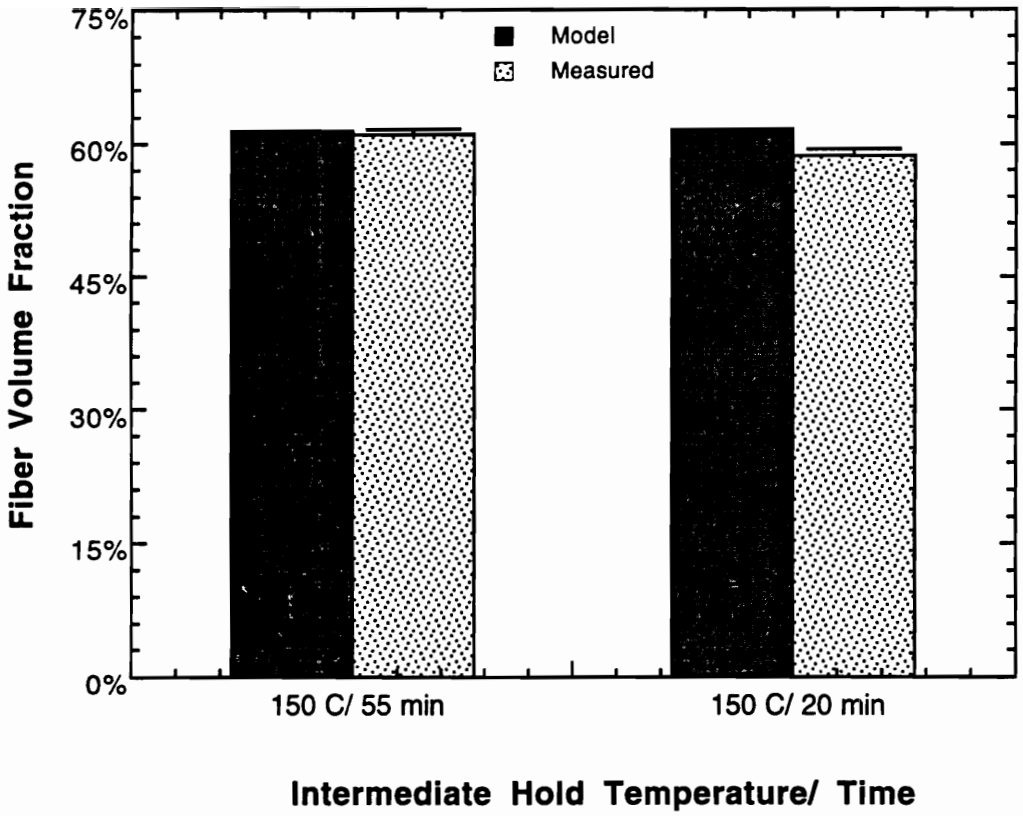

Figure 2.31 Comparison of model predicted and measured fiber volume fractions of the unidirectional AS4/toughened cyanate ester composite laminates.

60%. Thus, these results show that by closely following the model generated process cycles produce laminates with the desired fiber volume fraction.

A sample of the fully cured toughened cyanate ester resin, obtained from the panel production, was analyzed for the glass transition temperature, T_g, of the resin system. This analysis was performed by Thomas [29] using a Modulated Differential Scanning Calorimeter (MDSC). A recently developed thermal analysis technique, MDSC has the capability to easily detect close and weak transitions. Fig. 2.32 shows the results of a MDSC scan to analyze the change in the heat capacity of the resin system. The step change in heat capacity with increasing temperature, reflecting the glass transition temperature, is evident in the figure. However, the derivative of the heat capacity signal with respect to time, plotted along the second y-axis, indicates the existence of two transitions. One T_g, at ~ 255 °C, corresponds to the cross-linked cyanate ester thermoset while the other, at ~ 275 °C, corresponds to the amorphous thermoplastic toughener. The high T_g indicates that the resin is fully cured and the proximity of the two distinct T_g indicates the existence of two separate phases.

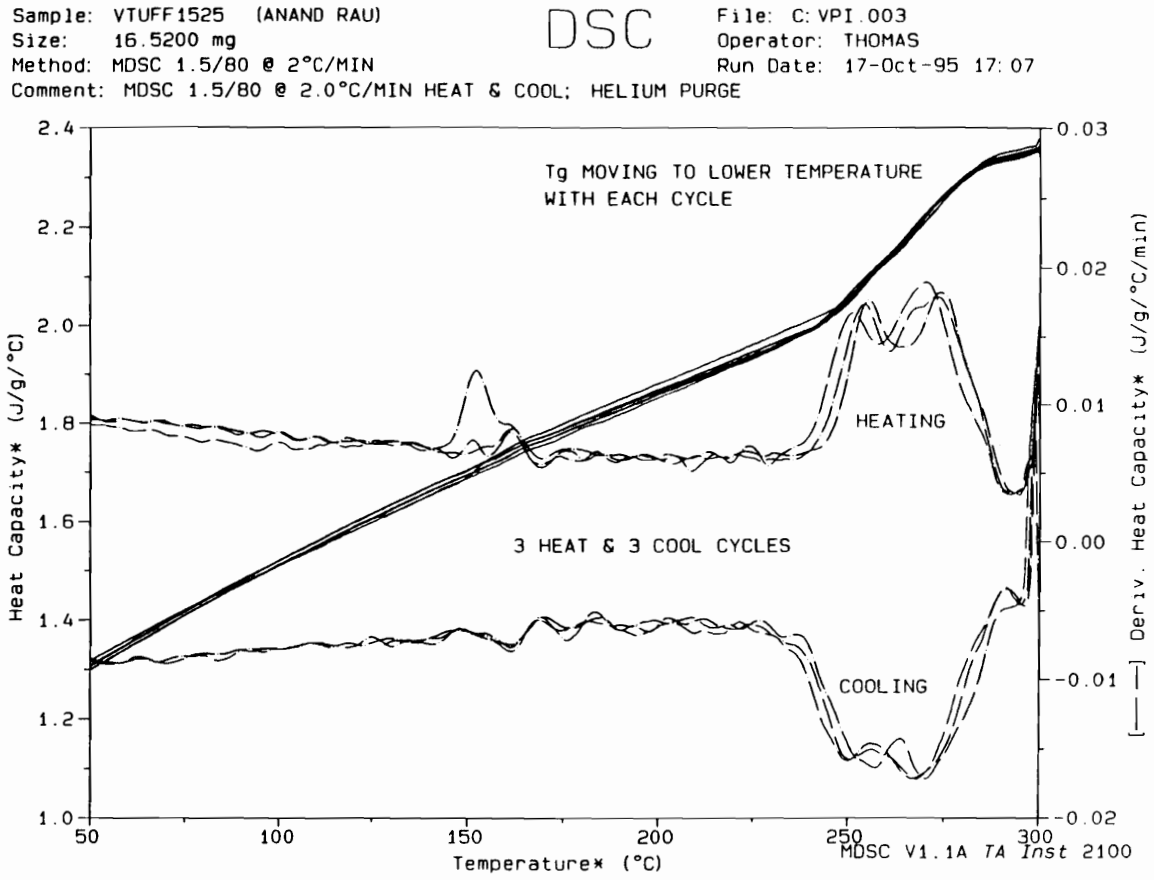

Figure 2.32 Modulated DSC scan of VTUFF1525 flash resin showing the existence of two T_g.

2.7.6 Microscopy

Optical microscopy of composite specimens from the 8-ply unidirectional and the 16-ply quasi-isotropic panels shows good consolidation of the prepreg plies and the composite to be free of visually detectable voids. Typical photomicrographs of the 8-ply unidirectional laminates at two different magnifications, 200X and 400X, are shown in Figs. 2.33 (top) and (bottom) respectively. Likewise, Figs. 2.34 (top) and (bottom) show photomicrographs of sections from the quasi-isotropic laminate. The photomicrograph in Fig. 2.34 (top) shows a typical 45°-0°-90° ply interface and a closer view of the 45°/0° ply interface is shown in Fig. 3.34 (bottom) . These micrographs are indicative of quality laminates.

Figure 2.35 shows a photomicrograph at 2500X of a typical section from a unidirectional laminate studied under a Olympus Image Analysis system to evaluate fiber volume fraction by image analysis. The local fiber volume fraction was found to be 63%. While this is a very localized measurement, the estimate of v_f obtained by this technique is consistent with the values obtained by density measurement technique.

TEM analysis of the flash resin from the manufacture of the 8-ply unidirectional panels shows a difference in the phase separated morphology in the cured toughened cyanate ester resin system, confirming the indications of the MDSC scan (Fig. 2.32).

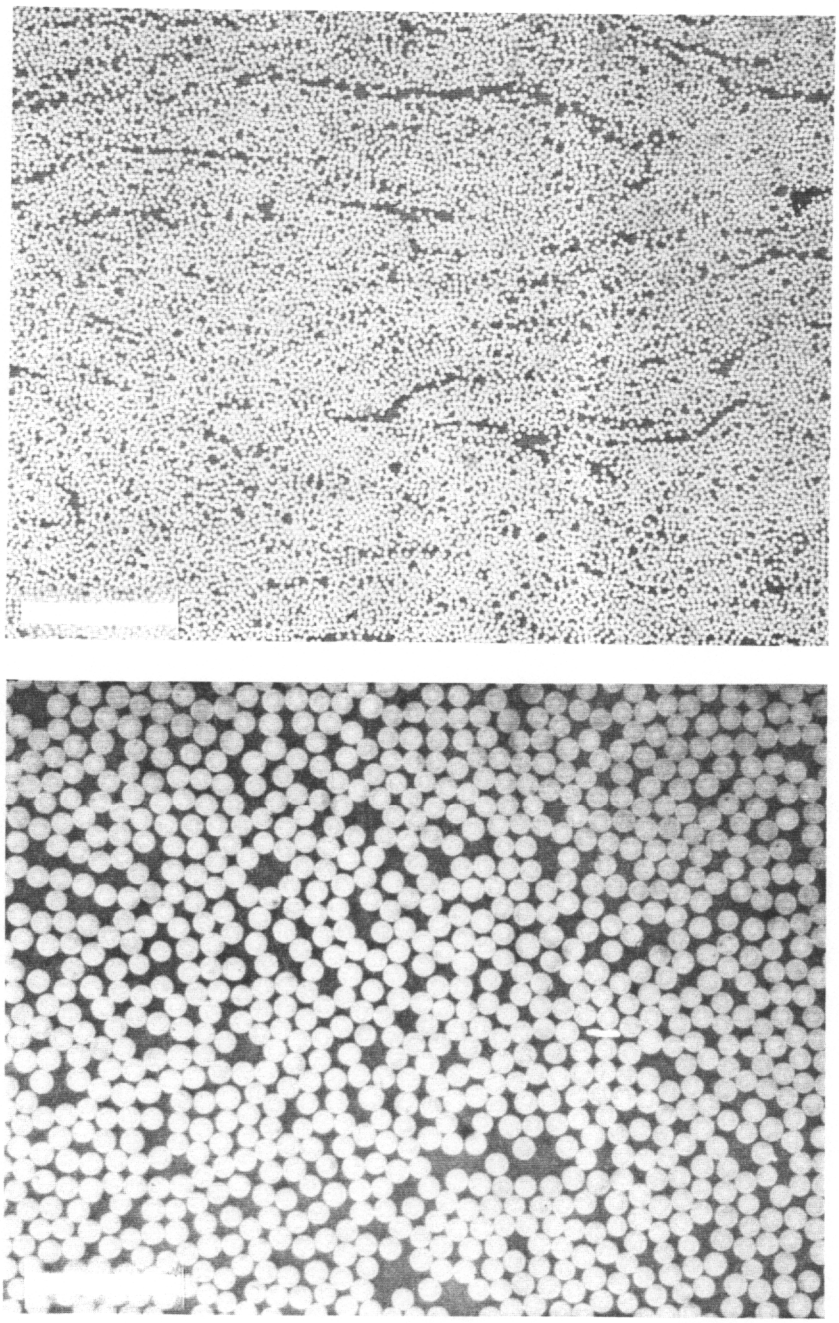

Figure 2.33 Photomicrographs of a typical section from the 8-ply unidirectional laminates at 200X [scale bar = 50 μm] (top), and at 400X [scale bar = 25 μm] (bottom).

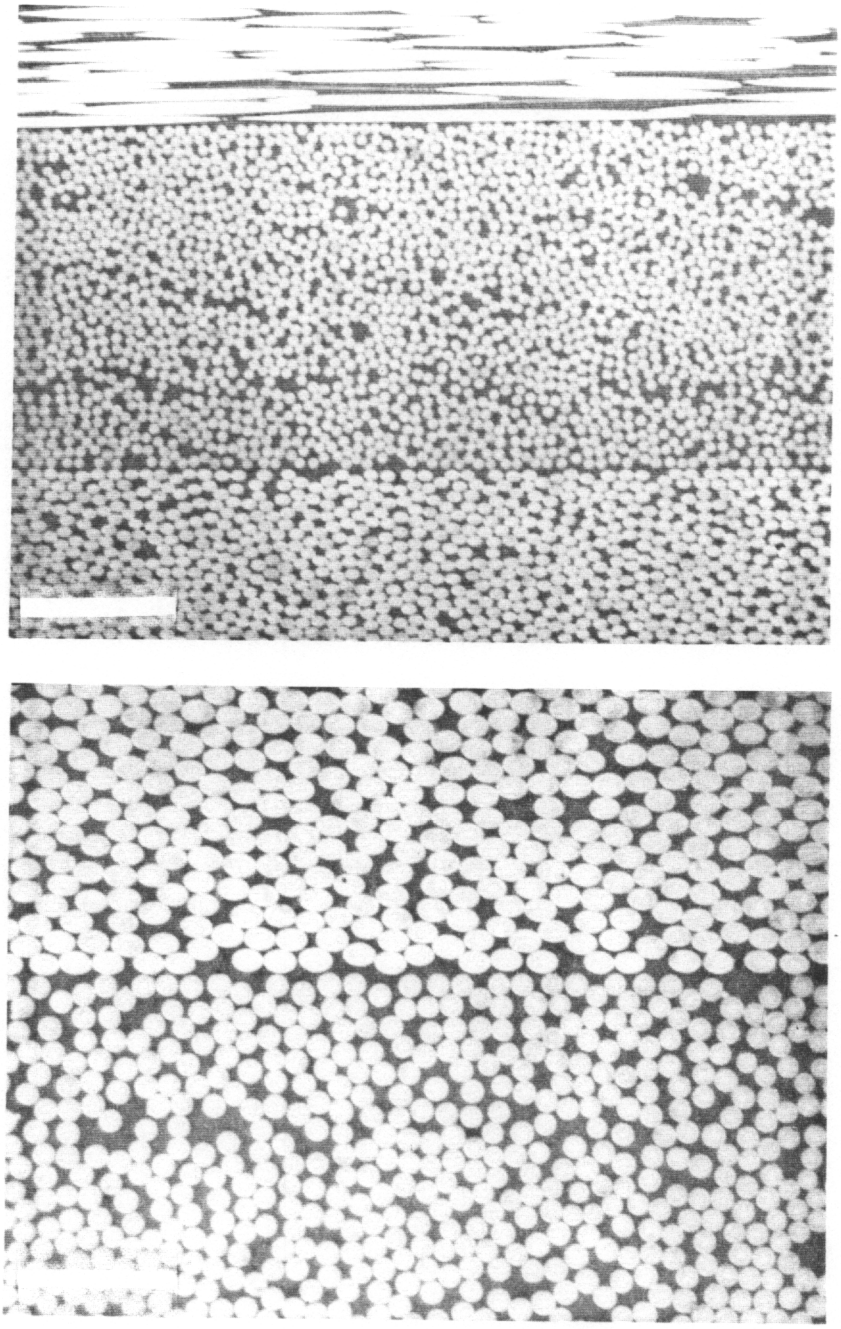

Figure 2.34 Photomicrographs of a typical section from the 16-ply quasi-isotropic laminate at 200X [scale bar = 50 μm] (top), and at 400X [scale bar = 25 μm] (bottom).

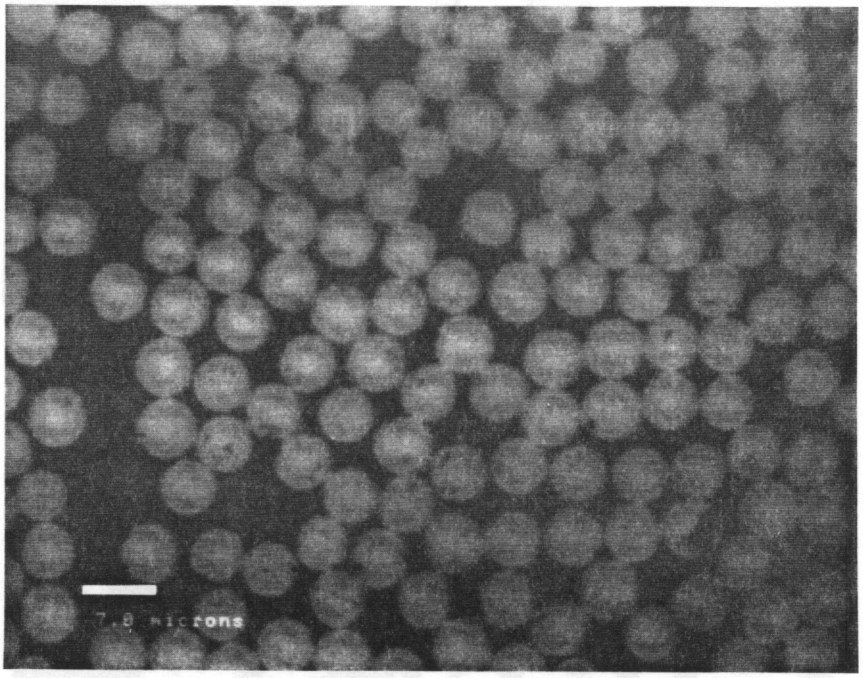

Figure 2.35 Photomicrographs of a typical section from a 8-ply unidirectional laminate for image analysis at 2500X magnification [scale bar = 10 μm].

Typical photomicrographs from the TEM analysis at a magnification of 25,000X is shown in Figs. 2.36 (top) and (bottom). Figure 2.36(top) shows the morphology developed in the resin system when processed with an initial hold of 20 minutes at 150 °C. The morphology developed in laminates processed with an initial hold of 150 °C for 55 minutes is shown in Fig. 2.36 (bottom). The micrographs indicate a nearly co-continuous morphology in both cases. However, in the second case a finer structure seems to occur. It is recognized that these observed morphology exist in the neat resin and may not necessarily exist in the same configuration in the matrix region between the fibers.

2.7.7 Iosipescu Shear

The unidirectional laminates processed under the two initial hold conditions were tested for inplane shear properties by the 90° Iosipescu shear test method. Three specimen from each of the four 8-ply unidirectional laminates were tested. The load-strain data acquired during testing were analyzed to obtain the shear strength, initial shear modulus and the shear strain at failure for these specimens.

Fig. 2.37 shows a plot of the shear strength of the AS4 carbon fiber reinforced, toughened cyanate composite material. The shear strengths of the laminates processed at 150 °C for 55 minutes indicate nearly equal shear strength, on an average, as compared with those processed at 150 °C for 20 minutes.

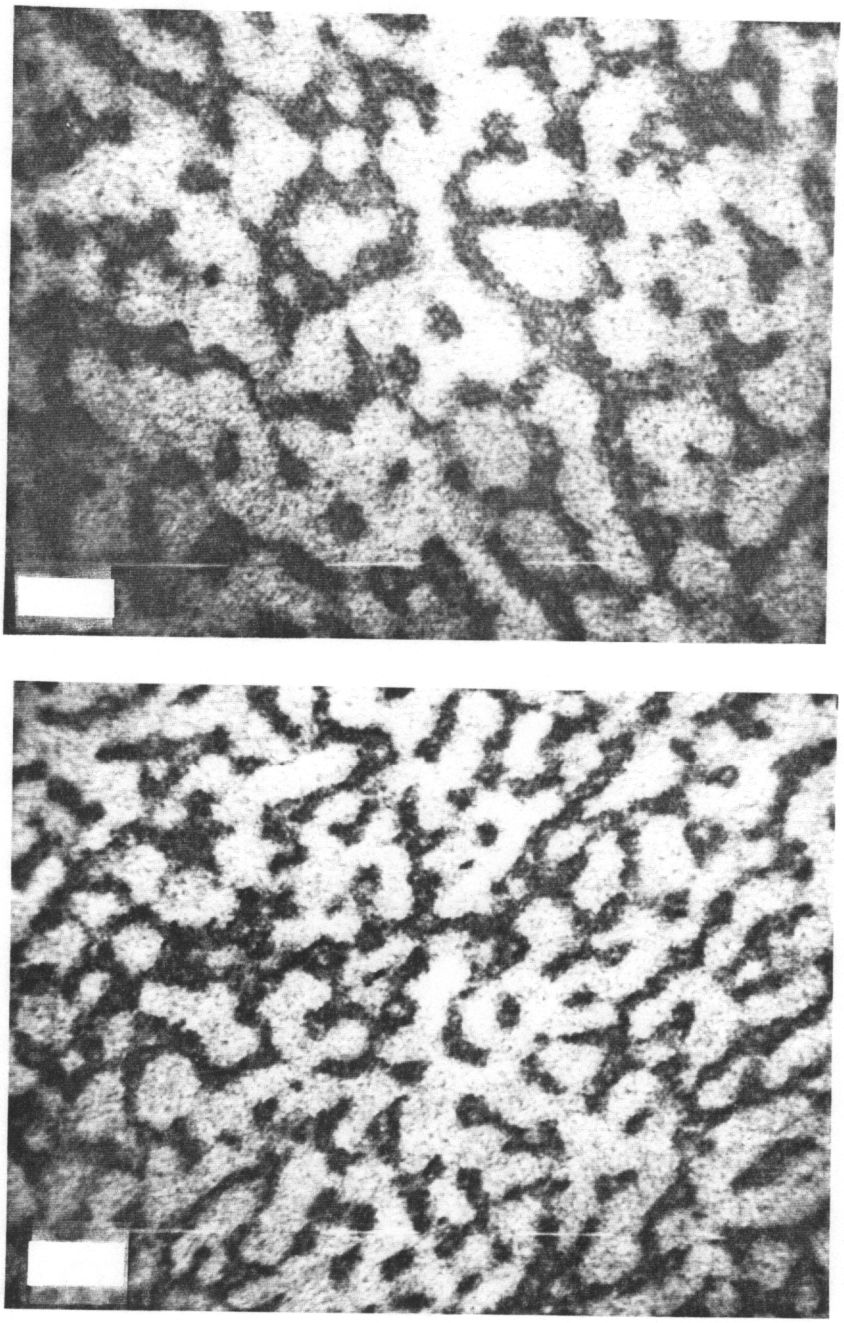

Figure 2.36 TEM photomicrographs of flash resin samples from the 8-ply unidirectional laminates processed at 150 °C/20 min (top), and at 150 °C/55 min (bottom). [Scale bar = 0.5 μm].

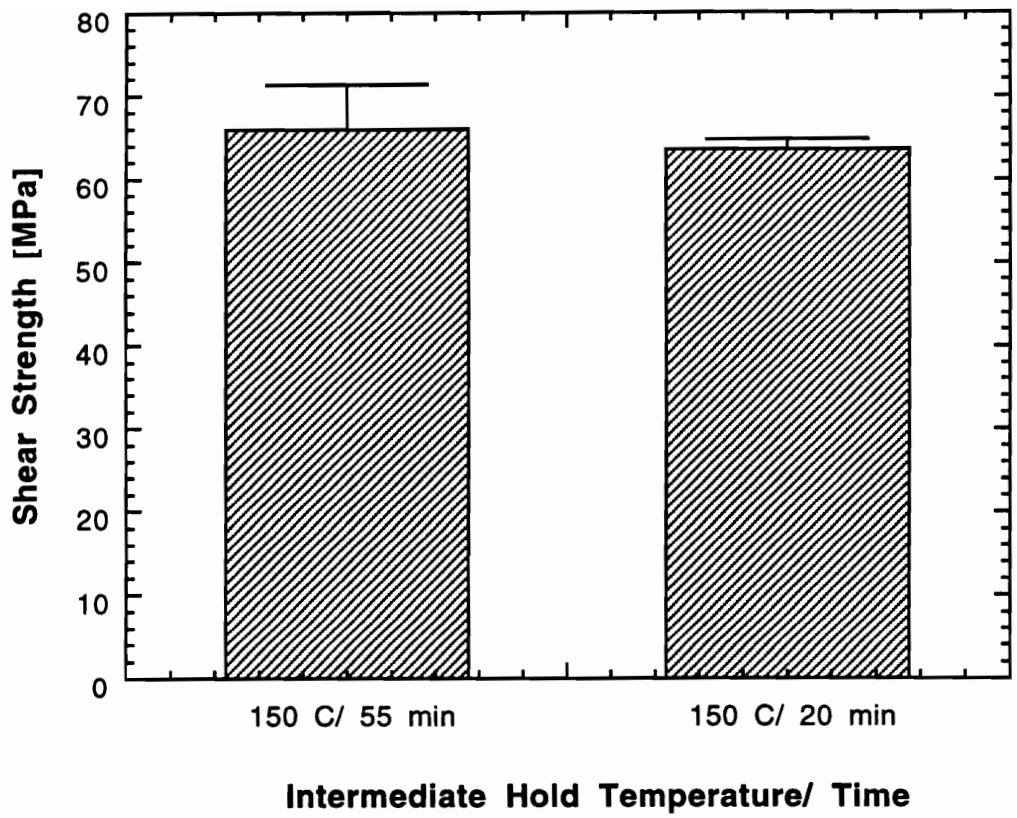

Figure 2.37 Iosipescu shear strengths of AS4 carbon fiber/ toughened cyanate ester resin composites processed under two different initial hold conditions.

However, the initial shear moduli, shown in Fig. 2.38, indicate a marked difference between the two cases. The processing condition which produced a finer phase-separated morphology (Fig. 2.36), 150 °C/55 min, results in a composite with about 20% higher modulus compared to laminates processed with initial hold of 20 minutes at 150 °C. Also, in Fig. 2.39, the shear strain at specimen failure is plotted against the processing condition. The results show a processing dependence again. The laminates subjected to a 20 minute hold indicate, on an average, about 30% higher strain to failure. While it can be argued that the strengths of the laminates resulting from changes in processing may lie with the experimental scatter, as indicated by the error bars, the trends indicated by the shear modulus and the strain to failure data appear to indicate real processing related differences in the composites.

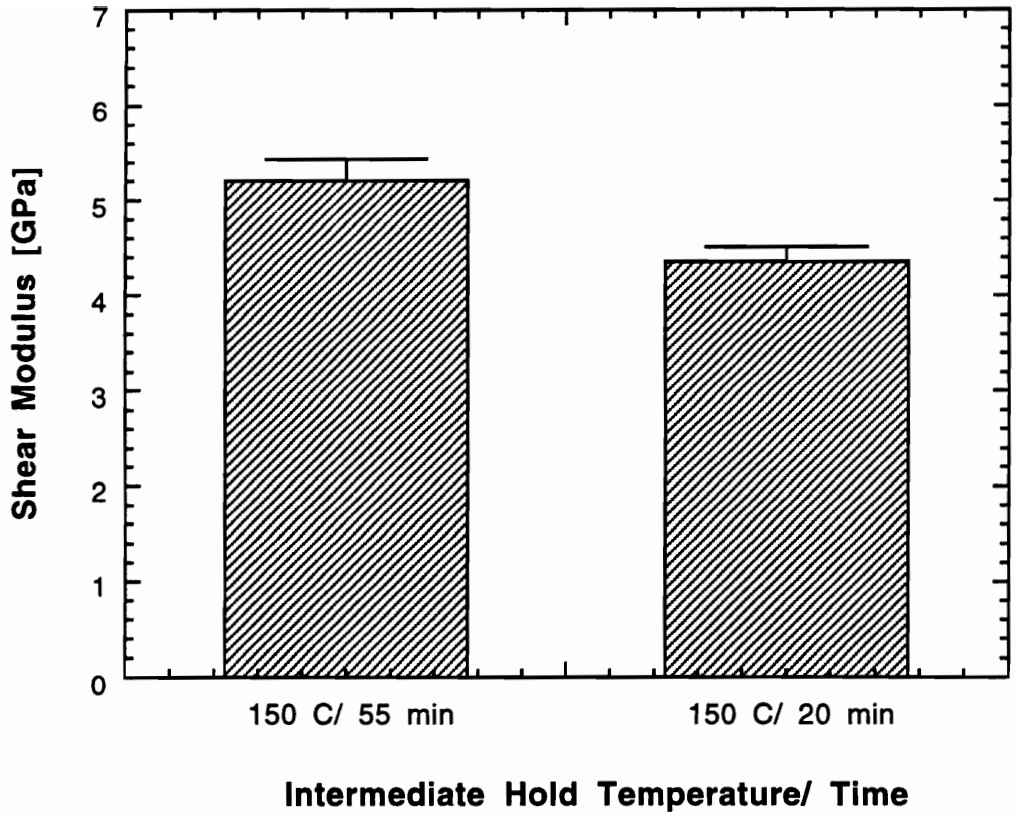

Figure 2.38 Initial Iosipescu shear modulus of AS4 carbon fiber/ toughened cyanate ester resin composites processed under two different initial hold conditions.

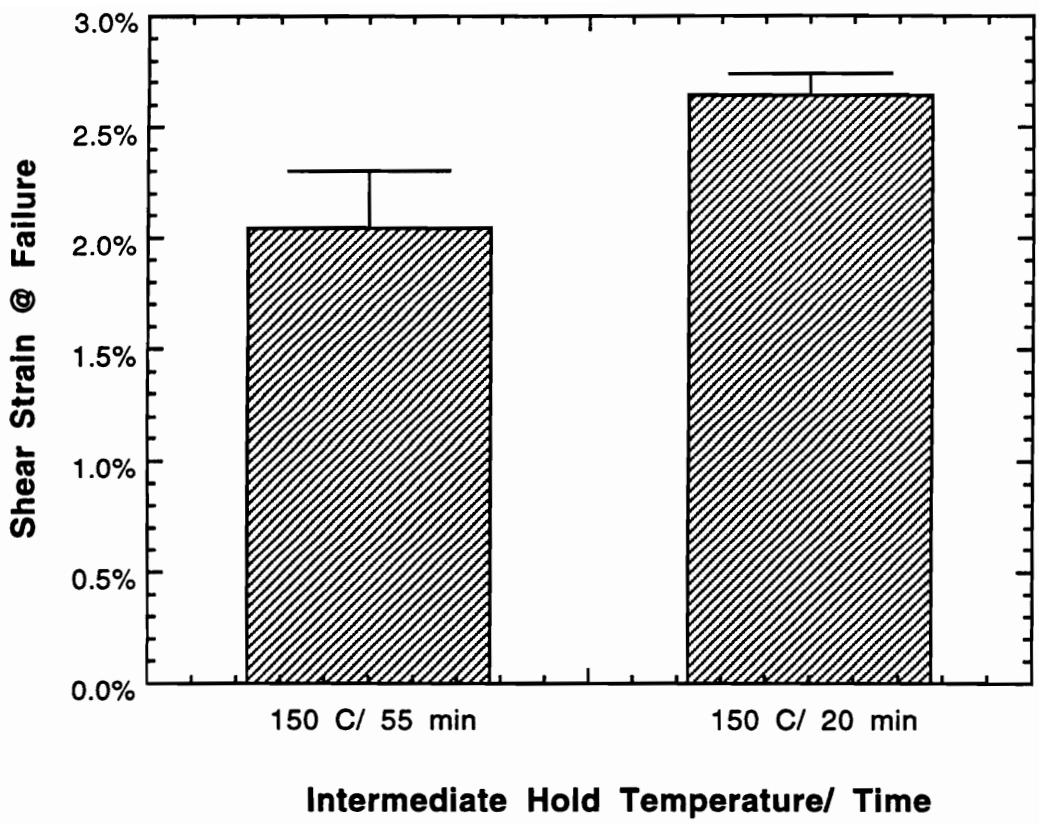

Figure 2.39 Shear strain at failure of AS4 carbon fiber/ toughened cyanate ester resin composites processed under two different initial hold conditions.

2.7.8 Impact Testing

Gas gun impact tests were performed on AS4/toughened cyanate ester, 16-ply quasi-isotropic laminates by measuring the damage area resulting from the impact of a projectile at four different incident velocities. A typical damage sustained by a specimen from this laminate, impacted at a velocity of 20 ms^{-1} (energy of ~ 14 J) was detected by ultrasonic C-scan shown in Fig. 2.40 (top) and x-ray radiograph shown in Fig. 2.40 (bottom). Fig. 2.41 (top) shows a comparison of the critical velocity to initiate damage, V_c , for three different material systems. While the reinforcement is the same in all three, 3502 represents a commercial brittle epoxy system, and APC-2 is a commercially available thermoplastic matrix composite material. The toughened cyanate ester composite shows nearly two-fold increase in V_c, indicating a higher resistance to the initiation of impact damage. It is, however, lower in the same measure when compared to the more tough thermoplastic material, as expected. In Fig. 2.41 (bottom), the damage growth rate, C, for these three material systems are shown. A brittle system, such as the 3502 matrix composite, exhibits a high value of C, indicating the development of a larger damage area with increasing velocity. A tough matrix composite, such as APC-2, on the other hand exhibits a low value of C. It was expected that the toughened cyanate ester would exhibit a growth rate value between those of a brittle epoxy and a tough thermoset. However, the C value of toughened cyanate ester composites was found to be about 20% higher than that for the AS4/3502 composites.

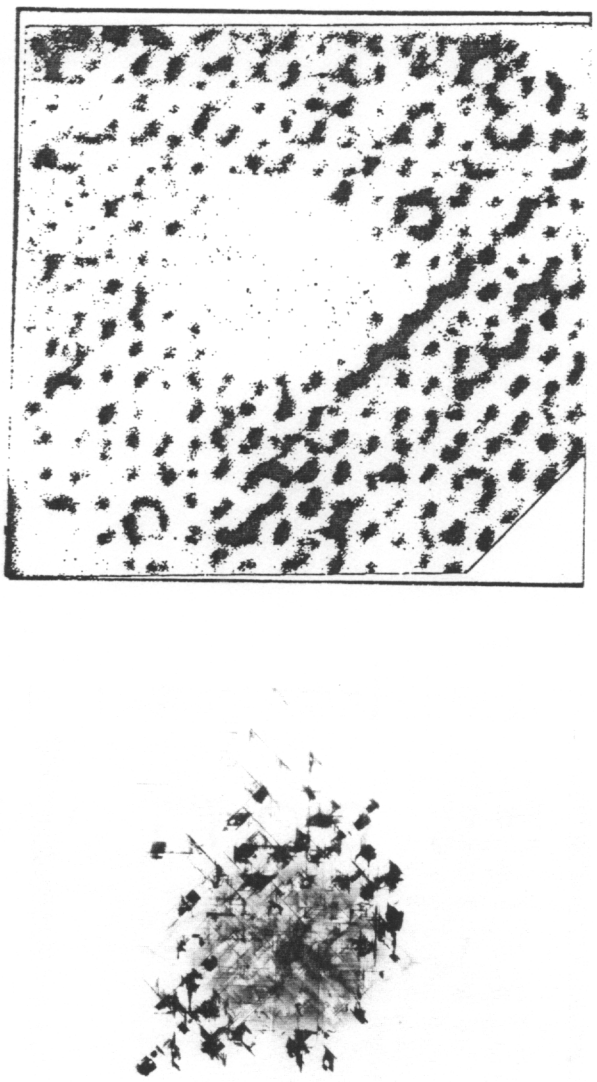

Figure 2.40 Impact damage area created by a projectile at 20 ms^{-1} in a 16-ply quasi-isotropic composite specimen. C-scan detected (top). X-ray detected (bottom)

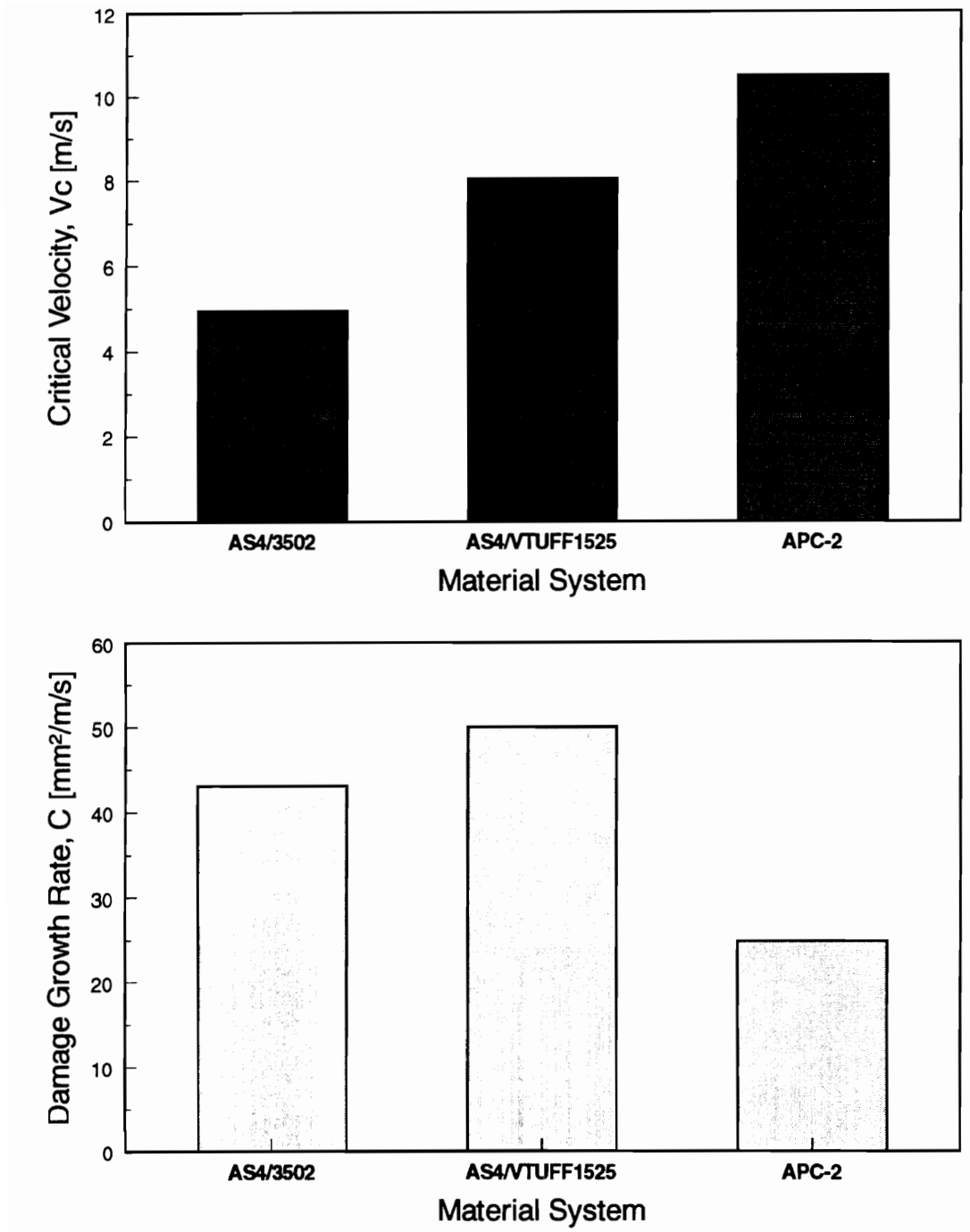

Figure 2.41 Comparison of impact damage resistance of carbon composites. Critical velocity to initiate damage, V_c (top). Damage growth rate, C (bottom).

2.8 SUMMARY AND CONCLUSIONS

The functionalized amorphous thermoplastic toughened cyanate ester resin system has been fully characterized. A new viscosity model which permits rapid viscosity characterization is proposed. The cure kinetics and viscosity models developed describe the resin behavior with good accuracy.

Unidirectional carbon fiber prepregs were successfully manufactured with the toughened cyanate resin using a solventless hot-melt technique. The low melt viscosity of the resin permits excellent wet-out of the reinforcing fiber tows producing void free prepregs with a controlled and uniform fiber and matrix distribution. The resin mass fraction of the prepregs was between 30 and 35%.

The carbon fiber, toughened cyanate ester prepreg was fabricated into composite panels for mechanical and physical testing. The manufactured laminates were well consolidated to the specified fiber volume fraction between 59 and 61%. Photomicrographs showed that the laminates are void free, the fiber and resin distribution is uniform and fiber wet-out is very good.

Mechanical tests were performed to measure the shear properties and impact damage resistance of the toughened cyanate ester resin composites. Small changes in processing conditions were shown to influence the shear performance of the carbon fiber/toughened cyanate ester composites. The results of the impact tests show improvements in the critical velocity to initiate impact damage compared with the commonly used hot-melt epoxy resin composites. There appears to be an anomaly in the

damage growth rate value for the toughened cyanate ester matrix composites. Further studies will be required to explain this trend. However, the use of toughened resin matrix is believed to only delay the onset of impact damage [23,30]. The improvement, that is evident from the V_c data, is gained without a sacrifice in the ease of processability of this resin system.

This investigation has ascertained that this new resin system is easily processed by the conventional prepregging route. The merits of adopting a model based approach to processing is demonstrated. The results also indicate that this material system has the potential for applications requiring improved damage resistance over conventional brittle epoxy systems.

2.9 CHAPTER REFERENCES

[1] Cano, R. J., M. B. Dow, "Properties of Five Toughened Matrix Composite Materials", NASA Technical Paper 3254, Langley Research Center, VA, 1992.

[2] Williams, J. G., "Effect Of Impact Damage and Open Holes On The Compression Strength Of Tough Resin/High Strain Fiber Laminates", in *Tough Composite Materials*, (L. F. Vosteen, N. J. Johnston, and L. A. Teichman, eds.), NASA Conference Publication 2334, Langley Research Center, VA, 1983, pp 61-79.

[3] Verchere, D., H. Sautereau, J. P. Pascault, S. M. Moschiar, C. C. Riccardi, and R. J. J. Williams, "Rubber-Modified Epoxies. I: Influence of Carboxyl-Terminated Butadiene-Acrylonitrile Random Copolymers (CTBN) on the Polymerization and Phase Separation Processes", J. App. Polym. Sci., Vol. 41, 1990, pp. 467-485.

[4] Verchere, D., J. P. Pascault, H. Sautereau, S. M. Moschiar, C. C. Riccardi, and R. J. J. Williams, "Rubber-Modified Epoxies. II: Influence of the Cure Schedule and Rubber Concentration on the Generated Morphology", J. App. Polym. Sci., Vol. 42, 1991, pp. 701-716.

[5] Moschiar, S.M., C. C. Ricardi, R. J. J. Williams, D. Verchere, H. Sautereau, and J. P. Pascault, "Rubber-Modified Epoxies. III: Analysis of Experimental Trends through a Phase Separation Model", J. App. Polym. Sci., Vol. 42, 1991, pp. 717-735.

[6] Verchere, D., J. P. Pascault, H. Sautereau, S. M. Moschiar, C. C. Riccardi, and R. J. J. Williams, "Rubber-Modified Epoxies. IV: Influence of Morphology on Mechanical Properties", J. App. Polym. Sci., Vol. 43, 1991, pp. 293-304.

[7] Verchère, D., J. P. Pascault, H. Sautereau, C. C. Riccardi, and R. J. J. Williams, "Rubber-Modified Epoxies: Analysis of the Phase-Separation Process", in *Toughened Plastics I Science and Engineering*, (C. Keith Riew and A.J. Kinloch, eds.), Advances in Chemistry Series 233, American Chemical Society, Chapter 14, 1993, pp. 335-363.

[8] Kubotera, K., and A.F. Yee, "Morphological and Fracture Studies of Alloys of Thermosets and Thermoplastics", *Back To The Future*, SPE ANTEC '92, Vol. II, May 1992, p. 2610.

[9] Srinivasan, S.A., et al, "Reactive Poly(Arylene Ether) Toughening of Cyanate Ester Networks Via Thermal and Microwave Curing", 39th International SAMPE Symposium, April 1994, pp. 60-71.

[10] Brown, J.M., S. Srinivasan, A.V. Rau, T.C. Ward, J. E. McGrath, and A. C. Loos, "Production of Controlled Networks and Morphologies in Toughened Thermosetting Resins Using Real-Time, In-Situ Cure Monitoring, 41st SAGAMORE Conf. on Intelligent Processes and Materials, US Army Research Lab., Materials Directorate (Polymer), Plymouth, MA, August 1994.

[11] Wilkinson, S.P., T.C. Ward, and J.E. McGrath, "Effect of Thermoplastic Modifier Variables on Toughening a Bismaleimide Matrix Resin for High - Performance Composite Materials", Polymer, Vol. 34, No. 4, 1993, p. 870.

[12] Srinivasan, S.A., "Toughening of Cyanate Ester Networks with Reactive Thermoplastic Modifiers", Doctoral Dissertation, Virginia Polytechnic Institute and State University, Blacksburg, Virginia, April 1994.

[13] Yoon, T.H., S.C. Liptak, D.B. Priddy Jr., and J.E. McGrath, "Adhesive and Mechanical Properties of Reactive Polysulfone Modified Epoxy Resins", J. Adhesion, Vol. 45, 1994, pp. 191-203.

[14] Lee, S.M., et al, "A New Toughened Epoxy Resin for Resin Transfer Molding Applications", 39th International SAMPE Symposium, April 1994.

[15] Brown, J. M., "Production of Controlled Networks and Morphologies in Toughened Thermosetting Resins Using Real-Time, In-situ Cure Monitoring", Doctoral Dissertation, Virginia Polytechnic Institute and State University, Blacksburg, Virginia, January 1994.

[16] Wong, D. G., M. F. DiBerardino, and R. C. Cochran, "Processing Evaluation of Toughened Epoxy Composites", 39th International SAMPE Symposium, April 1994, pp. 297-310.

[17] Chan, L. C. et al, "Rubber-Modified Epoxies: Cure, Transitions, and Morphology", in *Rubber Modified Thermoset Resins*, (C. Keith Riew and J. K. Gillham, eds.), Advances in Chemistry Series 208, American Chemical Society, Chapter 15, 1983, pp. 235-259.

[18] Chen, Y-T., and C.W. Macosko, "Chemorheology of Polycyanate for Resin Transfer Molding", 24th International SAMPE Technical Conference, October 20-22, 1992, p. T630.

[19] Castro, J.M., and C.W. Macosko, "Studies of Mold Filling and Curing in the Reaction Injection Molding Process", AIChE Journal, Vol. 28, No. 2, 1982, p. 250.

[20] DRNLIN, IMSL Statistical Subroutine, IMSL.

[21] Chmielewski, C., K. Jayaraman, and C. A. Petty, "An Experimental and Theoretical Study of Resin Impregnation Rates into Fiber Bundles Using a Wedge Slit Die", Polymer Composites ... April-June 1994? get full ref.

[22] Loos, A.C., and G.S. Springer, "Curing of Epoxy Matrix Composites", Journal of Composite Materials, Vol. 17, March 1983, p 135.

[23] Teh, K. T., "Impact Damage Resistance and Tolerance of Advanced Composite Material Systems", Doctoral Dissertation, Virginia Polytechnic Institute and State University, Blacksburg, Virginia, 1993.

[24] Deng, Y., and G.C. Martin, "Diffusion and Diffusion-Controlled Kinetics During Epoxy-Amine Cure", Macromolecules, Vol. 27, 1994, pp. 5147-5153.

[25] Wisanrakkit, G., and J.K. Gillham, "The Glass Transition Temperature (T_g) as an Index of Chemical Conversion for a High-T_g Amine/Epoxy System: Chemical and Diffusion Controlled Reaction Kinetics", J. Coatings Technology, Vol. 62, No. 783, April 1990, p. 35.

[26] Osei-Owusu, A., and G.C. Martin, "Analysis of the Curing Behavior of Cyanate Ester Resin Systems", Polym. Eng. Sci., Vol. 31, No. 22, Nov. 1991, p. 1604.

[27] Chen, Y-T., and C.W. Macosko, "Chemorheology of Polycyanate for Resin Transfer Molding", 24th International SAMPE Technical Conference, October 20-22, 1992, p. T630.

[28] Deng, Y., and G.C. Martin, "Modeling Diffusion during Thermoset Cure: An Approach Based on Dielectric Analysis", Macromolecules, Vol. 27, 1994, p. 5141.

[29] Thomas, L. C., Vice-President (Marketing), TA Instruments Inc., New Castle, Delaware, - personal communications.

[30] Babic, L., C. Dunn, and P. J. Hogg, "Damage Development and Its Significance in GRP Subjected to Impact", Plas. Rubber Process. Appl., Vol. 12, No. 4, 1989, pp. 199-207.

3.0 RESIN TRANSFER MOLDING (RTM) WITH CYANATE ESTER RESIN SYSTEMS

3.1 INTRODUCTION

Thermosetting resins such as epoxies and bismaleimides are commonly used materials for advanced composite matrices in the aerospace and electronic industries. These highly crosslinked materials are low cost, easy to process and offer excellent thermal and mechanical properties with outstanding adhesive properties. However, widespread use of these materials is limited in many high performance applications due to their inherent brittleness.

Various methods of improving the toughness of composites have been investigated. They include the use of high strain-to-failure reinforcing carbon fibers [1,2,3,7], woven fabric reinforcements [4,5], toughened matrix resins [1,2,6-10], and interleaf materials between the plies of a laminate [2,11,12]. Of these, perhaps the most widely studied approach has been on the use of toughened matrix resins for advanced composite

applications. Cano and Dow conducted a study of commercial toughened composite material systems for use in primary aircraft structures [6]. Brack et al., report on the selection of a toughened resin system for the manufacture of tilt rotor components for the Bell/Boeing V-22 Osprey aircraft [13]. The choice was made based on the ability of the material system to satisfy the processability and service requirements.

The benefits of matrix toughening for improving composite damage tolerance are well recognized today. Williams [7] draws the following conclusions based on impact studies comparing brittle and toughened matrix composites:

- Tough resin systems reduce the size of impact damage zone
- Tough resin systems can improve the compression strength of impact damaged laminates

In order to improve the toughness of brittle thermosetting resin systems, elastomers have been incorporated [14-17,24,31] into the base thermoset resin. The addition of an elastomeric second phase improves the toughness of thermosets. However, associated with this is a decrease in modulus and high temperature properties. This penalty precludes the use of elastomer toughened thermosets in many high performance structural composite applications.

McGrath and coworkers have demonstrated that the incorporation of tough ductile, functionally terminated, high temperature thermoplastic modifiers into thermosetting systems results in improvements in toughness along with retention of high modulus and thermal stability [10,19-25]. Resin toughening with reactive thermoplastics,

through chemical bonding between thermoplastic and thermoset phases, results in toughened resins with superior properties as compared to non-reactive thermoplastic modified systems.

Cyanate ester networks are emerging thermosetting resin systems with the potential to serve as the matrix in composite material systems. The resin under investigation is a Bisphenol-A cyanate ester toughened with hydroxy functionalized phenolphthalein based amorphous poly(arylene ether sulfone). The thermoplastic modified toughened networks exhibited improvements in the fracture toughness over the base cyanate ester networks without significant reductions in mechanical properties or glass transition temperature. Details of toughener chemistry and synthesis is reported by Srinivasan [22].

A variety of factors contribute to influence the properties of toughened thermosets including, toughener concentration, molecular weight, and formulation [14,17,21,24,30]. Further, cure conditions also have a significant effect on the development of morphology and on the mechanical behavior of the toughened system [15,17,20,26,31]. While improvement in toughness is achieved via the addition of a ductile second phase to the base thermoset resin, the viscosity of the toughened resin is significantly increased. Thermosets are easily processed, however, increased resin viscosity resulting from the toughening process has an adverse effect on the ease of processability. Therefore, in the manufacture of advanced fiber reinforced composites with toughened resin systems a good understanding of resin curing and viscosity behavior is necessary. Further, close control of process parameters is required to successfully manufacture high quality composites.

Addition of thermoplastic modifiers to thermosetting resins almost always results in a higher melt viscosity. This limits processability by RTM. It is therefore necessary to develop and utilize science based optimization/ simulation tools to select appropriate processing parameters

In order to efficiently manufacture composite components a model based approach to processing is necessary. The steps involved in such an approach to process development and material evaluation are schematically shown in Fig. 3.1. This approach involves characterizing fabric reinforcements and the resin systems as a first step. Understanding the flow characteristics of the fabric preform and the resin viscosity are essential for process development. Science based process simulation models, in conjunction with the characterization data, provide a means to develop processing cycles.

The model determined processing conditions, when applied during manufacture, produce quality composites without the need for extensive process trials. This necessitates the use of sophisticated control equipment for composite manufacture to faithfully follow desired process cycles. Composite parts thus produced are then subjected to physical and mechanical testing to evaluate their quality and performance. The results of the evaluation could provide sufficient information to "fine-tune" the processing conditions, if necessary. In this study, toughened resin systems are evaluated for processability by liquid molding techniques. The cyanate ester thermosetting resin and the functionalized thermoplastic toughener were formulated for this investigation by

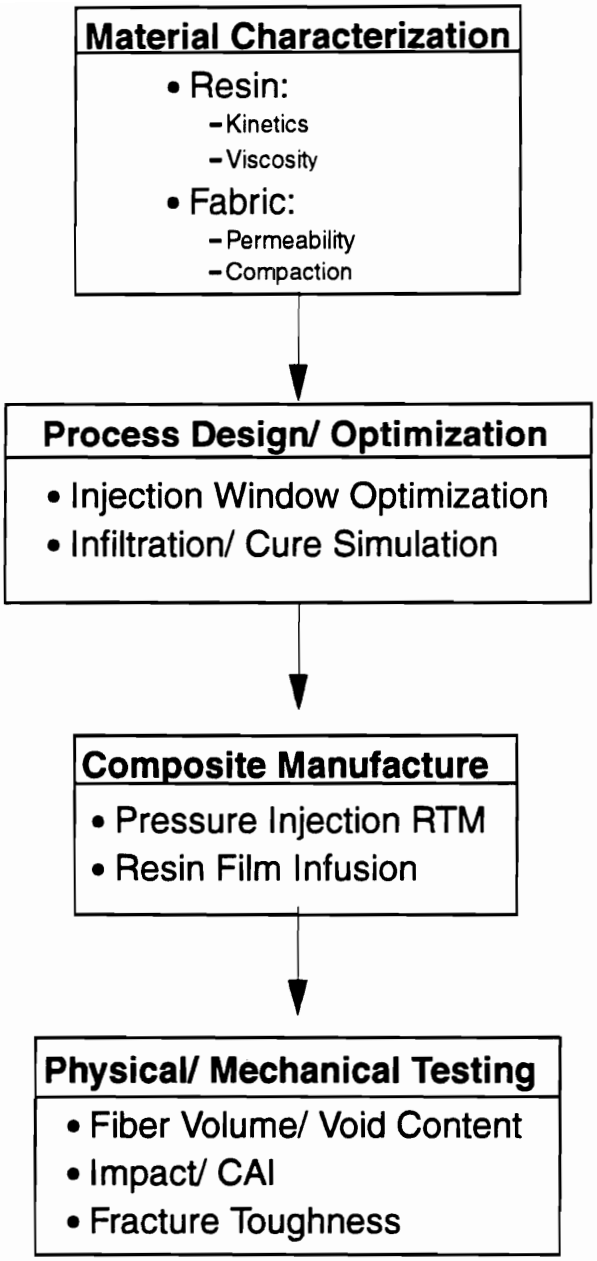

Figure 3.1 Schematic representation of a model based approach to composite processing by liquid molding techniques.

varying the concentration and the molecular weight of the toughener.

Carbon fabric composites were manufactured with the toughened and untoughened resin systems. Physical and mechanical tests were performed to evaluate the quality and performance of the composites. The performance of the toughened systems were compared to that of the untoughened system and other common thermosetting resin systems.

3.2 MATERIALS

In this investigation, seven different resin systems were chosen for use as composite matrix materials. Two type of carbon woven fabric construction constituted the reinforcements for the composites. Details of the materials used are presented in the following sections.

3.2.1 Matrix Resin Systems

A commercially available bisphenol-A based cyanate ester network system under the trade name AroCy B10 (T_g ~265-270 °C) provided by Ciba-Geigy, Inc. was the base thermosetting resin system. The thermoplastic toughener was a hydroxy functionalized phenolphthalein based amorphous poly(arylene ether sulfone) (T_g ~260 °C), synthesized at Virginia Tech by McGrath and coworkers [19,22]. The toughened resin systems formulated for this investigation had between 20 and 30 wt.% of the reactive toughener

dissolved in AroCy B-10 thermoset. The thermoplastic toughener with two different molecular weights (Mn = 15,000 and 20,000 g/mol) were used.

For convenience of reference, a designation system was developed to identify the toughened resin systems developed at Virginia Tech. Each of the four toughened resin formulation was designated by a "VTUFFmmww" code, where "mm" indicates the molecular weight of the toughener in kg/mol and "ww" indicates the concentration of the toughener in the formulation, expressed in weight percent (wt%). For example, the designation "VTUFF1525" would apply to a toughened system which contains 25% by weight of the 15,000 g/mol molecular weight thermoplastic toughener incorporated into the base cyanate ester thermoset. Details of the toughener molecular weight and concentration used to formulate the four different toughened resin systems and their respective designations are shown in Table 3.1.

The toughened resin systems were prepared, typically in batches of 150-200 grams, by incorporating required amounts of the thermoplastic modifier into molten cyanate ester thermoset. For example, in order to prepare a 100 gram batch of toughened resin with a toughener concentration of 25%, 25 grams of the toughener would be incorporated into 75 grams of molten thermoset. The AroCy B10 cyanate ester monomer, initially in a crystalline powder form, was first weighed into a twin-necked round bottom flask. The flask was then placed in an oil bath and heated to 115 °C. A mechanical stirrer with a PTFE paddle was fitted through one of the two necks of the round bottom flask.

Table 3.1 Designations and compositions of the thermoplastic toughened cyanate ester resin formulations.

Designation	Toughener Molecular Weight, g/mol	Toughener Concentration, wt %
AroCy B10	-	0
VTUFF1520	15,000	20
VTUFF1525	15,000	25
VTUFF1530	15,000	30
VTUFF2020	20,000	20

Also, the resin and oil bath temperatures were closely monitored using two separate thermocouples. As the temperature of the resin increased above the melting point (~ 89 °C), the B10 monomer melted to a very low viscosity clear liquid. After the resin temperature stabilized at 115 °C, the thermoplastic toughener of the desired molecular weight was weighed and gradually added via a powder funnel. During and after the addition of the thermoplastic powder, the resin in the flask was continuously stirred. The stirring was continued for approximately 1.5-2.0 hours until a clear, homogeneous dark yellow hot-melt solution was obtained. The toughened resin was then removed from the oil bath and allowed to cool down to ambient temperature.

The toughened resin was stored in the flask and catalyzed only prior to use in characterization or composite manufacture. Aluminum acetylacetonate [Al(acac)], at a concentration of 250 ppm, and nonyl phenol, at a concentration of 2 phr, constituted the catalysts for the cyanate ester family of resin systems. The quantities of the catalysts added to the four toughened resin systems were such that the required concentration with respect to the AroCy B10 cyanate ester resin content was maintained.

In addition to the five cyanate family of resin systems, two commercial epoxy resin systems were also used in this investigation. The epoxy systems were used to provide a reference for the purpose of comparing the mechanical performance of the untoughened and toughened cyanate ester resin systems. One epoxy used for initial evaluation was Shell RSL1895. This is a developmental resin system designed for composite manufacture by the RTM process. A proprietary curing agent "W", at 33% by

weight, is used to cure this resin system. The other epoxy resin used was 3501-6, a widely used hot-melt thermoset, from Hercules Inc.

3.2.2 Fabric Reinforcements

Two different types of carbon fiber fabrics were chosen for this study. For preliminary investigations, a 3k IM7 carbon fiber 8-harness satin woven fabric (IM7-3k-8HS) was used. Also, AS4 carbon fiber, in a plain weave construction (AS4-3k-PW), from Fabric Development Inc., Quakertown, Pennsylvania, was used as the reinforcement material for the majority of the composite laminates fabricated in this investigation.

3.3 MATERIALS CHARACTERIZATION

3.3.1 Resin Viscosity Characterization

The viscosity-time characteristics of the toughened cyanate resin system were measured at elevated temperatures using a Brookfield Model DVIII rheometer. Isothermal viscosity measurements were made using cylindrical spindle (SC4-21) and a disposable cup attachment. The isothermal measurements were made at three different temperatures between 100 and 150 °C for each of the toughened resin systems. From these measurements isothermal viscosity-time profiles were obtained.

3.3.2 Fabric Preform Characterization

Determining the compaction and permeability behavior of the preform as a function of the fiber volume fraction constitutes preform characterization. Information obtained from such characterization forms vital input data for RTM process modeling [5]. Extensive studies on preform characterization have been conducted at Virginia Tech [33-36]. Details of preform characterization techniques, considerations, and results are available in ref. [34].

3.3.2.1 Preform Compaction Behavior

In the fabrication of fabric composite laminates, pressure is applied on the dry preform to compress, or compact, the fabric preform to the desired thickness. Usually, the preform is held compressed at this thickness during resin infiltration and until the resin is fully cured. In RTM, a net shape manufacturing process, it is necessary to compact the preform to the final thickness of the mold before the resin is infiltrated. The fiber volume fraction, v_f, is defined as the ratio of the volume of the fibers to the total volume of the fabric preform. Typically, the preform occupies the entire volume of matched molds used in RTM. That volume not occupied by the fibers, also called "porosity", is the volume available for the infiltrating resin. The term porosity as applied to fabric prefroms is related to the fiber volume fraction and is different from porosity in the final composite which results from the presence of voids.

Therefore, knowing the desired composite fiber volume fraction, the required thickness of the fabric preform can be determined from the following expression [33],

$$v_f = \frac{n}{t_{fp}} \sum_{i=1}^{N} \frac{\xi_i}{(\rho_f)_i} \tag{3.1}$$

where, t_{fp} is the thickness of the fabric preform constructed by stacking "n" plies of the woven fabric. The fabric areal weight, ξ, is simply the weight of the fabric per unit area. The fiber density is represented by ρ_f. Eq. (3.1) represents a general case where each ply may be of different fiber densities and areal weights. If every ply in the preform stack is of the same fabric material (i.e., of the same areal weight and fiber density) then the above equation reduces to

$$v_f = \frac{n\ \xi}{t_{fp}\ \rho_f} \tag{3.2}$$

Characterizing the compaction behavior of a stacked multiple ply fabric preform involves the development of a relation between the applied compaction pressure and the resulting preform thickness, and hence the fiber volume fraction. Fig. 3.2 shows a schematic arrangement to determine this behavior experimentally.

Investigations of the compaction behavior of dry fabric preforms have been conducted in the recent years at Virginia Tech [33-36]. The procedure involves applying a known compaction load to a n-ply fabric preform and measuring the resulting thickness.

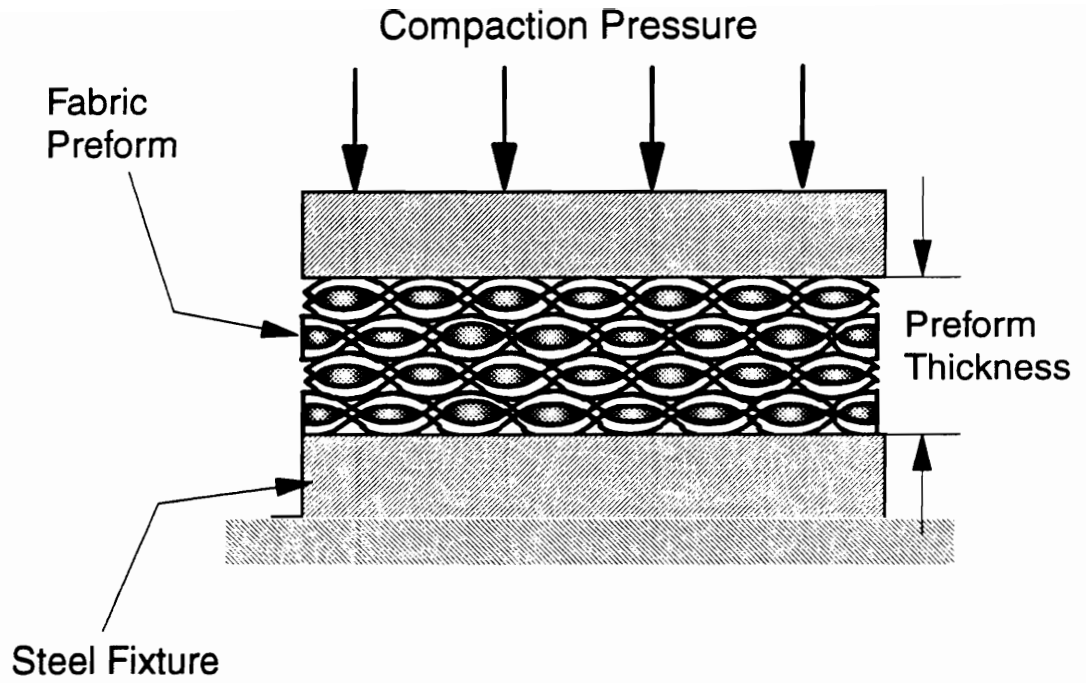

Figure 3.2 Schematic representation of the method to study fabric preform compaction behavior.

A computer controlled test apparatus, developed at Virginia Tech by Fingerson [35], uses a displacement transducer to accurately determine the preform thickness and a load cell to measure the applied load. Knowing the fabric areal weight and the fiber density, the fiber volume fraction is determined from Eq.(3.2). From the applied load and preform area, the compaction pressure, P_{comp} , is calculated. An empirical relation is used to relate fiber volume fraction to the applied compaction pressure, as follows

$$v_f = a\ (P_{comp})^b \tag{3.3}$$

where the parameters a and b are constants obtained by a power-law regression fit to the data from compaction tests.

During the manufacture of composites in a hot-platen press, it is necessary to apply and maintain the compaction pressure on the preform. The magnitude of the applied pressure will depend on the designed fiber volume fraction and the compaction behavior of the fabric. In matched molds designed to produce composite laminates of a specific thickness, an appropriate compaction pressure should be applied to maintain the desired fiber volume fraction and to avoid leakage of the infiltrating resin. In cases where vacuum is used to draw the resin into the mold, insufficient compaction pressure will result in the ingestion of ambient air into the composite thereby causing voids to occur.

3.3.2.2 Preform Permeability

A fabric preform is considered to behave as a porous medium and the flow of a fluid through the preform obeys D'Arcy's law. Permeability of a porous medium is a measure of the resistance offered to fluid flow. In RTM, the permeability of the preform influences the selection of injection/outlet ports, injection strategy and injection pressures. The degree of difficulty of RTM processing increases with decreasing preform permeabilities. A variety of factors affect preform permeability, including yarn bundle size, weave type/balance, interlace concentration, crimp angle, float length, and fiber volume fraction [25]. However, once a preform material is chosen, permeability has a direct dependence only on the fiber volume fraction.

Permeability measurements are performed using fixtures specifically designed for this purpose. A schematic diagram of a permeability fixture developed at Virginia Tech [33] is shown in Figure 3.3. This fixture is used to measure the in-plane permeability of a fabric preform. In a recent work, Fingerson et al. [35], have developed an advanced facility for permeability measurements. This computer controlled facility provides improved precision in measurements. Through the use of sensors and computer data acquisition, continuous measurements are made possible with the potential to calculate permeabilities in real time.

Two in-plane directions are typically associated with woven fabrics, the warp and the fill directions. The direction of the fabric roll is considered the warp direction. Usually, the permeabilities in these two directions are measured in separate tests.

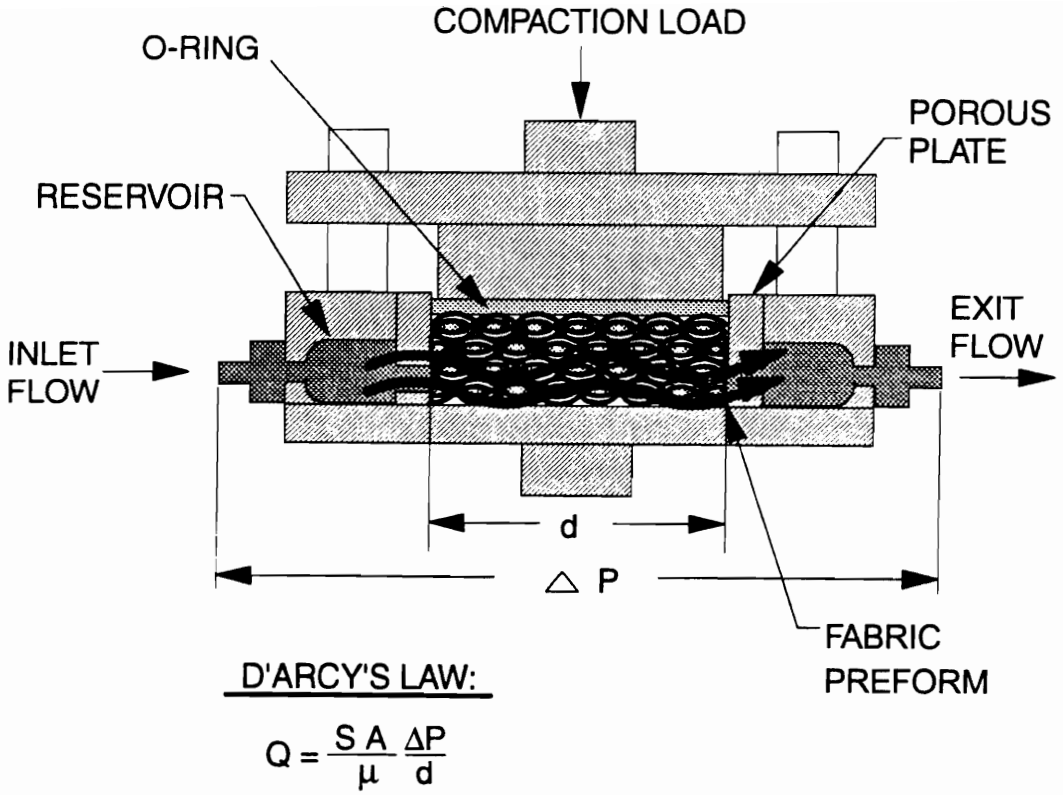

Figure 3.3 Schematic representation of a fixture to measure inplane permeability behavior of fabric preforms.

The permeability measurement procedure first involves cutting the woven fabric into 152 mm by 152 mm (6"x 6") plies for the Virginia Tech fixture. The desired number of plies are stacked, with all plies oriented in the same measurement direction, and placed into the cavity of the fixture. The fabric is then compacted by the plunger to the desired thickness or fiber volume fraction. A test fluid, corn oil, is pumped through the preform material at a constant flow rate. The pressure drop, ΔP, resulting from the flow of the fluid through the fabric is measured by pressure taps located at the inlet and outlet of the fixture.

By knowing the distance, L, over which the pressure drop occurs, and the flow rate, q, the viscosity of the test fluid, μ, and the cross sectional area normal to the flow, A, the permeability of the preform, S, can be calculated from D'Arcy's law which relates these parameters as

$$q = \frac{S}{A\mu} \frac{\Delta P}{L} \tag{3.4}$$

The pressure drop is measured for a series of flow rates at a given level of compaction or fiber volume fraction. A linear regression curve is fit to the flow rate-pressure gradient data and the slope ($S/A\mu$) gives the average permeability of the fabric. This process is repeated at various levels of preform compaction to obtain a relationship between the preform permeability and fiber volume fraction. An empirical, power law relationship between the fiber volume fraction and the corresponding permeability is developed similar to Eq.(3.3) for compaction and is given as

$$S = a\ (\ v_f\ )^b \tag{3.5}$$

where, parameters a and b are obtained from a non-linear least squares regression fit of the permeability-fiber volume fraction data. Also, the permeability is measured in both, the warp (S_{warp}), and the fill (S_{fill}) directions.

3.4 Composite Laminate Manufacture

3.4.1 Processing Cycles For Liquid Molding.

In the manufacture of composites by liquid molding, two main processing steps are identified as

(a) infiltration of the liquid resin into the dry preform

(b) full curing of the infiltrated preform to obtain the composite

To successfully complete the two steps, the process parameters associated with the two stages must be carefully selected. The critical process variables are the resin/mold temperatures, compaction and injection pressures.

Figure 3.4 shows a schematic arrangement of the Pressure-Injection Resin Transfer Molding (PI-RTM) process. In this process, the dry fabric preform is placed in a matched mold, usually made of metal, and compacted to the designed dimensions upon mold

closure. Liquid resin is then pumped into the mold cavity until the preform is fully infiltrated. Resin injection may be accomplished either by using a mechanical pump or with the pressure pot arrangement shown in Fig. 3.4. The resin is placed inside the pressure pot and is forced into the mold by pressurizing the pot with compressed air.

In the resin film infusion (RFI) process, a film of resin is cast and placed on the bottom of the mold. The dry preform is then stacked over the resin film. The resin flows into the preform under the application of heat and pressure. A schematic layout of the preform and resin film arrangement in the mold for the RFI process is shown in Fig. 3.5. Typically, this process is preferred for the manufacture of fabric composites with very viscous resin systems [40]. The mass of the resin film has to be accurately determined based on the compacted dimensions and the fiber volume fraction of the part being manufactured. In this process, the preform compaction and resin infiltration occur simultaneously. Unlike PI-RTM, where the preform is held compacted upon mold closure to the final dimensions of the mold cavity before infiltration.

In either process, temperature and pressure need to be properly selected. Temperature is perhaps the most important variable in the design and control of the RTM process. Both, the infiltration and the curing stages of the RTM process are strongly influenced by the processing temperature. The characteristics of the resin system drives

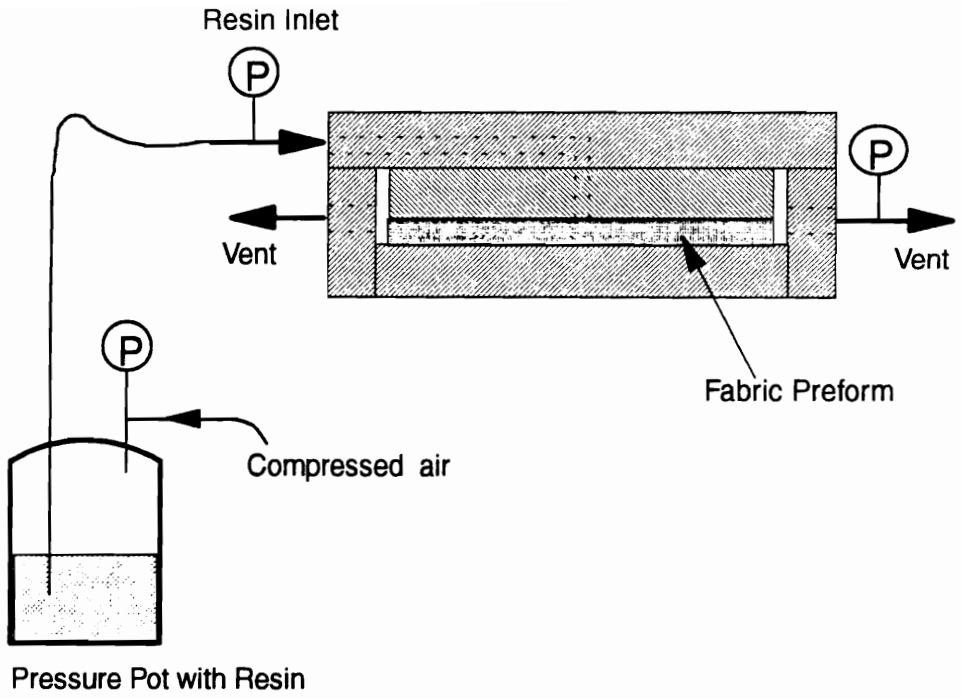

Figure 3.4 Schematic representation of a small scale setup for composite manufacture by the Pressure-Injection Resin Transfer Molding process.

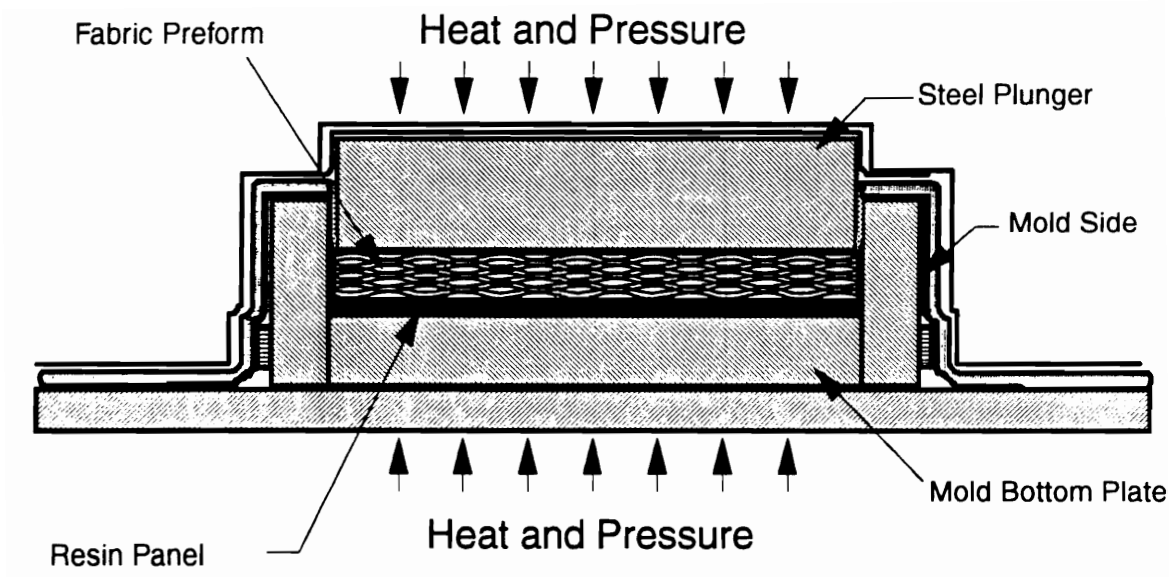

Figure 3.5 Schematic representation of a typical setup for composite manufacture by the Resin Film Infusion process.

the choice of injection and cure temperature. In RTM, most resin systems are injected at an elevated temperature in order reduce the resin viscosity and process cycle times [37]. The temperature of the mold may either be at or above the resin temperature.

The injection temperature of a catalyzed thermosetting resin system must be selected carefully. Elevated temperature reduces the magnitude of the melt viscosity but also accelerates cure, thereby reducing available injection time and increasing the required injection pressure. At lower temperatures which are closer to the ambient temperature, however, the magnitude of the melt viscosity may not be sufficiently reduced to ensure complete infiltration. Such conflicting effects result from the complex dependence of viscosity of thermosetting resins on temperature and cure state [38]. The cure state in turn, depends on temperature and prior thermal history. Further, thermosetting resin systems do not have a constant viscosity at elevated temperatures [38-42].

Temperature control provides the only means to control resin viscosity during injection. The selection of the appropriate temperature depends on the knowledge of the "right" resin viscosity. Hackett, et. al., [43], define an easily processed RTM resin as one having "sufficient time at sufficiently low viscosity to allow complete wet-out of all of the reinforcement and removal of any residual air pockets before the resin reaches gelation". The need for low resin viscosity is stated in literature concerned with the RTM process. However, the term "sufficiently low viscosity" is not quantified. Hayward and Harris [37] report that while a viscosity of ~0.25 Pa-s is generally considered appropriate, a wide range, 0.1-3.5 Pa-s was successfully used in a study of quality of RTM moldings.

Other researchers quote optimum resin viscosities of ≤ 0.5 Pa-s [44,45], and 0.1-0.25 Pa-s [46,47].

A typical time-temperature profile, also known as the cure cycle, is shown in Fig. 3.6. This is an example of a three stage cure cycle, referring to the three temperature steps, that the mold assembly is subjected to during infiltration and cure. Region 1, represents the initial heating-up or "ramp" at a constant rate up to an injection temperature, T_{inj}. When the mold temperature reaches this temperature, the resin injection or infiltration is started. The temperature is maintained constant during infiltration. The time at which the infiltration process is started is denoted t_s, and t_f, is the cycle time at which infiltration is completed. The time taken for infiltration is simply the difference between t_f and t_s.

On completion of the infiltration process, the matrix resin must be cured out. In order to carry out the curing process, the mold temperature is raised above the injection temperature, at a constant heating rate, to an initial hold temperature, denoted T_{ih} in the figure. This temperature is usually about 30-60 °C below the final cure temperature. This step, however, may be omitted depending on the resin system.

At the end of the hold period in region 2, the temperature is increased at a constant heating rate to a final cure temperature, T_{fh}. Region 3 represents the higher temperature hold wherein the composite is fully cured. This is then followed by a cool down to the ambient temperature.

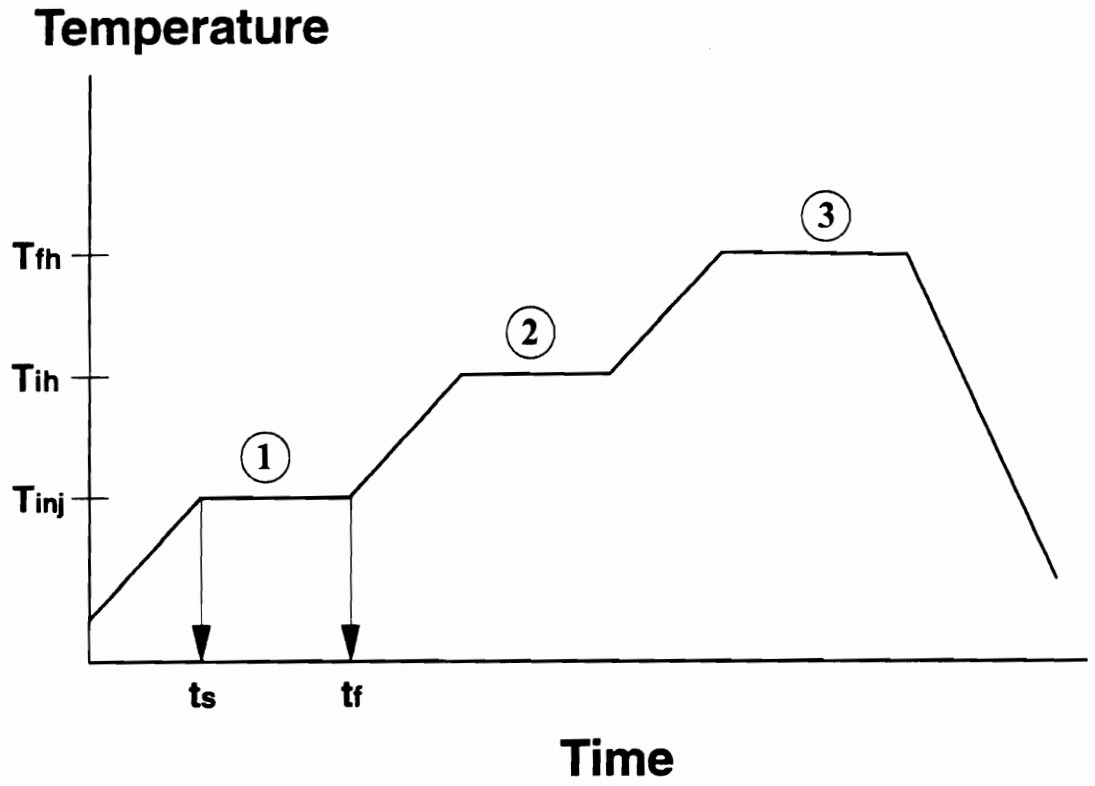

Figure 3.6 Example of a typical cure cycles showing different events during processing by liquid molding techniques.

Further, the choice of T_{fh} is based on the curing behavior of the resin. The temperature of the final hold must be sufficiently high in order to fully cure the resin, however, not so high as to cause thermal degradation.

In this study, the choice of the method of infiltration and the temperature, T_{inj}, for the various resin systems under investigation were based on the viscosity behavior. The temperatures and the duration of the initial and final hold steps were chosen either based on previous work or on the recommendations of the resin manufacturer.

3.4.2 Equipment and Procedure

The composite laminates manufactured for this investigation were of dimensions 152 x 152 mm (6 x 6 in) and of two different thicknesses. While the majority of the laminates were made to a nominal thickness of 3.2 mm (⅛ in), a preliminary set of laminates were manufactured to a nominal thickness of 6.4 mm (¼ in) for use in short block compression (SBC) testing.

The 6.4 mm thick laminates were made using the IM7/8HS fabric. In order to obtain a nominal fiber volume fraction of 60%, 16 plies were required as determined by eq. (3.2). All laminates manufactured with the AS4/PW fabric had a nominal thickness of 3.2 mm. Again, based on the fabric areal weight, 18 plies of the AS4/PW fabric were necessary to obtain a desired fiber volume fraction of 60%.

An aluminum mold was used in this investigation for the manufacture of the fabric composites by the PI-RTM and the RFI techniques. The mold consists of three parts, a bottom plate, a "picture" frame, and a top plunger plate. By assembling the bottom plate and the frame together, a mold cavity is created. The mold uses a flat bottom plate or a stepped bottom plate for making a 6.4 mm or a 3.2 mm thick laminate, respectively. A photograph of the mold can be found in Figure 3.7. Injection/vent ports are located on two opposite sides of the picture frame and in the top plunger plate. Further, 1.6 mm diameter blind holes were drilled into the picture frame, on all four sides. These blind holes were drilled into the picture frame to within 2 mm of the mold cavity. These holes were provided to accommodate thermocouples used to monitor the mold temperature during processing. A through hole into the mold cavity would only provide a leakage path for the resin.

In addition to the three main mold elements, a spacer plate with a machined channel is placed on top of the plunger plate to provide a flat bearing surface against the press platens. The machined channel provides access for routing resin tubing to the center port. Also, O-rings are used to seal the surfaces between the bottom plate and the picture frame, and between the top plate and the picture frame.

For the manufacture of laminates by the PI-RTM technique, a pressure pot was used to inject the resin, under a constant pressure, into the mold cavity containing the fabric preform. The pressure pot used was rated to operate at a maximum pressure of about 750 kPa (110 psi) at room temperature.

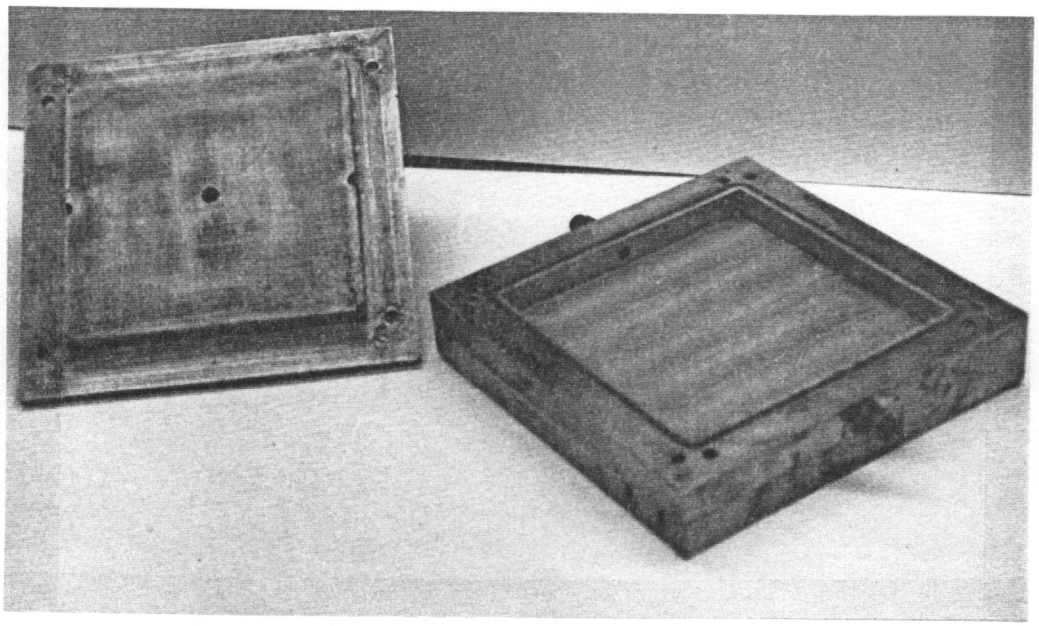

Figure 3.7 Photograph of the aluminum mold used to manufacture composites by liquid molding.

A blanket heater surrounding the pressure pot facilitated resin injection at elevated temperatures. For safety of operation, the maximum pressure at elevated injection temperatures was limited to about 650 kPa (95 psi).

In a typical elevated temperature injection, a measured amount of the resin is placed in a container which is then placed inside the pressure pot. A heat transfer oil (Mobiltherm 610) is used transport the heat from the walls of the pressure pot to the resin container. The temperature of the resin is maintained at the injection temperature. The mold containing the dry preform is placed between the platens of the computer controlled hot-platen press. The required compaction pressure is applied and the platens are heated to the injection temperature. Once the mold reaches the injection temperature, the pressure pot is pressurized with compressed air and the resin is pumped into the mold through PTFE tubing. The tubing leading up to the mold is also heated with a heating tape to maintain the resin at the injection temperature.

Vents are installed at the inlet and outlet ports of the mold. A bleed line is attached to the resin tubing, close to the mold, to facilitate the removal of air from the lines prior to injection. After the air in the line are bled, the inlet valve is opened allowing the resin into the mold. Thermocouples are used to monitor the resin, mold, and the inlet tube temperatures. Further, in order to measure and control the resin pressure during the injection, a high temperature pressure transducer (Model S from Sensotec, Ohio) is mounted at the mold inlet. A fitting was fabricated to connect the pressure transducer to the resin inlet tubing. The output signal from the transducer is recorded by

the data acquisition system. A sharp fluctuation in the sensor signal when the inlet valve is opened indicates the onset of injection. From the acquired data, the cycle time at which this event occurs can be identified to provide the injection start time, t_s in Fig. 3.6. When the resin is sighted at an exit port, the corresponding cycle time, t_f , can be recorded. Also, a thermocouple placed in the exit port is used to provide an indication of the completion of infiltration. Again, a spike is detected in the output signal when the hot resin comes in contact with the thermocouple.

A typical setup for the manufacture of fabric composite by the PI-RTM technique is shown in Fig. 3.8. The resin enters the mold cavity from the center port in the top plate of the mold and exits from the two side ports after full infiltration of the preform. Also seen in the figure are the pressure pot with the PTFE tubing leading into the mold, and the computer controlled hot-platen press with the mold between the platens.

In the manufacture of fabric composites by the RFI technique, the pressure pot is not used. The side ports and the top center port of the mold are plugged to prevent resin leakage. An appropriate quantity of resin is weighed, cast into a film and placed into the mold cavity. Fabric plies cut to the exact inside dimensions of the mold cavity are stacked on top of the resin film in the mold cavity. The top plate is placed over the moldcavity and the assembly is placed between the platens of the press. The mold is heated to infiltration temperature, and upon reaching the infiltration temperature, compaction pressure is applied, followed by curing of the resin.

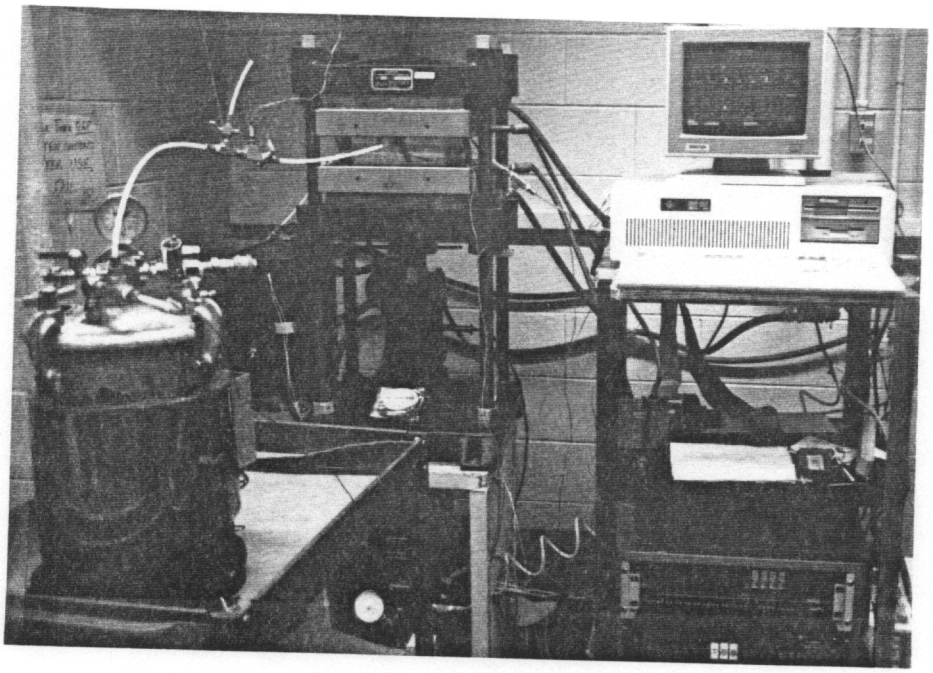

Figure 3.8 Photograph of the setup for composite manufacture by the Pressure-Injection Resin Transfer Molding technique.

A series of AS4/PW fabric reinforced composite laminates were manufactured for end-notched flexure testing. These laminates were manufactured with the untoughened and toughened cyanate ester resin systems and with the 3501-6 epoxy resin system either by PI-RTM or by RFI. In all cases, a 38 mm wide strip of 2 mil thick Kapton® film was placed between the ninth and tenth ply of the 18-ply fabric stack. This strip, placed at one end of fabric preform, extended the entire width of the preform and aided in developing a starter crack at the mid-plane of the fabric composite during testing.

At the end of the process cycle, the platens and the mold were cooled down to ambient temperature and the laminate was easily removed from the mold. A stub of resin from the inlet to the mold, attached to the panel, was carefully removed and identified for later testing.

The injection temperatures, the initial and final hold temperatures, and the duration of the respective hold periods used for all the resin systems considered in this study are given in Table 3.2. These cure cycle parameters correspond to the events described in Fig. 3.6.

Table 3.2 Cure cycle parameters used for composite manufacture with the resin used in this study.

Resin System	T_{inj} [°C]	T_{ih} [°C]	Hold time [min]	T_{fh} [°C]	Hold time [min]
AroCy B10	95	-	-	200	90
VTUFF1520	115	150	20	200	55
VTUFF1525	120	150	20	200	55
VTUFF1530	135	150	20	200	55
VTUFF2020	120	150	20	200	55
RSL 1895/W	85	147	20	177	150
3501-6	110	-	-	177	90

3.5 PHYSICAL AND MECHANICAL TESTING

3.5.1 Physical Testing

In order to evaluate the quality of the fabric reinforced toughened cyanate ester composites manufactured for this study a series of non-destructive tests were performed. Initially, the composites examined by the ultrasonic C-scan technique. However, when fabric composites are C-scanned, dubious results are obtained due the undulations in fabric causing attenuation of the ultrasonic signals. The 6.4 mm laminates could not be scanned at all with the equipment available at Virginia Tech. The C-scan images show that the panel contains voids and imperfections when the composite is actually well consolidated and void free. In this investigation, C-scan was useful in detecting the damaged area in impact testing.

The composites manufactured were grouped into three categories for measurement of the composite density and fiber volume fraction. They were, composites manufactured with IM7/8HS fabric reinforcements for SBC testing, a set of AS4/PW fabric composites manufactured for impact damage evaluations, and a set of AS4/PW fabric reinforced composites for evaluation of fracture toughness properties.

The composite fiber volume fraction was estimated using the density measurement procedure described in Section 2.6.1. Knowing the matrix resin and fiber densities (ρ_m and ρ_f, respectively), the fiber volume fraction is determined from the rule of mixtures given by

$$\rho_c = \rho_f v_f + \rho_m v_m \tag{3.6}$$

where, ρ_c is the composite density, v_f and v_m are the fiber and matrix volume fractions, respectively. By rearranging eq. 3.6, the fiber volume fraction can be solved for, recognizing that $v_f + v_m = 1$, as

$$v_f = \frac{\rho_c - \rho_m}{\rho_f - \rho_m} \tag{3.7}$$

Also, the fiber volume fraction of the composite can be estimated from the final thickness of the laminates (see eq. 3.2), assuming that the fibers are uniformly distributed in the composite. This procedure requires that the fabric areal weight, the number of plies in the composite, and the fiber density be known, and provides an estimate of the fiber content in the composite. Again, from the rule of mixtures (eq. 3.6), the composite density can be calculated based on this estimate of fiber volume fraction and the resin and fiber densities.

The composite density and the fiber volume fraction of composite laminates can be estimated by these two methods. In the second method, based on the composite thickness measurements, it is assumed that the fraction of the volume occupied by the fiber is constant for a given composite thickness. Further, in calculating the composite density by this method, it is assumed that the matrix resin completely occupies the fraction of the composite volume *not* occupied by the fibers. That is, this represents an

ideal composite in which no voids are present. However, real composites, almost always, contain voids to some degree. The level of the void content can vary from visibly porous to virtually undetectable. An argument can be made that in a given volume of composite, the voids can only displace the volume available for the matrix resin to occupy. The composite density measurement based on the liquid displacement method is influenced by the inevitable presence of voids. Hence, the composite density estimated by these two methods differ owing to the existence of voids.

In this investigation, void contents in the composites were estimated following an approach similar to the ASTM D 2734-91 Standard Test Methods for Void Content of Reinforced Plastics [50]. The ASTM test procedure involves measuring densities of the matrix resin, the reinforcement and the composite by the liquid displacement technique (ASTM D 792 test standard [51]). The composite density measured is called the measured density (M_d). The resin content is measured by burn-off or by acid digestion techniques, in accordance with ASTM test method D 2584 [52]. From the measured resin content and the fiber and resin densities, the composite density is computed and termed the theoretical density (T_d). The void content is estimated as

$$v_v = 100 \frac{(T_d - M_d)}{T_d} \tag{3.8}$$

from the difference between the theoretical and measured densities.

Where, v_v is the void content in the composite expressed in volume percent. In the present investigation, the procedure was modified slightly by using thickness measurement method (eq. 3.2) to estimate the theoretical density, T_d.

In both, the ASTM and the present methods of void content measurement, potential sources of error in the estimation of void content exist. The resin density is assumed to be the same in the composite as in the bulk resin. Void content estimates may seem lower than the actual content when bulk resin densities are used in the calculations [50]. The ASTM standard ascribes this source of error to a higher resin density in the composite as compared to that in bulk resin. This difference, however, results only in a small magnitude of error. Further, surface porosity can exist in composite laminates. The extent of such surface porosity can influence the measured (by liquid displacement) composite density. In cases of extensive porosity, the ASTM standard recommends coating the specimen surfaces with a known amount of a sealing agent, of a known density. Corrections to the calculations will then be necessary to account for the added material.

3.5.2 Microscopy

The cured resin stubs obtained from composite manufacture were used in transmission electron microscopy (TEM) analysis. This analysis was performed on the stubs from the AS4/PW carbon fabric, toughened cyanate ester composites. The objective of this analysis was to detect the phase-separated morphology in a resin sample, which

had also been subjected to the same thermal cure cycle as the composite. The resin samples were microtomed and stained with ruthenium oxide to enhance the contrast between the thermoset and the thermoplastic phases. TEM photomicrographs were then produced of the morphologies considered most representative of the specimen.

3.5.3 Gas Gun Impact Testing

Evaluation of impact damage properties of the carbon fabric composites manufactured were performed with the gas-gun impact testing instrument developed at Virginia Tech. The panels manufactured by liquid molding techniques were machined into four 65 mm x 65 mm test specimens. The test, originally developed by Teh [32], was is performed on quasi-isotropic composites constructed from prepreg tapes. In this investigation, only fabric reinforcements were used. This test was performed to evaluate the impact damage resistance of the epoxy (RSL1895/W), the untoughened and toughened cyanate ester matrix composite material systems.

3.5.4 Compression Strength After Impact

The composite specimen subjected to gas-gun impact damage were evaluated for impact damage tolerance properties. Compression tests performed on specimens machined from the damaged impact specimens provide information on the load carrying ability of the material systems, and is referred to as the Compression After Impact (CAI) test. The residual compression strength of the composites characterize the *impact damage tolerance*

of the material systems. The procedure used in this investigation was developed by Teh [32].

A compression test coupon of dimensions 52 mm x 25 mm is machined from the center of the impact specimen such that the impact location is at the center of the coupon. Fig. 3.9 shows the location of the compression after impact coupon with respect to the impact specimen and the dimensions of the test coupon. The CAI tests were performed using compression fixture developed by Gürdal [53]. Undamaged compression coupons were tested to provide a reference for comparing with the damaged specimens. From this test procedure, the residual compressive strength of the composites damaged at various incident energies is obtained.

3.5.5 Short Block Compression

Short Block Compression (SBC) tests were performed on a of fabric composites, manufactured by the RTM process. The material systems used for this test were the AroCy B10, VTUFF1525, and the RSL1895/W, reinforced with 16 plies of IM7/8HS woven fabric. The composites were machined to provide test specimen in both, the warp and fill directions of the fabric preform. The SBC test specimen is 44 mm x 38 mm (1.75 in long by 1.5 in wide) and of a nominal thickness of 6.35 mm (0.25 in).The edges of the specimen are ground parallel. Fig. 3.10 shows a photograph of the SBC fixture with a test specimen.

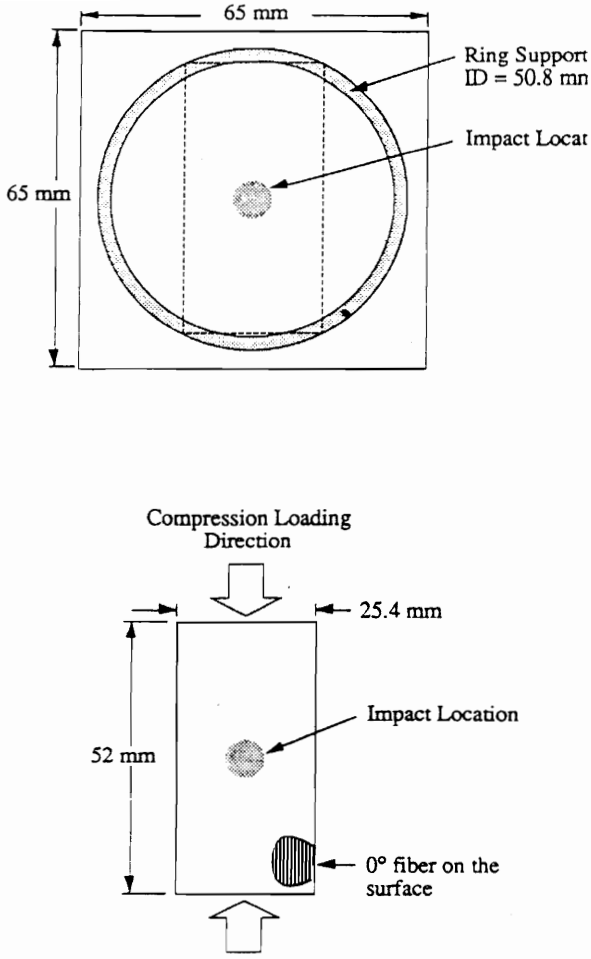

Figure 3.9 Location and dimensions of the compression-after-impact test coupon (fromTeh [32]).

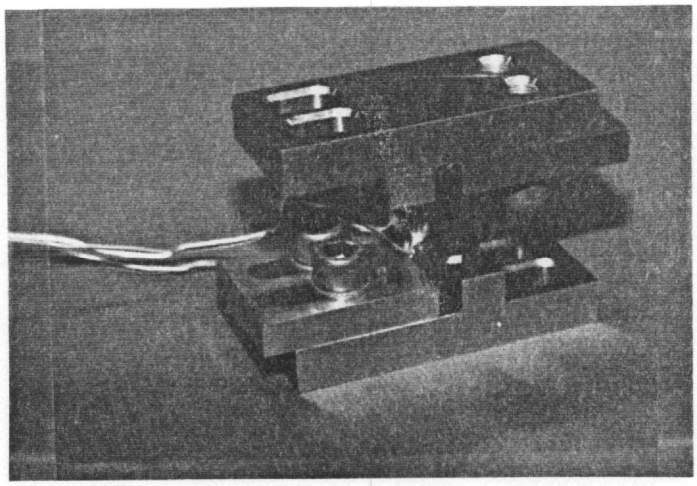

Figure 3.10 Test fixture and specimen for the short block compression test.

The specimens were carefully loaded in the test fixture and tested to failure on a Tinius-Olsen universal testing machine at a crosshead speed of 1.27 mm/min (0.05 in/min). In this evaluation, only the strengths at failure were determined for the three material systems mentioned above.

3.5.6 End-Notched Flexure

The recognition of interlaminar cracking or delamination as a significant fracture mode has led to numerous research studies to characterize the interlaminar fracture behavior of composite materials. The weakest failure mode in laminated composite material is delaminations [54]. Interlaminar cracks grow under the action of tensile, shear, or compressive stresses, especially in the vicinity of holes and free edges [55].

Further, low energy impact can initiate interlaminar defects, which subsequently may grow under loading. The resistance to delamination is an important issue in the evaluation of damage tolerance of composite materials. The critical strain energy release rate, G_c, is a key parameter used in the study of delamination type failure thorough a fracture mechanics approach [54-57].

Interlaminar crack propagation occurs under different modes. There are three basic interlaminar fracture modes shown schematically in Figure 3.11 [58].

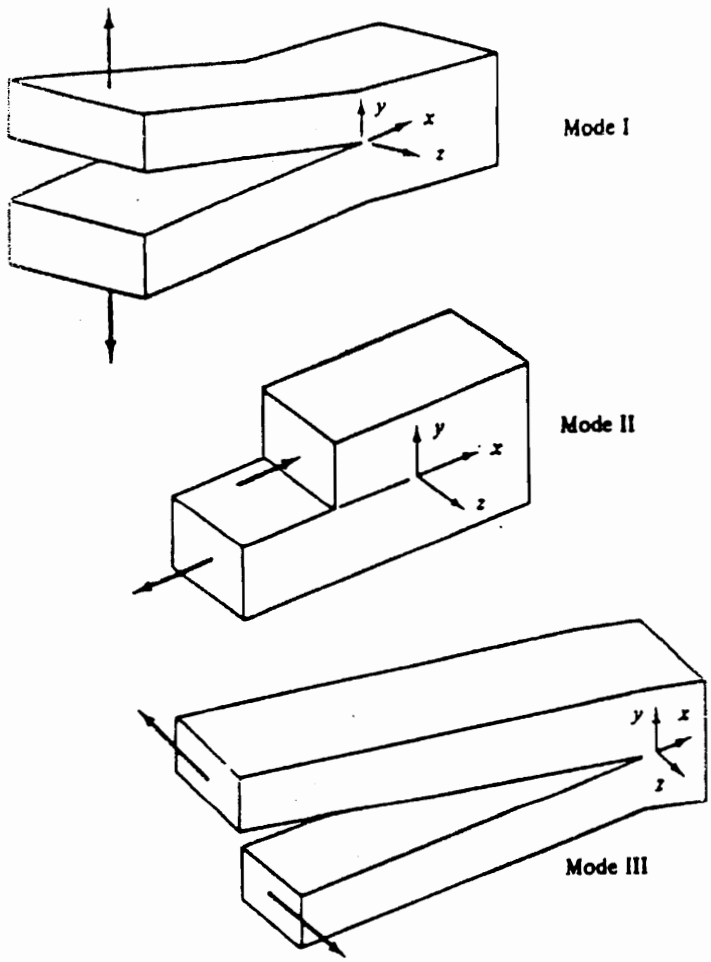

Figure 3.11 Interlaminar crack propagation modes (from Wilkinson [62]).

In mode I, a crack is propagated by a tensile forces acting normal to the plane of crack propagation. Mode II crack propagation occurs when shear forces act in the plane of the crack front, and in the direction of crack propagation. Under mode III, crack propagation occurs due to shear forces acting in the plane of the crack front but in a direction normal to that of crack propagation. These three modes are also referred to as the peel or opening mode (mode I), the sliding shear mode (mode II), and the tearing or twisting shear mode (mode III) [54]. A typical interlaminar fracture may occur under one or more of these three modes.

Traditionally, the double cantilever beam test is used to experimentally determine the strain energy release rate, G_{Ic}, a measure of the interlaminar fracture toughness under mode I conditions. Mixed mode tests exist when the crack is propagated in a combination of modes. For example, interlaminar fracture toughness as evaluated by the cracked lap-shear (CLS) specimen combines modes I and II in the crack propagation, wherein the mode I component was evaluated to be about 20% [56]. For pure mode II studies, the end-notched flexure specimen was developed by Russell and Street [56]. Figure 3.12 shows the details of the specimen geometry and loading.

The specimen for the end-notched flexure (ENF) test as originally designed by Russell and Street is 150 mm long and about 20 mm wide, and 3 mm thick. A starter crack of a desired length is introduced at one end of the specimen. This is usually accomplished by placing a film about 2 mil thick of PTFE or a similar material along the mid-plane of the laminate during manufacture. Usually, the film extends about 40 mm

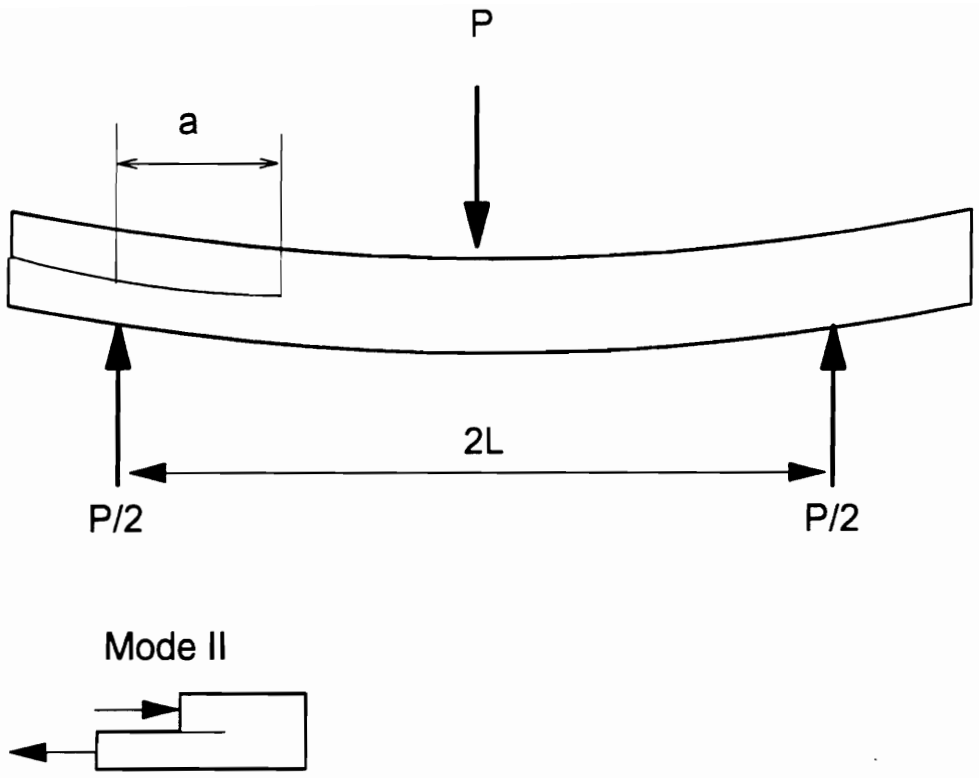

Figure 3.12 Geometry and loading details of the end-notched flexure test specimen for evaluating the mode II strain energy release rate.

from the end of the specimen. The specimen is loaded in a three-point flexure test fixture with a span length (2L in Fig 3.12) of 100 mm until an initial crack length, a_0, of 25 mm, measured from one support pin, extends into the span. Thus, the root of the starter crack would lie midway between the end support and the center loading pin, resulting in the crack length to half-span ratio, a/L, of 0.5. Whitney [54] recommends the use of ASTM Standard D-790 as a general guide for selecting L/h (the span to thickness ratio) and loading rates. For graphite/epoxy materials, a L/h ratio of 32 is recommended. The ENF test is performed by loading the specimen in flexure until a crack grows from the root of the starter crack. This crack grows rapidly until it reaches the mid-span of the specimen and arrests at the position of the load nose.

By providing a large overhang at the unnotched end, the specimen is shifted over and reloaded to obtain a second fracture energy value. The unstable nature of the crack growth allows only two values of G_{IIc} to be obtained. However, the first value of fracture energy obtained by extending the crack from the root of the starter crack is usually higher and is usually ignored because it is affected by the presence of a resin rich pocket at the root. Other researchers have precracked the ENF specimen in mode I, before performing the test to measure G_{IIc} [43]. However, the procedure outlined by Russell and Street [55,56] and Whitney [54] involves precracking the specimen to extend the initial crack beyond the starter crack root in flexure mode.

In the ENF test, the strain energy release rate in mode II is determined from the Irwin strain energy release rate relationship [55],

$$G_c = \frac{P^2}{2b}\frac{dC}{da} \tag{3.9}$$

where, G_c is the critical strain energy release rate, P is the critical load for crack extension and b is the specimen width. The term dC/da represents the rate of change of the compliance, C, with crack length, a. For determining the mode II fracture energy by the ENF test procedure, Russell and Street developed a compliance versus crack length relationship based on a beam theory analysis, expressed in the form

$$C = \frac{\delta}{P} = \frac{(2L^3 + 3a^3)}{16E_x^b bh^3} \tag{3.10}$$

where, δ is the beam deflection under the load nose, E_x^b is the effective bending modulus of the specimen, h is the half-thickness of the specimen. Substituting eq.(3.10) into eq.(3.9), the expression for the critical strain energy release rate in mode II is obtained as follows:

$$G_{IIc} = \frac{9a^2P_c^2}{64E_x^b b^2h^3} \tag{3.11}$$

Again, by combining eqs. (3.10) and (3.11), an alternate form of the expression for G_{IIc} is obtained as

$$G_{IIc} = \frac{9a^2P_c\delta_c}{4b(2L^3+3a^3)} \quad (3.12)$$

where, P_c and δ_c are the critical values of the load, P, and the deflection,δ, associated with the onset of crack growth [54].

While the test was originally developed for unidirectional laminates this method has been applied to woven fabric (IM7/plain weave) reinforced composite laminates by Hackett et al [43]. In the present investigation, the ENF tests were performed on AS4/plain weave carbon fabric composites. The resin systems used for the tests included the untoughened and toughened cyanate ester resin systems and the 3501-6 epoxy resin system. The laminates were manufactured by either the PI-RTM or the RFI processes. A 2 mil thick film of Kapton® was used to provide the starter crack. The composites were successfully manufactured despite of the challenge posed by the presence of the Kapton® film along the mid-plane of the 18-ply preforms, especially in the case of the laminates manufactured by the RFI process. Test specimens were cut from the laminates to the required dimensions on a diamond saw. A L/h ratio of 32 was used and the specimens were tested on an Instron testing machine interfaced to a computer. The specimens were loaded at a rate of 1 mm/min and the load-deflection data were acquired at a rate of 5 samples per second on a PC with the Labview© data acquisition and control software. The compliance of the specimen at different crack lengths was measured by loading the specimen to a maximum load of about 150 N. The new crack position was

marked and the specimen was loaded so as to maintain the a/L ratio of 0.5. The specimen was then loaded to failure. Here, failure is defined as the point at which the crack rapidly propagates to the center load nose and the load drops sharply.

The mode II strain energy release of composite material systems appears to be an important parameter as an indicator of the impact damage tolerance of composites materials [63,65]. The results obtained by Recker, et al. [63], based on impact damage studies of certain toughened thermosets, show a strong linear correlation between the compression strength after impact and G_{IIc} for both, AS4 and IM7 fiber reinforced composites. They conclude that improved mode II fracture toughness translates into higher compression after impact strength. While these results were for unidirectional composites, the test data generated by Hackett et al [43] on IM7 fabric reinforced composites manufactured by the resin transfer molding process also indicate a similar linear correlation. The plot shown in Figure 3.13, indicates that the compression strength after impact increases with increasing G_{IIc}. Caution must be exercised when comparing the G_{IIc} of woven fabric reinforced composites with that of unidirectional composites. It is, however, reasonable to make comparisons when the reinforcing fabric is of the same material and construction and only the matrix material is varied.

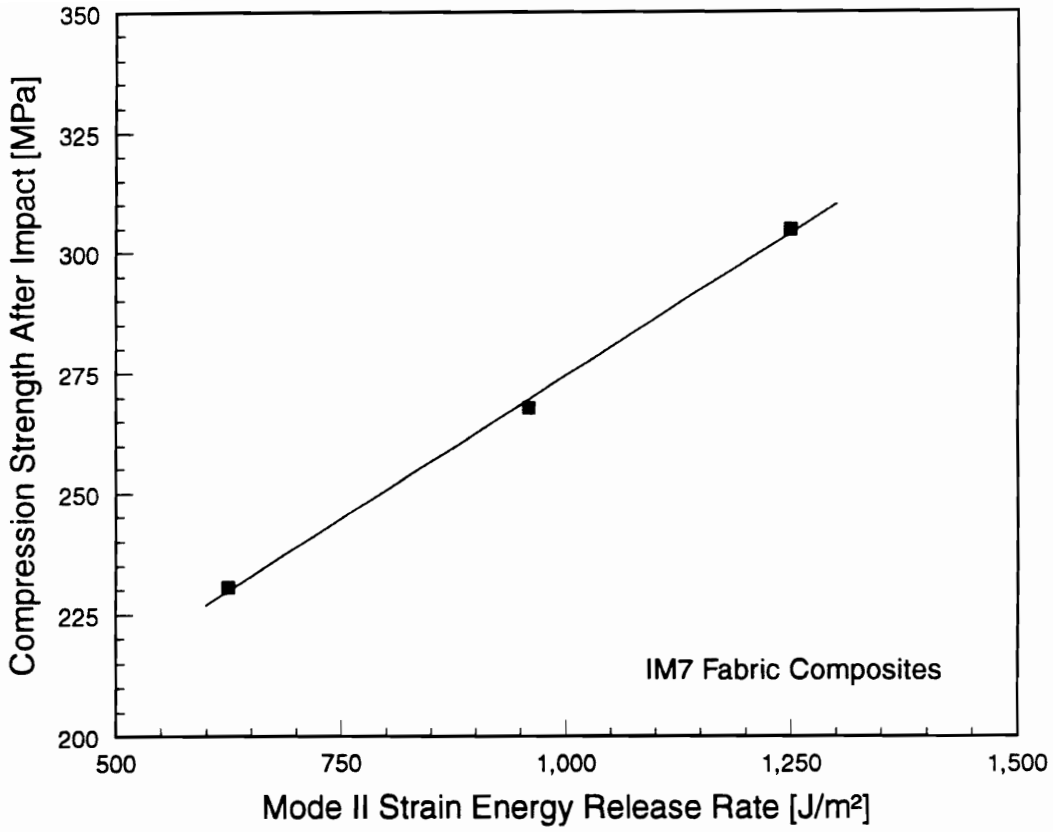

Figure 3.13 Correlation between CAI strength and the mode II fracture toughness for woven fabric composites (from Hackett et al [43]).

3.6 RESULTS AND DISCUSSION

3.6.1 Material Characterization

The viscosity behavior of the resin systems used in this investigation were measured as a function of temperature and time. The Shell RSL 1895/W epoxy resin system was characterized by Hammond, et. al. [34] and the Hercules 3501-6 epoxy system was characterized by Chiou and Letton [60]. Of the four different toughened cyanate ester resins, viscosity models were developed only for VTUFF1525 as described in Chapter 2.

The viscosity-time profiles generated in this study were used to select appropriate injection temperatures. For the untoughened cyanate ester, AroCy B10, the melt viscosities at 90 and 100 °C were measured. At these temperatures, the minimum resin viscosity were about 0.008 and 0.006 Pa·s, respectively. Also, the viscosity remained nearly constant for an extended period of time indicating a negligible cure reaction rate for the temperature.

The four toughened cyanate ester resin systems had much higher melt viscosities compared to the AroCy B10 system due to the presence of the dissolved thermoplastic toughener. Fig. 3.14(top) shows the isothermal viscosity-time profiles generated for the VTUFF1520 resin system at 115, 125, 135, and 150 °C. The initial viscosity at 115 °C was about 0.6 Pa·s, an increase of two orders of magnitude over the untoughened system at 90-100 °C. Further, with increasing measurement temperature, the increase in viscosity is accelerated as a result of the higher rates of cure reaction.

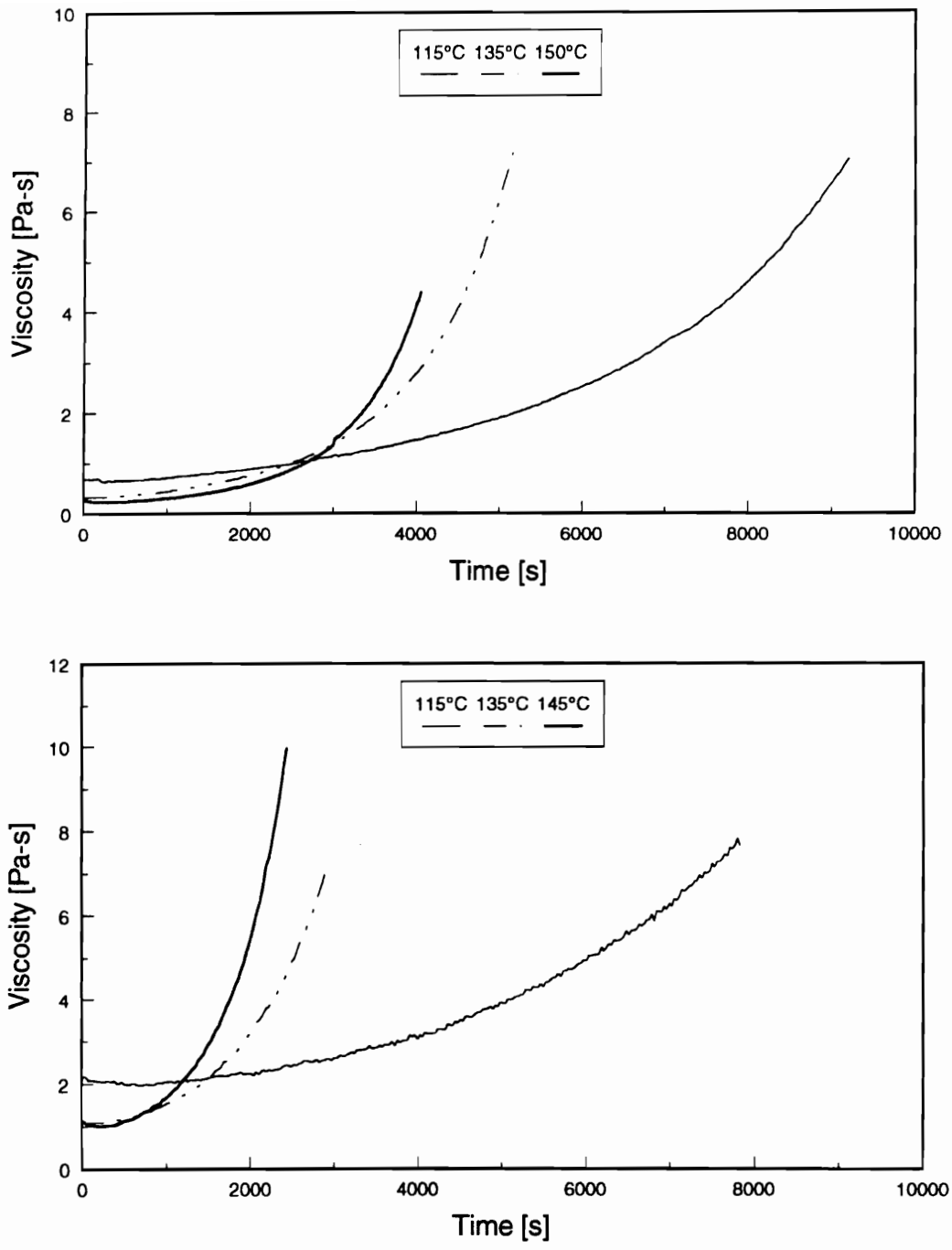

Figure 3.14 Viscosity time profiles at different temperatures for VTUFF1520 (top), and for VTUFF1525 (bottom).

These profiles serve as a guide in selection of the resin temperature such that sufficient time is available for injection before the onset of the rapid increase in viscosity. The measurements were terminated soon after the onset of this rise in viscosity due to operating constraints of the viscometer used for this investigation. The measured viscosity-time profiles for VTUFF1525 are shown in Fig. 3.14(bottom), and those for VTUFF1530 and VTUFF2020 are shown in Figs. 3.15(top) and (bottom), respectively.

In Fig. 3.16, the measured isothermal viscosity-time profiles for the four toughened cyanate ester resin systems at 135 °C are shown. It is evident from the plot that the initial viscosities of the toughened resin systems increase with increasing concentration of the toughener. Also, comparing the curves corresponding to VTUFF1520 and VTUFF2020, the effect of increasing the molecular weight of the toughener, while keeping the concentration the same, is seen. The initial viscosity of VTUFF2020 is nearly three time higher than that of VTUFF1520. The rates of viscosity increase are different for each of the four resin systems. This result seems to indicate the influence of toughener concentration and molecular weight not only on the initial melt viscosity, but also on the cure behavior.

The results of the compaction characterization for the AS4/PW fabric material is shown in Fig. 3.17. The solid line represents the power law fit to the data. The parameters a and b in eq. 3.3 were determined as a = 0.2149, and b=0.1331.

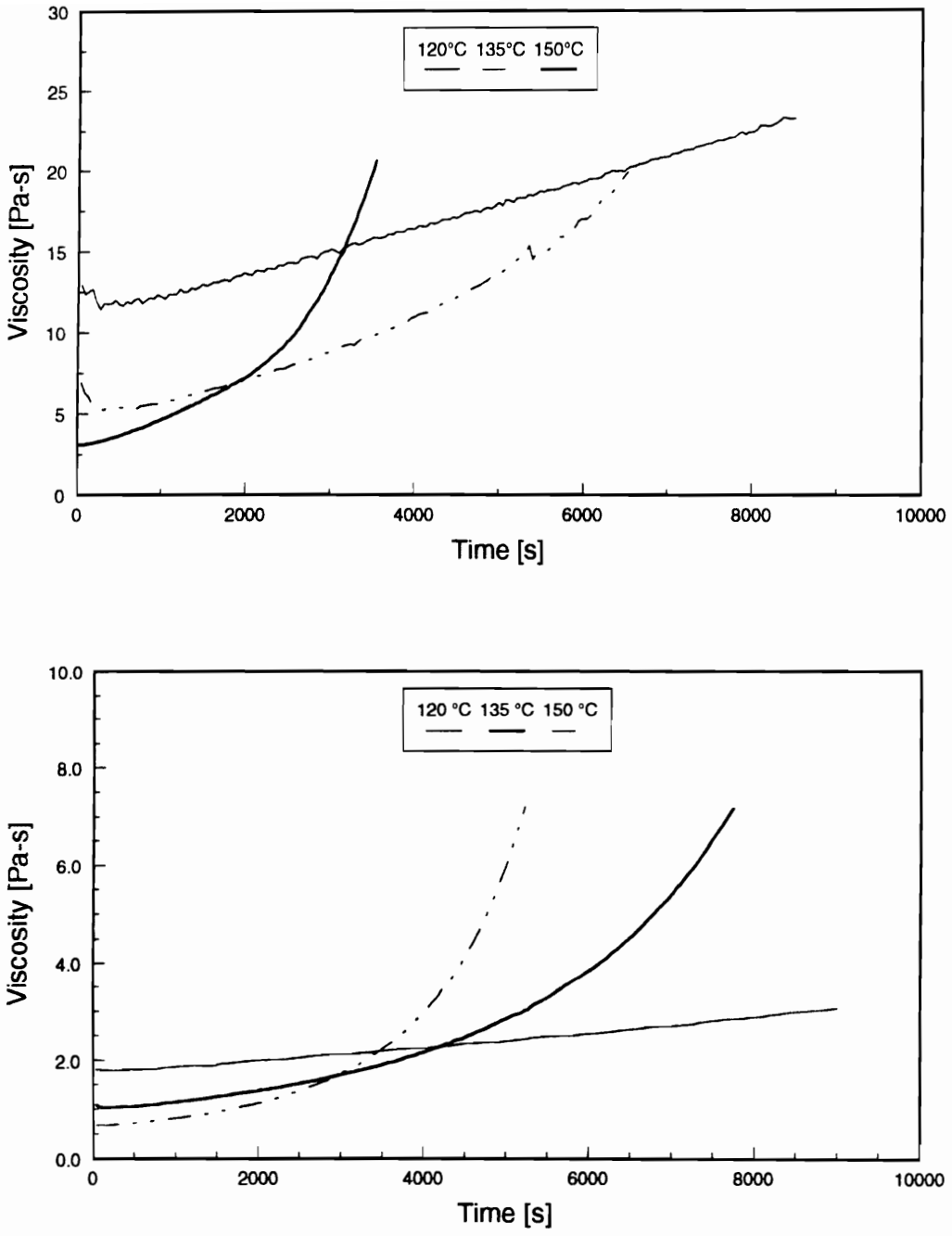

Figure 3.15 Viscosity time profiles at different temperatures for VTUFF1530 (top), and for VTUFF2020 (bottom).

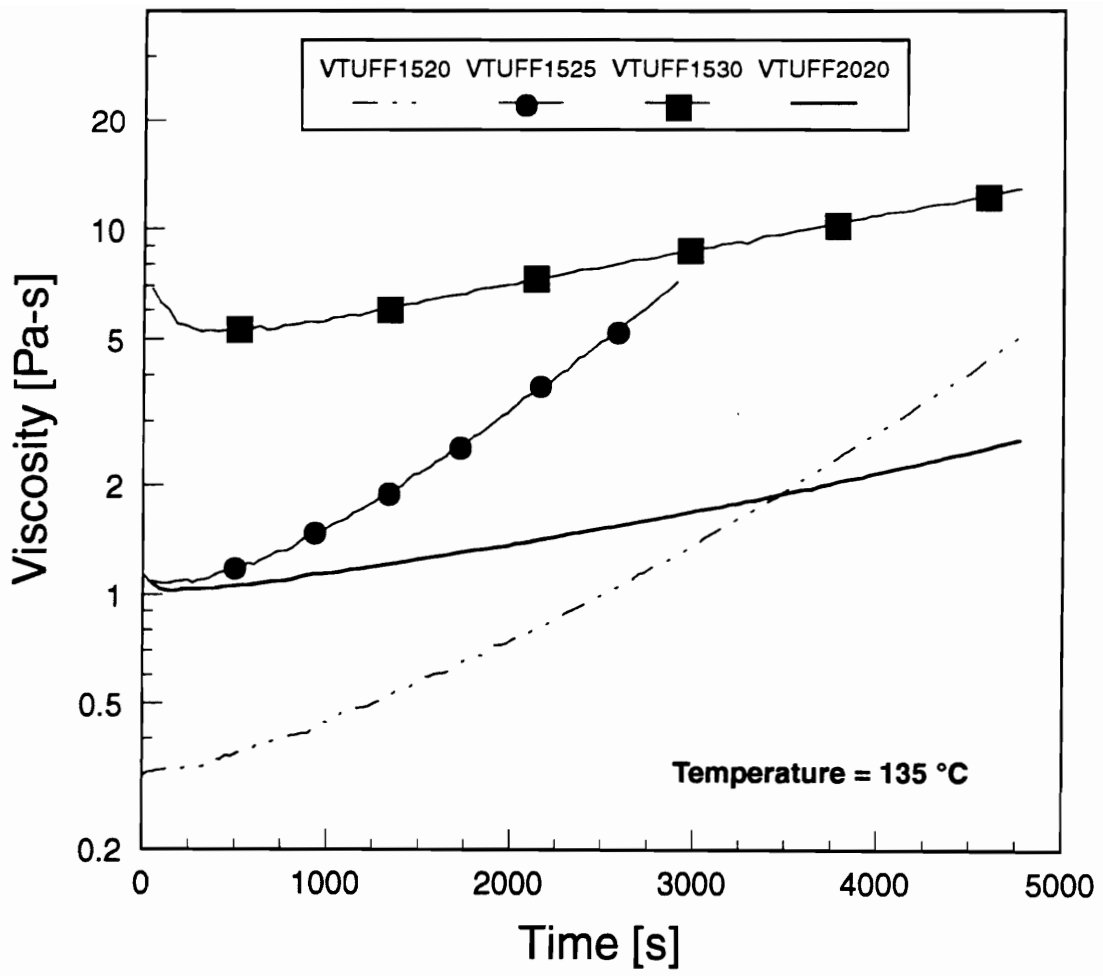

Figure 3.16 Comparison of isothermal viscosity-time curves for the toughened cyanate ester resin systems, at 135 °C.

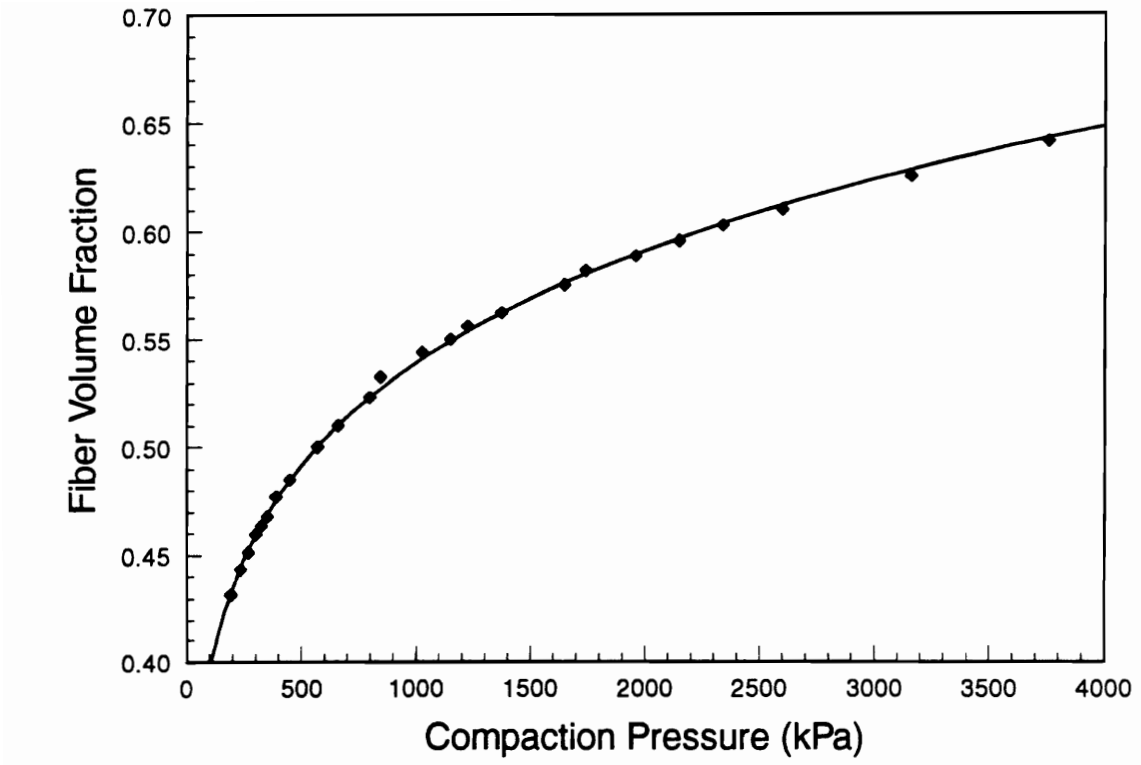

Figure 3.17 Compaction behavior of AS4/PW fabric preform as a function of the fiber volume fraction.

The in-plane permeability behavior of the AS4/PW fabric material was characterized by measuring the permeability in the warp and fill directions of the fabric preform at different levels of applied compaction pressure. Fig. 3.18 shows the variation of the permeability with fiber volume fraction in the warp and fill directions. The results show that the fabric material is more permeable in the fill direction when compared to the warp direction. At a fiber volume fraction of 60%, the ratio of the permeability in the fill direction to that in the warp direction is approximately 3.0. Typically, this ratio changes with the level of compaction of the fabric [35]. The knowledge of the preform permeability in these directions aid in designing injection strategies. In an earlier study, the IM7-3k-8HS fabric has been characterized by Hammond [34].

3.6.2 Physical Testing

The fiber volume fractions of the IM7/8HS fabric reinforced composites manufactured with the RSL1895/W, the AroCy B10, and the VTUFF1525 resin systems are shown in Fig. 3.19. These laminates were manufactured by PI-RTM for initial processability evaluation and short block compression testing. The nominal thickness of these laminates was 6.35 mm and the target fiber volume fraction was about 59%. The measured values are in close agreement with the designed values and the small scatter in the data suggests uniform fiber contents in the composites.

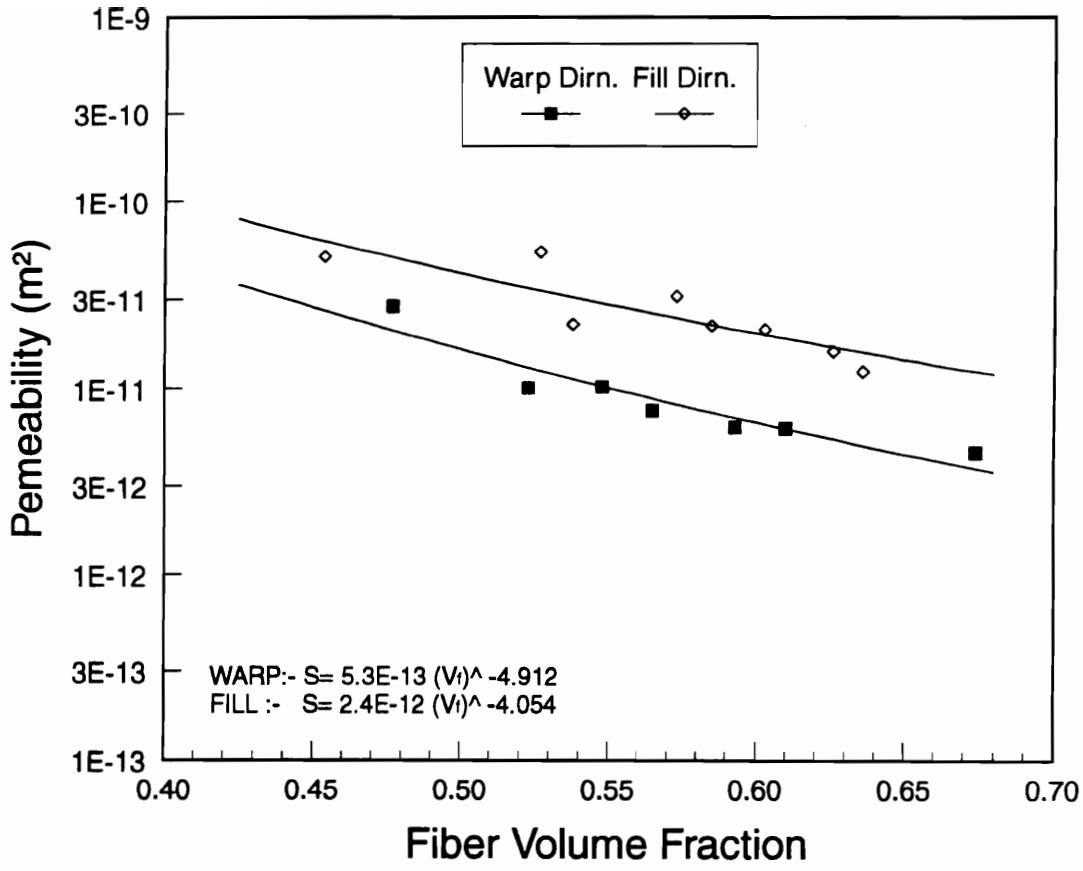

Figure 3.18 Permeability behavior of AS4/PW fabric preform as a function of the fiber volume fraction in warp and fill directions.

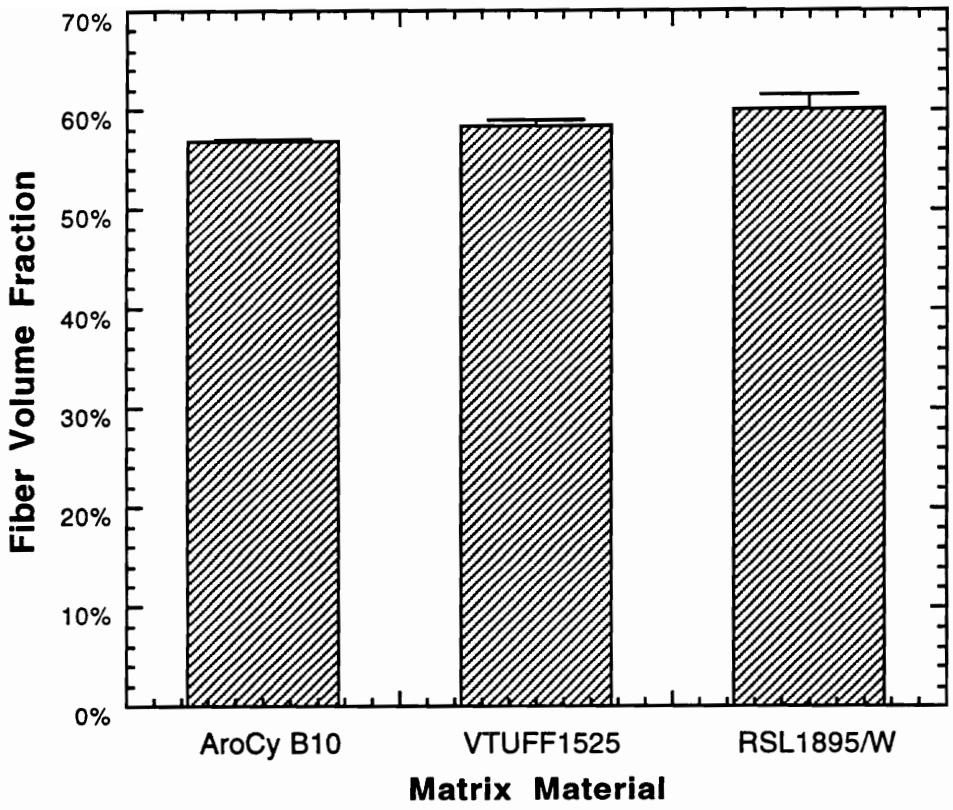

Figure 3.19 Fiber volume fractions for IM7/8HS fabric composites manufactured by the PI-RTM process.

A second set of composites were manufactured with the AS4/PW fabric for impact damage studies. The resin systems used included the untoughened and toughened cyanate ester resins and RSL1895/W epoxy resin. All the composites were manufactured either by PI-RTM or by RFI except for the VTUFF1525 matrix composites. A total of three VTUFF1525 composite were manufactured for impact studies. Two were manufactured by the RFI process and one by the PI-RTM process. Fig. 3.20 shows the measured fiber volume fractions of the composites manufactured for impact damage studies. Again, the target fiber volume fraction was about 60%. A minimum of four specimens, representing the majority of the laminate volume, were used to estimate the fiber content. The fiber volume fraction estimate for the VTUFF1525 system combines the results from laminates manufactured by both processes. In all composites, except the VTUFF1525 matrix laminates, the scatter in the data were small, indicating uniformity of fiber volume fraction throughout the entire composite.

The void contents were measured for the untoughened and toughened cyanate ester resin composites by the method outlined in Section 3.5.1, and the results are shown in Fig. 3.21. In a recent work, Demaree [61] classified composite laminates into three categories based on the void content. A composite laminate with a void content less than 1% by volume was classified as "void free". Composites with void contents between 1 and 2% were considered "low void" laminates and those with voids in excess of 2% were considered "high void" composites. Based this classification, the data shows all the composites to have low void content.

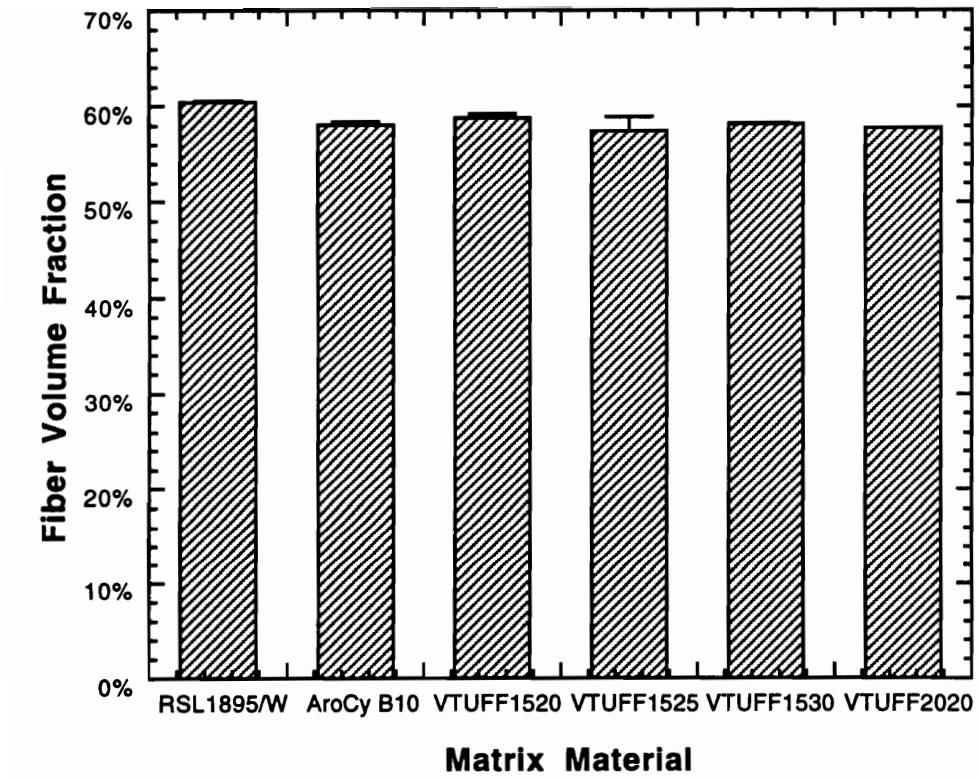

Figure 3.20 Fiber volume fractions for AS4/PW fabric composites manufactured for impact damage evaluations.

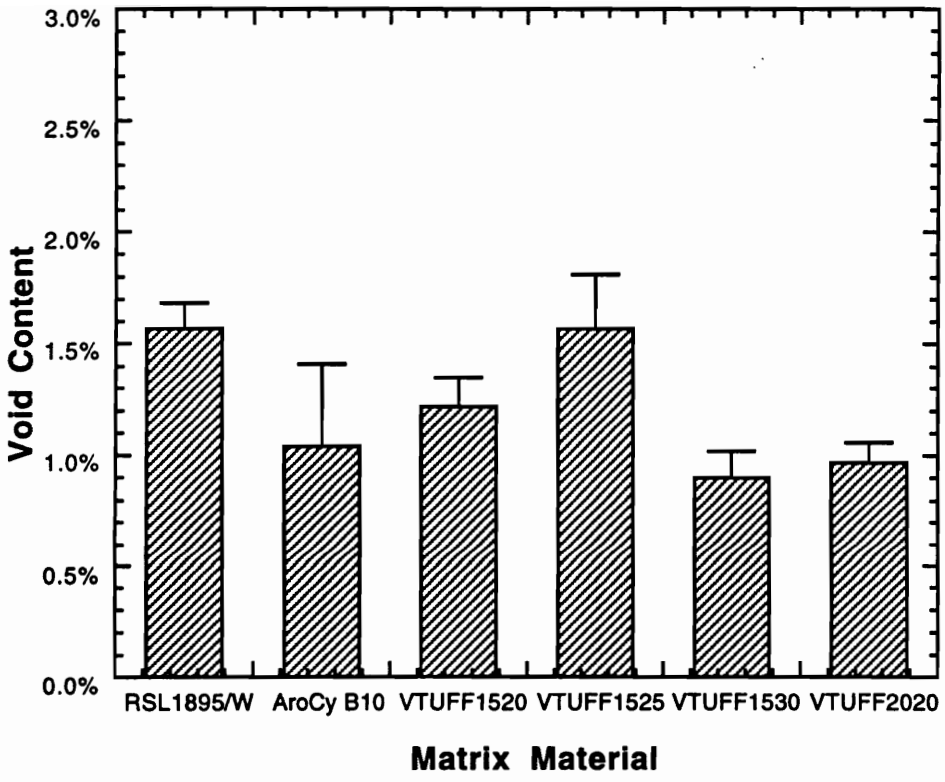

Figure 3.21 Void content estimates for AS4/PW fabric composites manufactured for impact damage evaluations.

Although the a wide scatter in the void content is seen for the AroCy B10 and the VTUFF1525 matrix composites, it must be noted that the average void contents are about 1.0% and 1.5%, respectively. Clearly, the data shows the VTUFF1530 laminates to be "void-free", in the context of the above classification.

A third set of composites were manufactured for evaluating the fracture toughness by end-notched flexure test of the untoughened and the toughened cyanate ester resins. The fiber volume fractions and void contents for these composites are shown in Figs. 3.22 and 3.23, respectively. Again, the data represent an average of at least five specimens taken from across the width of the composite. The results indicate uniformity of the fiber content across each panel. The void content estimates for these composites are shown in Fig. 3.23 and indicate that all the composites, except VTUFF1520, have very low void contents. Although the estimated void content is higher in this composite compared to the rest of the composites in this group, the void content is below 2.0%. Further, the wide scatter in the data for the very low void content composite perhaps reflects a limit in the resolution of this technique.

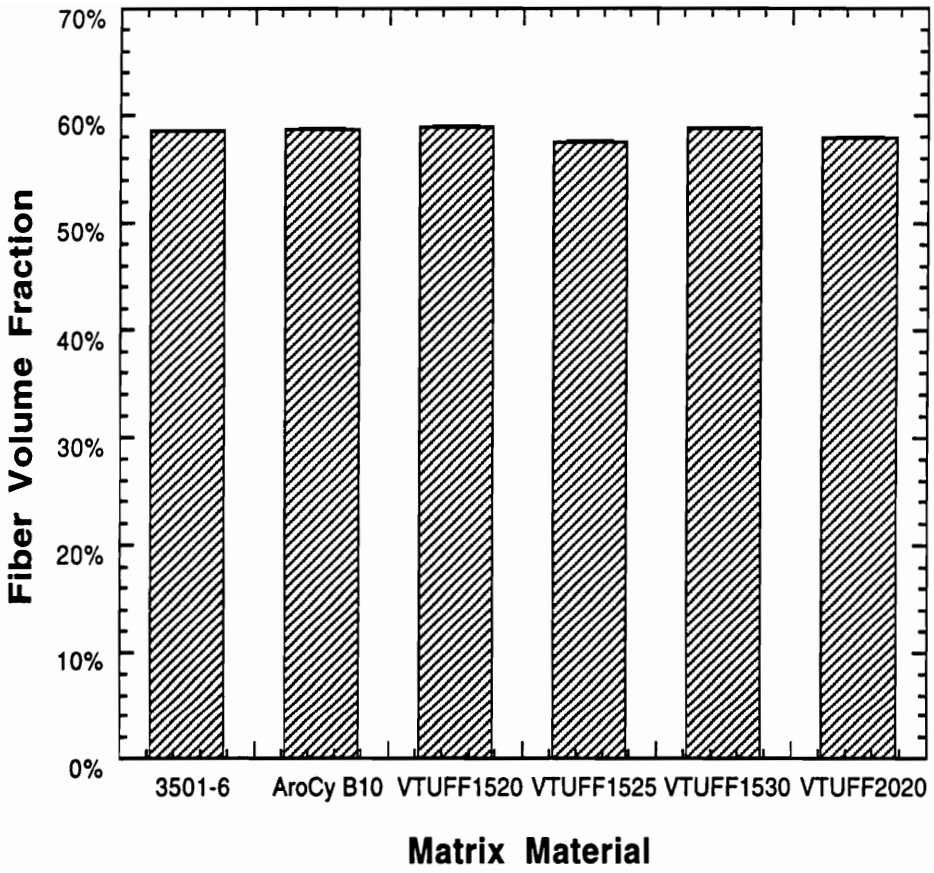

Figure 3.22 Fiber volume fractions for AS4/PW fabric composites manufactured for fracture toughness evaluations.

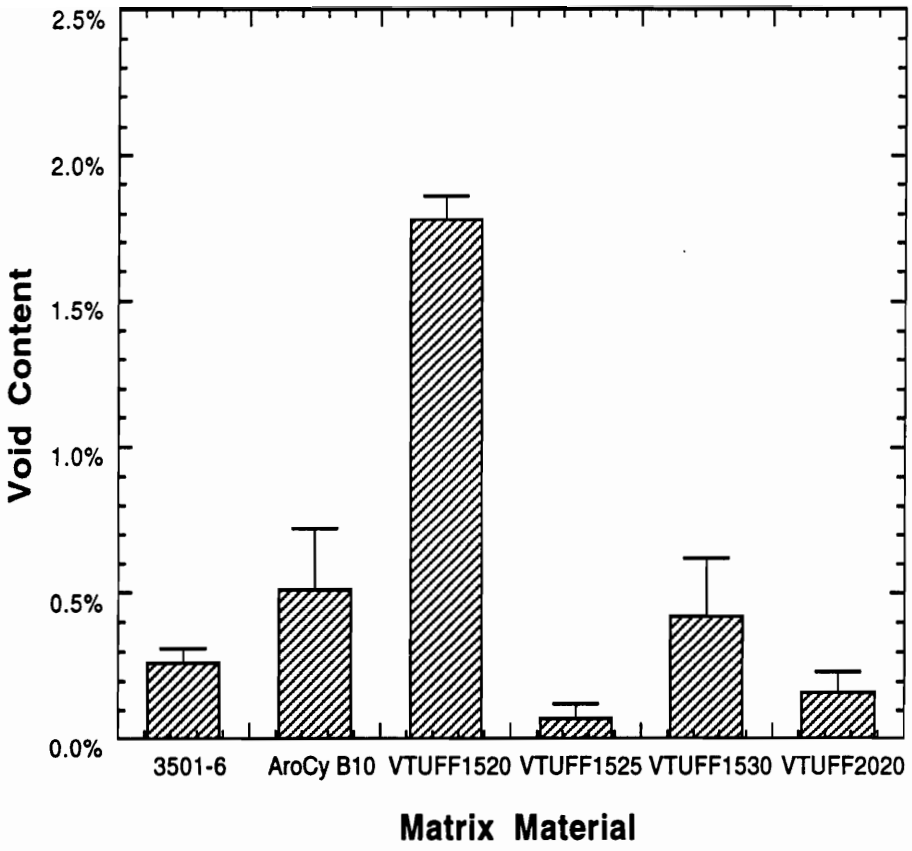

Figure 3.23 Void content estimates for AS4/PW fabric composites manufactured for fracture toughness evaluations.

3.6.3 Microscopy

Upon completion of infiltration all the toughened cyanate ester composites were manufactured using identical cure cycles. The details of the cure cycle used were shown in Table 3.2. TEM analysis of the resin stems from the panel manufacture show differences in the phase separated morphology in the fully cured toughened cyanate ester resin systems. TEM micrographs, at 6,400X magnification, for VTUFF1520 and VTUFF1525 are shown in Figs. 3.24(top) and (bottom), respectively. Figs. 3.25(top) and (bottom) show the micrograph for VTUFF1530 and VTUFF2020 resin systems, respectively. The lighter phase in the micrographs is the thermoplastic toughener phase. The two micrographs in Fig. 3.24 show phase separation, with a co-continuous structure evident in the resin systems. With the increase in the concentration of the 15k molecular weight toughener from 20 to 30%, a finer structure seems to result. However, with an increase in the toughener molecular weight from 15k to 20k, at a constant concentration of 20%, a phase-inverted structure develops, as shown in Figs. 3.24 (bottom) and 3.25(bottom). In a phase inverted structure, the thermoplastic phase becomes the continuous phase, with the thermoset phase dispersed within. In a study on thermoplastic toughened bismaleimide resins, Wilkinson [62] suggests that a phase-inverted morphology helps improve the resistance to solvent attack. While these morphologies have been detected in the unreinforced toughened resin, the morphology within the composite may not necessarily be similar to those developed in the neat resin primarily due to the presence of the reinforcing fibers.

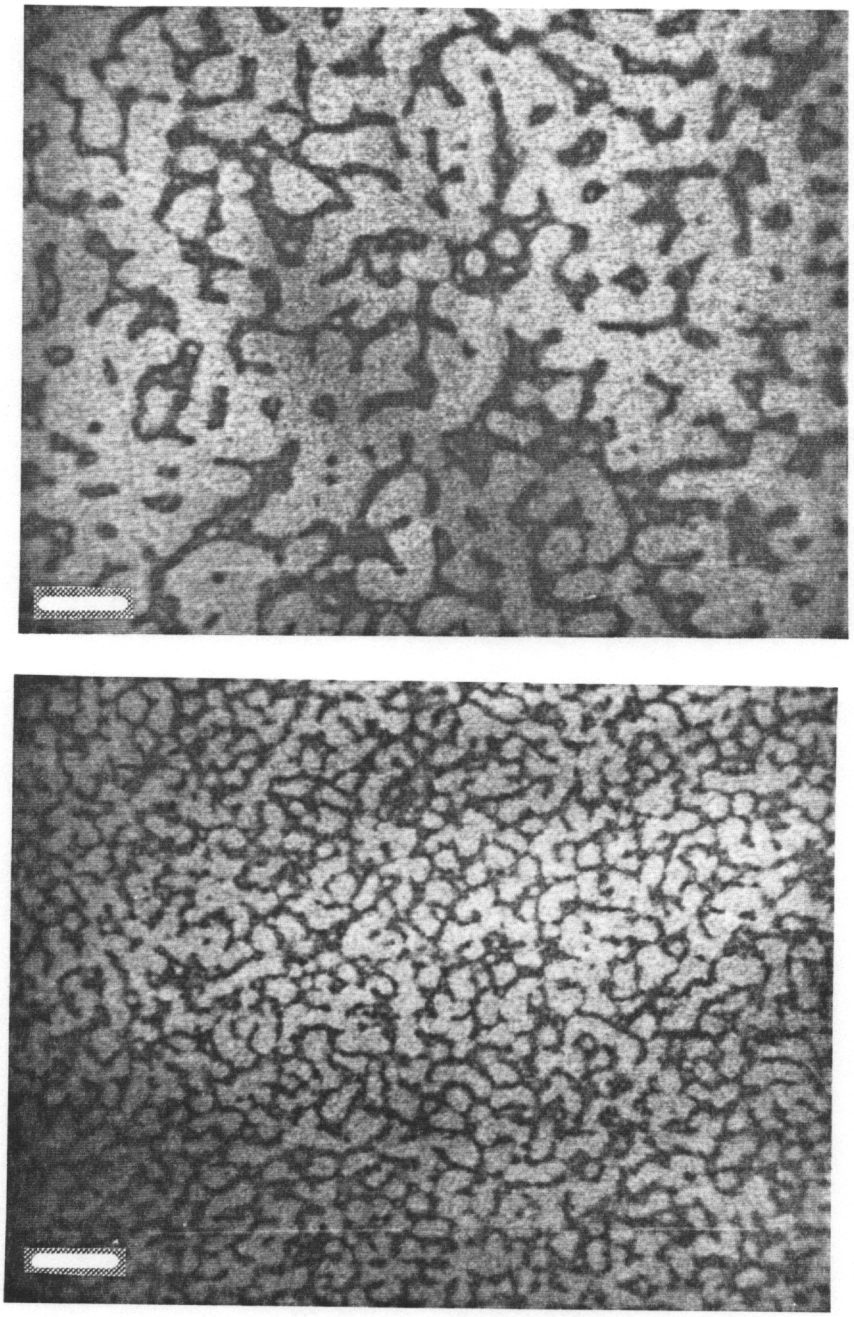

Figure 3.24 TEM analysis of resin morphology for VTUFF1520 (top), and for VTUFF1525 (bottom). (Scale bar = 2 μm).

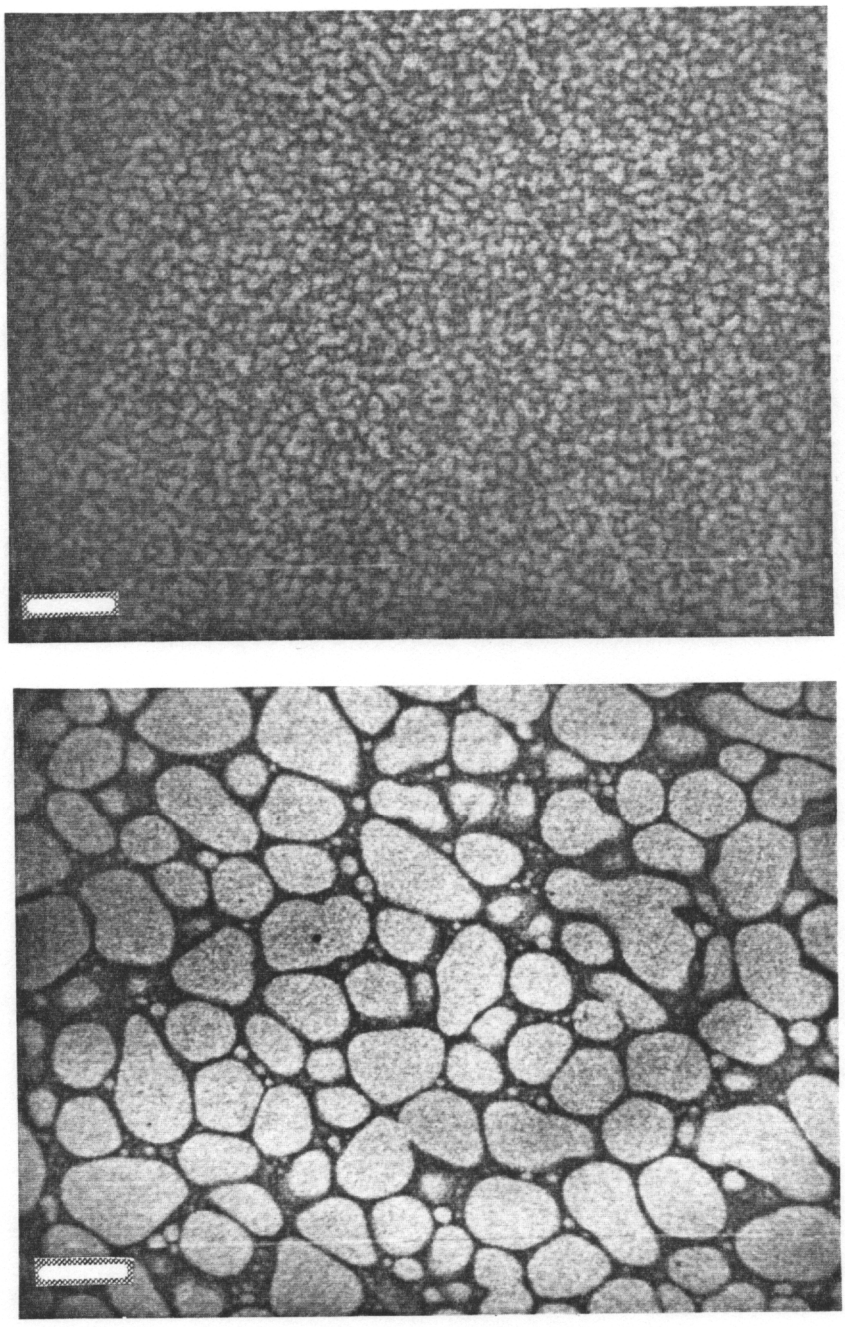

Figure 3.25 TEM analysis of resin morphology for VTUFF1530 (top), and for VTUFF2020 (bottom). (Scale bar = 2 μm).

3.6.4 Short Block Compression Testing

The IM7/8HS fabric composites were tested to failure in compression using the NASA short block compression test procedure. This test was performed on untoughened AroCy B10 cyanate ester, VTUFF1525 toughened cyanate ester, and RSL1895/W epoxy matrix composites. Test specimens from the composites were machined in the fabric warp and fill directions. The compression strengths are plotted in Figs. 3.26(top) and (bottom), for the warp direction and fill directions respectively. The results show an increase in the compression strength as a result of toughening the AroCy B10 resin system. The compression strength of the VTUFF1525 resin system seems to be of the same level as that for the RSL1895/W epoxy system.

3.6.5 Gas-Gun Impact Testing

The gas-gun impact tests were performed on the AS4/PW fabric composites manufactured with the RSL1895/W epoxy, the AroCy B10 cyanate ester, and the VTUFF series toughened cyanate ester resin systems. The parameters measured from this test that describe the impact damage resistance were the critical velocity to initiate damage, V_c, and the growth rate, C, of the damage with respect to the incident velocity of the impactor. The damage area was measured from the ultrasonic C-scan detected images of the damaged specimen. Fig. 3.27 shows the critical velocities for the composites fabricated with different matrix materials.

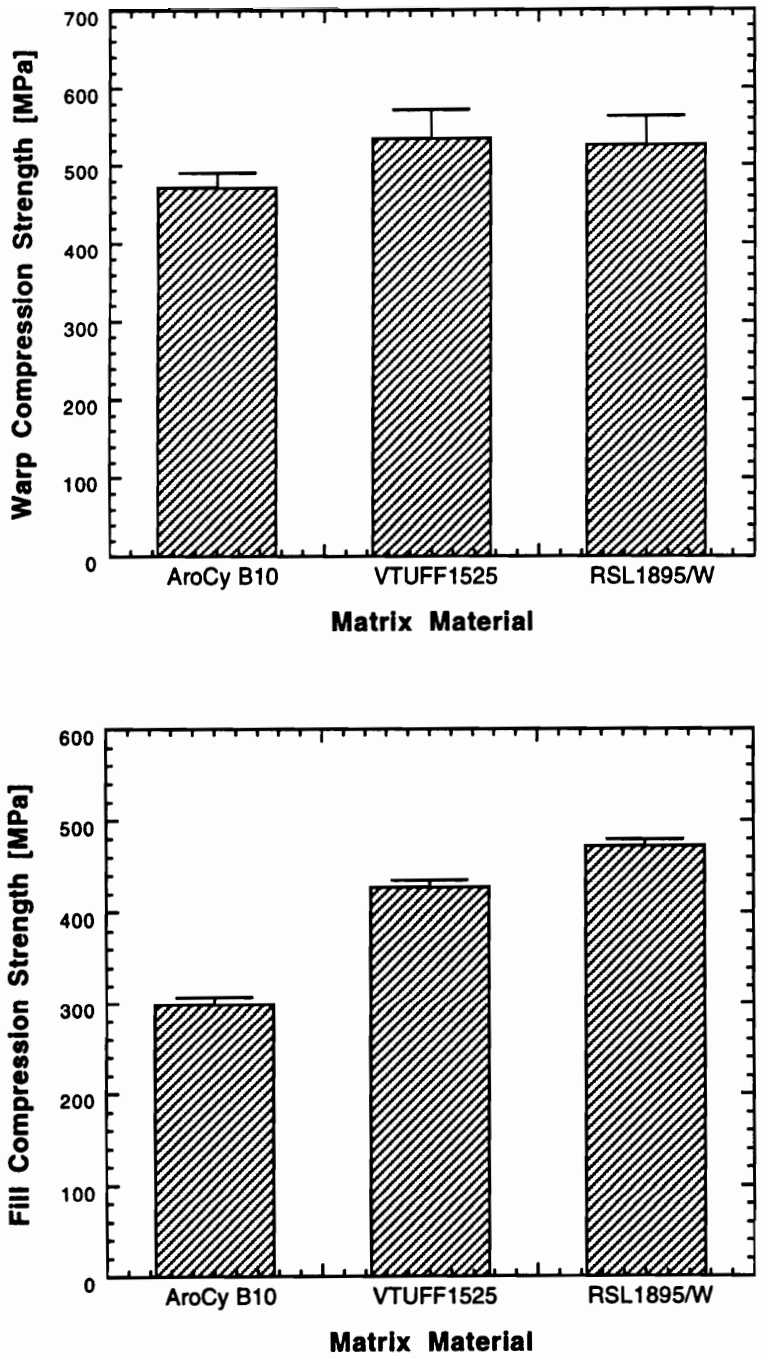

Figure 3.26 Short block compression strengths for IM7/8HS fabric composites in the warp direction (top), and fill direction (bottom).

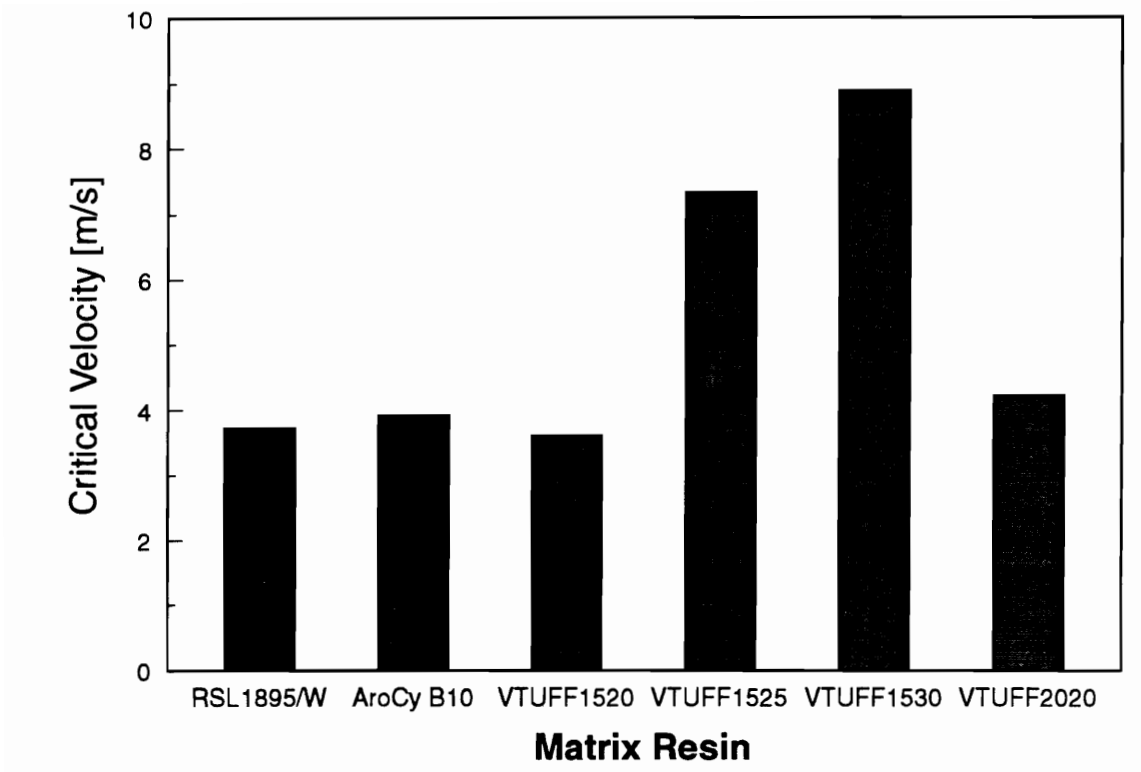

Figure 3.27 The critical velocity, V_c , to initiate impact damage for AS4/PW fabric composites measured from gas-gun impact tests.

Generally, materials with high V_c and low C values are indicative of superior resistance to impact damage [32]. The toughened cyanate ester matrix composites with a toughener composition of 25% or higher exhibit a higher V_c compared with the AroCy B10 composite. The cyanate ester matrix composites with a 20% toughener concentration have the same V_c as the untoughened composite.

The damage growth rate, C, is plotted for the various material systems in Fig. 3.28. Typically, a lower "damage growth rate" is desirable for improved resistance to impact damage. The data seem to show higher "growth rates" for the VTUFF1525 and VTUFF1530 composite laminates as compared with the AroCy B10 composites. This result seems to be anomalous because the previous work of Tea [32] on quasi-isotropic tape laminates shows a lower "growth rate" for thermoplastic matrix composites, which are widely known to be tough and exhibit high damage resistance.

In using the C-scan technique to detect damage area, the total delaminated area resulting from the impact is not accounted for. In the C-scan technique, only a projected damage area is measured. Due to an impact, delamination may occur at one or more ply interfaces. That is, the "total damage area" created by an impact is the sum of the surface areas at each inter-ply delamination and not the projected delamination area [32]. This inability to differentiate between the total and projected damage area is a limitation of this test procedure. Further, correlations between projected area and the impact velocity reported in Ref. 32 were for quasi-isotropic laminates and not for fabric composites. The onset of damage is easily detected by the C-scan technique and hence the parameter V_c

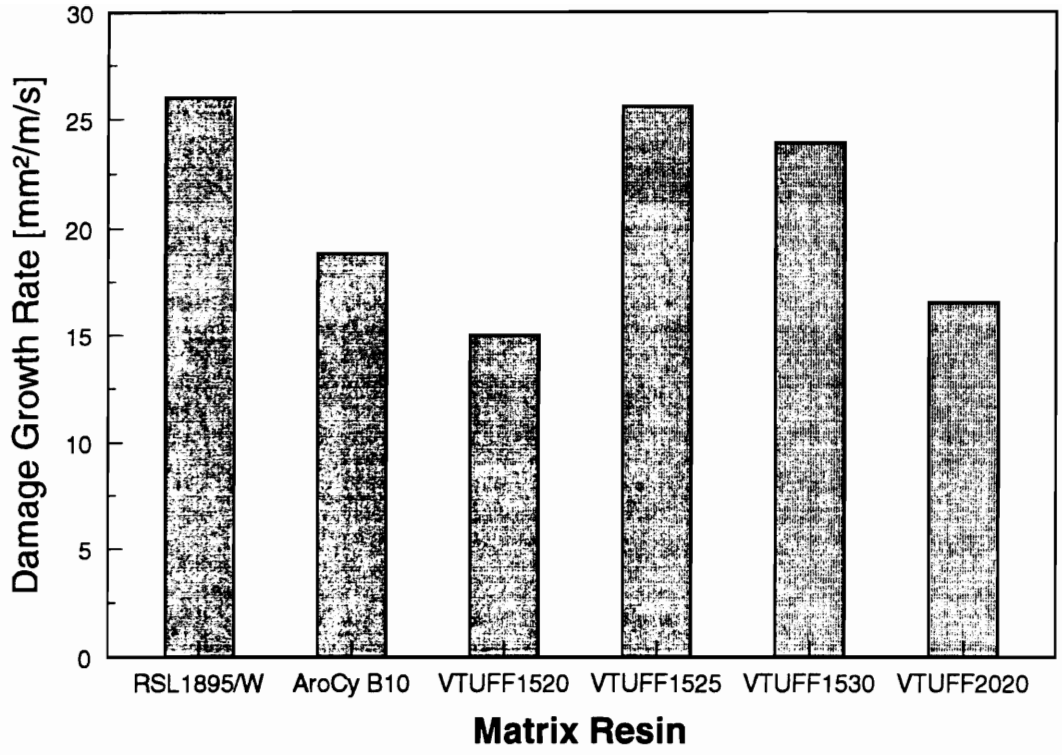

Figure 3.28 The growth rate of impact damage,C, for AS4/PW fabric composites measured from gas-gun impact tests.

may perhaps be a more reasonable measure of impact damage resistance in this study. Clearly, more studies are required to better understand and interpret the trends seen in the "damage growth rate" data.

Based on impact studies on glass fiber reinforced composites, Babic et. al., [66] conclude that the use of toughened resin matrices leads to improvements in the *resistance* to damage formation. A material system exhibiting a high value of V_c may successfully *resist* impact damage under conditions where damage is induced in a less damage resistant materials which exhibit a low value of V_c.

3.6.6 Compression After Impact

Following the gas-gun impact tests on the fabric composite material systems, compression after impact (CAI) tests were performed to determine the impact damage tolerance of these materials. A set of undamaged test specimens for each material system were tested to measure the undamaged compressive strengths. Fig. 3.29 shows the undamaged strengths in compression for the fabric reinforced composites. These tests were performed on 52 mm x 25 mm test specimens. The data show a slight decrease in the compression strength with increasing concentration of toughener as expected. The maximum reduction in compression strength between AroCy B10 and VTUFF2020, was less than 13%.

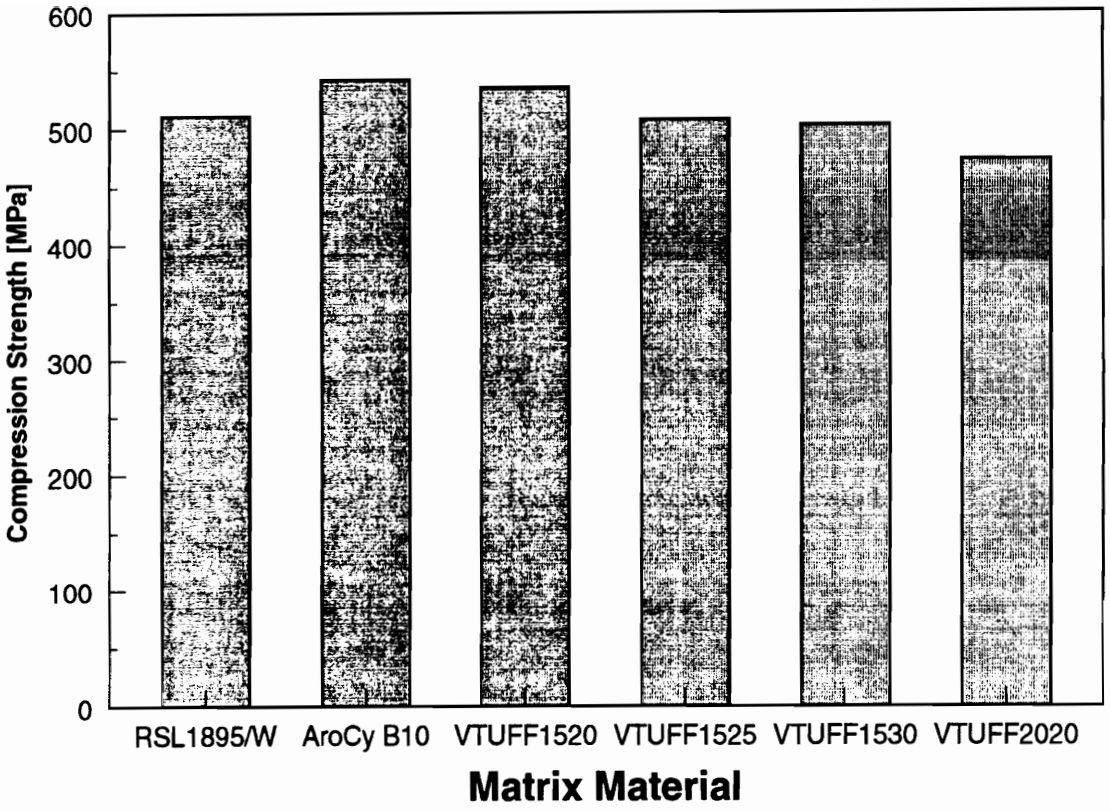

Figure 3.29 Compression strengths of undamaged AS4/PW fabric composites.

Composite specimens that were impacted at a different velocities were machined to the required size and tested to failure in compression as described in Section 3.5.4. Plots of the residual compression strength as a function of the incident impact energy were generated following the procedure adopted by Teh [32]. The compression strengths of the damaged specimens were normalized by compression strengths of the respective undamaged reference specimens. Fig. 3.30 compares the normalized residual compressive strengths plotted as a function of the incident impact energy for the RSL1895/W epoxy and the AroCy B10 cyanate ester matrix composites. This plot shows the ability of the composite material to "tolerate" damage. Clearly, the untoughened cyanate ester composites are significantly more damage tolerant than the RSL1895/w epoxy composites.

Now to assess the damage tolerance of the VTUFF series of toughened cyanate ester matrix composites, the normalized residual compression strengths are similarly plotted as a function of the incident impact energy. The CAI data for the untoughened AroCy B10 is plotted for comparison. From Fig. 3.31, the improvement in the damage tolerance of the VTUFF1520 matrix composites over the untoughened cyanate ester composites is evident.

In general, an increase in the concentration of the 15k toughener improves the damage tolerance of the fabric composites as shown in Figs. 3.32 and 3.33 for VTUFF1525 and VTUFF1530 matrix composites, respectively. However, in Figure 3.32 large scatter in the residual compression strength data for the VTUFF1525 composites is seen.

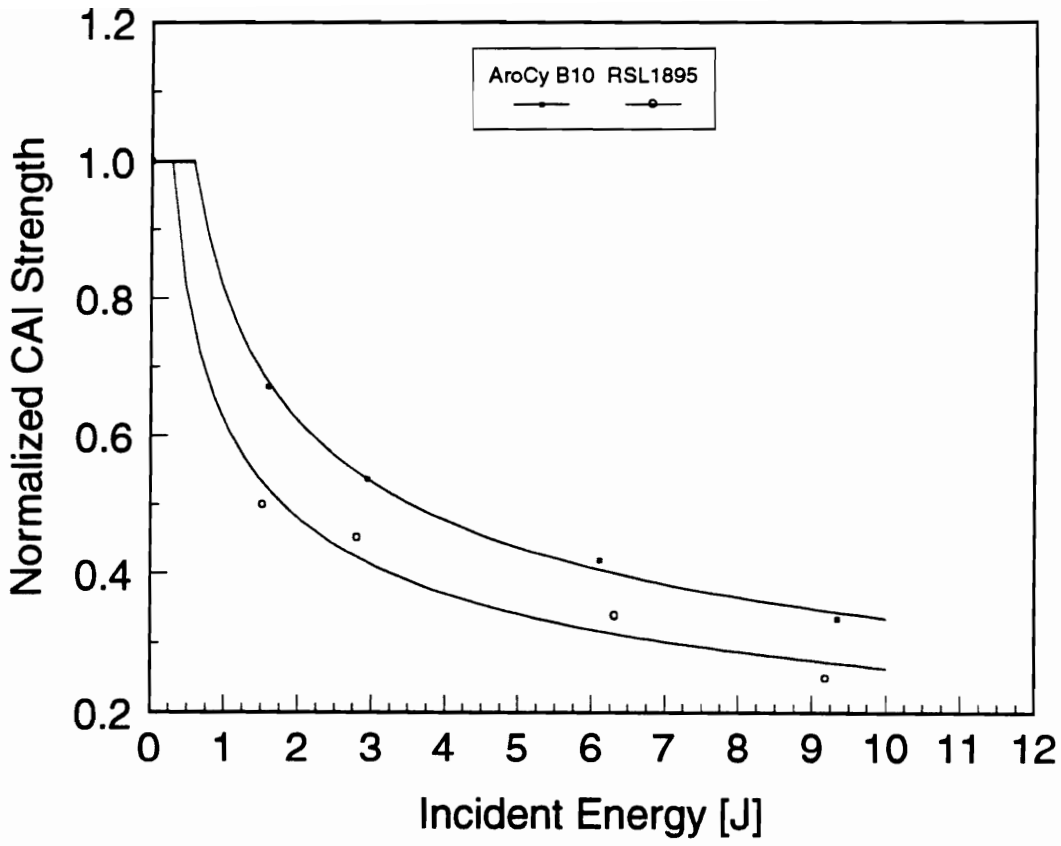

Figure 3.30 Normalized residual compression strength as a function of incident impact energy for AS4/PW fabric AroCy B10 and RSL1895/W composites.

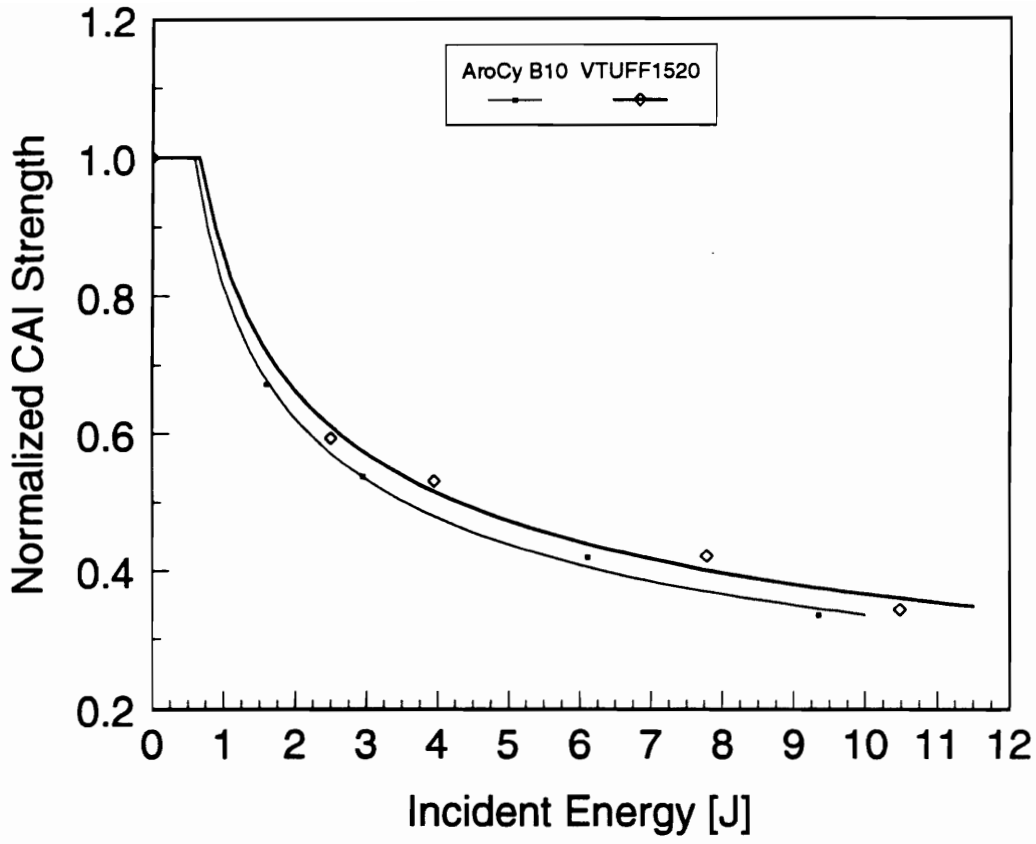

Figure 3.31 Normalized residual compression strength as a function of incident impact energy for AS4/PW fabric AroCy B10 and VTUFF1520 composites.

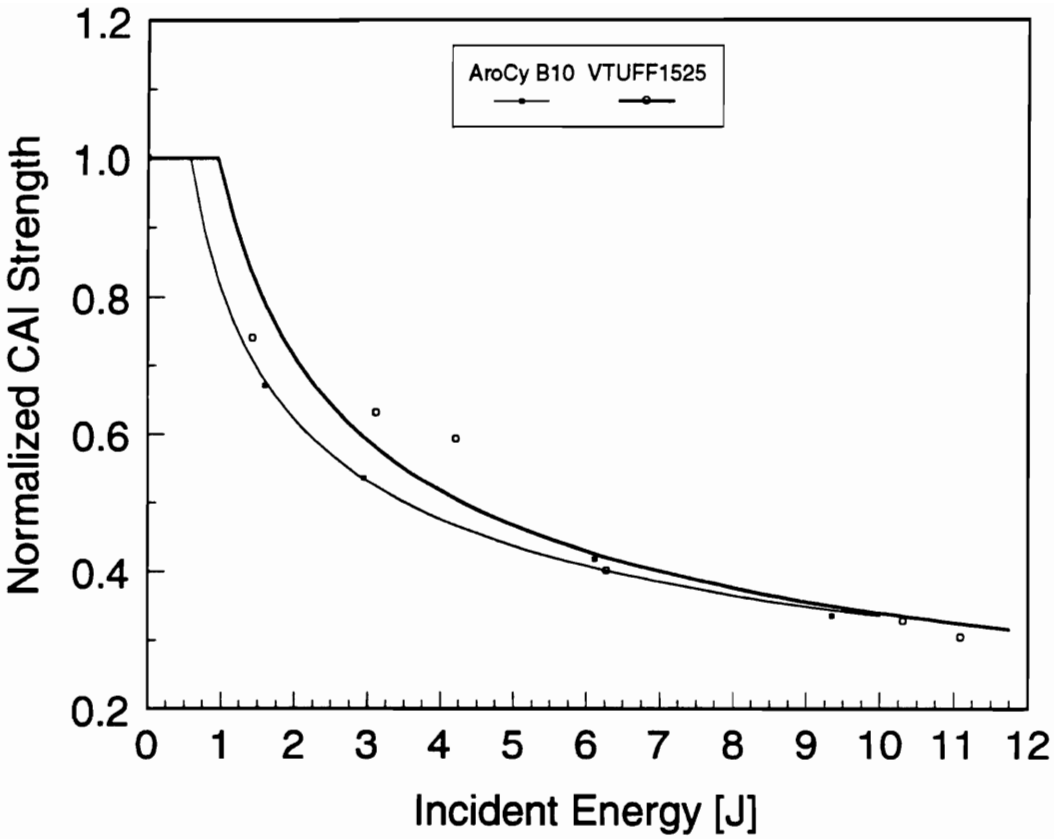

Figure 3.32 Normalized residual compression strength versus incident impact energy for AS4/PW fabric AroCy B10 and VTUFF1525 composites

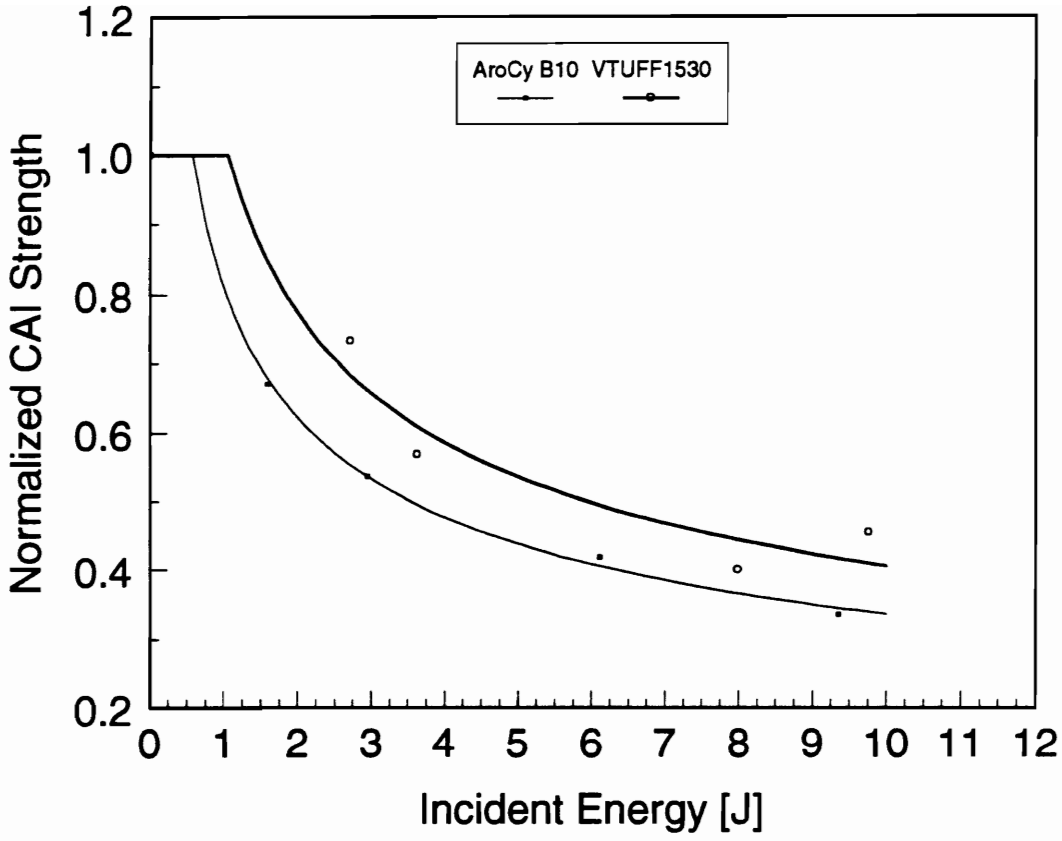

Figure 3.33 Normalized residual compression strength versus incident impact energy for AS4/PW fabric AroCy B10 and VTUFF1530 composites.

The curve, fitted to the data, does not show a significant improvement in the damage tolerance over the AroCy B10 composites. Further, at the higher levels of incident energy (above ~ 6 joules), there appears to be no improvement over the untoughened cyanate ester composites. It must be noted here that the impact test specimens for this material system were obtained from three different panels. Two panels were manufactured by the RFI process, and one by the PI-RTM process. Two test specimens were prepared from each panel. For all other material systems, the four test specimen were obtained from a single panel.

The plot in Fig. 3.34 compares the damage tolerance of the VTUFF2020 toughened matrix composites with that of the AroCy B10 composites. Again, an improved performance with the toughened system is seen without any ambiguity. Finally, in Fig. 3.35, a comparison of the CAI data for VTUFF1520 and VTUFF2020 matrix composites shows the effect of increasing the toughener molecular weight while maintaining an identical concentration of 20%. The resin system with the 20k molecular weight toughener, VTUFF2020, seems to exhibit higher damage tolerance than that with 15k toughener, VTUFF1520.

Although the CAI data do show an improvement in the impact damage tolerance of the toughened cyanate ester composite materials, it is recognized that additional CAI strength data for the material systems would help establish the trends with more certainty, especially for the VTUFF1525 matrix composites. The compression tests performed on the damaged specimens according to the procedure developed by Teh [32] may need to

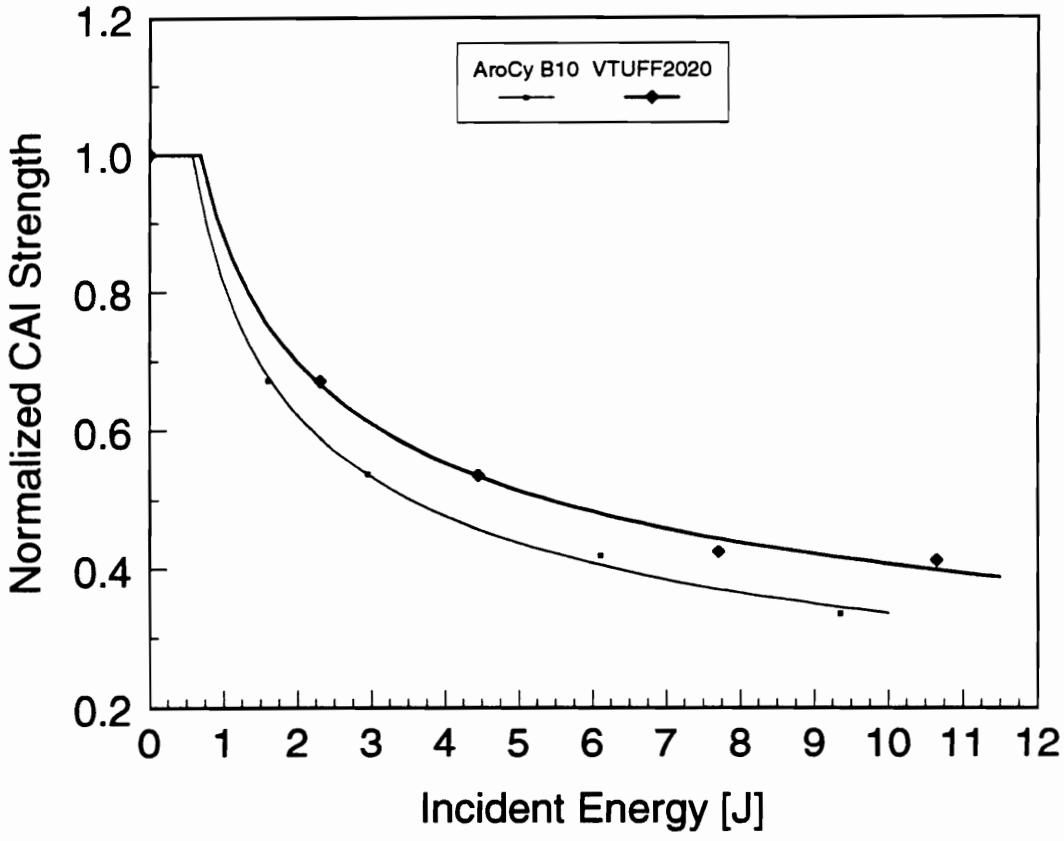

Figure 3.34 Normalized residual compression strength versus incident impact energy for AS4/PW fabric AroCy B10 and VTUFF2020 composites.

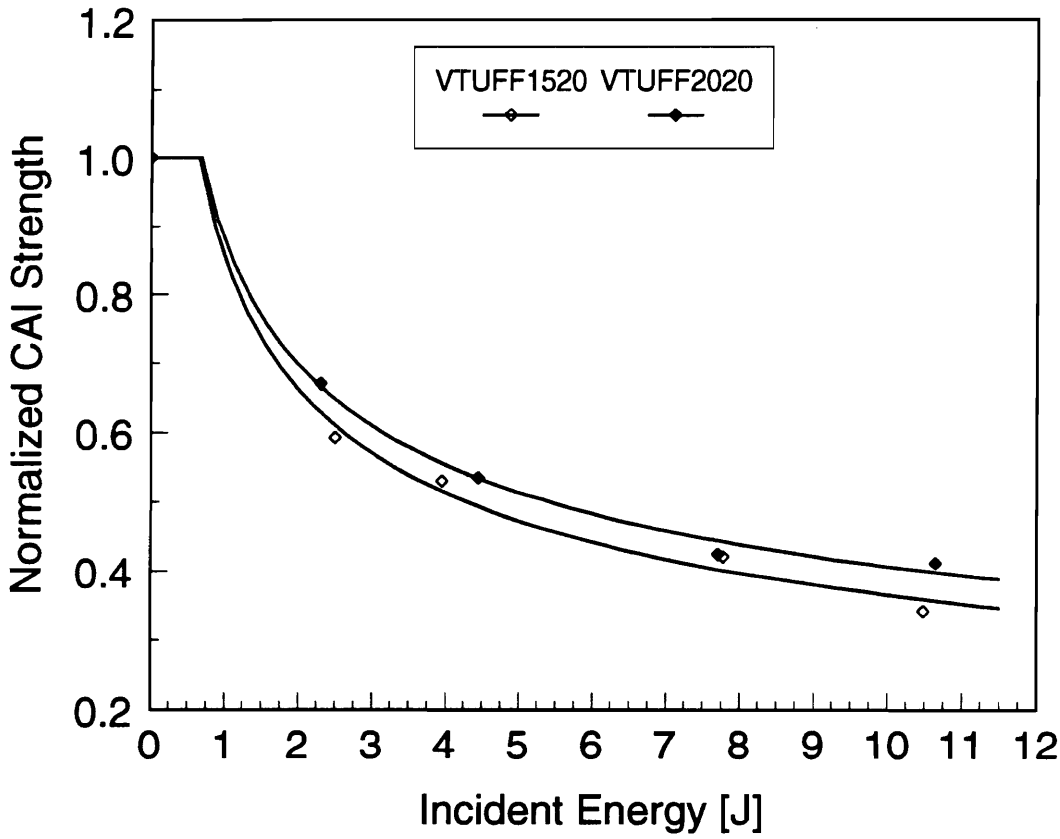

Figure 3.35 Normalized residual compression strength versus incident impact energy for AS4/PW fabric VTUFF1520 and VTUFF2020 composites.

be revised. As explained in Section 3.5.4, the 52 mm x 25 mm compression specimens were machined out of the 65 mm x 65 mm gas-gun impact specimen. The compression strength measurements made with these specimens may be adversely affected by machining. In particular, when the size of the damage area in the specimens impacted at higher energies is on the order of the width of the compression test specimen, pronounced machining effects may occur. Also, it is assumed that the damage is centrally located in the CAI specimen. Hence, machining the compression specimen from the impact specimen such that the damage area, not completely visible to the naked eye, is located centrally may have practical limitations. These effects may be the cause of the scatter seen in the data from some of the material systems at the higher incident energy levels, above 6 joules. Perhaps, these concerns may be eliminated by performing the compression tests on the 65 mm x 65 mm impact specimen, without any machining. This may require modifications to the existing compression fixture in order to accommodate a larger test specimen.

3.6.7 End-Notched Flexure

The mode II critical strain energy release rate, G_{IIc}, for the AS4/PW fabric reinforced composites was measured by end-notched flexure tests, according to the procedure explained in Section 3.5.7. In the first step of the test, the flexural modulus of each composite specimen was measured in the warp direction. The measured moduli

of the material systems are plotted in Fig. 3.36. The 3501-6 epoxy composite shows a higher modulus as compared to that of the untoughened cyanate ester composites. While the flexural modulus seems to increase with an increase in the concentration of the toughener, an increase in the toughener molecular weight from 15k to 20k, for a concentration of 20%, does not seem to affect the modulus.

Fig. 3.37 shows the influence of toughener concentration on the mode II critical strain energy release rate for the VTUFF toughened systems with 15k toughener. Also shown in the figure are G_{IIc} values for the AroCy B10 and the 3501-6 epoxy system. Clearly, dramatic improvements result from increasing toughener concentration. The untoughened cyanate ester composite shows about an 84% higher fracture toughness when compared with the 3501-6 matrix composite. Further, increasing the toughener concentration from 20 to 30% results in an improvement in G_{IIc} ranging from about 230 to nearly 300%, compared with that of the 3501-6 system. With the AroCy B10 resin system as a reference, incorporation of 20% of the 15k toughener results in about 25% improvement in G_{IIc}. Similarly, the VTUFF1525 and the VTUFF1530 matrix composites show, on an average, about 52% and 58% improvement, respectively. Considering the scatter in the data, the fracture toughness values for the VTUFF1525 and the VTUFF1530 resin systems do not seem to differ significantly.

In Fig. 3.38, the influence of the toughener molecular weight on the measured G_{IIc} is shown. The VTUFF1520 and the VTUFF2020 toughened systems are compared with the AroCy B10 untoughened system and the 3501-6 epoxy system.

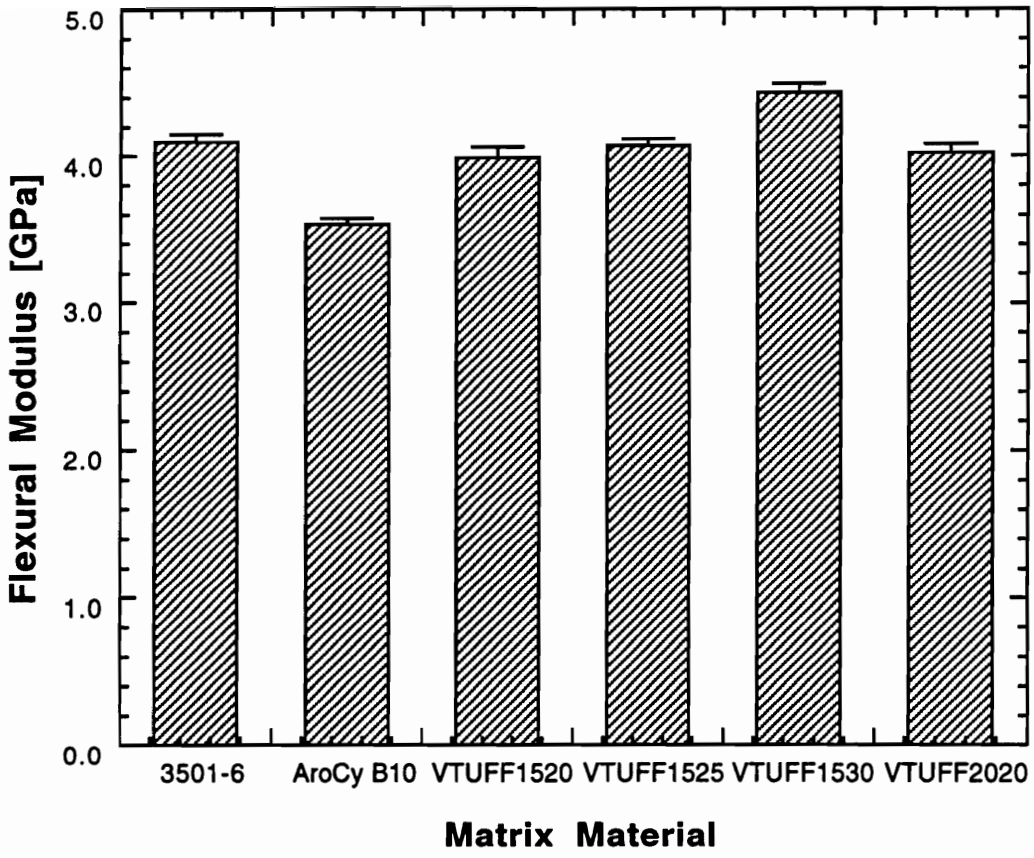

Figure 3.36 Flexural modulus of the AS4/PW fabric composite material systems.

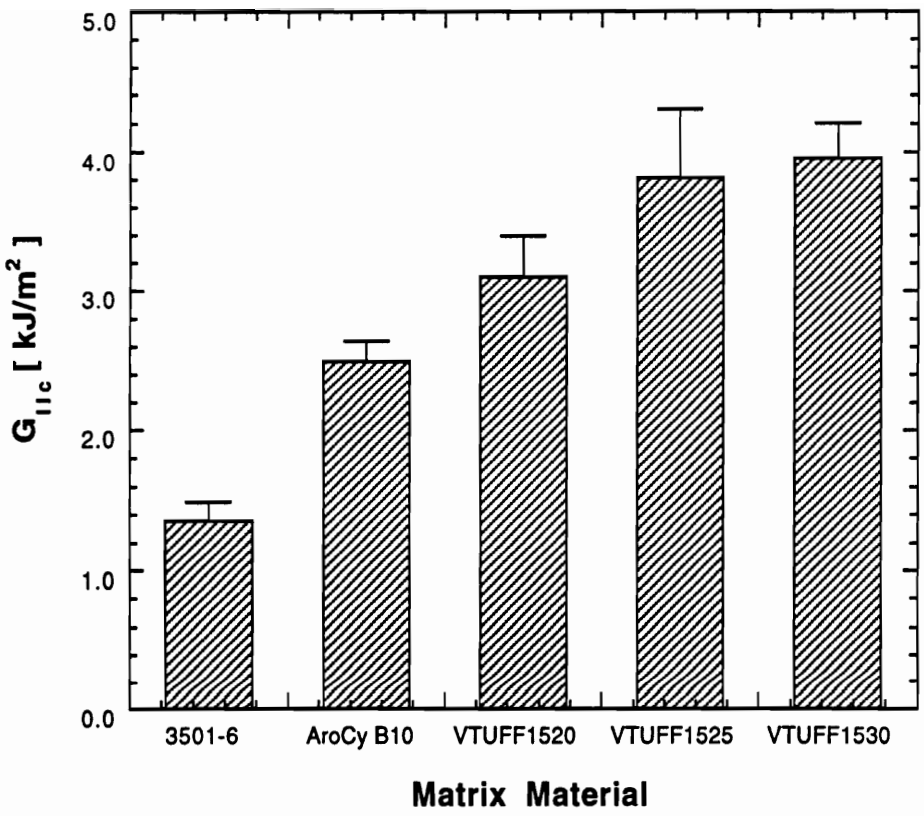

Figure 3.37 The effect of toughener concentration on the mode II critical strain energy release rate, G_{IIc}, of AS4/PW fabric composites.

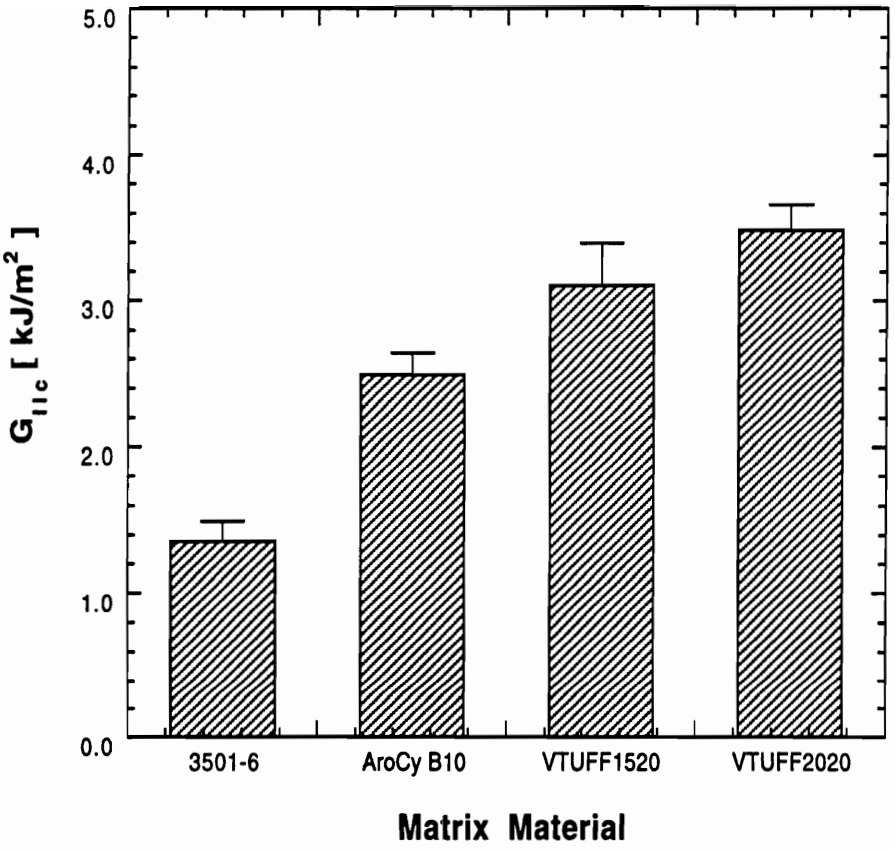

Figure 3.38 The effect of toughener molecular weight on the mode II critical strain energy release rate, G_{IIc}, of AS4/PW fabric composites.

While an improvement of about 25% over AroCy B10 system results through the use of 20%, by weight, of the 15k molecular weight toughener, at the same concentration, the 20k molecular weight toughened system shows about 40% increase in the G_{IIc} over the untoughened cyanate ester resin system. The VTUFF2020 matrix composites show a 260% higher fracture toughness than that of the 3501-6 epoxy system.

3.7 SUMMARY AND CONCLUSIONS

In this investigation, a series of novel toughened cyanate ester resin systems were used to successfully manufacture carbon fabric reinforced composite laminates. The manufactured laminates were manufactured to the target fiber volume fraction between 57 and 60%. A modified non-destructive method was used to estimate the void contents in fabric reinforced composites. By this method, the laminates manufactured were found to have void contents less than 2%, at the maximum.

Mechanical tests were performed to measure the impact damage resistance and damage tolerance properties of the toughened cyanate ester resin composites. The results show improvements in both impact damage resistance and residual compression strengths after impact compared with commonly used hot-melt epoxy resin composites. Although, the gas-gun impact and CAI test results do not seem to conclusively indicate superior damage tolerance of the toughened resin, they do show a general trend to that effect. However, through the mode II critical strain energy release rate results, in conjunction with the well established correlation between the G_{IIc} and the CAI strength, the vastly improved impact properties of the toughened cyanates are demonstrated.

This investigation has ascertained that the new series of toughened cyanate ester resin systems developed are easily processed by liquid molding techniques and exhibit good damage resistance properties and also display enhanced fracture toughness as indicated by the mode II strain energy release rate measurements.

3.8 CHAPTER REFERENCES

[1] Poon, C., R. F. Scott, and S. Lee, "Testing of New-Generation Carbon Fiber/Toughened Resin Epoxy Systems", Polymer Composites, Vol. 9, No. 5, October 1988, pp. 318-329.

[2] Morton, J., and E. W. Godwin, "Impact Response of Tough Carbon Fibre Composites", Composite Structures, Vol. 13, No. 1, 1989, pp. 1-19.

[3] Cantwell, W. J., P. T. Curtis, and J. Morton, "An Assessment of the Impact Performance of CFRP With High Strain Carbon Fibres", Composite Science and Technology, Vol. 25, No. 2, 1986, pp. 133-148.

[4] Wang, Y., and D. Zhao, "Mechanical and Interlaminar Fracture Properties of Woven Fabric Reinforced Composites", 39th International SAMPE Symposium, April 11-14, 1994, pp. 2693-2705.

[5] Ishikawa, T., and T. W. Chou, "Stiffness and Strength Behaviour of Woven Fabric Composites", J. Material Science, Vol. 17, 1982, pp. 3211-3220.

[6] Cano, R. J., M. B. Dow, "Properties of Five Toughened Matrix Composite Materials", NASA Technical Paper 3254, Langley Research Center, VA, 1992.

[7] Williams, J. G., "Effect Of Impact Damage and Open Holes On The Compression Strength Of Tough Resin/High Strain Fiber Laminates", in *Tough Composite Materials*, (L. F. Vosteen, N. J. Johnston, and L. A. Teichman, eds.), NASA Conference Publication 2334, Langley Research Center, VA, 1983, pp. 61-79.

[8] Lee, S. M., T. Golato, M. Thiede-Smet, H. Girardy, and G. Chekherdemian, "A New Toughened Epoxy Resin for Resin Transfer Molding Applications", 39th International SAMPE Symposium, April 11-14, 1994, pp. 133-144.

[9] Hong, Su-Don, S. Y. Chung, R. F. Fedors, J. Moacanin, and A. Gupta, "Morphology and Dynamic Mechanical Properties of Diglycidyl Ether of Bisphenol-A Toughened with Carboxyl-Terminated Butadiene-Acrlonitrile, in *Tough Composite Materials*, (L. F. Vosteen, N. J. Johnston, and L. A. Teichman, eds.), NASA Conference Publication 2334, Langley Research Center, VA, 1983, pp. 285-294.

[10] Wilkinson, S. P., S. C. Liptak, J. J. Lesko, D. A. Dillard, J. Morton, J. E. Mcgrath, and T. C. Ward, "Toughened Bismaleimides and Their Carbon Fiber Composites

for Fiber-Matrix Interphase Studies", Proc. Sixth Japan-U.S. Conference on Composite Materials, June 22-24, 1992, pp. 240-249.

[11] Woo, E. M., and K. L. Mao, "Evaluation of Interlaminar-Toughened Poly(ether imide)-modified Epoxy/Carbon Fiber Composites", Polymer Composites,> October 1995.

[12] McGrail, P. T., S. D. Jenkins, "Some Aspects of Interlaminar Toughening in Thermosetting Composites", Polymer Preprints, Vol. 33, No. 1, 1992, pp. 360-361.

[13] Brack, R. A., R. M. Chris, and D. F. Sims, "Material and Process Development of a Fiberglass/Carbon-Reinfored Toughened Epoxy for Tiltrotor Components", 39th International SAMPE Symposium, April 11-14, 1994.

[14] Verchere, D., H. Sautereau, J. P. Pascault, S. M. Moschiar, C. C. Riccardi, and R. J. J. Williams, "Rubber-Modified Epoxies. I. Influence of Carboxyl-Terminated Butadiene-Acrylonitrile Random Copolymers (CTBN) on the Polymerization and Phase Separation Processes", J. App. Polym. Sci., Vol. 41,1990, pp. 467-485.

[15] Verchere, D., J. P. Pascault, H. Sautereau, S. M. Moschiar, C. C. Riccardi, and R. J. J. Williams, "Rubber-Modified Epoxies. II: Influence of the Cure Schedule and Rubber Concentration on the Generated Morphology", J. App.Polym. Sci., Vol. 42, 1991, pp. 701-716.

[16] Moschiar, S. M., C. C. Ricardi, R. J. J. Williams, D. Verchere, H. Sautereau, and, J. P. Pascault, "Rubber-Modified Epoxies. III: Analysis of Experimental Trends through a Phase Separation Model", J. App. Polym. Sci., Vol. 42, 1991, pp. 717-735.

[17] Verchere, D., J. P. Pascault, H. Sautereau, S. M. Moschiar, C. C. Riccardi, and R. J. J. Williams, "Rubber-Modified Epoxies. IV. Influence of Morphology on Mechanical Properties", J. App. Polym. Sci., Vol. 43, 1991, pp. 293-304.

[18] Kubotera, K., and A.F. Yee, "Morphological and Fracture Studies of Alloys of Thermosets and Thermoplastics", *Back To The Future*, SPE ANTEC '92, Vol. II, May 1992, p. 2610.

[19] Srinivasan, S.A., et al, "Reactive Poly(Arylene Ether) Toughening of Cyanate Ester Networks Via Thermal and Microwave Curing", 39th International SAMPE Symposium, April 1994, pp. 60-71.

[20] Brown, J.M., S. Srinivasan, A.V. Rau, T.C. Ward, J. E. McGrath, and A. C. Loos, "Production of Controlled Networks and Morphologies in Toughened Thermosetting Resins Using Real-Time, In-Situ Cure Monitoring, 41st SAGAMORE Conf. on Intelligent Processes and Materials, US Army Research Lab., Materials Directorate (Polymer), Plymouth, MA, August 1994.

[21] Wilkinson, S.P., T.C. Ward, and J.E. McGrath, "Effect of Thermoplastic Modifier Variables on Toughening a Bismaleimide Matrix Resin for High - Performance Composite Materials", Polymer, Vol. 34, No. 4, 1993, p. 870.

[22] Srinivasan, S.A., "Toughening of Cyanate Ester Networks with Reactive Thermoplastic Modifiers", Doctoral Dissertation, Virginia Polytechnic Institute and State University, Blacksburg, Virginia, April 1994.

[24] Verchère, D., H. Sautereau, J. P. Pascault, S. M. Moschiar, C. C. Ricardi, and R. J. J. Williams, "Rubber-Modified Epoxies: Analysis of the Phase-Separation Process", in *Toughened Plastics I Science and Engineering*, (C. Keith Riew and A.J. Kinloch, eds.), Advances in Chemistry Series 233, American Chemical Society, Chapter 14, 1993, pp. 335-363.

[25] Yoon, T.H., S.C. Liptak, D.B. Priddy Jr., and J.E. McGrath, "Adhesive and Mechanical Properties of Reactive Polysulfone Modified Epoxy Resins", J. Adhesion, Vol. 45, 1994, pp. 191-203.

[26] Wong, D. G., M. F. DiBerardino, and R. C. Cochran, "Processing Evaluation of Toughened Epoxy Composites", 39th International SAMPE Symposium, April 1994, pp. 297-310.

[30] Brown, J. M., "Production of Controlled Networks and Morphologies in Toughened Thermosetting Resins Using Real-Time, In-situ Cure Monitoring", Doctoral Dissertation, Virginia Polytechnic Institute and State University, Blacksburg, Virginia, January 1994.

[31] Chan, L. C., J. K. Gillham, A. J. Kinloch, and S. J. Shaw, "Rubber-Modified Epoxies: Cure, Transitions, and Morphology", in *Rubber Modified Thermoset Resins*, (C. Keith Riew and J. K. Gillham, eds.), Advances in Chemistry Series 208, American Chemical Society, Chapter 15, 1983, pp. 235-259.

[32] Teh, K. T., "Impact Damage Resistance and Tolerance of Advanced Composite Material Systems", Doctoral Dissertation, Virginia Polytechnic Institute and State University, Blacksburg, Virginia, 1993.

[33] Weideman, M. H., A. C. Loos, H. B. Dexter, G. H. Hasko, "An Infiltration/Cure Model for Manufacture of Fabric Composites by the Resin Transfer Molding Process", Center For Composite Materials and Structures Report Series, CCMS-92-05, Virginia Polytechnic Institute and State University, Blacksburg, Virginia, 1992.

[34] Hammond, V.H., A.C. Loos, H.B. Dexter, and G.H. Hasko, "Verification of a Two-Dimensional Infiltration Model for the Resin Transfer Molding Process", Virginia Tech Center for Composite Materials and Structures Report, CCMS-93-15, Blacksburg, VA, August 1993.

[35] Fingerson, J. C., A. C. Loos, H. B. Dexter, "Verification of a Three-Dimensional Resin Transfer Molding Process Simulation Model", Center For Composite Materials and Structures Report Series, CCMS-95-10, Virginia Polytechnic Institute and State University, Blacksburg, Virginia, September, 1995.

[36] Verghese, K. E., "An Infiltration/Cure Model for Manufacture of Fabric Composites by the Resin Transfer Molding Process", Center For Composite Materials and Structures Report Series, CCMS-92-05, Virginia Polytechnic Institute and State University, Blacksburg, Virginia, 1996.

[37] Hayward, J.S. and B. Harris, "Effect Of Process Variables On The Quality Of RTM Mouldings", SAMPE Journal, Vol. 26, May/June 1990, p. 39.

[38] Roller, M.B., "Rheology of Curing Thermosets: A Review", Polym. Eng. Sci., Vol. 26, No. 6, March 1986, p.432.

[39] Hasko, G., H.B. Dexter, A.C. Loos, and D. Kranbuehl, "Science-Based RTM For Fabricating Primary Aircraft Structures", 39th International SAMPE Symposium, April, 1994, p.779.

[40] Ahn, K.J., J.C. Seferis, and L. Letterman, "Autoclave Resin Infusion Process: Anaysis and Prediction of Resin Content", SAMPE Quarterly, January 1990, p 3.

[41] Loos, A.C., and G.S. Springer, "Curing of Epoxy Matrix Composites", J.Composite Materials, Vol. 17, March 1983, p 135.

[42] Hou, T.H., and J.M. Bai, "A Semi-Empirical Approach for the Chemoviscosity Modeling of Reactive Resin System", SAMPE Journal, Vol. 24, No. 6, Nov/Dec, 1988, p. 43.

[43] Hackett, S.C., P.C. Griebling, and A.M. Hine, "Unique Advanced Materials With

High Performance and Resin Transfer Molding Characteristics", *Advanced Materials: Cost Effectiveness, Quality Control, Health and Environment*, Eds. A. Kwakernaak and L. van Arkel, SAMPE/Elsevier Science Publishers B.V., 1991.

[44] Puckett, P.M., and W.D. White, "Thermoset Resin Systems And Manufacturing Technology For RTM", Resin Transfer Molding for the Aerospace Industry, SME Conference Proceedings, Manhattan Beach, CA, March 1990.

[45] Strömbeck, A., "Optimization of the Resin Transfer Molding Process for Advanced Composites", ICCM/9, Spain, 1993, p. 497.

[46] Gebart, B.R., "Analysis of Heat Transfer and Fluid Flow in the Resin Transfer Moulding Process", Doctoral Thesis, Swedish Institute of Composites, Piteå and Luleå University of Technology, Luleå, Sweden, March 1993.

[47] Cai, Z., "Mold Filling Analysis of RTM Process", J. Composite Materials, Vol. 26, No. 9, 1992.

[48] Castro, J.M., and C.W. Macosko, "Studies of Mold Filling and Curing in the Reaction Injection Molding Process", AIChE Journal, Vol. 28, No. 2, 1982, p. 250.

[49] Chen, Y-T., and C.W. Macosko, "Chemorheology of Polycyanate for Resin Transfer Molding", 24th International SAMPE Technical Conference, October 20-22, 1992, p. T630.

[50] ASTM D 2734-91, "Standard Test Methods for Void Content of Reinforced Plastics", *Annual Book of ASTM Standards*, Vol. 08.02, pp. 115-117.

[51] ASTM D 792-86, "Test Method for Specific Gravity (Relative Density) and Density of Plastics by Displacement", *Annual Book of ASTM Standards*, Vol. 08.01, pp. 299-302.

[52] ASTM D 2734-91, "Test Method for Ignition Loss of Cured Reinforced Resins", *Annual Book of ASTM Standards*, Vol. 08.02, pp. 115-117.

[53] Gürdal, Z., and J. M. Starbuck, "Compresssive Characterization of Unidirectional Composite Materials", Analytical and Testing Methodologies for Design with Advanced Materials, 1988, pp.337-347.

[54] Whitney, J. M., "Experimental Characterization of Delamination Fracture", in *Interlaminar Response of Composite Materials*, (N.J. Pagano, ed.), Elsevier

Science Publishers 1989, pp.161-240.

[55] Russell, A. J., and K. N. Street, "Factors Affecting the Interlaminar Fracture Energy of Graphite/Epoxy Laminates", in *Progress in Science and Engineering of Composites*, (T. Hayashi, K. Kawata, and S. Umekawa, eds.), ICCM-IV, Tokyo 1982, pp.279-286.

[56] Russell, A. J., and K. N. Street, "Moisture and Temperature Effects on the Mixed-Mode Delamination Fracture of Unidirectional Graphite/Epoxy", in *Delamination and Debonding of Materials*, (W. S. Johnson, ed.), ASTM STP 876, 1985, pp.349-370.

[57] Wang, S. S., "Fracture Mechanics for Delamination Problems in Composite Materials", in *Progress in Science and Engineering of Composites*, (T. Hayashi, K. Kawata, and S. Umekawa, eds.), ICCM-IV, Tokyo 1982, pp.287-294.

[58] Wilkinson, S. P., "Toughened Bismaleimides, Their Carbon Fiber Composites and Interphase Evaluation Studies", Ph.D. Dissertation, Virginia Polytechnic Institute and State University, Blacksburg, Virginia, 1991.

[59] Davies, P., W. Cantwell, C. Moulin, and H. H. Kausch, "A Study of the Delamination Resistance of IM6/PEEK Composites", Composite Science and Technology, Vol. 36, 1989, pp.153-166.

[60] Chiou, P., and A. Letton, "Reaction Kinetics and Chemoviscosity of a Thermoset Exhibiting Complex Curing Behavior", in *Processing Of Polymers And Polymer Composites*, (A. A. Tseng, and S. K. Soh, eds.), The American Society of Mechanical Engineers, MD-Vol. 19, November 1990, pp. 35-48.

[61] Demaree, R. J.,"The Effects of Process Parameters on the Properties of Resin Transfer Molded Composites", Master of Science Thesis, Virginia Polytechnic Institute and State University, Blacksburg, January 1996.

[62] Wilkinson, S. P., T. C. Ward, and J. E. McGrath, "Effect of thermoplastic modifier variables on toughening a bismaleimide matrix resin for high-performance composite materials", Polymer, Vol. 34, No.4, 1993, pp.870-884.

[63] Recker, H. G., V. Altstädt, W. Eberle, T. Folda, D. Gerth, W. Heckmann, P. Ittemann, H. Tesch, und T. Weber, "Toughened Thermosets for Damage Tolerant Carbon Fiber Reinforced Composites", Sampe Journal, Vol. 26, No. 2, March/April 1990, pp. 73-78.

[64] Babic, L., C. Dunn, and P.J. Hogg, "Damage Development and Its Significance in GRP Subjected to Impact", Plast. Rubber Process. Appl., Vol. 12, No. 4, 1989, pp. 199-207.

[65] Odagiri, N., T. Muraki, and K. Tobukuro, "Toughness Improved High Performance Torayca Prepreg T800H/3900 Series", in *Materials - Pathway to the Future*, SAMPE, California, 7-10 March, 1988, pp. 272-283.

4.0 DESIGNING THE INJECTION PARAMETERS FOR THE RTM PROCESS.

4.1 INTRODUCTION

In the manufacture of composites by liquid molding techniques, the first step is to infiltrate the resin into the dry preform. In order to fully infiltrate a perform, the process parameters associated with this step must be carefully selected. The key process variables are the resin injection temperature and the injection pressure. An appropriate choice of these variables ensures successful completion of this process.

In recent years, numerous investigations have been carried out on the RTM process, but a clear technique to select infiltration process parameters has not yet evolved. In 1990, Hayward and Harris[1] noted that in spite of a large number of investigations on the process, there was insufficient information in the literature to base the choice of process variables. Again, in 1993, Verheus and Peeters[2] refer to the ad hoc nature of the selection of injection parameters which are largely based on the operator's experience.

Thus, the need for a systematic method for the selection of the injection parameters is well recognized.

The influence of various process parameters on the quality and void content in composites manufactured by the RTM process has been studied by Hayward and Harris[1], and Gebart [4]. Gebart presents a qualitative assessment of the process variables on void production in composites. Again, the injection pressure and the temperature of resin/ mold at injection are identified as the most significant variables that affect composites manufactured by RTM.

In RTM, most resin systems are injected at an elevated temperature in order reduce the viscosity and process cycle times [1]. The characteristics of the resin system drives the choice of the injection temperature as thermosetting resin systems do not have a constant viscosity at elevated temperatures due to the complex dependence of viscosity on temperature and cure state [3,5,6,7]. The cure state, in turn, depends on temperature and prior thermal history.

Temperature controls resin viscosity during injection. The injection temperature is selected to give an initial resin viscosity in the range of 0.1-3.5 Pa-s. Hasko et al [3], comparing viscosity behavior of two epoxy resin systems, 3M PR500 and Hercules 3501-6, state that the 3501-6 resin system can not be used in PI-RTM owing to a limited minimum in viscosity. The authors also suggest that the PR500 resin system can be injected - "if the process is designed around the limited viscosity window". Knowing that the viscosity window is limited and also that the viscosity is not constant, an injection

temperature which provides a maximum window below a predetermined viscosity level. Once the injection temperature is determined, the viscosity profile corresponding to that injection temperature can be determined from the viscosity and cure kinetics models.

The injection pressure now remains to be determined. The injection pressure must be selected such that infiltration is completed well before the resin viscosity rapidly increases above a "critical" or "cut-off" value. Again, the selection of an injection pressure depends on the geometry of the component to be manufactured, the permeability of the preform material, and on the mold configuration and injection strategy. The pressure capabilities of injection equipment place a limit on the maximum pressure that can be safely used for injection.

Resin flow simulation models can be used for the selection of the injection pressure. Resin infiltration is the most widely studied aspect of the RTM process and a number of researchers have directed efforts towards the development of flow simulation models using various numerical techniques. A finite element method/control volume based flow model has been developed by MacRae and Loos [8] and validated by Hammond, et. al.[9]. These flow models, when used in conjunction with optimization schemes, help in the complete design of the RTM process.

In this study, a method was developed for a well characterized resin system that can be used to determine the injection temperature for liquid molding processes. Further, based on the viscosity profile generated for the selected injection temperature, the time required for the infiltration of a 152 mm x 152 mm preform will determined at different

levels of applied pressure. The infiltration time for different injection pressures will be determined with the aid of the two-dimensional flow simulation model developed by MacRae and Loos [8]. The analysis will be performed on two different epoxy resin systems to demonstrate the approach.

4.2 MATERIALS

In this investigation, two different resin systems were chosen for study. The first, Shell RSL1895/W, is an epoxy resin system designed specifically for use in the RTM process. The second, Hercules 3501-6, a hot-melt epoxy resin system designed for prepregs. This resin system, however, is commonly used for composite manufacture by the resin film infusion (RFI) technique.

Further, for the purpose of flow modeling, the characteristics of a preform, at a fiber volume fraction of 60%, constructed from AS4-3k-PW fabric will be used. Specifically, the permeability of this fabric material obtained from the earlier characterization, in Section 3.6.1, will form a part of input data for the flow model.

4.3 INJECTION TEMPERATURE

In a typical liquid molding process, the resin temperature is raised at a constant heating rate, β, to an injection temperature, T_{inj}. Infiltration of the preform is commenced

once the resin temperature reaches T_{inj}. Usually the mold containing the preform is also maintained at the injection temperature.

As the temperature is increased, the resin viscosity decreases. Upon reaching T_{inj}, the temperature is maintained constant until the completion of the infiltration process. Beginning at the onset of this hold period, the resin viscosity increases, from a minimum value, due to the progress of the cure reaction. The viscosity minimum at the onset point and the rate of increase in viscosity are influenced by the choice of the injection temperature and the heating rate, β.

The heating rate and the injection temperature must be selected with the objective to provide the largest possible window for resin infiltration. In order to determine the processing window, an objective function, I_μ , is constructed

$$I_\mu = \int_{t_i}^{t_f} [\mu_c - \mu(T,\alpha)]\, dt \qquad (4.1)$$

where, μ_c is defined as a user specified "cut-off" viscosity. $\mu(T,\alpha)$ is the resin viscosity expressed as a function of the cure state and temperature as obtained from resin characterization (Section 2.7.1). Fig. 4.1 shows a schematic representation of a typical viscosity-time profile corresponding to a ramp-hold temperature-time profile. Also shown in the figure are, t_i, the time at which the resin viscosity first reaches the μ_c value during the heat-up to T_{inj} , and t_f the time at which the resin viscosity reaches the cut-off

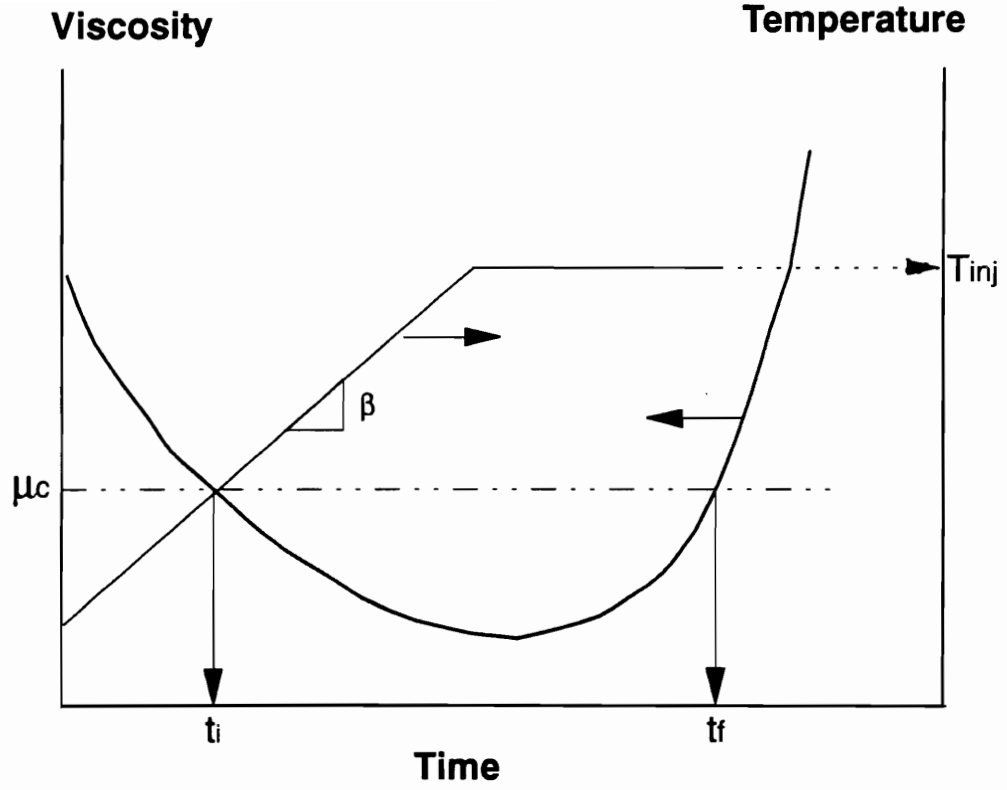

Figure 4.1 Schematic representation of a temperature-time profile and the corresponding viscosity-time profile.

viscosity during the hold at the injection temperature. The function I_μ represents the area between μ_c and the viscosity-time curve, bounded on the time axis between t_i and t_f. The time interval between t_i and t_f is defined as the window time, Δt_{win}.

Ideally, if μ_c is considered that level of viscosity above which the ease of resin infiltration is diminished, then the infiltration of the preform should be completed within the available window time. The choice of the value of the cut-off viscosity may depend on the characteristics of the resin system, the permeability of the preform material, etc. The question as to what is the "right viscosity" for the RTM process, still remains unanswered.

Now, if the viscosity-time area represented by I_μ is increased a dual benefit of reduced viscosity and an expanded window time can be realized. Two extreme situations can be envisioned. First, with reference to a specified μ_c, the resin viscosity can reach a very low value over a short window time, as would occur with the choice of a very high T_{inj}. Choosing an injection temperature which is much lower than that in the first case leads to the second case where, for the same value of μ_c, the resin viscosity is higher than in the previous case, and may result in an extended Δt_{win}. The injection temperature can range between a lower bound of ambient temperature and an upper bound of the maximum cure temperature. Neither of the above mentioned cases may provide the largest I_μ. This fact is demonstrated in Figure 4.2, where the function I_μ, calculated for the RSL1895/W resin system, is plotted as a function of injection temperature.

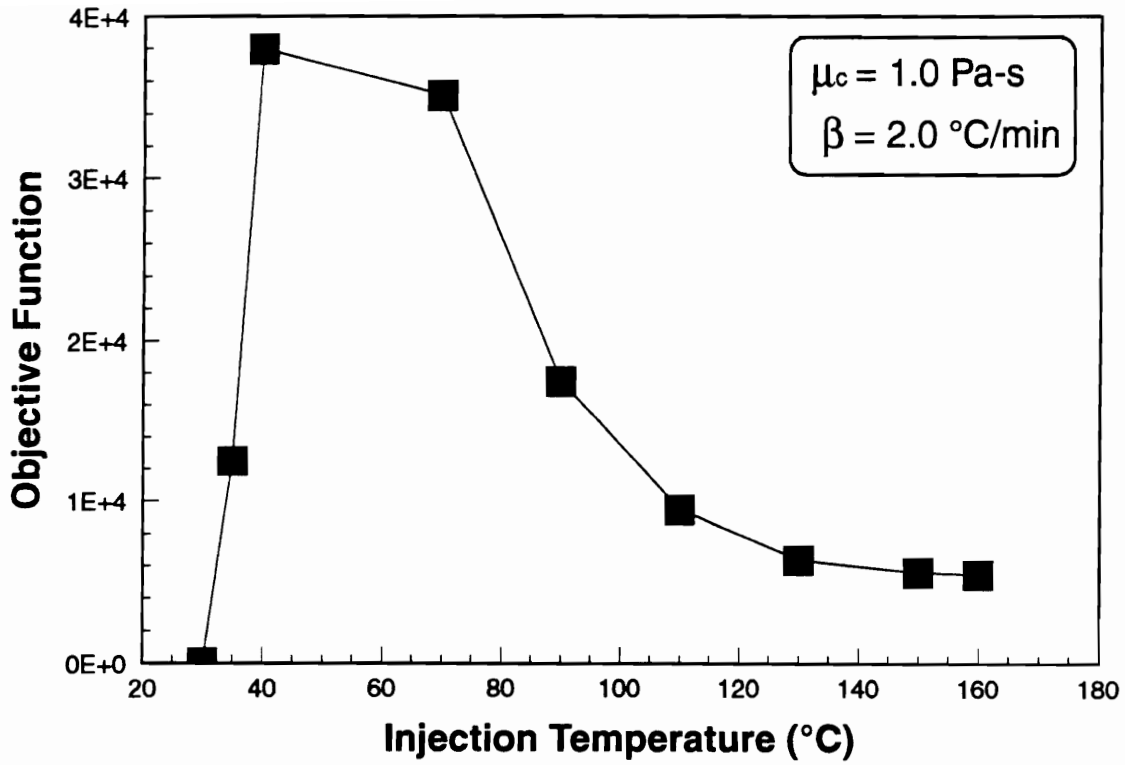

Figure 4.2 Objective function, I_μ, as a function of the injection temperature for RSL1895/W resin system (μ_c = 1.0 Pa-s; β = 2.0 °C/min).

The function I_μ (eq. 4.1) was calculated by increasing the resin temperature, at a rate of 2.0 °C/min, to a preselected injection temperature. The procedure was repeated for different values of preselected T_{inj}, ranging from 20 °C to 160 °C. In the calculations, μ_c was specified as 1.0 Pa-s. In Fig. 4.2, the calculated values of I_μ are plotted as a funtion of the corresponding injection temperature. Clearly, I_μ is a unimodal function, exhibiting a maximum value at some injection temperature between the ambient and maximum cure temperatures.

This behavior provides an opportunity to utilize numerical optimization schemes to identify the parameters which provide the best value of the objective function, I_μ, for a given resin system. Hence, in this study, an attempt is made to find a T_{inj} which maximizes the objective function, for a set of heating rate and cut-off viscosity conditions. The optimization is performed with a computer code which uses the golden section search technique, a line search algorithm [10]. In order to study the effects of heating rate and cut-off viscosity on the optimal injection temperature, nine different cases were analyzed for each of the two resin systems. For the RSL1895/W resin system, cut-off viscosity values of 0.25, 0.50, and 0.75 Pa-s were selected. For each value of μ_c, three different heating rates, 1.0, 2.0, and 4.0 °C/min were examined. For the Hercules 3501-6 resin system, the same three heating rates were used at cut-off viscosities of 2.5, 5.0, and 7.5 Pa-s. This analysis would then provide the data required to study the dependence of the maximum objective function and the optimal injection temperatures on the heating rate and the cut-off viscosity.

4.4 INJECTION PRESSURE

The magnitude of the injection pressure during the RTM process depends on the geometry, preform permeability, resin viscosity, and the location of the injection ports and vents in the mold. Capabilities of the injection equipment places a limitation on the maximum useable pressure. Typically, the magnitude of the injection pressure is selected to completely infiltrate the preform in the shortest possible time.

Numerical models of the infiltration process can aid in determining the required injection pressure for complete infiltration of a preform. In this investigation a flow simulation model, RTM2D Version 1.1A [11], based on the Finite Element Method/Control Volume technique was used to determine the time required for the infiltration of a flat, 152 mm x 152 mm preform. The analysis was performed for the center-injection configuration, where the resin is injected at an inlet port at the center of the mold cavity, flows through the preform and exits from vents located on two opposite sides of the preform. The injection configuration is shown schematically in Fig. 3.4 and the details of the mold in Fig. 3.7. The time required to infiltrate the preform was calculated for the a constant resin pressure at the inlet to the mold. The analysis was repeated for various of inlet pressures, thereby providing the information required to correlate model predicted infiltration time with injection pressure.

A uniform mesh of 36 x 36 linear quadrilateral elements was used to model the preform. User input to the model included preform permeabilities in the warp and fill directions, fiber volume fraction, and resin viscosity-time and injection pressure-time

profiles. The values of the AS4-3k-PW fabric preform permeabilities in the warp and fill directions were 6.5 x 10^{-12} and 1.9 x 10^{-11} m^2, respectively (Section 3.6.1). These values correspond to a fiber volume fraction of 60%. The viscosity-time profile within the window time, generated from the analysis of the previous section, was input into the model. For the Hercules 3501-6 resin system, the viscosity-time profile used was generated for the optimal injection temperature case of μ_c = 2.5 Pa-s and a heating rate of 2.0 °C/min. The model predicted infiltration times for the center port injection scheme were generated at pressures ranging between 103 kPa (30 psi) and 1034 kPa (150 psi). Based on the results obtained from the analysis, the limits of injection equipment, and the injection window time, Δt_{win}, generated in the previous section, the feasibility of injecting the 3501-6 resin system into the AS4-3k-PW fabric preform was assessed.

4.5 Results and Discussion

The optimization scheme generated injection temperatures which maximizes the objective function, I_μ, for both the resin systems considered for this analysis. The optimal injection temperatures were generated for a total of nine different combinations of heating rate and cut-off viscosity levels. The development of the optimal solutions for one combination of heating rate and cut-off viscosity are shown in Fig. 4.3 for Hercules 3501-6 (top) and RSL1895/W (bottom) resin systems.

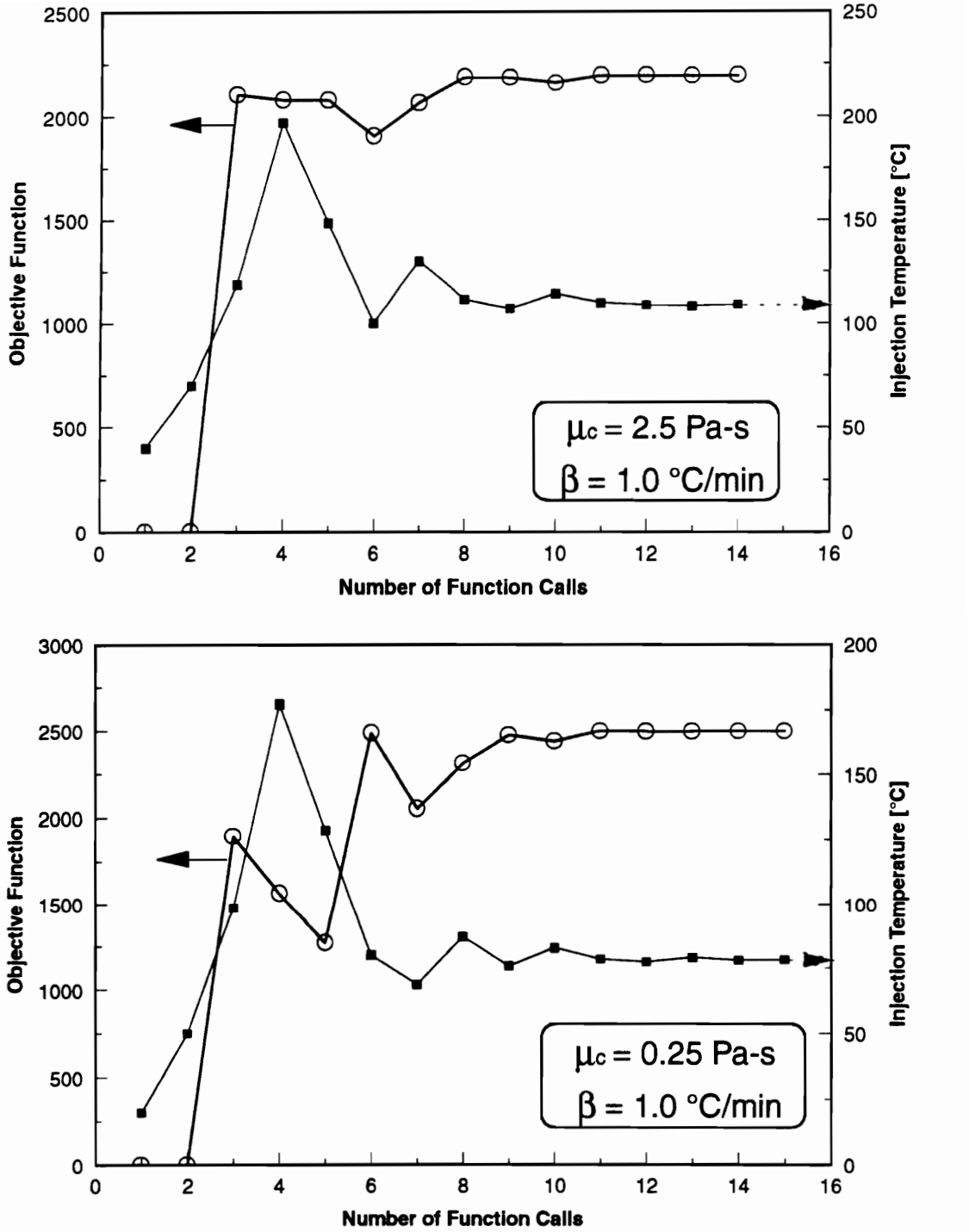

Figure 4.3 Development of optimal solution for Hercules 3501-6 (top) and RSL1895/W (bottom) resin systems.

In the golden section search technique, the optimal solution is determined based only on function evaluations. In Fig 4.3, the objective function and the injection temperature (the design variable) are plotted versus the number of function calls at the lowest heating rate (1.0 °C/min) and the lowest level of cut-off viscosity (2.5 Pa-s for Hercules 3501-6, and 0.25 Pa-s for RSL1895/W). The optimization calculations were repeated for the remaining 8 combinations of β and μ_c for each resin system.

In Fig. 4.4, the optimal values of the objective function are plotted as a function of the heating rate for the two resin systems, 3501-6 (top) and RSL1895/W (bottom). The results are plotted for the low, the medium, and the high values of cut-off viscosities chosen for each resin system. The results indicate that for a given level of cut-off viscosity, the optimal solution is not influenced by the rate of heating, up to the injection temperature. The increase in the objective function with an increase in the value of μ_c reflects the increase in the area represented by I_μ. The optimal values of the injection temperature are, however, influenced by the choice of the cut-off viscosity. Fig. 4.5 shows the optimal values of the injection temperature, T_{inj}, obtained for the nine cases analyzed for each resin system. The results for the 3501-6 resin system show that an increase in the heating rate causes a decrease in the optimal injection temperature. However, for the RSL1895/W resin system, the injection temperature is independent of heating rate.

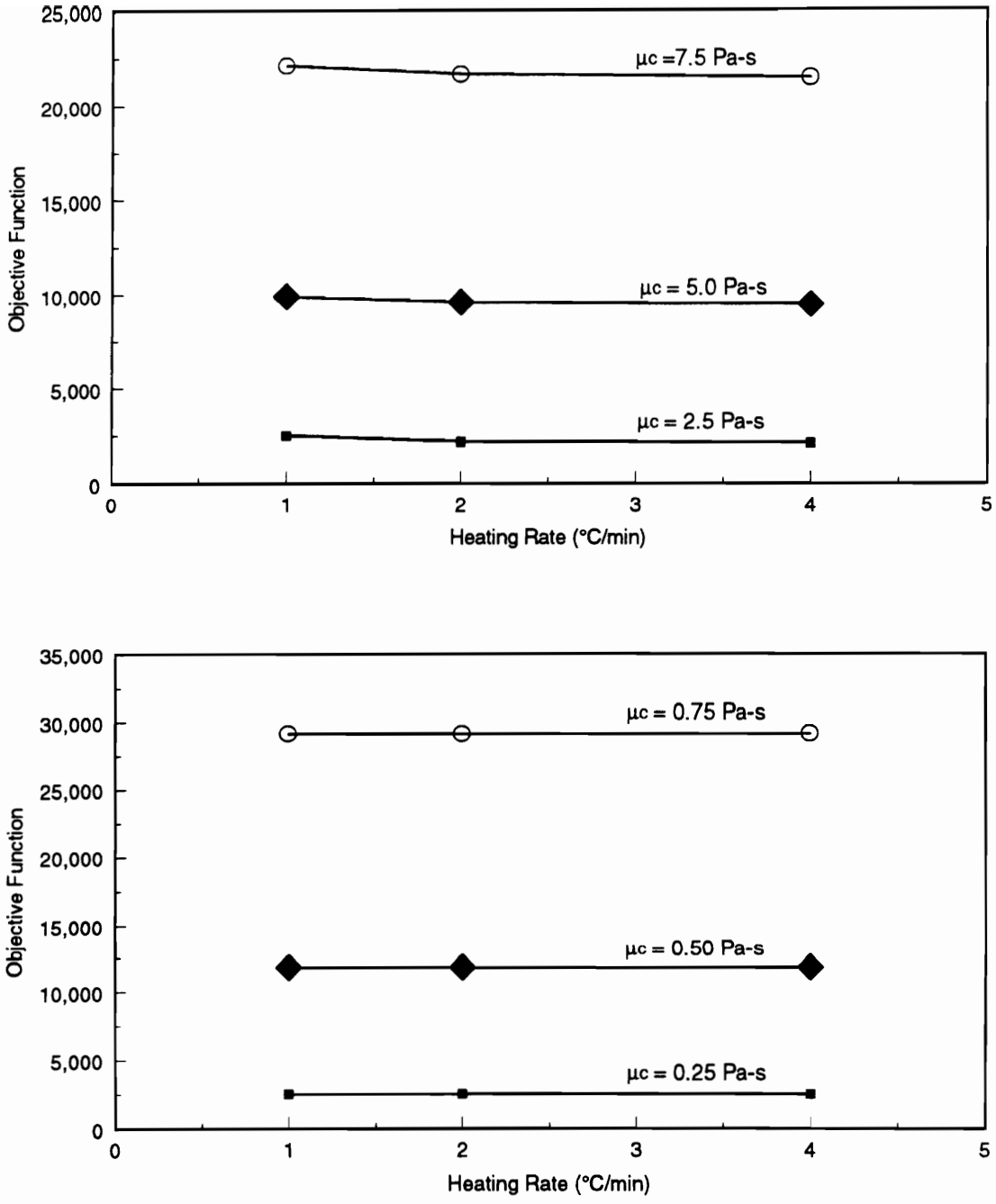

Figure 4.4 Influence of the heating rate on the maximal objective functions for Hercules 3501-6 (top), and RSL1895/W (bottom) resin systems.

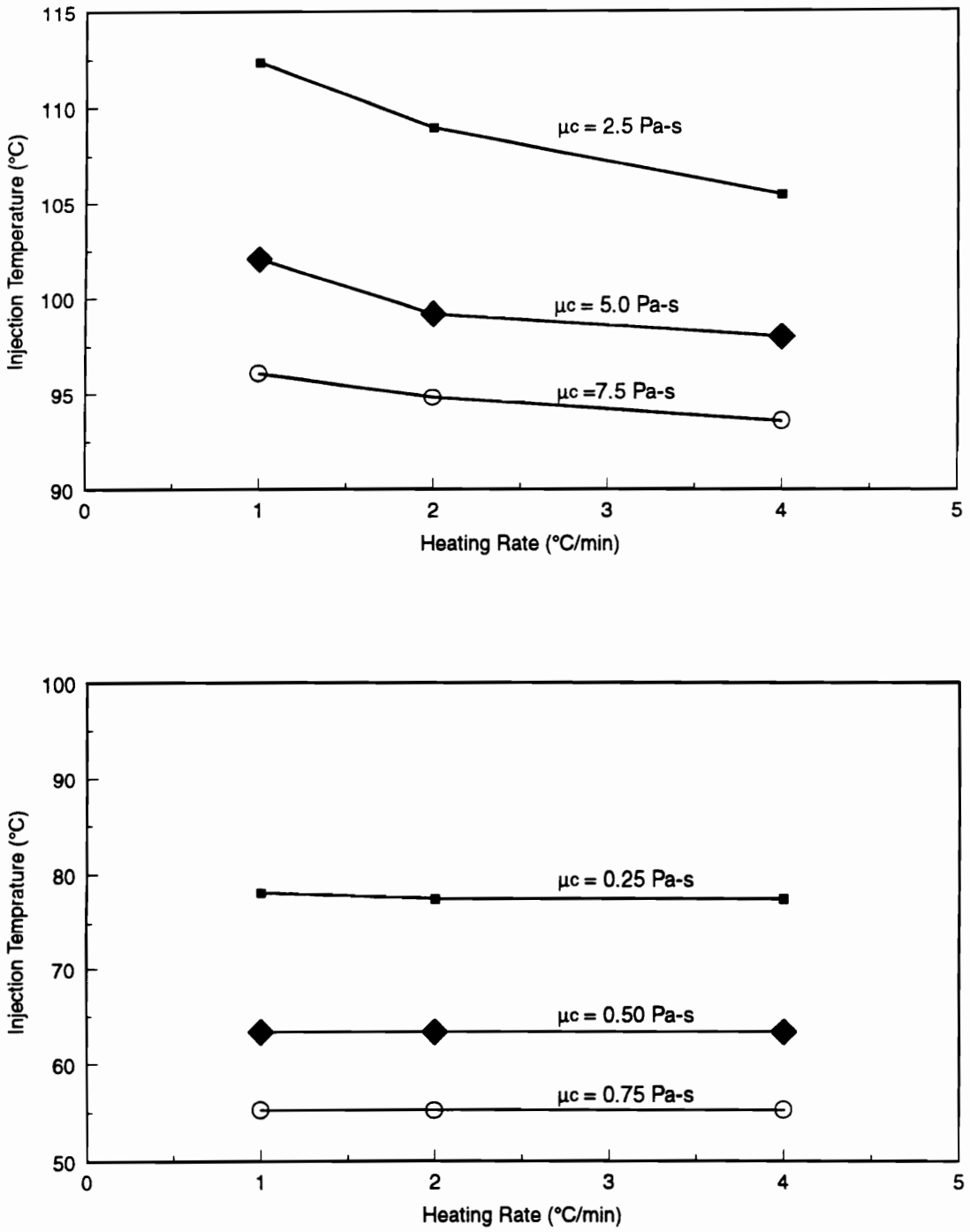

Figure 4.5 Influence of the heating rate on the optimal injection temperature for Hercules 3501-6 (top), and RSL1895/W (bottom) resin systems.

The viscosity-time profiles generated from the injection window analyses are shown in Fig. 4.6 for RSL1895/W resin system. For cut-off viscosities of 0.25, 0.50, and 0.75 Pa-s at a heating rate of 2.0 °C/min the optimal injection temperature were 77.5, 63.3, and 55.2 °C, respectively. As the plot indicates, with an increasing T_{inj} the magnitude of the viscosity minimum decreases, forced by the choice of the cut-off viscosity.

Similarly, Figure 4.7 shows the viscosity-time profiles of the Hercules 3501-6 resin system for cut-off viscosities 2.5, 5.0, and 7.5 Pa-s, and a heating rate of 2.0 °C/min. The optimal injection temperatures obtained for these cases were 109, 99, and 95 °C, respectively.

The effect of varying the heating rate on the viscosity-time profiles is shown in Fig. 4.8, for RSL1895/W, and in Fig. 4.9, for 3501-6. These viscosity-temperature-time plots, generated for the optimal injection temperatures corresponding to a cut-off viscosity of 0.5 Pa-s for RSL1895/W, and 5.0 for 3501-6. Both plots show that the magnitude of the viscosity minimum does not change with a change in the rate at which the injection temperature is reached. However, the location of the viscosity minimum **does** vary, occurring earlier in time, with increasing heating rate. This is a significant result because the injection window is not influenced by the heating rate and the resin viscosity minimum occurs earlier at high heating rates. This provides an opportunity to reduce the overall injection process time. By heating up to the optimal injection temperature at the highest possible rate, the resin injection can be initiated at an early cycle time.

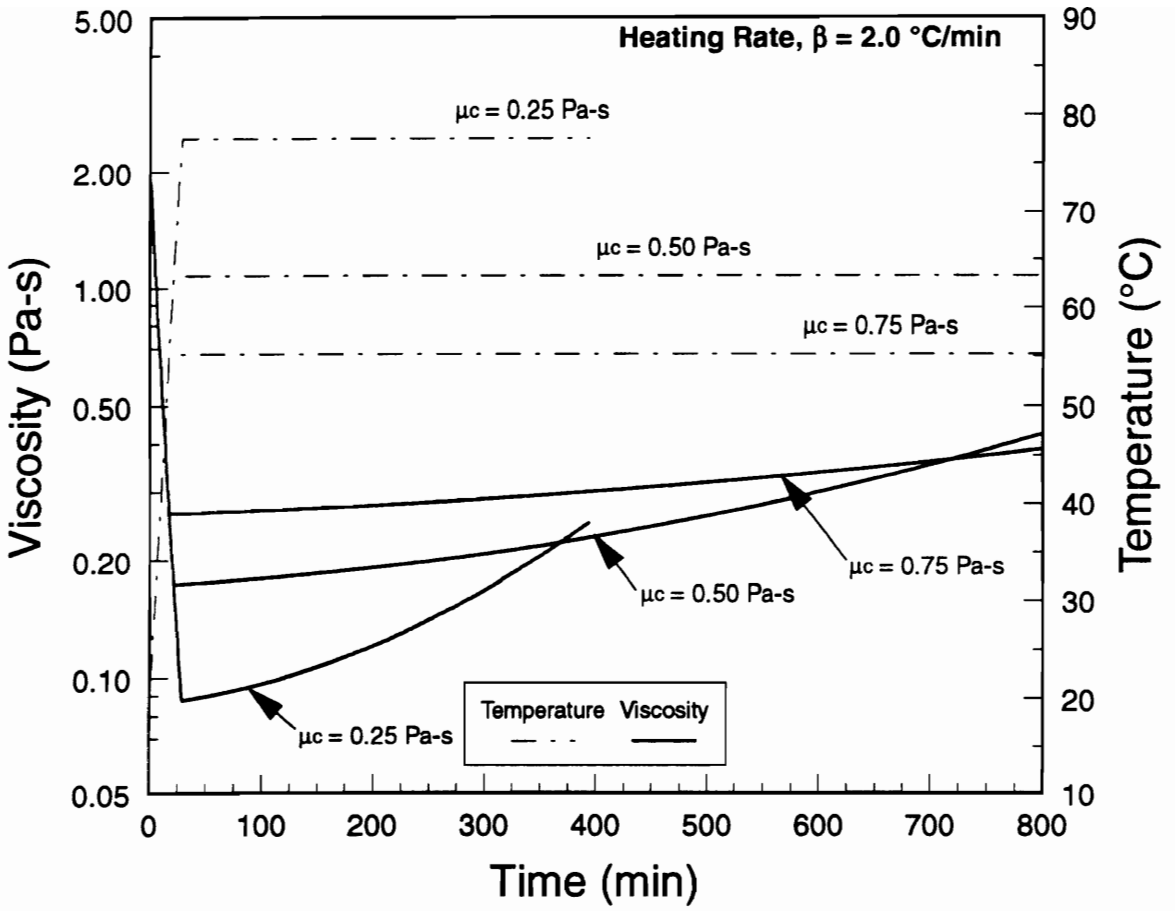

Figure 4.6 Viscosity-time profiles for RSL1895/W resin system at the optimal injection temperatures for β= 2.0 °C/min and at the three levels of μ_c.

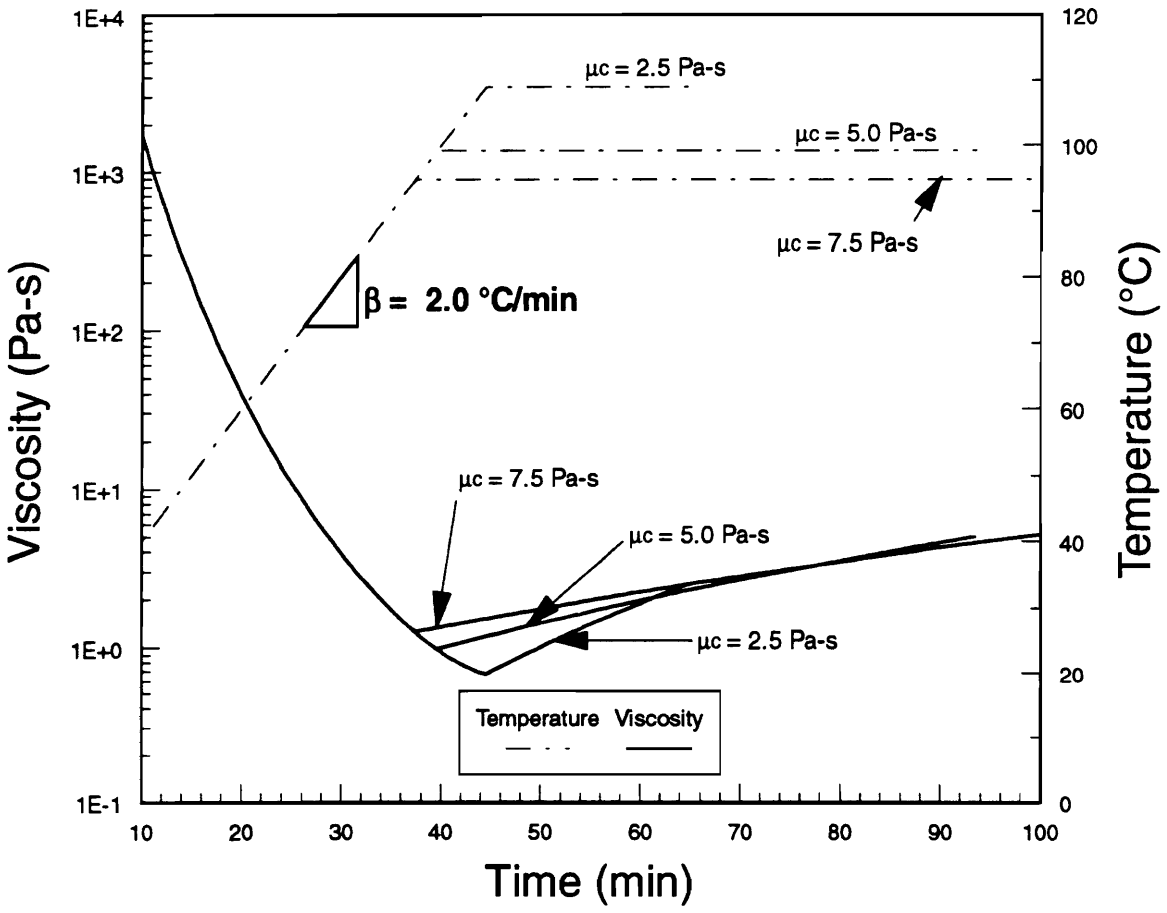

Figure 4.7 Viscosity-time profiles for Hercules 3501-6 resin system at the optimal injection temperatures for β= 2.0 °C/min and the three levels of μ_c.

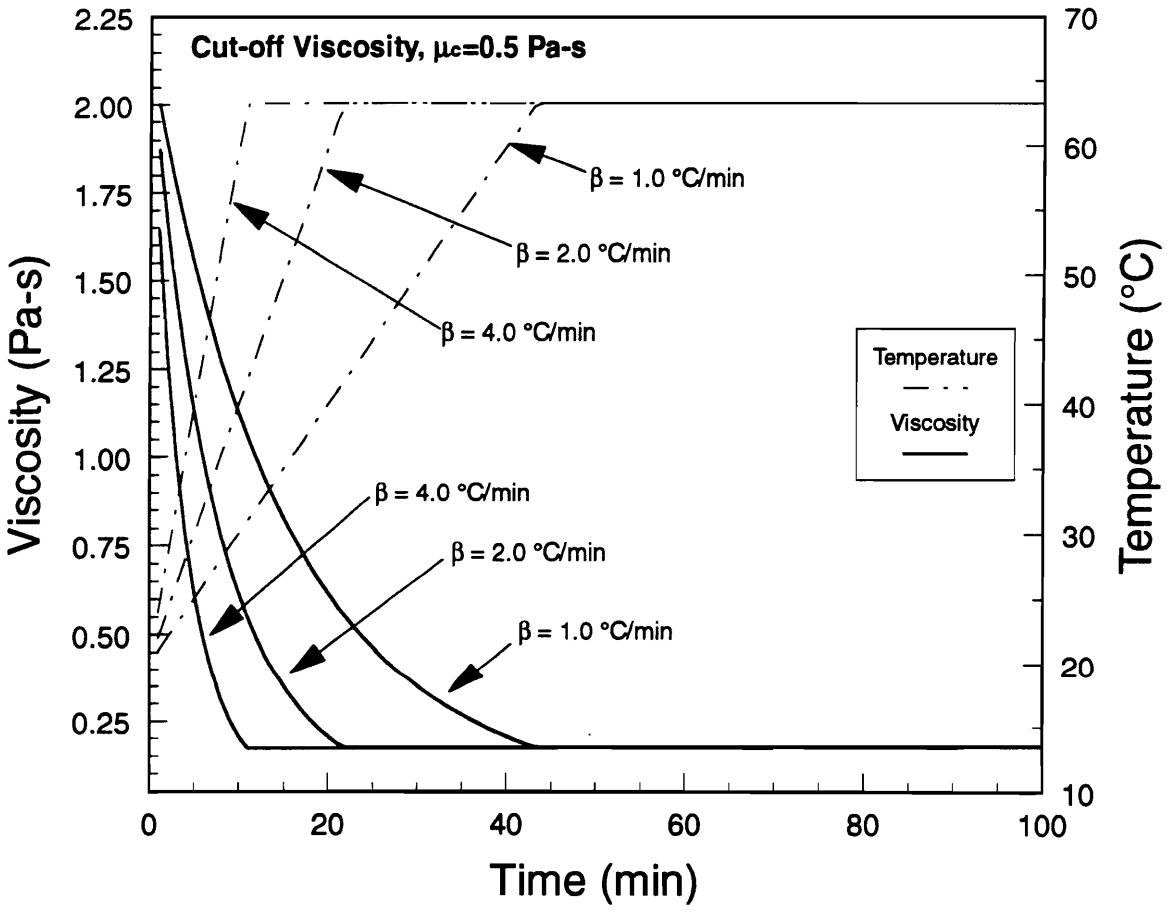

Figure 4.8 Viscosity-time profiles of the RSL1895/W resin system at the optimal injection temperatures for heating rates of 1, 2, and 4 °C/min and μ_c = 0.5 Pa-s.

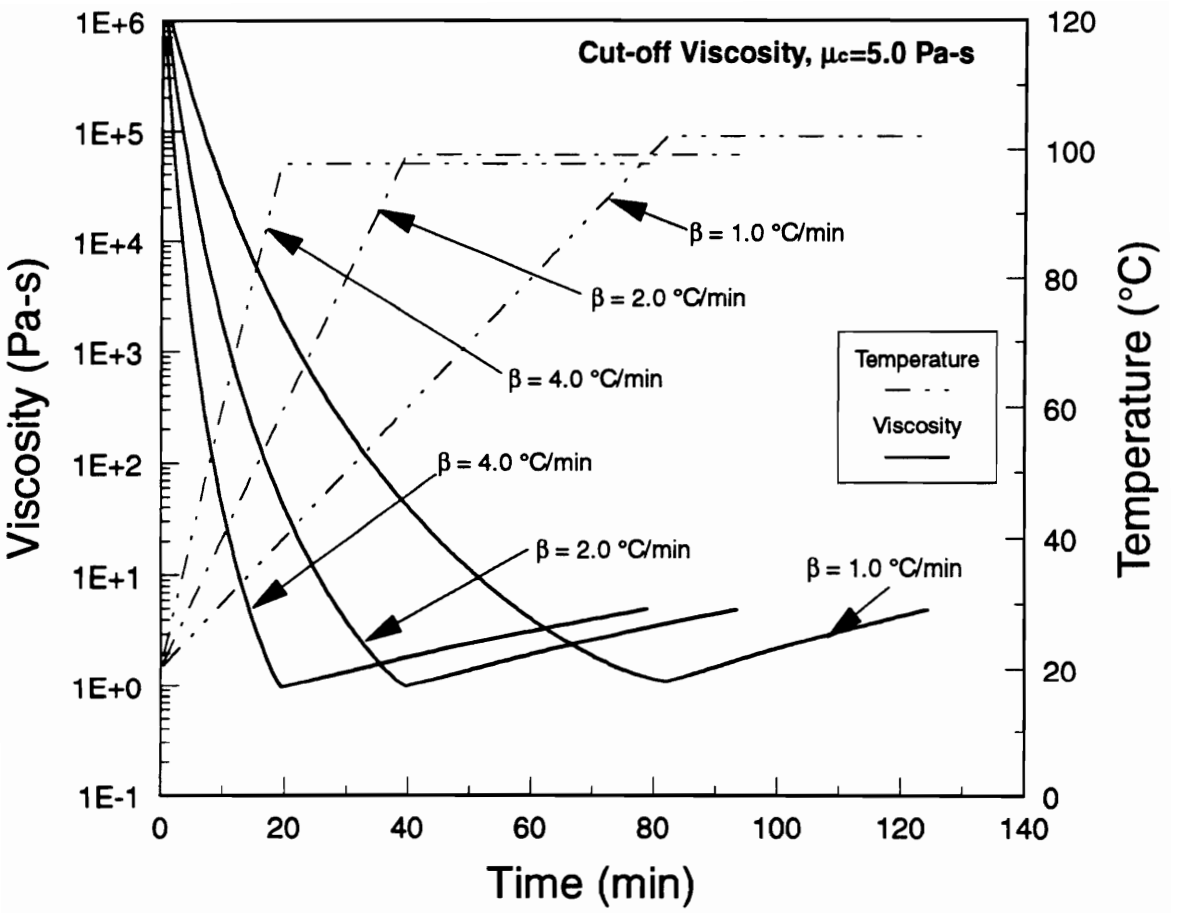

Figure 4.9 Viscosity-time profiles of the 3501-6 resin system at the optimal injection temperatures for heating rates of 1, 2, and 4 °C/min and μ_c = 0.5 Pa-s

For instance, employing heating rates of 1, 2, and 4 °C/min, from Fig. 4.9, the location of the viscosity minimum is shown to occur at about 80, 40, and 18 minutes, respectively, from the start of the process cycle.

Based on the viscosity profiles generated for the optimal injection temperatures, the injection pressures required for complete infiltration of a fabric preform was determined through the use of the flow simulation model. This procedure is demonstrated for the case of the optimal injection temperature obtained for the Hercules 3501-6 resin system (T_{inj} = 109 °C), with a heating rate of 2.0 °C/min, and the cut-off viscosity of 2.5 Pa-s. The viscosity-time profile generated for this thermal cycle was input into the RTM2D flow simulation code and the infiltration times generated for a range of inlet pressures. Shown in Fig. 4.10 are the model predicted infiltration times as a function of the injection pressure. The injection window time, Δt_{win}, predicted by the optimization scheme was 1950 seconds (32.5 minutes). The minimum injection pressure required to completely infiltrate the preform within the injection window time was 655 kPa (95 psi). Infiltration times predicted up to an injection pressure of 1043 kPa (150 psi) are also shown in the figure. In practice, the maximum usable pressure is limited by the specific equipment employed. The pressure pot used in this investigation was rated at 655 kPa (95 psi) while operating at typical injection temperatures and at 760 kPa (110 psi) for room temperature applications.

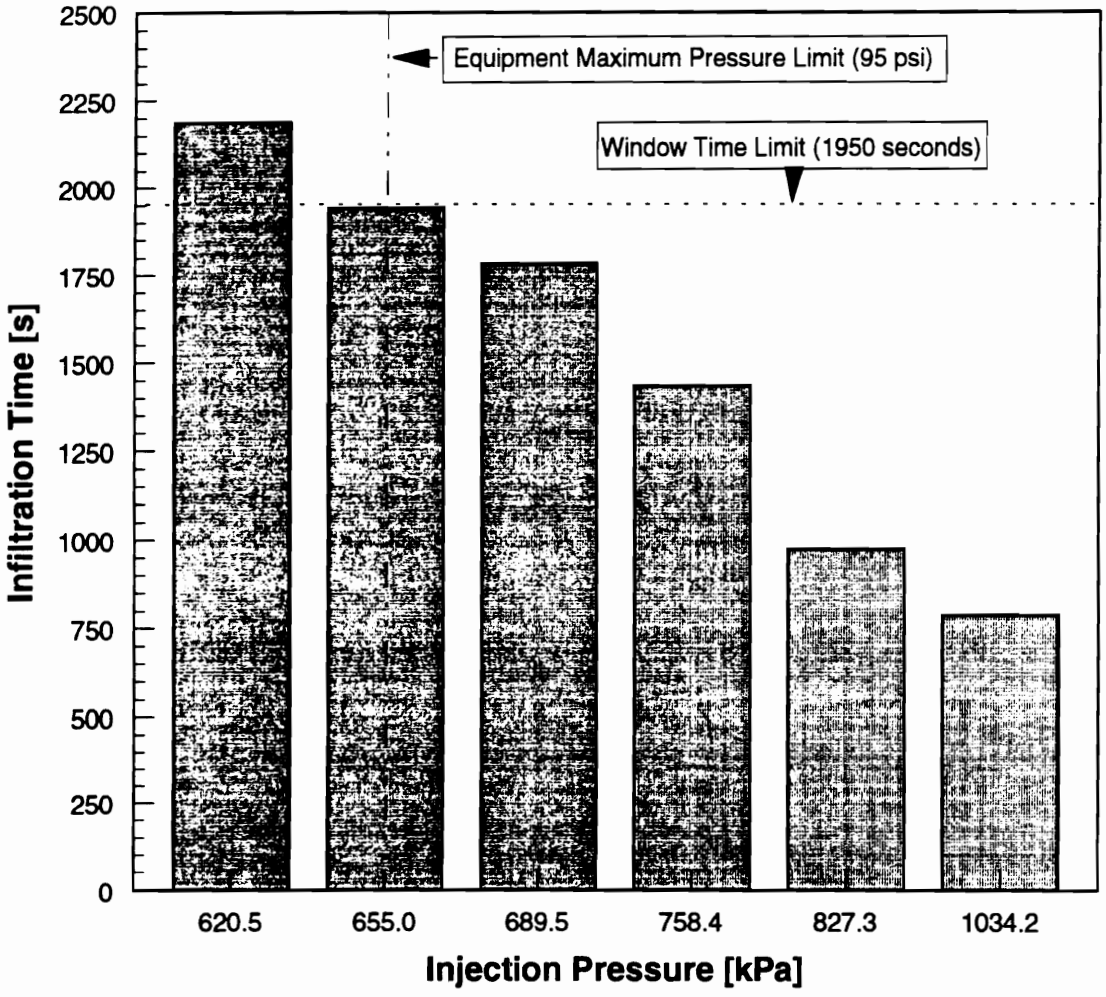

Figure 4.10 Model predicted infiltration time as a function of injection pressure for Hercules 3501-6 resin system (T_{inj} =109 °C; β = 2.0 °C/min; μ_c = 2.5 Pa-s).

Therefore, in order to infiltrate a AS4-3k-PW fabric preform, compacted to a fiber volume fraction of 60%, the injection must be performed at the threshold of the equipment maximum capacity. It must be mentioned here that the required injection pressure depends on the mold geometry, preform type, and injection procedures

A flow simulation was also performed to analyze the infiltration of 3501-6 resin into preform constructed from Style 162 E-glass fabric material. The permeability of this fabric, at a fiber volume fraction of 60%, was 1.8×10^{-11} and 2.4×10^{-11} m^2 in the warp and fill directions, respectively [9]. The viscosity-time profile corresponding to the optimal injection temperature of 109 °C, for $\beta = 2.0$ °C/min and $\mu_c = 2.5$ Pa-s, was used in the analysis. The flow simulation was performed for a resin injection at a constant pressure of 414 kPa (60 psi), through the center port. The model predicted an infiltration time of 1110 seconds (18.5 minutes) for complete infiltration of a preform of the same dimensions as that for the carbon fabric preform. Based on this analysis an E-glass fabric/3501-6 composite laminate was successfully manufactured by pressure injection RTM. However, a visual inspection of the panel revealed dry areas at the corners of the laminate. Also, a region with surface porosity was noticed. These defects could have been due to poor control of the pressure pot temperature. While the mold temperature was monitored and controlled with precision by the computer controlled hot-platen press, the pressure pot temperature was controlled manually with a simple thermostat switch.

Also, it is argued in literature that apriori simulation and optimization results can not take into consideration batch-to-batch variations that may exist in material properties

[13]. The flow behavior of the resin systems changes with the state of cure, and for even the same batch of resin, prior handling can influence the cure state. The initial cure state of the resin must be verified before manufacture because model generated process cycles may be invalid if the resin degree of cure at the beginning of injection is different from that used in the model. In the development of the optimal injection temperatures, the resin systems were assumed to be uncured. This is a valid assumption for resin systems which are processed immediately after the addition of catalysts, or curing agents, or both. However, with resin systems which are supplied premixed with curing agents and catalysts, "out-time" can influence the state of cure. Out-time refers to the length of time a resin system, which perhaps is refrigerated during storage, is exposed to ambient temperature in the process of handling. Manufacturers often provide viscosity traces of resin subjected to various levels of out-time.

An analysis was performed to study the influence of the initial degree of cure on the objective function, I_μ, for the RSL1895/W resin system. A heating rate of 2.0 °C/min and a cut-off viscosity of 0.25 Pa-s were chosen. The analysis was performed for a wide range of initial degree of cure, from 0.001 to 0.05. Figure 4.11 shows the influence of the initial degree of cure on the objective function and on the window time, Δt_{win}, available for injection. The results show a four-fold decrease in the window time over the selected degree of cure range.

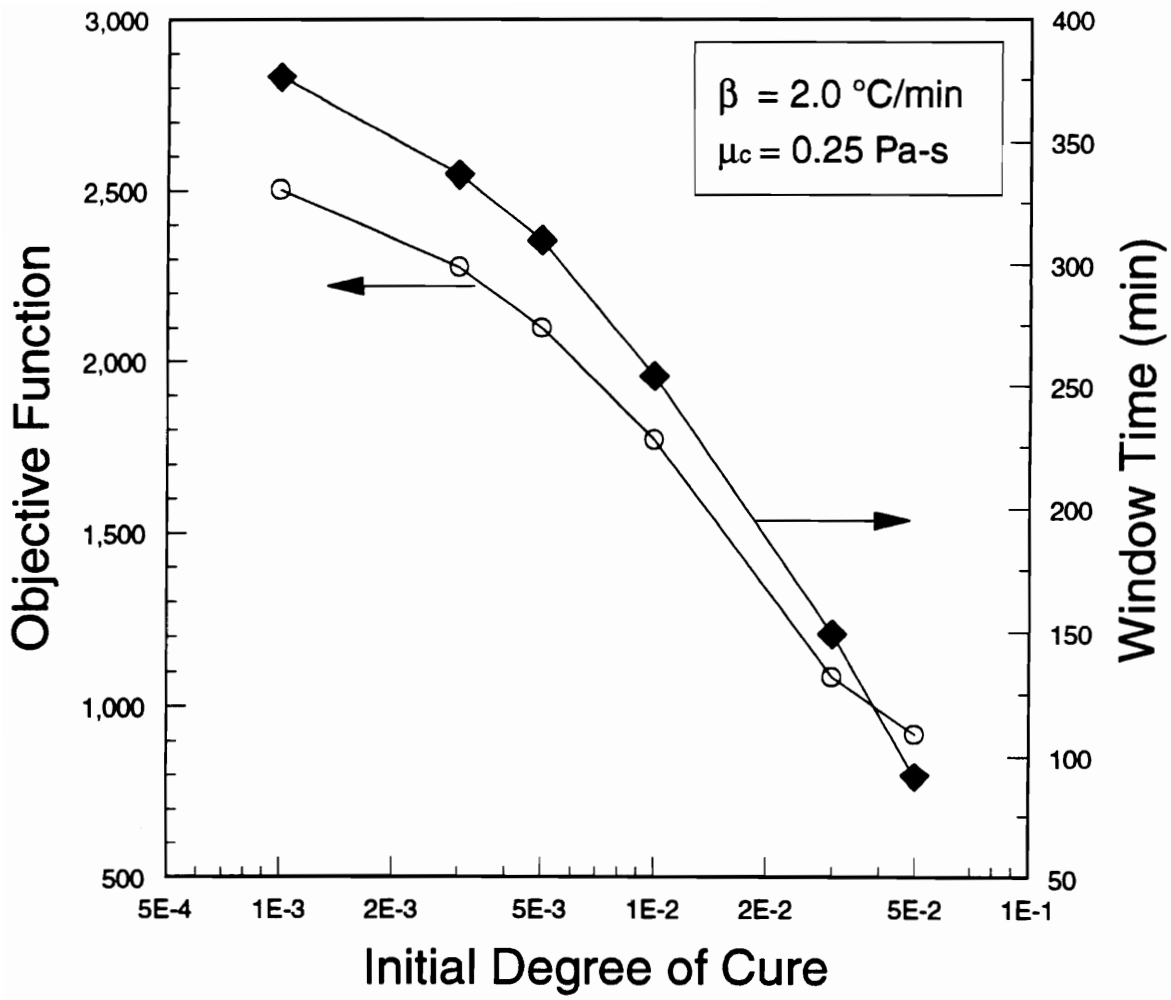

Figure 4.11 Influence of the initial degree of cure on the objective function, I_μ, and the injection window time, Δt_{win}, for RSL1895/W resin system (β = 2 °C/min; μ_c = 0.25 Pa-s)

4.6 SUMMARY AND CONCLUSIONS

In this study, a method has been developed to aid in the selection of the injection parameters for liquid molding processes. The method involves the use of a simple line search algorithm to generate optimal injection temperatures. These temperatures were generated at various levels of "cut-off" viscosity. At the present time, there is uncertainty in specifying the "right viscosity" for RTM.

The optimization scheme was used to generate optimal injection temperatures for two epoxy resin systems, Shell RSL1895/W and Hercules 3501-6. The rate of heating the resin up to the injection temperature does not seem to significantly influence the optimal solutions. However, increasing the heating rate was shown to help in reducing the overall process cycle time. It was also shown that resin injection can be initiated prior to reaching the "injection temperature", at the point when the resin viscosity drops below the cut-off viscosity.

Also, an analysis was performed to study the effect of the initial resin degree of cure on the optimal solutions. A small increase in the initial cure state was shown to result in a four-fold decrease in the injection window time.

A two-dimensional flow simulation model was used to help correlate the infiltration time and injection pressure, for a constant pressure, center injection configuration. The analysis was performed for the pressure injection of the 3501-6 resin system into a carbon fabric preform. As predicted by the model, the low permeability of the carbon preform necessitated a high injection pressure, in excess of 95 psi, to fully

infiltrate the preform. However, substituting the permeability characteristics of the carbon fabric preform with that of a E-glass fabric preform, resulted in model predictions of complete infiltration of the preform well within the window time available for H3501-6 resin system. Further, this was predicted to happen at an injection pressure of 60 psi. Based on this analysis, a E-glass/3501-6 composite laminate was successfully manufactured by the pressure injection RTM process. Cai [12] introduced a process design chart where the ratio of preform permeability to resin viscosity is considered to relate mold filling time, a characteristic length and pot life limit of the resin. This approach emphasizes the need to consider resin viscosity in conjunction with preform characteristics in process design.

4.7 REFERENCES

[1] Hayward, J.S. and B. Harris, "Effect Of Process Variables On The Quality Of RTM Mouldings", SAMPE Journal, Vol. 26, May/June 1990, p. 39.

[2] Verheus, A. S., and J. H. A. Peeters, "The Role Of Reinforcement Permeability In Resin Transfer Moulding", Composites Manufacturing, Vol.4, No.1, 1993, pp.33-38.

[3] Hasko, G., H.B. Dexter, A.C. Loos, and D. Kranbuehl, "Science-Based RTM For Fabricating Primary Aircraft Structures", 39th International SAMPE Symposium, April, 1994, p.779.

[4] Gebart, B.R., "Analysis of Heat Transfer and Fluid Flow in the Resin Transfer Moulding Process", Doctoral Thesis, Swedish Institute of Composites, Piteå and Luleå University of Technology, Luleå, Sweden, March 1993.

[5] Ahn, K.J., J.C. Seferis, and L. Letterman, "Autoclave Resin Infusion Process: Analysis and Prediction of Resin Content", SAMPE Quarterly, January 1990, p 3.

[6] Loos, A.C., and G.S. Springer, "Curing of Epoxy Matrix Composites", Journal of Composite Materials, Vol. 17, March 1983, p 135.

[7] Roller, M.B., "Rheology of Curing Thermosets: A Review", Polym. Eng. Sci., Vol. 26, No. 6, March 1986, p.432.

[8] MacRae, J.D., "Development and Verification of a Resin Film Infusion/Resin Transfer Molding Simulation Model for Fabrication of Advanced Textile Composites", M.S. Thesis, Virginia Polytechnic Institute and State University, Blacksburg, Virginia, December 1994.

[9] Hammond, V.H., A.C. Loos, H.B. Dexter, and G.H. Hasko, "Verification of a Two-Dimensional Infiltration Model for the Resin Transfer Molding Process", Virginia Tech Center for Composite Materials and Structures Report, CCMS-93-15, Blacksburg, VA, August 1993.

[10] Arora, J. S., "*Introduction To Optimum Design*", McGraw-Hill Book Company, 1989.

[11] MacRae, J. D., and A. C. Loos , "*RTM2D Version 1.1A User Guide*", Aug., 1994.

[12] Cai, Z., "Mold Filling Analysis of RTM Process", J. Composite Materials, Vol. 26, No. 9, 1992.

[13] Ciriscioli, P.R., and G.S. Springer, *Smart Autoclave Cure of Composites*, Technomic Publishing Company, Inc., Lancaster, PA, 1990.

5.0 CONCLUSIONS AND FUTURE WORK

5.1 CONCLUSIONS

This study has shown that the hydroxy functionalized, phenolphthalein based poly(arylene ether sulfone) thermoplastic toughened cyanate ester resin systems are candidate materials for high performance, damage tolerant advance composites. The untoughened AroCy B10 cyanate ester resin composites were found to be more damage tolerant and tougher compared with the hot-melt epoxy systems evaluated in this study. The choice of a specific toughened resin system is application and component end-use dependent. Applications of high performance toughened resin matrix composites, for instance, are in primary aircraft structural components like horizontal and vertical tails on Boeing 777 commercial aircraft, and in nose radomes on military aircrafts.

From the end-notched flexure tests, the mode II strain energy release rates for the Hercules 3501-6 epoxy, the AroCy B10 cyanate ester, and the VTUFF1520, VTUFF1525, VTUFF1530, and VTUFF2020 toughened cyanate ester matrix fabric composites were 1.35, 2.49, 3.10, 3.81, 3.94, and 3.48 kJ/m^2, respectively. Improvements in the mode II fracture toughness of the VTUFF series of modified resins further translated into

improvements in the impact damage performance and fracture toughness of the fabric composites.

The incorporation of the thermoplastic toughener in varying concentrations and molecular weights resulted in a corresponding increase in the melt viscosities. The tradeoff in enhancing the toughness of thermosetting resin system by this procedure is the ease of processablity. Although the average mode II fracture toughness of the VTUFF1530 composite was higher than that of the VTUFF1525 composite by about 5%, the penalty on processability was the increased melt viscosity of the VTUFF1530 resin system.

At the same level of concentration (20%), increasing the molecular weight of the toughener from 15k to 20 k resulted in about 12% increase in the G_{IIc}, and also improved the damage tolerance of the composites. While the VTUFF1520 permitted the manufacture of composites by pressure injection RTM, the VTUFF2020 composites were manufactured only by the RFI technique. Therefore, the choice of a particular matrix material depends on the application and economic trade-offs.

Through the use of science based simulation models, the processability of any resin system can be evaluated prior to manufacture. If deemed processable, process parameters such as temperature, consolidation/injection pressures, can be chosen so as to yield composites in the desired configuration upon manufacture. For the manufacture of unidirectional carbon fiber prepreg composites, the CUREV1 process simulation model generated two-stage cure cycles with hold temperatures at 150 and 200 °C. The use of

two different hold periods at 150 °C, 20 minutes and 55 minutes, resulted in a 30% change in the composite shear strain-at-failure.

The advantage of following a simulation model based approach to process design was further demonstrated by the successful manufacture of a glass fabric composite panel with a typical high-viscosity epoxy resin system, Hercules 3501-6. The results of this investigation suggests that resin systems with viscosities up to about 2.5 Pa-s can be used for composite manufacture by the pressure injection RTM process. While this viscosity level may be considered an upper bound, the results can not be generalized to specify a single value or a narrow range of viscosity that is suitable for all RTM applications. The geometry of the component targeted for manufacture, the injection procedure used, the permeability and compaction level of the prefom material, and the specific resin system together influence the choice of process parameters. Hence, process design can only be performed on a case by case basis.

The contribution resulting from this work to the field of composite materials and their processing include:

(a) The development of a low-cost, modular computer controlled hot-platen press which is capable of interfacing with a wide variety of sensors for process control, from conventional thermocouples to advanced fiber-optic devices. The utility of such a process control equipment in accurately following model generated cure cycles with excellent repeatability was demonstrated. The need for operator intervention is minimized and provides reliability in composite processing.

(b) The verification of the processability of the recently developed series of toughened cyanate ester resin systems. The results of the resin characterization and mechanical tests add to an evolving database on toughened matrix composites.

(c) The development of a modified test method for rapid estimation of the void content in fabric composites manufactured by the RTM/RFI processes.

(d) The demonstration of the utility of a model based approach for composite processing. A procedure was developed for designing the injection parameters for the RTM process. Also, this procedure can easily be applied to other composite manufacturing processes such as pultrusion, prepregging, and continuous RTM (CRTM®).

5.2 Recommendations for Future Work

Although this investigation has demonstrated the processability and the improvements in the impact damage tolerance of the toughened cyanate ester resin composites, it is by no means an exhaustive study. However, this work has helped identify a few future opportunities in the various aspects of composite manufacturing.

Materials Characterization

In this study only the VTUFF1525 resin system was fully characterized and cure kinetics and viscosity models were developed. By completely characterizing the other

resin VTUFF series resin systems and the AroCy B10, the simulation models can be applied to develop process cycles.

Process Simulation and Optimization

The Model 30 prepregger control parameters were selected by process of trial and error in the manufacture of the carbon fiber prepregs. A science based simulation model which describes the impregnation of a fiber tow in the wedge-slit die is available in the literature. This model does not, however, take into account the resin uptake in the fiber tow in the resin bath. In this investigation it was observed that the resin content in the fiber tow was dependent on the level of resin in the resin pot, suggesting a dependence of the resin uptake on the residence time of a tow section in the resin. An opportunity exists to investigate this observation and suitably modify the existing model.

Simulation model generated process cycles are, in general, based on user input of key raw material properties and variables that are experimentally determined. The model predictions are valid only if these parameters accurately represent the materials to be processed. The level of accuracy required of the various parameters can be ascertained by a sensitivity analysis on the results of process simulation.

The constants associated with the resin characterization models and the mass fraction of resin in prepregs are determined experimentally. The influence of errors in the measurement of these constants on the model predictions can be studied by statistical methods such as response surface analysis. From the expected minimum and maximum

values of the experimentally determined constants, a statistically valid analysis surface can be generated (IMSL Statistical Library Routine - **RCOMP**). Based on the model predictions for the analysis surface, a response surface can be generated and thereby providing information on the level of significance to which each input variable needs to be determined (Meyers, R.H., *Response Surface Methodology*, Allyn and Bacon, Boston, 1971).

The procedure developed in this study for the design of the injection parameters for the RTM process demonstrated the potential of a simulation model/optimization based approach. The current method requires the specification of a cut-off viscosity and heating rate to develop an injection temperature profile. But, the resin viscosity needs to be "low enough, long enough" to complete the infiltration. Therefore, a unique solution may exist for each combination of component geometry, resin system, preform characteristics, injection procedure, equipment capabilities, and quality constraints. The next logical step would be to develop an optimization scheme which incorporates a flow analysis submodel. Modeling the component geometry and any necessary preprocessing required for the flow model can be performed using PATRAN® as it was done in this study. The objective of the optimization process would be to find the temperature-time profile and the injection pressure required to minimize not only the infiltration time, but the overall cycle time as well. It was shown in this study that increasing the heating rate to the injection temperature allows the infiltration step to be completed early in the cure cycle. However, unless a rationale is developed to "trade-off" injection pressure, the upper bound

allowed on the pressure will be returned as the "optimal" solution which minimizes infiltration time. Toward this end, quality constraints need to be introduced. The quality constraints should be based on the flow rates within the fabric preform which do not promote or induce void formation. Obviously, very "low" flow rates are not desirable for shortening the time required for infiltration and the suspicion is that void content increases at very "high" flow rates. High flow rates may also cause fiber-wash and misalignment of fibers in the composite. In order to sustain a specified flow rate during infiltration, different levels of injection pressures may be necessary depending the factors mentioned above. What then is the "right" flow rate or range of flow rates?

This can perhaps be answered by estimating the void content distribution across a composite panel. Injecting a constant viscosity resin into a preform at a constant inlet pressure results in a decrease in flow rate with increasing distance of the flow front from the inlet. Panels can be manufactured at different injecion pressures, fiber volume fractions, and fabric types. Specimens, identified by location on the panel, can be cut and their void contents estimated using the procedure used in this study and by other techniques. A flow simulation model can be used to determine average flow rates as a function of location on the panel. The objective of this study will be to determine the range flow velocities which are ideal for minimizing the void content in the composite. This information will help in providing a basis in the optimization scheme for determining the injection pressure. Thus, a complete procedure can be developed to design the

injection parameters for RTM and such a tool would be of immense use to the composite manufacturing industry.

Process Control Equipment

Currently, the platen heaters on the computer controlled hot-press are accurately controlled to follow a specified temperature-time profile. The application of compaction pressure is also controlled in a closed loop, through pressure transducers and a motorized pressure regulator. However, for the pressure injection RTM process, the pressure pot and resin feed lines are not controlled by the computer. Only the acquisition of temperature data is performed. Also, the pressure pot in use is not designed for RTM. A complete redesign of the pressure pot will be necessary to improve the accuracy of temperature control, and the ease of operation. Also, by installing a motorized pressure regulator on the pressure pot, the injection pressure can be controlled by the computer. Already, a high temperature pressure transducer is used to monitor the inlet pressure. By providing the output of this sensor as a feedback signal to the computer, the injection pressure can be set with greater accuracy. Operator intervention is further reduced.

Implementing this change to the current system opens yet another opportunity. A flow simulation model can be used to predict the inlet pressure-time profile required to ensure a constant flow rate injection into the preform. The model predicted pressure profile can be easily programmed into the control software and the motorized pressure regulator can be controlled to change the injection pressure accordingly. To date, constant

flow rate injection is carried out only with the aid of gear pumps and other devices which are expensive. Generating constant flow-rates with a pressure pot simplifies the maintenance and clean-up as compared to these devices.

VITA

Anand Rau was born in Madras, India, on August 29th 1963. In 1985 he obtained a Bachelor of Engineering degree in Mechanical Engineering. Anand was then employed by Hindusthan Aeronautics Ltd. (HAL), Bangalore, India. He was sponsored by HAL for graduate study at the Indian Institute for Technology at Madras. After his Master's program he assumed the duties of Engineer at the Aircraft Division of HAL, at Bangalore. In 1989, Anand left HAL to pursue a doctoral program at Virginia Tech. He received his Ph.D. degree in Engineering Mechanics, under the guidance of Dr. Alfred C. Loos, in November 1996.